THE UNIVERSITY
of EDINBURGH

“It is our choices, Harry, that show what we truly are, far more than our abilities”

Harry Potter and the Chamber of Secrets 1992

Constitutive Activation of the ATM DNA Damage Response Pathway in Cancer Represents a Deregulated Pathway

Shahida Din

Thesis submitted for the degree of Doctor of Philosophy

University of Edinburgh

2014

Doctor of Philosophy University of Edinburgh 2014

Abstract

Constitutive activation of the ATM dependent DNA damage response and repair pathways have been reported in pre-malignant and malignant human tissues and may undermine the efficacy of genotoxic cancer therapies. Therefore, ATM inhibitors may overcome resistance to current cytotoxics and potentiate the effects of radiotherapy. A colorectal cancer model was investigated to develop a framework for the rational use of ATM inhibitors.

HCT116 p21-/- cells display constitutive activation of the ATM DNA damage response but display a defect in the ionising radiation induced S-phase checkpoint, termed radioresistant DNA synthesis. This radioresistant phenotype is associated with increased basal levels of Cdc25A protein, deficient DNA damage-induced degradation of Cdc25A and Chk2 mis-localisation. HCT116 p21-/- and SW620 cells, which exhibit basal Chk2 threonine-68 phosphorylation, were unable to abrogate the S-phase checkpoint when treated with an ATM inhibitor, suggesting that the ATM–Chk2 arm is non-functional in these cells: inhibition of ATM did not potentiate the efficacy of ionising irradiation.

To assess activation of the pathway a tumour microarray was created using 179 treatment naïve sporadic colorectal cancers; 152 were of the microsatellite stable phenotype. Phosphorylated Chk2 threonine-68 was present in 22 % of microsatellite-stable colorectal tumours and 33 % of tumours with the microsatellite instability phenotype.

In a colorectal cancer cell line model constitutive activation of the ATM DDR pathway reflected an attenuated ATM-Chk2 axis and inhibition of ATM in these circumstances was unable to potentiate the efficacy of ionising irradiation. Basal Chk2 threonine-68 phosphorylation may reflect a deregulated ATM DNA damage response pathway and/or checkpoint adaption and therefore use of an ATM inhibitor in this background may have limited efficacy.

A predictive model is proposed that integrates functionality of the ATM-Chk2 axis, p53 mutation status and defects in DNA repair pathways when considering ATM inhibitor therapy. Ultimately, molecular phenotyping and functional analysis of processes deregulated in cancer will permit individualisation of current treatment modalities, improving their efficacy and limiting patient toxicity.

Declaration

I hereby declare that I am the author of this thesis and that I performed all the work described herein, except where specifically stated. The work described in this thesis has not been accepted in any previous form for application for a higher degree.

Shahida Din 2014

Acknowledgements

Firstly, I would like to thank all my supervisors through this epic journey who have guided me throughout my PhD studies; Professor Duncan Jodrell, Dr Sylvie Guichard, Professor David Harrison and Professor Ted Hupp. I am indebted to Dr Bernard Ramsahoye for his meticulous guidance in developing the radionucleotide DNA synthesis assay and to Professor John Bartlett and his team for answering my never ending questions in immunohistochemistry. I would also like to thank all the staff, past and present, at the CRUK Laboratories, especially Jayne Culley, Jacqueline Dickson, Maciej Kalicszak, Janet Macpherson and Catherine Naughton, for their invaluable support. Special thanks to Morwenna Muir for the animal work and Euan Gibson (BSc Honours student) for creating the human CRC microarray and working with myself in optimising the antibodies for immunohistochemistry.

To my husband and daughters who have supported me throughout this period and have never questioned my early starts and late finishes.

I am grateful to CRUK for the funding that I received.

Abbreviations

53BP1	tumor suppressor p53-binding protein 1
Ab	antibody
AGT	alanine-glyoxylate aminotransferase
AKT	RAC-alpha serine/threonine-protein kinase
APC	adenomatous polyposis coli protein
ARF	cyclin-dependent kinase inhibitor 2A - interacting protein
AT	ataxia-telangiectasia
ATLD	ataxia-telangectasia-like disorder
ATM	serine/threonine-protein kinase ataxia-telangiectasia mutated
ATR	serine/threonine protein kinase Ataxia-telangectasia mutated-Rad3 related
ATRIP	serine/threonine protein kinase Ataxia-telangectasia mutated-Rad3 related-interacting protein
BCA	bicinchoninic acid
Bcl	B cell lymphoma protein
BRCA1	breast cancer (type 1/2) susceptibility protein
BSA	bovine serum albumin
CAK	cyclin dependent kinase-activating kinase
Cdc25	cell division cycle 25
Cdk	cyclin-dependent kinase
Chk1	serine/threonine-protein kinase checkpoint kinase 1
Chk2	serine/threonine-protein kinase checkpoint kinase 2
CPT	camptothecin
CRC	colorectal cancer

CRUK	cancer research United Kingdom
DAB	3,3'-diaminobenzidine
DAPI	4',6-diamidino-2-phenylindole
DDR	deoxyribonucleic acid damage response
DMEM	Dulbecco's modified eagle's medium
DMSO	dimethyl sulfoxide
DNA	deoxyribonucleic acid
DNA-PK	deoxyribonucleic acid -dependent protein kinase
DPX	dibutyl phthalate xylene
DSB	double-strand breaks
DTT	1,4-dithiothreitol
ECL	enhanced chemiluminescence
EDTA	ethylenediaminetetraacetic acid
FA	Fanconi anaemia
FACS	fluorescence-activated cell sorting
Fas	Tumor necrosis factor receptor superfamily member 6
FISH	fluorescence in situ hybridisation
FITC	fluorescein isothiocyanate
FSC	forward scatter
G1	Gap 1
G2	Gap 2
GAPDH	Glyceraldehyde-3-phosphatedehydrogenase
Gy	Gray
H2AX	histone 2AX
H&E	hematoxylin and eosin
hMLH1	human Mut L homologue
hMSH2 (6)	human Mut S homologue
HNPCC	hereditary non-polyposis colon cancer
HR	homologous recombination
HRP	horseradish peroxidase

hSMG-1	Serine/threonine-protein kinase SMG1
HUS 1	checkpoint protein HUS 1
IκB	inhibitor kappaB
IgG	immunoglobulin G
IHC	immunohistochemistry
IKK	inihibitor kappaB kinase
INK	family of cdk inhibitors
IR	ionising radiation
kDa	Kilodalton
MEF	mouse embryonic fibroblasts
MDC1	mediator of deoxyribonucleic acid damage checkpoint protein 1
Mdm2	E3 ubiquitin-protein ligase mouse double minute 2
Mdm4	protein mouse double minute 4
MGMT	O-6-methylguanine deoxyribonucleic acid methyltransferase
MMR	mismatch repair
MOPS	4-Morpholinepropanesulfonic acid
MRN	Mre11–Rad50–Nbs1/Nibrin
mRNA	messenger ribonucleic acid
MSI	microsatellite instability
MSS	microsatellite stable (cancers containing no alterations in the standard microsatellite panel)
mTOR	mammalian target of rapamycin
NBS	Nijmegen breakage syndrome
NCS	neocarzinostatin
NER	nucleotide excision repair
NF-κB	nuclear factor- kappaB
NHEJ	non-homologous end joining
NP40	nonidet P40
PAGE	polyacrylamide gel electrophoresis

PARP	poly (adenosine diphosphate-ribose) polymerase
PBS	phosphate-buffered saline
PCNA	proliferating cell nuclear antigen
PCR	polymerase chain reaction
PI3K	phosphoinositide 3-kinase
PIKK	phosphoinositide 3-kinase-related kinase
PMS1/2	PMS1 protein homolog 1/2
PVDF	polyvinylidene difluoride
qRTPCR	quantitative real time polymerase chain reaction
Rad 1	cell cycle checkpoint protein RAD1
Rad 9	cell cycle checkpoint protein RAD9
Rad 17	cell cycle checkpoint protein RAD17
RDS	radioresistant deoxyribonucleic acid synthesis
RNA	ribonucleic acid
RNF8	E3 ubiquitin-protein ligase RING finger protein 8
RPA	replication protein A
RTPCR	real time polymerase chain reaction
SCID	severe combined immunodeficiency
SDS	sodium dodecyl sulphate
SiRNA	small interfering ribonucleic acid
SMC1	structural maintenance of chromosomes protein 1
SRB	sulforhodamine B
TBST	tris-buffered saline tween 0.001%
TCA	trichloracetic acid
TMA	tissue microarray
UV	ultraviolet

Table of Contents

Chapter 1
Introduction

Chapter 2

Materials & Methods

Chapter 3

Expression of DNA Damage Response Proteins in Sporadic Colorectal Cancer

Chapter 4

p21-Null Cells Display Radioresistant DNA Synthesis

Chapter 5

p21 Regulates DNA Damage Induced Cdc25A Degradation

Figures and Tables

Chapter 1. Introduction

1.1 DNA Damage

DNA damage occurs continuously in eukaryotic organisms and cells have developed sophisticated networks for dealing with this type of genotoxic insult. The purpose of such networks is to enable the cell to halt division (cell cycle arrest) and undergo DNA repair or programmed cell death (apoptosis) (Zhang *et al.*, 2004). Defects in the DNA damage response (DDR), occurring in both recognition or repair pathways, will undermine genome integrity and allow the propagation of detrimental mutations. DNA damage can be induced by a variety of mechanisms, including physiological processes (i.e., reactive oxygen species and replication stress) and exogenous compounds such as ultraviolet (UV) radiation and cytotoxic therapies including ionising radiation (IR). The type of DNA damage created depends on the insult, but may include altered bases, single- and double-strand breaks (DSB), interstrand cross-links and bulky DNA adducts (Norbury and Hickson, 2001).

1.2 DNA Damage Response

DDR pathways are highly conserved and much insight has been gained by studying the mechanisms in simple organisms (Sancar *et al.*, 2004). The DDR pathway essentially has three components: sensors that recognise DNA damage, transducers that relay signals to effectors that execute the desired outcome (Figure 1.1) (Lukas *et al.*, 2004b). The general principles of signal transduction are common; however, it is clear that more than one response pathway exists and that the response is dictated by the type and severity of DNA damage (Kastan and Bartek, 2004). Examples of

sensor proteins include replication protein A (RPA), breast cancer (type 1/2) susceptibility protein (BRCA1), the Rad family of proteins and the Mre11–Rad50–Nbs1 (MRN) complex, which are all recruited early to the sites of DNA damage (Niida and Nakanishi, 2006). Phosphoinositide 3-kinase-related kinases (PIKK) comprise a family of proteins, including DNA-dependent protein kinase (DNA-PK), serine/threonine-protein kinase ataxia-telangiectasia mutated (ATM), serine/threonine-protein kinase ATM-Rad3 related (ATR); serine/threonine-protein kinase SMG1 (hSMG-1) and serine/threonine-protein kinase mammalian target of rapamycin (mTOR). These family members have been shown to have important roles in DNA damage recognition and repair (Abraham, 2004; Abraham, 2001; Lempiainen and Halazonetis, 2009; Russell, 1998; Shiloh, 2003).

ATM is primarily involved in the recognition and processing of DNA DSB (see below), whereas ATR has a more pertinent role in the detection of UV-induced DNA damage and stalled replication forks that occur during DNA replication (Heffernan *et al.*, 2002). However, this relationship is not definitive; in reality, both kinases have considerable overlap in activating DNA damage signalling and in their downstream substrates (Jazayeri *et al.*, 2006). A large-scale proteomic analysis has indicated that over 700 proteins are phosphorylated in an ATM- and ATR-dependent manner in response to ionising radiation (IR) (Matsuoka *et al.*, 2007). In separate publications, Bennetzen (2010) and Bensimon (2010) extended this panel of substrates using a mass spectrometry-based proteomics approach; they identified many thousands of protein phosphorylation events occurring in response to IR and radiomimetic treatments. ATM and ATR were originally considered to be direct sensors of DNA damage yet recent data has suggested that they are in fact activated by

intermediaries: the MRN trimeric complex and RPA–ATRIP (ATR-interacting protein)–ATR that bind to sites of double- and single-strand DNA breaks, respectively (Zou and Elledge, 2003). Jazayeri *et al.*(2006) have since confirmed that IR (which induces DSB) efficiently induces checkpoint kinase 1 (Chk1) serine-317 phosphorylation and requires functional ATM, ATR and Nbs1. Specifically, ATM and Mre11–Nbs1 cooperate in RPA focus formation, thus facilitating ATRIP–ATR recruitment and subsequent Chk1 phosphorylation . In general, transducer molecules are kinases such as ATM, ATR, Chk1 and checkpoint kinase 2 (Chk2) that amplify the initial signal and activate effector molecules. Effector proteins include p53, which controls G1/S-phase cell cycle arrest, and phosphatases involved in G2 arrest. hSMG-1 is the newest member of the PI3K family to be discovered and appears to have dual roles in DNA damage sensing and quality control of mRNA prior to protein translation (Abraham, 2004). DNA-PK has a defined role in both DNA repair and apoptotic mechanisms but has yet to be implicated in DNA damage recognition cascades (Burma and Chen, 2004). The outcome of the DDR is the activation of cell cycle checkpoints, to allow adequate time for DNA repair processes or the induction of apoptosis, if the DNA repair processes are inefficient (Shiloh, 2006).

1.3 DNA Damage Responses to Double Strand Breaks

1.3.1 DNA damage sensing

DSB comprise one of the most detrimental types of DNA damage; they occur frequently as a result of exogenous insults such as ionising radiation or cytotoxic agents and endogenously via reactive oxygen species and mechanical stress on chromosomes (Carney *et al.*, 1998; Dasika *et al.*, 1999). DSB have an essential physiological role in V(D)J recombination during the development of the immune

system. They also occur during DNA synthesis when replication forks arrest and collapse (Kuzminov, 2001a; Kuzminov, 2001b) and as a therapeutic consequence of cytotoxic chemotherapy that creates interstrand cross-links or other structural modifications to DNA (Sancar *et al.*, 2004). Many proteins, including the MRN complex, histone 2A (H2A), tumor suppressor p53-binding protein 1 (53BP1), BRCA1 and mediator of DNA damage checkpoint protein 1 (MDC1) (Bekker-Jensen *et al.*, 2006; DiTullio *et al.*, 2002; Schultz *et al.*, 2000), are rapidly recruited to the sites of DNA DSB (or chromatin alterations), forming complexes termed foci (Lisby and Rothstein, 2005). Their precise roles and positions within the damage-sensing cascade remain under investigation. Emerging data has suggested that access to condensed chromatin is tightly regulated and additional mechanisms exist to allow the DDR to access damage chromatin in a highly organised manner E3 ubiquitin-protein ligase RNF8nuclease complex (Kitagawa *et al.*, 2004). The MRN complex has been shown to aid the recruitment and activation of ATM at sites of DNA damage (Carson *et al.*, 2003; D'Amours and Jackson, 2002; Falck *et al.*, 2005; Lee and Paull, 2005; Uziel *et al.*, 2003). Current data suggest that the Mre11–Rad50 dimer translocates to the sites of DNA damage and association with Nbs1 creates a bridge for the attachment of ATM (Assenmacher and Hopfner, 2004; Carney *et al.*, 1998; Cerosaletti and Concannon, 2004; Falck *et al.*, 2005; Lavin, 2004) and linkage to MDC1 bound to damaged chromatin (Lukas *et al.*, 2004a). ATM phosphorylates H2AX (Stucki and Jackson, 2006) and creates a further focus for the attachment of MDC1(Xie *et al.*, 2007); subsequently recruiting E3 ubiquitin-protein ligase RING finger protein 8 (RNF8) as part of a ubiquitylin signalling cascade (Lukas *et al.*, 2011). RNF8 ubiquitinylates H2AX creating a focus for the stable attachment of

oligomerised 53BP1 (Kolas *et al.*, 2007; Mailand *et al.*, 2007). 53BPI in turn stimulates ATM activity through the MRN complex resulting in amplification of the ATM signal (Lee and Paull, 2007). This function appears to be important at the early stages of low-level DNA damage (Cerosaletti and Concannon, 2004). Nbs1 itself is a target for ATM phosphorylation (on serine-278 and serine-343); this appears to be a prerequisite for the activation of DNA damage checkpoints (S phase and G2/M) (Falck *et al.*, 2005; Lim *et al.*, 2000; Zhao *et al.*, 2000), as well as facilitating ATM-dependent phosphorylation of downstream substrates such as Chk2, FAND2, histone H2A and structural maintenance of chromosomes protein 1 SMC1 (Assenmacher and Hopfner, 2004).

The MRN complex is involved not only in DSB signalling with ATM but also in DSB repair, maintenance of the S-phase checkpoint and telomere stability (Lavin, 2004; Shiloh, 2001). Ataxia telangectasia is an autosomal recessive condition in which the *ATM* gene is mutated (Gatti *et al.*, 1988) (see below). The Ataxia-telangectasia-like disorder (ATLD) bears a striking clinical resemblance to ataxia-telangectasia (AT) and is caused by a defect in the *MRE11A* gene (Stewart *et al.*, 1999). Similarly, Nijmegen breakage syndrome (NBS), which is caused by a mutated *NBM* gene, displays some clinical features resembling the AT phenotype, but is also characterised by developmental defects (Carney *et al.*, 1998; Varon *et al.*, 1998). *MRE11A* and *NBN* mutations are hypomorphic (mutations that partially inactivate the gene), and null phenotypes of any component of the MRN complex lead to early embryonic lethality (Luo *et al.*, 1999; Xiao and Weaver, 1997; Zhu *et al.*, 2001), thus highlighting their essential role in cell survival.

1.3.2 Signal transduction

ATM is a nuclear protein kinase that orchestrates the response to DNA DSB; much of this data has been deduced by studying genomic instability syndromes. The *ATM* gene, located on chr11q22.3 (Gatti *et al.*, 1988), is mutated in the autosomal recessive disorder AT that is characterised by extreme sensitivity to radiation (and other agents causing DSB) and susceptibility to developing malignancies, especially those of lymphoid origin (Savitsky *et al.*, 1995). Cells from AT patients are defective in processing DSB and in DNA damage checkpoint controls (Meyn, 1995; Shiloh, 2003). *ATM* homozygotes have chromosomal instability, associated with gaps/breaks, translocations involving the T cell receptor locus, telomere–telomere fusions, reduced telomere length and increased rates of intrachromosomal recombination (Enoch and Norbury, 1995; Kirsch, 1994). AT cells also display radioresistant DNA synthesis, a consequence of the failure to activate the S-phase checkpoint control in response to ionising radiation (Houldsworth and Lavin, 1980; Painter and Young, 1980; van den Bosch *et al.*, 2003).

Elegant studies by Bakkenist and Kastan (2003) revealed that ATM is a 350 kDa nuclear protein kinase, which exists as an inactive homodimer that rapidly dissociates and autophosphorylates at serine-1981 following low-dose ionising radiation. A conformational change then allows dimer dissociation and formation of ATM monomers. Their initial hypothesis suggested that ATM activation occurs in response to subtle changes in the highly organised structure of DNA (i.e., chromatin alterations); however, emerging data has confirmed that the MRN trimeric complex is an important intermediary in ATM activation (Carson *et al.*, 2003; D'Amours and

Jackson, 2002; Lee and Paull, 2004; Lee and Paull, 2005; Petrini, 2000; Uziel *et al.*, 2003; Zhao *et al.*, 2000).

1.3.3 Effector pathways

The DDR to DSB is complex and remains an area of intense investigation. Components (sensors, transducers and effectors) of the DDR pathways appear to have multiple roles, both upstream and downstream of ATM. The role of activated ATM is discussed with particular reference to the cell cycle, as many of its substrates are involved in cell cycle arrest, DNA repair, apoptosis and senescence.

1.3.4 Cell cycle arrest

During normal cellular growth, entry into the cell cycle is dependent on cyclin–Cdk (cyclin-dependent kinase) complexes, termed replication checkpoints, that monitor various aspects of DNA synthesis (Vermeulen *et al.*, 2003). Eukaryotic cell division is divided into four stages: mitosis (M), gap1 (G1), DNA synthesis (S) and gap2 (G2) phases. In the G1 phase, cells are preparing for DNA synthesis; at G1, cells may exit into G0 if the conditions for cell division are unfavourable. G1 also contains a mitogen-dependent restriction checkpoint, or the point of no return: if mitogens are limited before G1 phase, then cells enter G0; conversely, if essential components are limited after this phase, then cells continue their progression through the cell cycle. DNA synthesis occurs during S phase, which is followed by G2 phase, in which cells prepare for mitosis. Finally, cells undergo cell division during M phase. During normal cellular growth, entry into and progression through the cell cycle is tightly regulated and dependent on a series of serine/threonine kinases termed Cdks, which

bind activating partners termed cyclins (Sherr and Roberts, 1995). Cdk levels are relatively stable throughout the cell cycle, but the expression of cyclins fluctuate (Diehl *et al.*, 1997), regulating cdk-cyclin kinase activity. As well as requiring cyclin partners, Cdks must be phosphorylated on specific residues by the Cdk7–cyclin H complex [termed the Cdk-activating kinase (CAK)] for full activation (Malumbres and Barbacid, 2005). In addition to these control mechanisms, a third level of regulation is provided by the Wee1 and Myt1 kinases, which inactivate Cdks by phosphorylating residues threonine-14 and tyrosine-15, respectively (Watanabe *et al.*, 1995). Inactivating phosphorylation at these sites must be removed by the Cdc25 dual specificity phosphatases (subtypes A, B and C) to allow programmed entry into the cell cycle (Hoffmann *et al.*, 1994; Russell and Nurse, 1986). Additional constraints are provided by other inhibitory proteins, designated Cdk inhibitors. There are two major families: members of the INK family group bind to Cdk4 and Cdk6, thereby preventing association with cyclin D; and cip/kip family members, including p21, universally inhibit Cdk/cyclin complexes. p21 can also inhibit DNA synthesis by binding to the proliferating cell nuclear antigen (PCNA), a subunit of DNA polymerase delta. Under mitogenic stimuli, G1 cell cycle entry is initiated by cyclin D binding to Cdk4 and Cdk6 (Figure 1.2). The active Cdk4–Cdk6–cyclin D complex phosphorylates the retinoblastoma (Rb) protein, thus allowing the release and activation of E2F transcription factors, which leads to the transcriptional upregulation of proteins necessary for S-phase progression, including Cdc25, cyclin A and cyclin E (Sherr and Roberts, 1995; Vigo *et al.*, 1999; Weinberg, 1995). The subsequent formation of the Cdk2–cyclin E complex initiates DNA synthesis at the G1/S transition point (Hoffmann *et al.*, 1994; Jinno *et al.*, 1994). Further, cyclin A-

dependent Cdks control initiation of DNA replication by activating DNA polymerase alpha primase. Once DNA synthesis is complete, Cdk1 becomes the dominant Cdk, binding first to cyclin A and then to cyclin B1 during mitosis.

Despite the level of complexity in the regulation of cellular division, additional protective mechanisms termed DNA damage checkpoints delay cell cycle progression to allow the repair of damaged DNA (Figure 1.2), thus preventing the propagation of mutations (Russell, 1998). Checkpoint proteins negatively regulate the cell cycle in response to DNA damage (Enoch and Norbury, 1995). Four DNA damage checkpoints function in different parts of the cell cycle: G1/S checkpoint (pre-DNA synthesis), intra-S phase checkpoint (during DNA synthesis), G2/M checkpoint (pre-mitosis) and the mitotic or spindle checkpoint (during M phase). In response to DSB, ATM and ATR coordinate phosphorylation of Chk1 and Chk2. Chk2 levels are relatively constant during the cell cycle; in contrast, Chk1 levels are low in early G1 and rise to a maximum in S phase.

1.3.4.1 G1/S phase

The G1/S checkpoint prevents replication of damaged DNA through the activation, stabilisation and accumulation of p53 in response to IR via the ATM and other pathways. ATM phosphorylates Chk2 on threonine-68 (Ahn *et al.*, 2000; Matsuoka *et al.*, 1998); in turn, activated Chk2 phosphorylates p53 on serine-20, which inhibits p53 binding to E3 ubiquitin-protein ligase Mdm2 (Mdm2) (Bartek and Lukas, 2003; Chehab *et al.*, 2000; Craig *et al.*, 2003; Falck *et al.*, 2001; Hirao *et al.*, 2000; Shieh *et al.*, 2000; Shieh *et al.*, 1997). Mdm2 is a negative regulator of p53 that functions by (1) binding to the transactivation domain of p53 and inhibiting its transcriptional

activity, (2) exporting p53 from the nucleus and (3) targeting p53 for ubiquitin-mediated proteolysis (Dasika *et al.*, 1999; Haupt *et al.*, 1997; Kubbutat *et al.*, 1997; Momand *et al.*, 2000). ATM phosphorylation of Mdm2 at serine-395 prevents the nuclear export of p53. Hence, the accumulation of nuclear p53 activates the gene encoding p21 an inhibitor of cdks (e.g., Cdk2–cyclin E), resulting in G1 arrest (Brugarolas *et al.*, 1999). Additionally, direct ATM phosphorylation of p53 serine-15 induces an allosteric change that enables the binding of p300, thereby stabilising and further enhancing the transcriptional activity of p53 (Dornan and Hupp, 2001; Kastan and Lim, 2000). Two further p53-inducible genes encode 14–3-3σ and Gadd45; these inhibitory proteins are suspected to be involved in G2 arrest following DNA damage (see below). The protein Mdm4 is an mdm2 homologue that is also able to bind p53 and inhibit its transcriptional activity. ATM-induced p53 phosphorylation of Mdm4 at serine-403 and Chk2-dependent phosphorylation at serines 342 and 367 promote its Mdm2-dependent ubiquitination and degradation (Chen *et al.*, 2005c). Mdm4 serine-367 phosphorylation facilitates its interaction with the 14-3-3 protein, which is essential for the regulation of Mdm4 (LeBron *et al.*, 2006). The induction of multiple genes following DNA damage can take several hours; therefore, the initial rapid cellular response is mediated by Cdc25A degradation (Busino *et al.*, 2003; Donzelli *et al.*, 2002; Jin *et al.*, 2003). ATM-dependent Chk2-mediated degradation of Cdc25A is an important axis of the G1/S-phase DNA damage checkpoint. Cdc25A is a dual specificity phosphatase that removes inhibitory tyrosine and threonine phosphorylation from the Cdk2–cyclin E complex, thus promoting S-phase entry.

1.3.4.2 S phase

The S-phase checkpoint is less well characterised but appears to function when DNA is damaged during the early stages of DNA synthesis. In ATM-deficient cells this checkpoint is defective, which allows the cells to continue DNA synthesis in the presence of DNA damage, a phenomenon termed radioresistant DNA synthesis. There appear to be two distinct S-phase checkpoints, depending on the type of DNA damage incurred during DNA synthesis. However, both inhibit the initiation of replicons, the structures at which replication occurs (Kastan and Lim, 2000). The first checkpoint involves Cdc25A phosphatase inactivation, which inhibits cyclin E–Cdk2 and causes cell cycle arrest. This mechanism is orchestrated by either an ATR–Chk1-dependent pathway (e.g., by stalled replication forks), involving ATRIP, RPA and the Rad family of proteins (Osborn *et al.*, 2002), or the ATM–Chk2-dependent pathway (Bartek *et al.*, 2004; Bartek and Lukas, 2003; Mailand *et al.*, 2000). The second checkpoint pathway involves ATM-dependent phosphorylation of Nbs1 on serine-343 (Gatei *et al.*, 2000b; Lim *et al.*, 2000) and phosphorylation of cohesin protein SMC1 following IR-induced DSB (Heffernan *et al.*, 2002; Kastan and Bartek, 2004; Shiloh, 2003). Much of the role of Nbs1 during S phase has been deduced by analysing the differences between AT and NBS cells. Zhao *et al.* (2003) showed that ATM complementation in AT cells restored Nbs1 serine-343 phosphorylation after IR. In addition, substitution of Nbs1 serine-343 (and serine-278) site with an alanine residue failed to correct the radioresistant DNA synthesis in S phase when transfected into NBS cells. Similarly, Wu *et al.* (2000) and Lim *et al.* (2000) noticed a slower migration of p95/Nbs1 by SDS gel electrophoresis after irradiation and demonstrated that this effect was due to phosphorylation. Nbs1

phosphorylation is delayed in irradiated AT cells (occurring after 24 h) but is restored to within 30 min following the expression of functional ATM protein.

1.3.4.3 G2/M phase

The final G2/M checkpoint serves to repair DNA damage that occurs during DNA synthesis and prevent the segregation of damaged chromosomes during mitosis (Dasika *et al.*, 1999). The nuclear serine/threonine kinase Chk1 (and to a lesser extent, Chk2) has a major role in the G2/M phase checkpoint by preventing premature mitotic entry following IR (Matsuoka *et al.*, 1998). Chk1 is phosphorylated on serines 345 and 317 by ATM and ATR, respectively. Both Chk1 and Chk2 phosphorylate and inactivate the dual specificity phosphatase Cdc25C that maintains the G2-phase progression by dephosphorylating and activating cyclin B–Cdc2. Cdc25C phosphorylation on serine-216 creates a binding site for the 14–3-3σ protein and Cdc25C–14-3-3σ complex undergoes nuclear export, leading to cytoplasmic sequestration of Cdc25C and thereby activating the G2/M checkpoint (Lopez-Girona *et al.*, 1999). The product of the p53-induced gene, *GADD45*, interferes with cyclin B–Cdc2 association, inhibits Cdc2 kinase activity and leads to cytoplasmic sequestration of cyclin B, thus augmenting G2 arrest (Jin *et al.*, 2002; Zhan *et al.*, 1999).

1.3.5 DNA double strand break repair

In humans, DSB are repaired by homologous recombination (HR), nonhomologous end joining (NHEJ) and single-strand annealing (Khanna and Jackson, 2001). NHEJ is believed to be the dominant process in mammalian cells and occurs throughout the cell cycle, whereas HR usually occurs during the S and G2 phases (Tauchi *et al.*,

2002). During HR, the complementary strand of the homologous chromosome acts as a template for the damaged chromosome and allows error-free repair, thus maintaining genomic integrity (Haber, 2000; Johnson and Jasin, 2001). HR is also regulated during the cell cycle (Valerie and Povirk, 2003). Nonhomologous repair involves excising the damaged DNA and ligating the cut ends of the single-strand DNA (Takata *et al.*, 1998). However, unlike HR, this process is error prone and can lead to deletion of tumour suppressor genes, amplification of oncogenes (by removing inhibitory signals) or translocations that deregulate or alter the functions of proto-oncogenes, thus predisposing to tumorigenesis (Hefferin and Tomkinson, 2005). Defective DNA damage repair mechanisms promote genetic instability, including major chromosomal translocations (Richardson and Jasin, 2000).

The direct involvement of ATM in DNA repair is less well characterised. In response to DSBs, ATM requires to process the DNA lesions resulting in the downstream activation of ATR-Chk1 (Bensimon *et al.*, 2010; Cuadrado *et al.*, 2006; Jazayeri *et al.*, 2006). This modulation may facilitate the cell cycle stage dependent recruitment of the MRN complex and other nucleases to direct cell cycle arrest and DNA repair (Jazayeri *et al.*, 2006; Xu *et al.*, 2002; Yang *et al.*, 2004; Yarden *et al.*, 2002). It may also explain the topography of ATR-Chk1 activation in ATM deficiency following the generation of DNA DSBs (Bekker-Jensen *et al.*, 2006; Byun *et al.*, 2005; Myers and Cortez, 2006).

Other components of the DDR signalling cascade have more fundamental roles in DNA repair 53BP1 and BRCA1 appear to have opposing roles. 53BP1 has an essential role in directing the type of DNA repair that is undertaken. In G1 it prevents

the resection of the damaged ends promoting direct ligation by the NHEJ pathway (Chapman *et al.*, 2012). ATM involvement in DNA repair may also be mediated by Chk2 phosphorylation of BRCA1 on serine-988; BRCA1 is involved in both HR and NHEJ (Burma *et al.*, 2006; Cortez *et al.*, 1999; Gatei *et al.*, 2000a; Zhang *et al.*, 2004). Upon entry into S phase, BRCA1 appears to exclude 53BPI bound complexes from the double strand break thus promoting extensive resection of the damaged ends in preparation for HR. (Escribano-Diaz *et al.*, 2013). A similar re-arrangement of proteins occurs in G2 phase cells whereby BRCA1 displaces 53BP1 facilitating the POH1 dependent removal of RAP80 allowing ubiquitin chain degradation in preparation for DNA end terminal resection and subsequent HR (Kakarougkas *et al.*, 2013).

NBS1 is also as an essential component of HR but not of NHEJ (Tauchi *et al.*, 2002). NHEJ is directed by DNA-PK; however, it has been demonstrated that ATM phosphorylates and may activate Artemis. Artemis is one of the many proteins that is mutated in severe combined immunodeficiency (SCID), which displays defects in DNA repair (Jeggo and Lobrich, 2005).

1.3.6 Apoptosis

Apoptosis or programmed cell death (Kerr *et al.*, 1972) is an evolutionary conserved mechanism that normally occurs during embryo development and in response to cellular stresses (Rich *et al.*, 2000). However, the aberrant activation of this process is also associated with cancer, autoimmune conditions, inflammatory diseases and infections. Apoptosis occurs when DNA repair mechanisms are unable to resolve damaged DNA. DNA damage can activate the extrinsic death receptor pathway

(tumor necrosis factor receptor superfamily member 6, caspases) and/or the intrinsic mitochondrial pathway (B cell lymphoma-2 protein family) (Roos and Kaina, 2006). ATM induces the direct (p53 serine 15) (Shieh *et al.*, 2000) and indirect phosphorylation of p53 (serine 20) and Mdm2, resulting in increased levels of p53 protein (Canman *et al.*, 1998). Increased p53 activation can result in the transcriptional regulation of both anti and pro apoptotic genes with dual roles in promoting DNA repair and delivering apoptosis dependent on the DNA lesion (Roos and Kaina, 2013).

In addition to the established role of ATM-p53 in apoptosis, ATM has been implicated in the *in vivo* activation of the nuclear transcription factor nuclear factor KappaB (NF-κB) an anti-apoptotic mediator (Piret *et al.*, 1999). NF-κB activity is tightly regulated in the cytoplasm by an inhibitor factor κappaB (IκB) that conceals the nuclear localisation signal (Karin and Ben-Neriah, 2000; Molitor *et al.*, 1990). Following the generation of DNA DSB, NF-κB essential modulator (NEMO) is anchored at sites of DSBs promoting ATM dependent phosphorylation and other post translational modifications of NEMO (Huang *et al.*, 2003). The subsequent ATM-NEMO composite relocates to the cytoplasm and activates Inhibitor factor κappaB kinase (IKK) (Brzoska and Szumiel, 2009). IKK phosphorylates IκB identifying IκB for ubiquitinlation and degradation hence, the nuclear localisation signal is revealed and NF-κB translocates to the nucleus (Karin and Ben-Neriah, 2000). The physiological significance of the detailed signalling hierarchy requires to be assessed in the development of human cancers.

The majority of earlier chemotherapeutic drugs have focussed on inducing DNA damage to induce apoptotic pathways/cytotoxic cell death; the realisation that loss of function of p53 occurs in the majority of cancers may limit this approach. An alternative mechanism of cancer therapy involves the induction of permanent growth arrest termed senescence, discussed next.

1.3.7 Senescence

Senescence is defined as an irreversible growth arrest in the G1 cell cycle phase, but not the arrest of cellular/metabolic functions, suppressing cancer development *in vitro*. Senescence can be activated by loss of replicative ability (telomere induced) and stress induced; both forms are characterised by altered cellular morphology, gene expression and activation of the DDR and tumour suppressors (Harley *et al.*, 1990; Schmitt *et al.*, 2007). Stress induced senescence is considered to be the predominant form in cancer robustly stimulated by the p53/p21 and retinoblastoma (Rb) protein pathways (Ben-Porath and Weinberg, 2005). The senescent phenotype requires continuing signalling through the DDR pathways including chromatin alterations and γ-H2AX foci (Bartkova *et al.*, 2006; Passos *et al.*, 2010). Initially described as a barrier to carcinogenesis, senescent cells can also develop a senescent associated secretory phenotype, stimulating the neighbouring matrix and microenvironment to promote neoplastic transformation *in vitro* (Coppe *et al.*, 2010). The induction of cellular senescence following cytotoxic drug administration in cultured cells is an alternative high risk strategy to restrict disease progression (cytostatic therapy) as cells can theoretically re-enter the cell cycle (Saretzki, 2010). The combination of genotoxic therapy to induce premature senescence and abrogation of senescence by

ATM inhibition may improve drug cytotoxicity (Crescenzi *et al.*, 2008) in certain cancers. However, cancer cells are inherently programmed to continually adapt and progress by several mechanisms including the engagement of redundant pathways.

1.3.8 Redundancy

High throughput analyses of cancer models and tissues interrogating cancer addiction to functional pathways have permitted the rational design of specific targets for cancer therapy. Yet, inherent redundancy between these dynamic processes and feedback loops can limit the efficacy of targeted treatment. Targeted therapy can be ineffective for multiple reasons including second mutation in the target, mutations in downstream molecules and up regulation of redundant processes or pathways. This has been elegantly demonstrated in patients with colorectal cancer treated with epidermal growth factor receptor antagonists who can subsequently develop and/or potentiate mutations in downstream genes, *KRAS* and *BRAF*, resulting in therapy resistance (Diaz *et al.*, 2012; Misale *et al.*, 2012).

Similarly, the PIKKs share substrate specificity during DNA damage and repair but are distinct in their response to the type of DNA lesions, activation signals, and kinetics (Culligan *et al.*, 2006; Falck *et al.*, 2005; Helt *et al.*, 2005). ATM primarily responds to DNA double strand breaks and ATR to single stranded DNA coated with replication protein A; however, these DNA lesions have been shown to be interchangeable suggesting redundancy between the kinases (Cimprich and Cortez, 2008; Reaper *et al.*, 2011). The redundancy can exist at multiple levels including the checkpoint kinases 1 and 2 (Bartek and Lukas, 2003; Bekker-Jensen *et al.*, 2006;

Brown and Baltimore, 2003; Shieh *et al.*, 2000) and DNA repair proteins (see section *1.3.5 DNA Repair*).

ATR responds to DSB, although to a lesser extent than ATM, and both ATM and ATR phosphorylate common substrates (Bartek and Lukas, 2003; Brown and Baltimore, 2003; Shiloh, 2003). Overexpression of ATR can partially rescue the phenotype of ATM deficiency (Cliby *et al.*, 1998) and ATR has been shown to be constitutively activated in cells that lack functional ATM (Khanna and Jackson, 2001) serving as a "back-up" pathway functioning in the absence of ATM (Shiloh, 2003). Conversely, ATM does not appear to rescue an ATR deficiency phenotype as demonstrated by the embryonic lethality of ATR null and genotoxic sensitivity of ATR hypomorphic mutations *in vitro* (Brown and Baltimore, 2003; Gamper *et al.*, 2013; Lewis *et al.*, 2005; Nghiem *et al.*, 2001; Wright *et al.*, 1998).

hSMG-1 can also phosphorylate Chk2, H2A and p53 in response to IR; however, detailed analysis this effect remains under investigation (Abraham, 2004).

1.4 DNA Damage Response and Cancer

1.4.1 Cancer Susceptibility and DNA damage response

Patients with the related inherited conditions, AT, ATLD and NBS, are all susceptible to cancer development (Jaspers *et al.*, 1988; Kastan and Bartek, 2004). Inactivating *ATM* mutations have also been reported in a selection of sporadic malignancies (Shiloh, 2003). Promoter hypermethylation leads to gene silencing and has been seen in key genes (*APC, ATM* and those related to DNA MMR) implicated in colon cancer at the adenoma stage (Bai *et al.*, 2004). In cases of *ATM*

hypermethylation, there was an association with reduced protein expression. Female *ATM* heterozygotes have an increased risk of breast cancer (Bernstein *et al.*, 2002; Heikkinen *et al.*, 2005; Renwick *et al.*, 2006). One per cent of the general population are *ATM* heterozygotes, and these individuals have a 3–5-fold increased risk of developing cancer if they have a blood relative with ataxia-telangiectasia (Swift *et al.*, 1991). In addition; downstream targets of ATM such as Chk2 and p53 are implicated in cancer development (Bartkova *et al.*, 2004; Bartkova *et al.*, 2005b). *CHEK2* mutations have been reported in a subset of families diagnosed with Li-Fraumeni syndrome without concomitant *TP53* mutations (Lee *et al.*, 2001). Mutations within the noncoding region of the *MRE11A* gene have been reported in colorectal (Giannini *et al.*, 2002), endometrial, ovarian (Giannini *et al.*, 2004), stomach (Ottini *et al.*, 2004) and lymphoid malignancies (Ham *et al.*, 2006). This relationship suggests that the DDR protects against the development of cancer.

1.4.2 DNA damage response biomarkers

The functional assessment of the DDR in cancer is limited by the ability to study these dynamic processes during cancer development and treatment. Therefore, biomarkers that can objectively measure the biological processes (BDWG, 2001) in the DDR are urgently required. One such method may be the analysis of the downstream signalling molecules using immunohistochemistry in normal and cancer specimens. A large study evaluated the expression and activation of both ATM and Chk2 in normal tissues (Bartkova *et al.*, 2005a). Only two tissues demonstrated significant ATM and Chk2 phosphorylation: the bone marrow and testis, both sites of V(D)J recombination. Gorgoulis *et al.* (2005) determined activation of the DDR pathway in human lung hyperplasia and adjacent normal tissue via examining γ-

H2AX and Chk2 phosphorylation, 53BP1 localisation and p53 protein levels. They reported that the DDR pathway was not activated in normal tissue but was activated in hyperplastic lung tissue, which also showed evidence of apoptosis. Similarly, the pathway was activated in dysplastic and cancerous tissue, although with less apoptosis compared with hyperplastic lung tissue. The apparent reduction in apoptosis was thought to represent nonfunctional p53 (mutant p53 or reduced wild-type p53 protein expression). Bartkova *et al.* (2004) used a similar approach in human urinary bladder cancer, premalignant bladder cancer and normal tissue. They demonstrated activation of the ATM pathway (via ATM, Chk2, γ-H2AX and p53 phosphorylation) in preinvasive cancers of the bladder, breast, colon and lung (Bartkova *et al.*, 2005b), suggesting that the activation of the pathway limits the progression of lesions and prevents malignant transformation. Moreover, ATM and Chk2 activation preceded *TP53* mutations and genetic instability was associated with ATM and Chk2 defects (Bartkova *et al.*, 2005b). A subset of surgically resected breast, lung (DiTullio *et al.*, 2002) and bladder (Bartkova *et al.*, 2004) cancers from untreated patients showed Chk2 phosphorylation in the absence of DNA damage. However, in approximately 10% of bladder cancer patients in the Bartkova study, an absence of Chk2 phosphorylation was also observed, thus linking Chk2 inactivation to bladder cancer invasion. Activation of this pathway may be tissue specific, as Bartkova *et al.* (2005a) demonstrated a reduced degree of ATM–Chk2 pathway activation in testicular germ cell tumours. Activation of DDR in the early stages of prostate cancer has also been identified. Thirty-five primary prostate cancers were analysed immunohistochemically and increased levels of phosphorylated ATM and Chk2 were demonstrated in preinvasive cancers (intraepithelial neoplasias) compared

with normal prostate tissue and carcinomas (Fan *et al.*, 2006). Nuciforo *et al.* (2007) also confirmed these findings in studies into lung cancer development: phosphorylated forms of ATM and Chk2 were present in inflamed tissue and preinvasive lung specimens, but gradually diminished as cancers progressed.

It is not known why the ATM-dependent DDR pathway is activated in premalignant lesions and lost during cancer development. Current hypotheses suggest that it may be a consequence of (1) replication stress in rapidly growing cancer cells, (2) telomere dysfunction or (3) a physiological response that acts as an anti-cancer barrier (Bartkova *et al.*, 2005b; Gorgoulis *et al.*, 2005). Cells with constitutively activated DDR pathways would be expected to undergo prolonged cell cycle arrest or cellular senescence. It is speculated that activation of the DDR pathway in some cancers may select for mutations in genes involved in DNA damage cell cycle checkpoints, DNA repair, cellular senescence and apoptosis, thus driving cancer progression (Bartkova *et al.*, 2004; DiTullio *et al.*, 2002). Zoppoli *et al.* (2012) analysed the National Cancer Institute panel of 60 cell lines and concluded that Chk2 threonine-68 phosphorylation was only present in cancer cell lines with a concomitant *TP53* mutation. As expected, increased basal Chk2 phosphorylation also correlated with an abnormal number of chromosomal arrangements (i.e., instability) and was associated with downregulation of DNA repair proteins. This was interpreted as reflecting an activated DDR when DNA repair pathways are compromised, presumably due to either an increased burden of DNA damage or a compensatory increase in parallel redundant DNA repair pathways. In breast cancers, mutant *TP53* status appears to be associated with an intact ATM signal transduction pathway (but without evidence for activation) and wild-type *TP53* is associated with

a defective ATM pathway (Craig and Hupp, 2004). The inverse correlation between ATM functionality and *TP53* status suggests that the progression of these cancers is independent of the signals for cell cycle arrest via the DDR pathway, but may also indicate the presence of functional prosurvival repair pathways that are amenable to therapeutic manipulation. As a model to study the DDR process in detail, colorectal cancer has a defined sequence of progression from adenoma to carcinoma, including alterations in the DDR and also has a particular type involving deficiencies in the DNA mismatch repair system. (Bartkova *et al.*, 2005b).

1.5 DNA Damage Response in Colorectal Cancer

1.5.1 DDR & molecular phenotype of colorectal cancer

Colorectal cancer is a multistep process, showing progression from adenoma to carcinoma by the accumulation of defects in genes that regulate cell survival and apoptosis (Figure 1.3) (Lane and Crawford, 1979). Additionally, it is a well characterised model to study the DDR as multiple important DDR components are deregulated in isolation during the development of colorectal cancer. The proportion of colorectal cancers with intact and functional DDR pathways is unknown. Historically, there are two main types of genetic aberrations in colorectal cancer: chromosomal instability (referring to the gross rearrangement of whole chromosomes), which is commonest in sporadic cancers; and microsatellite instability (MSI) that accounts for over 90% of hereditary nonpolyposis colon cancers (HNPCC) (Lengauer *et al.*, 1998; Wheeler *et al.*, 2000) and up to 15% of sporadic tumours (Lynch *et al.*, 1993).

Chromosomal instability is a prominent feature of sporadic cancers, in which mutations in several genes, including *APC*, *KRAS* and *TP53*, lead to the development of invasive cancer (Li *et al.*, 2003). Moreover, replication stress associated chromosomal instability resulted in a positive feedback loop increasing the number of chromosomal instability lesions (Burrell *et al.*, 2013). *Loss of heterozygosity i*n the short arm of chromosome 11 (Connolly *et al.*, 1999; Konstantinova *et al.*, 1991), as well as in chromosome 17p and 17q21, has frequently been reported in colon cancer. This locus contains genes encoding *ATM* (Rasio *et al.*, 1995; Sugai *et al.*, 2001; Uhrhammer *et al.*, 1999), *CHEK1* (Sanchez *et al.*, 1997), *TP53* (Lane and Crawford, 1979) and *BRCA1* (Garcia *et al.*, 2003) respectively that are involved in the DDR. Promoter hypermethylation and subsequent reduced ATM protein expression have been reported in a series of colorectal adenomas and carcinomas (Bai *et al.*, 2004). Furthermore, chromosomal instability is a key feature of the AT phenotype (Shiloh, 2003). A comprehensive analysis of the genetic mutations that trigger chromosomal instability showed that *MRE11A* was the most frequently mutated gene in chromosomally unstable colorectal cancers (Wang *et al.*, 2004b). Defects in the double-strand break repair pathway are associated with chromosomal instability in colorectal cancer (Wang *et al.*, 2004b).

Microsatellite instability (MSI) occurs in up to 15% of sporadic colorectal cancers but in >90% of hereditary nonpolyposis colon cancers (Ionov *et al.*, 1993; Khanna and Jackson, 2001; Lengauer *et al.*, 1998; Thibodeau *et al.*, 1993; Wheeler *et al.*, 2000; Yamamoto *et al.*, 2002). Microsatellites are mononucleotide repeat sequences dispersed throughout noncoding regions of the genome. Their integrity is maintained by the MMR system that recognises and repairs mismatched and unpaired bases that

occur through DNA replication errors and other processes (Jiricny and Nystrom-Lahti, 2000). Mutations within genes of the MMR machinery underlie the cancer predisposition in HNPCC (Markowitz, 2000). As the defective MMR machinery is unable to correct replication errors, mutations accumulate throughout the whole genome. The most commonly affected MMR genes in HNPCC are *MLH1*, *MSH2*, *MSH6*, *PMS1* and *PMS2* (in reducing frequency) (Akiyama *et al.*, 1997; Boyer *et al.*, 1995; Fishel *et al.*, 1993; Lindblom *et al.*, 1993; Miyaki *et al.*, 1997; Nicolaides *et al.*, 1994; Ponz de Leon *et al.*, 1999; Thibodeau *et al.*, 1996). Hypermethylation of the *MLH1* promoter underlies the MSI phenotype seen in sporadic colorectal cancers (Cunningham *et al.*, 1998; Thibodeau *et al.*, 1998) . A panel of five microsatellite markers (three dinucleotide markers D2S123, D5S346, D17S250 and two mononucleotide markers BAT25, BAT26, known as the Bethesda panel) are commonly used to assess for MSI (Boland *et al.*, 1998). 'MSI high' cancers are defined as cancers containing MSI in >30% of the standard microsatellite panel; 'MSI low' cancers are defined as containing MSI in <30% of the standard panel and 'Microsatellite stable (MSS)' cancers are defined as those containing no alterations in the standard panel. Microsatellite instability can also be inferred by a lack of MMR protein expression by immunohistochemistry (IHC) analysis. In addition to mutations that occur in noncoding microsatellite sequences, mutations in genomic DNA can also promote cancer progression. Ejima *et al.* (2000) have proposed that the shortening of intronic mononucleotide repeat sequences within the *ATM* gene is a feature of MSI, as it occurs in colon cancer cell lines with MSI. Gianni *et al.* (2004) reported that mutations within the polythymine repeat sequence in intron 4 of the *MRE11A* gene resulted in a truncated protein with reduced activity that was present

only in colon cancer cell lines and primary cancers with the MSI phenotype. The MSI phenotype is not restricted to colorectal cancers but has also been demonstrated in gastric cancers with frameshift mutations in key DNA repair genes such as *ATR, BRCA1* and *RAD50* (Li *et al.*, 2003).

In an attempt to understand the functional consequence of the DDR Bartkova *et al* (2004) demonstrated activation of the ATM pathway in preinvasive colon cancer suggesting the DDR may limit the progression of lesions and prevent malignant transformation. This group also demonstrated that the DDR pathway appeared to be downregulated when invasive cancer had developed (Bartkova *et al.*, 2005b). In a more recent attempt Stawinska *et al* (2010) reported an increased Chk2 threonine 68 phosphorylation staining pattern accompanied tumour invasion to lymph nodes indicating that an activated pathway was unable to prevent cancer progression or reflects an increased burden of DNA damage and repair.

Grabsch *et al.* (2006) showed that ATM or BRCA1 protein expression predicted the survival of colorectal cancer patients and that low ATM expression was associated with loss of MLH1 and MSH2 a feature of MSI phenotype. Conversely, reduced ATM expression was an independent marker of poor disease-free survival in colorectal cancer with a hazard ratio of 1.67 (95% CI 1.11-2.50, p=0.015) suggesting that downregulation of the DDR was associated with cancer progression (Beggs *et al.*, 2010).

Currently, there is a lack of data available to determine how a deregulated DDR pathway modulates cancer progression, treatment response and ultimately survival.

1.5.2 Current treatment strategies for colorectal cancer

Current treatment regimens for colorectal cancer are dictated by the site and location of disease either local or advanced (metastatic). Curative surgery is the most appropriate therapy (Table 6.2); preoperative chemoradiotherapy is considered for patients with high risk locally advanced cancer (NICECG131, 2011). Adjuvant therapy is recommended for stage III colon cancer to reduce local and metastatic recurrence and control disease. This can involve first line therapy with capecitabine monotherapy or oxaliplatin in combination with 5-fluorouracil and folinic acid. First line chemotherapy for patients with advanced (metastatic) disease may include combinations of oxaliplatin or irinotecan with 5-flourouracil and folinic acid or capecitabine or irinotecan as a single agent therapy. The particular combination and sequence of therapy will be guided by the side effect profile and patient acceptability. Raltitrexed is an alternative in patients with advanced colorectal cancer who are unable to tolerate 5-fluorouracil based regimens. Biological agents (cetuximab, bevacizumab and panitumumab) are currently not recommended for patients with advanced and metastatic colorectal cancer after failure to control disease with first line therapy (NICETA242, 2012); but may be available on a compassionate basis or as part of large multicentre trials.

1.5.3 Role of DNA damage response and therapy in colorectal cancer

The role of the DDR and current colorectal cancer therapy strategies has not been studied in a systematic manner. However, there are isolated reports evaluating the effect of the DDR in both *in vivo* and *in vitro* models.

The DNA mismatch repair system appears to be implicated in the processing of low dose 5-flourouracil (clinically relevant) induced DNA damage. MMR deficient cell lines (HCT 116 and HCT15) did not activate the ATM dependent signalling cascade compared with the MMR proficient HT29 cell line when treated with a bolus of 5-flourouracil; this response may also be modulated by *TP53* status (Adamsen *et al.*, 2011). MMR deficiency is considered an inherent mechanism of cancer chemoresistance due to the inability to recognise and repair 5-flourouracil-DNA lesions (Li *et al.*, 2009). A more recent Australian study analysed 882 patients with colorectal cancer and reported a higher burden of CIN as opposed to single gene mutations were associated with progressively poorer disease free survival (Mouradov *et al.*, 2010).

1.6 Therapeutic Strategies Targeting DNA Damage Repair and DNA Repair

The ultimate goal of cancer chemotherapy is to create sufficient DNA damage to overwhelm the dividing cell, thus directing it towards cell death. Constitutively activated DDR and repair pathways may undermine the efficacy of such approaches. It has been suggested that chemotherapeutic drugs that produce DSB are ineffective in this type of cancer because of the ability of ATM pathway to sense and repair the resulting DNA damage (Madhusudan and Middleton, 2005). MSI cell lines that harboured multiple heterozygous mutations in DNA repair genes are hypersensitive

to the effect of DNA DSB-inducing chemotherapy (Li *et al.*, 2004). Therefore, the DNA DSB response pathway is an attractive therapeutic target; inhibition of this DDR pathway may overcome resistance to current cytotoxics and potentiate the effects of radiotherapy (Martin, 2001).

1.6.1 Synthetic lethality

Cancer therapy is inherently limited by the narrow therapeutic index and toxicity that accumulates in normal non-cancerous cells. Exploiting cancer specific addictions or deficiencies can limit the toxicity to normal cells and improve the efficacy of treatment; this is the concept of synthetic lethality (Hartwell *et al.*, 1997; Kamb, 2003). Synthetic lethality was initially used to describe two genetic mutations which singularly are viable but together induce death (Guarente, 1993). This concept is discussed next, in more detail with specific DDR inhibitors.

1.6.2 ATM inhibitors

The AT phenotype demonstrates marked sensitivity to IR; as such, inhibition of ATM may improve the efficacy of current cancer treatments. Caffeine and wortmannin are nonspecific PIKK inhibitors; caffeine primarily inhibits ATM (Sarkaria *et al.*, 1999; Zhou and Elledge, 2000) and ATR, and wortmannin inhibits ATM, DNA-PK and ATR (Sarkaria *et al.*, 1998). Hickson *et al.* (2004) identified a specific small molecule ATM inhibitor, KU-55933, which sensitises U20S cells to camptothecin (a topoisomerase I inhibitor), doxorubicin, etoposide (a topoisomerase II inhibitor) and IR. The inhibitor had no appreciable effect on sensitivity to alkylating (chlorambucil, cisplatin and melphalan,) and cross-linking (mitomycin B)

agents. There was a reduction in phosphorylation of Chk1, γ-H2AX, Nbs1 and SMC1 (ATM targets) after IR in the presence of KU-55933 and cells accumulated in the G2/M phase, similar to AT cells. In DNA-PK-deficient cells, the addition of KU-55933 sensitised cells to the effects of etoposide. However, AT cells showed no significant increase in radiosensitivity when exposed to ATM inhibitor, suggesting that ATM expression and activation is necessary for ATM inhibitor activity. Using the same compound, Cowell *et al.* (2005) demonstrated a reduction in breast cancer cell survival (using the colony formation assay) after IR therapy (1–5 Gy) in cells pretreated with KU-55933. As an alternative method of silencing ATM by the use of retroviral vectors expressing anti-*ATM* small hairpin RNAs Mukhopadhyay *et al.* (2005) reported increased sensitivity of mutant p53 prostate cancer cells to the DNA damaging agent doxorubicin. Disruption of the G2 checkpoint by ATM inhibition is thought to render cells more sensitive to DNA damage (Eastman, 2004; Guha *et al.*, 2000; Uziel *et al.*, 2003). Importantly, reducing *ATM* gene expression in normal human fibroblasts did not increase doxorubicin cytotoxicity. Antisense gene therapy and small interference RNA-mediated gene silencing has also been successfully used to increase radiosensitivity in brain tumour cell lines (Guha *et al.*, 2000) and in human cervical cancer cells and prostate cells (Collis *et al.*, 2003; Li *et al.*, 2006), respectively.

Jiang *et al.* (2009) proposed that a mutant p53 status may determine the efficacy of ATM inhibitor therapy. Cancers that are mutated for *TP53* are sensitive to ATM inhibitors, presumably because the DNA damaged-induced S and G2 checkpoints are abrogated, thus directing cells towards mitotic catastrophe. This would support the observation by Zoppoli that cancer cells are dependent on a chronically activated

ATM-directed DDR in the presence of *TP53* mutations and DNA repair defects; downregulation of ATM or Chk2 in these cells may therefore potentiate cancer therapy. Inhibition of ATM in a wild-type p53 background appears to promote cell survival, perhaps through ATM-independent cell cycle arrest or inefficient ATM–Chk2–p53 apoptotic signalling. Cancers that retain wild-type p53 status (and thus the capacity to induce apoptosis) may be under less selective pressure, and abrogating the (functionally) normal ATM–Chk2 DDR axis in this circumstance may promote genetic instability and thus cancer progression. However, it can be difficult to ascertain in which order the constraining mechanisms were circumvented in these cancers and therefore to identify the appropriate stage of cancer development to target DDR.

Additionally, if the cancer is defective in some checkpoint controls and/or repair mechanisms; inhibiting the remainder may be sufficient to trigger the apoptotic machinery or promote catastrophic mitosis. This could also increase the specificity of treatment for cancer cells by reducing the cytotoxic effect on normal tissues. One such example is the autosomal recessive disorder Fanconi anaemia (FA), which manifests as a cellular defect in DNA repair that results in hypersensitivity to DNA cross-linking agents *in vitro* and promotes the development of haematological cancers *in vivo*. ATM was reported to be constitutively activated in FA-derived cell lines, suggesting that the ATM pathway is stimulated by either DNA damage or defective DNA repair. Short-term inhibition of ATM function in FA-derived cells results in apoptotic cell death (Annexin V assay) and a reduction in colony formation, 47.4% +/- 4.2%, at 14 days, in the absence of additional exogenous DNA

damage. In the FA complemented cells, ATM inhibition did not increase apoptosis nor reduce colony formation, 94.% =/- 3.7, demonstrating the selectivity of such an approach for cancer cells (Kennedy *et al.*, 2007).

1.6.3 DNA repair inhibitors

Accurate DNA repair is an essential mechanism for maintaining genome fidelity. Cancers that are inherently defective in a particular DNA repair protein/pathway can be specifically targeted by inhibiting a parallel pathway (Figure 1.4). Noncancerous cells are protected if the DNA repair defect is acquired and not genetically inherited. An example is the use of PARP [poly (ADP-ribose) polymerase] inhibitors in cancers that are deficient in HR.

1.6.3.1 PARP inhibitors

PARP is a nuclear protein that cleaves NAD^+ to nicotinamide and ADP-ribose, thus forming negatively charged long-branched polymers on glutamic residues on itself and on target proteins. PARP is involved in processing DNA single-strand breaks created during base excision repair of DNA adducts and in NHEJ, where it modifies the activity of DNA-PK (Veuger *et al.*, 2004). PARP inhibition in combination with DNA damaging agents might potentiate the cytotoxicity of anti-cancer agents (Bryant and Helleday, 2004; Haince *et al.*, 2005). Bryant and Helleday (2006) demonstrated that AT cells are sensitive to PARP inhibition and that, conversely, PARP-deficient cells are sensitive to ATM inhibition. PARP inhibition allows single-strand breaks to persist; that if these are formed during replication, this may lead to the collapse of replication forks into DSB. DSB are repaired by HR during replication, and inhibiting critical components of this pathway may result in DNA

defects being repaired by NHEJ (which is error prone) or in cell cycle arrest or apoptosis. The inability to activate the DNA repair process via ATM (required for both HR and NHEJ) is thought to represent the detrimental lesion in both scenarios. Taking this concept further, they demonstrated that *BRCA1*$^{-/-}$ cells defective in HR are highly sensitive to PARP inhibition, represented by a reduction in the cloning efficiency of cultured cells (Bryant *et al.*, 2005). Similarly, Farmer *et al.* (2005) proposed that cancer cells which are defective in HR (*BRCA1*$^{-/-}$ and *BRCA2*$^{-/-}$) can be arrested at the G2/M phase (and then undergo apoptosis) if the single-strand break repair protein, PARP, is inhibited by small interfering RNA (siRNA). A reduction in cell survival has been reported following PARP inhibition combined with either inhibition of components of the DDR pathway (ATM, ATR, Chk1, Chk2 and Nbs1) or inhibition of proteins integral to HR repair (McCabe *et al.*, 2006).

Selective targeting of cancer cells by taking advantage of somatic mutations in tumour cells is an attractive concept and could create a significant therapeutic index for ATM and PARP inhibitors. However, to date, no criteria have been established that allow the rational selection of human colorectal cancers for treatment using this novel approach. Similarly, no pharmacodynamic or therapeutic endpoint has been developed to assess the efficacy of small molecule inhibitors that inhibit the DDR and repair pathways.

1.7 Aims

DNA damage response and repair pathways are frequently disrupted during cancer development resulting in the loss of DNA damage induced checkpoint controls, which promote genetic instability and defects in executing apoptosis. Constitutive activation of the ATM dependent DDR has been reported in several human cancers (Bartkova *et al.*, 2005b).

My hypothesis is that constitutive activation of the ATM dependent DNA damage response, when present in cancer, represents a deregulated pathway as the cancer has developed and/or progressed despite the active signalling network. In this situation, use of an ATM inhibitor may not potentiate the cytotoxicity of chemoradiotherapy. The overall aim of this thesis was to develop a framework for the rational use of ATM inhibitors using colorectal cancer as a model. In order to investigate this it is important to;

- determine the proportion of sporadic human (colorectal) cancers that demonstrates constitutive activation of the ATM-dependent DDR using tissue microarray technology.
- determine whether a constitutively activated DDR represents a functional DDR pathway.
- ascertain the efficacy of ATM inhibitor therapy in the presence of a constitutively activated DDR pathway.
- create a model for the rational use of ATM inhibitor therapy.

These aims are important to allow selection of the patients who will benefit from the use of ATM inhibitors in combination with current treatment modalities.

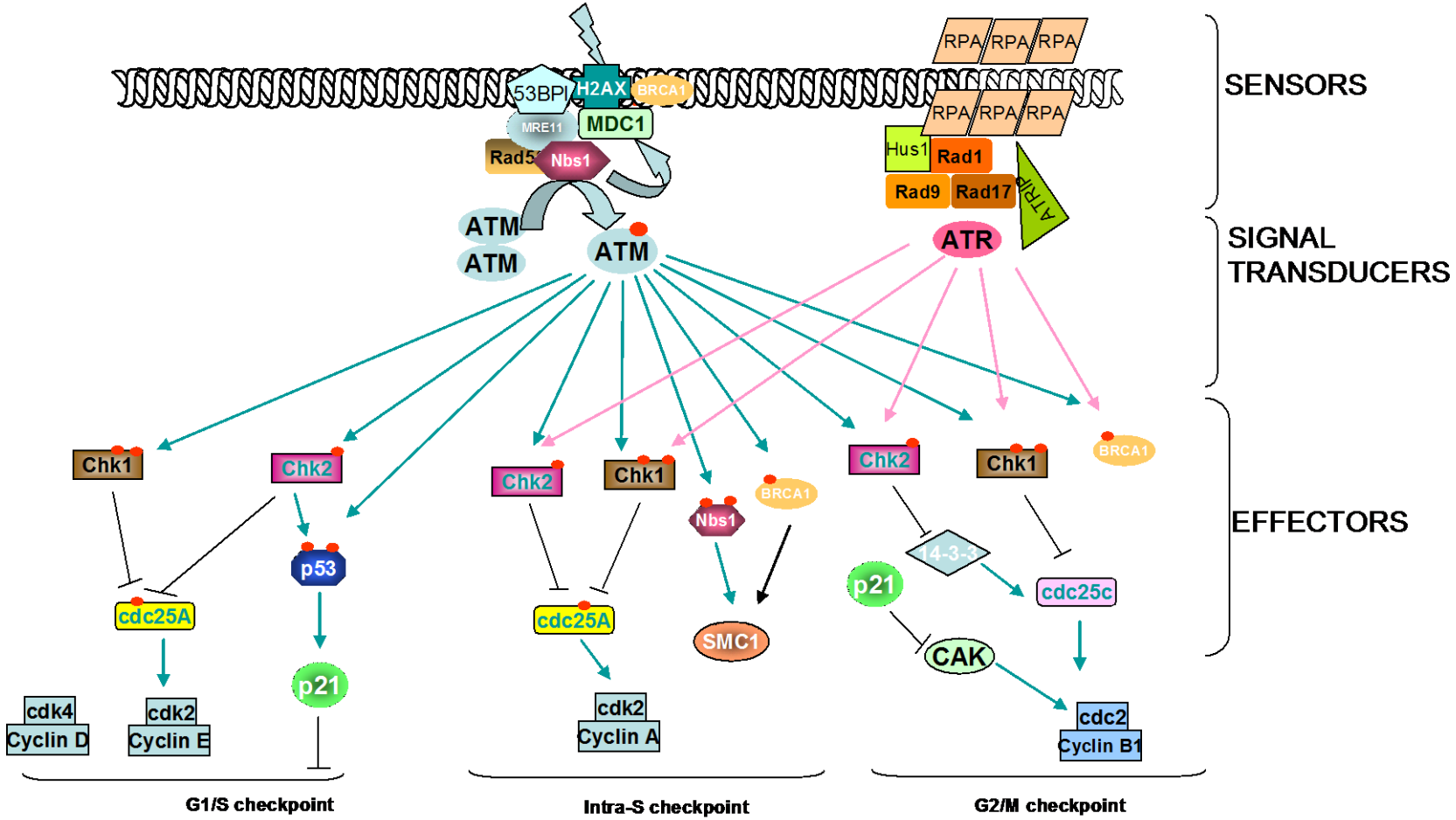

Figure 1.1. DNA damage response to double-strand breaks.

Double-strand breaks are sensed by an assembly of protein molecules which induce the correct localisation and activation of ATM, the main transducer molecule. ATM phosphorylation of substrates leads to the downstream activation of proteins involved in cell cycle arrest, DNA repair, apoptosis and cellular senescence. ATR is also activated during DNA double strand breaks. Red dots represent phosphorylation sites. This figure template kindly was provided by Dr Sylvie Guichard and modified by Shahida Din.

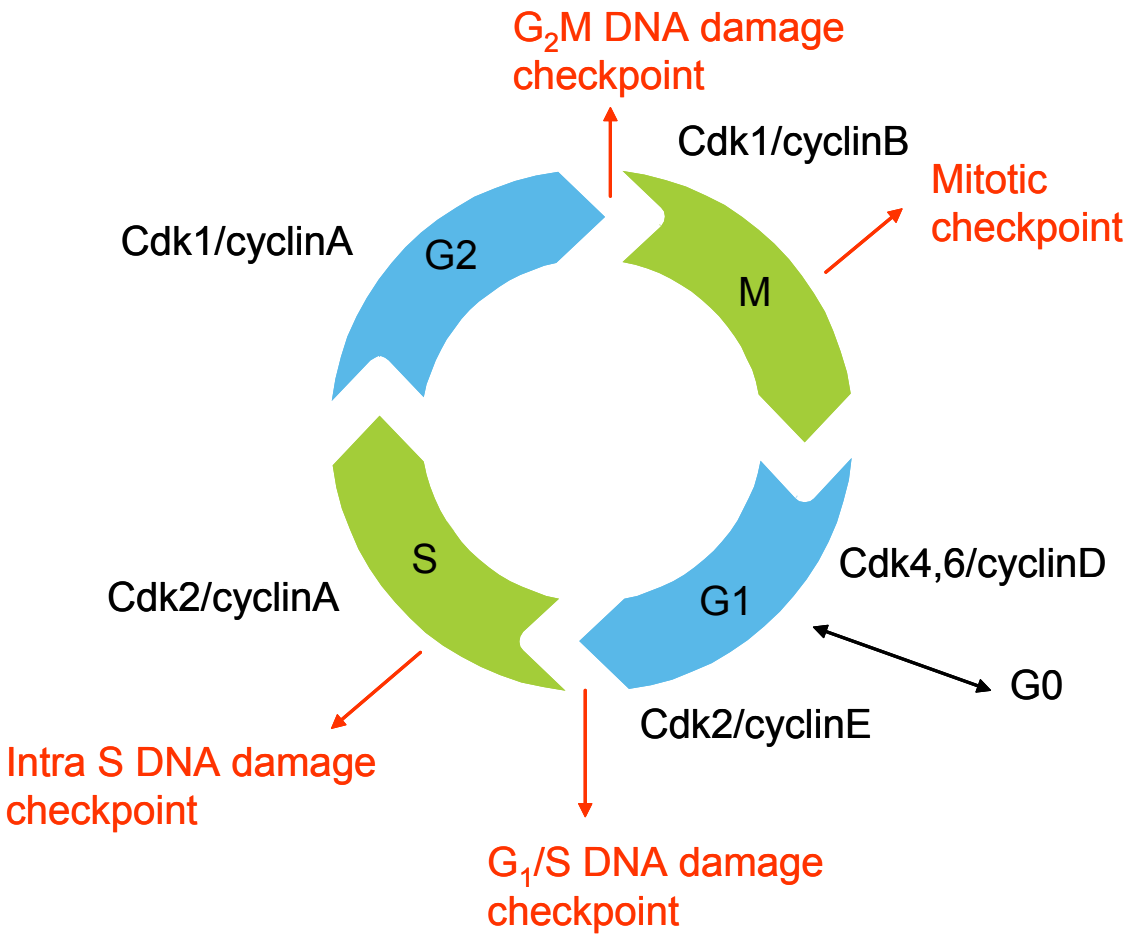

Figure 1. 2 Cell Cycle, cdk/cyclins and DNA damage induced checkpoints.

Specific cdk/cyclin complexes regulate passage through the cell cycle at G1 (Gap 1); S (S phase), G2 (Gap 2) and M (Mitosis) phases.

If conditions are unfavourable for cell division in G1 then cells can enter a reversible G0 phase.

The DNA damage and mitotic checkpoints are indicated in red.

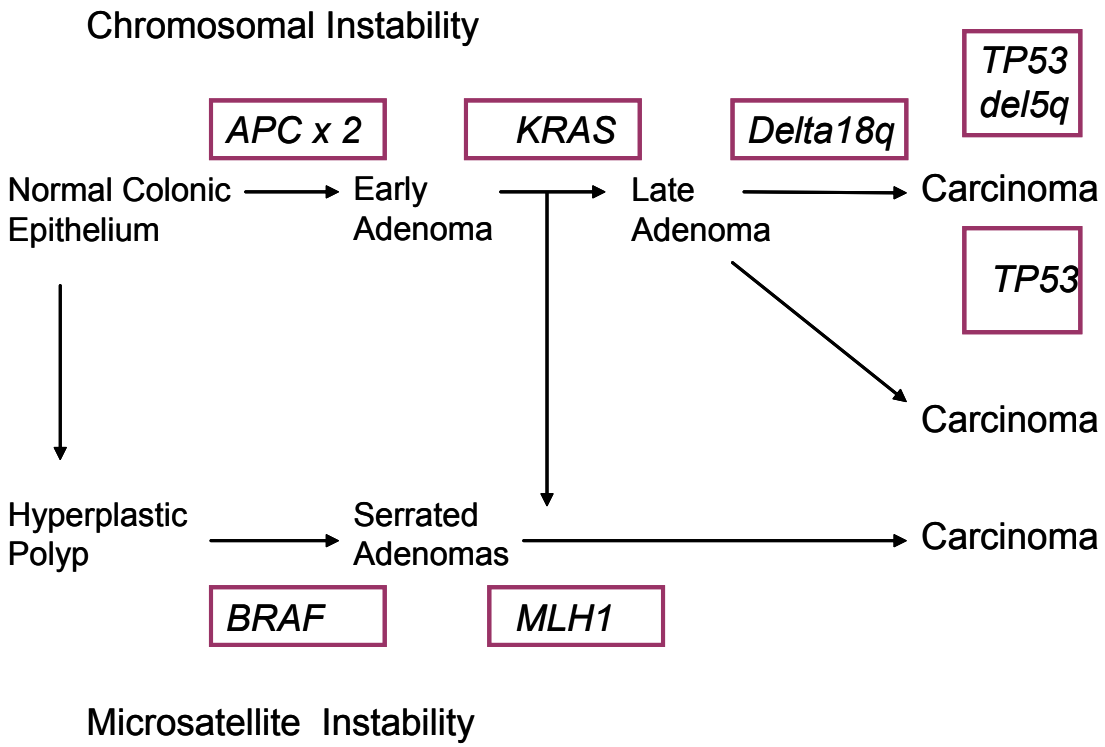

Figure 1.3. Multistep progression of sporadic colorectal cancer.

Chromosomal instability occurs in up to 85% of sporadic colorectal cancers and sequential gene inactivation (purple box) promotes cancer progression. Microsatellite instable cancers also demonstrate sequential gene inactivation especially hypermethylation of the *MLH1* (Mut L homologue) promoter. Adenomatous polyposis coli, APC; proto-oncogene B-Raf, BRAF; proto-oncogene KRAS.

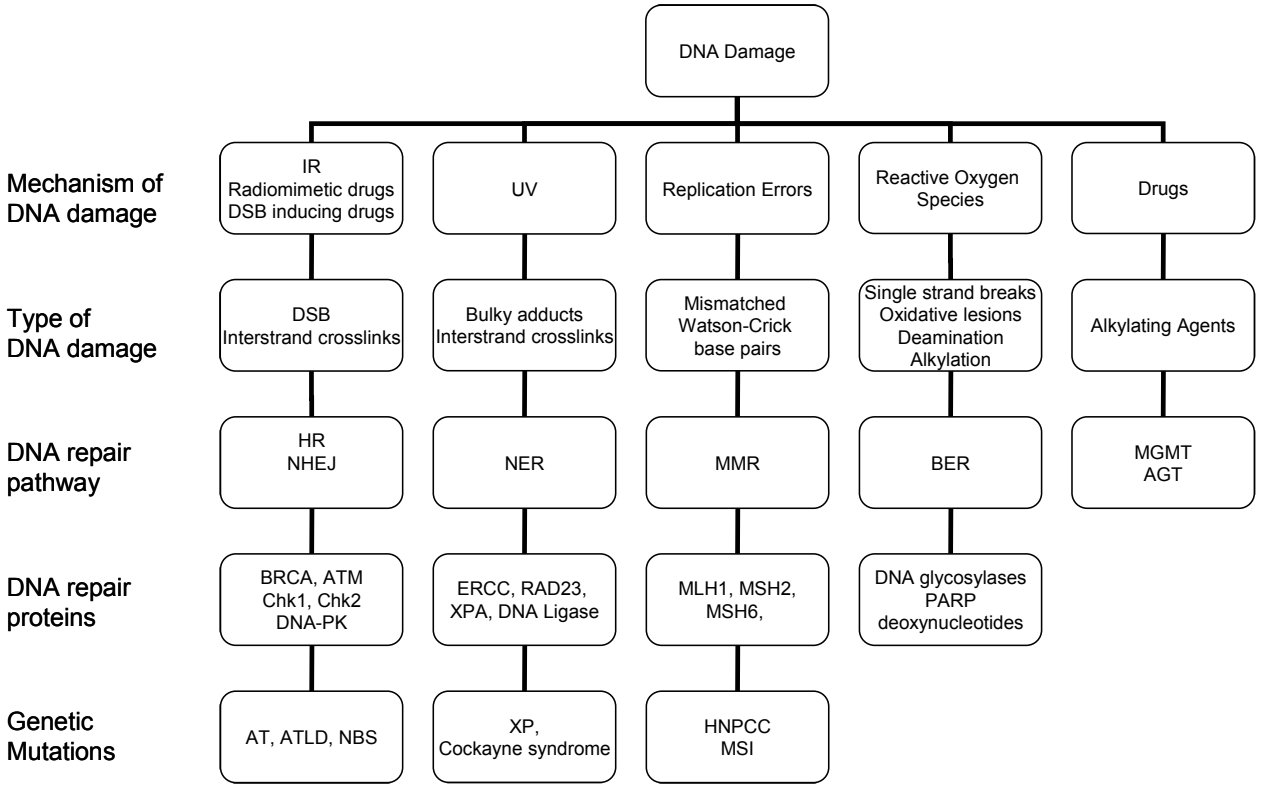

Figure 1.4. DNA Repair Pathways.

(Opposite page for legend details)

Chapter 2. Materials & Methods

2.1 General Reagents

Tissue culture media and supplements were purchased from Invitrogen. All chemicals and reagents were purchased from Sigma and BDH unless otherwise stated.

2.2 Consumables

Tissue culture and other general use plastic ware were purchased from TPP or Starlabs unless otherwise stated.

2.3 Cell Culture

2.3.1 Human cell lines

Colon cancer cell lines were obtained from American Type Culture Collection (Rockville, MD, USA) and European Collection of Cell Cultures (Salisbury, UK); HCT116, HCT15, HCT-8, HT29, SW-620, SW480. p53-null and p21-null HCT116 cells generated by targeted homologous recombination (Bunz *et al.*, 1998) were a gift from Professor Vogelstein (John Hopkins University, U.S.A.) U-20S human osteosarcoma cell line was obtained from Cancer Research United Kingdom (CRUK) research services (London UK). AT fibroblasts GM09607 were obtained from the Coriell Institute (Camden, New Jersey, USA). The p53 and mismatch repair mutational status of the cell lines is described in Table 6.3.

2.3.2 Recovery of frozen cells and storage

To thaw cell lines for culture, aliquots of cells stored in CryoTube™ vials were thawed rapidly with agitation in a 37°C water bath. The cell suspensions were transferred to a 10 cm universal tube with 10 ml of appropriate media (see below) supplemented with 10 % (w/v) foetal calf serum. The cell pellet was collected by centrifugal force of 1200 rpm at room temperature for 2 min and dispersed into 10 ml of fresh culture media into a 25 cm^2 tissue culture flask. When storage of cell stocks was necessary this was undertaken by collecting the cells as for subculturing (see below), transferring the pellet into storage medium (90 % foetal calf serum and 10 % dimethyl sulfoxide (DMSO)) into CryoTube™. This was snap frozen in liquid nitrogen and maintained in nitrogen storage tanks.

2.3.3 Cell culture maintenance

Unless stated, all media and supplements were heated to 37°C in a bench top water bath. Colon cancer cell lines were grown as monolayer cultures in 75 cm^2 tissue culture flasks maintained in Roswell Park Memorial Institute (RPMI) 1640 media containing 2 mM glutamine, 5 % foetal calf serum (Harlan) and 1 % penicillin/streptomycin. U-20S and GM09607 were grown in Dulbecco's Modified Eagle Medium (1 % w/v L-glutamine) supplemented with 100 units/ml penicillin G, 100 µg/ml streptomycin and 10 % foetal calf serum (Harlan). Cells were maintained at 37°C in the presence of 5 % CO_2 in a humidified atmosphere in Hera CO_2 incubators and regularly checked for mycoplasma contamination (Venor®*GEM* Mycoplasma PCR Detection Kit, Cambio Ltd, Cambridge,UK) and were negative at all times during the period of study.

2.3.4 Sub-culturing

Cells were cultured in 75 cm^2 tissue culture flasks with 12 ml of media; this was replaced every 48 h. When cells reached a confluency of 70–80 % medium was aspirated off and cells were washed in phosphate-buffered saline (PBS). The PBS was aspirated and the cells were incubated at 37°C in 2 ml of trypsin (0.05% trypsin / 0.02 % ethylenediaminetetraacetic acid (EDTA)) for 2–3 min. Once the cells were lifting off when gently tapped the trypsin was neutralised with 5 ml of culture media and single cell suspensions were created by passing through a Pasteur pipette. The cell suspension was transferred to a 10 ml centrifuge tube and pelleted at 1200 rpm for 2 min. The solution was removed and the pelleted cells were washed in PBS, centrifuged again for 2 min at 1200 rpm. The washed pellet was resuspended into 10 ml of media and cells were counted on a Coulter Counter. Cells were subcultured at a density of 2×10^6 cells/ml.

2.3.5 Cell harvest for protein extraction

Cells were collected by removing old culture media and washing twice with ice cold PBS. Adherent cells were removed from the plastic surface in 5 ml of ice cold PBS using a cell-scraper; the resultant suspension was collected in a 10 ml centrifuge tube on ice and pelleted at 2000 rpm for 4 min at 4°C in a bench top centrifuge. All of the PBS was aspirated off and the pellets were subsequently frozen in liquid nitrogen and stored at – 70°C until required.

2.4 Manipulation of Cell Lines

2.4.1 Ionising radiation treatment

Cell lines were subcultured in 10 cm Petri dishes or 6-well plates at an initial density of 1.5–1.7 × 10^6 and 1 × 10^6 cells, respectively. Cells were irradiated with overlying fresh medium (8 mls/10 cm dishes and 2 mls/well/6well plate) for 2 Gray (Gy)/min at 120 kVP using a Faxitron X-ray source (Unit 43855D Faxitron X-ray Corporation) to induce DNA damage and harvested at the indicated time points. Control cells were mock irradiated. Doses of 5Gy had demonstrated a robust activation of the DDR in HCT 116 cell lines in preliminary experiments (data not shown) and were used in the majority of the studies. A dose of 20Gy was used in Chapter 6 to overcome any inherent ability of the different cell lines to induce the DDR at low doses (Takemura *et al.*, 2006).

2.4.2 Ultraviolet radiation treatment

Cells were plated in 10 cm Petri dishes and allowed to attach for 24–48 h. The cells were exposed to UV irradiation 10 J/m^2 (CL-1000 UV Crosslinker, Ultraviolet Products Ltd, Cambridge, UK) with overlying 8 ml of media and harvested at the indicated time points; control cells were mock irradiated.

2.4.3 Drug treatment

Drugs were supplied by Sigma unless otherwise stated. KU-55933 was a gift from KUDOS pharmaceuticals. All drugs were dissolved in 100 % tissue culture grade DMSO (Sigma) and diluted into the appropriate volume of media for the final concentration. The IC50 of KU-55933 for all the cell lines is detailed in Appendix 1.

A dose of 10 μM KU-55933 has been shown to inhibit ATM kinase activity *in vitro (Hickson et al., 2004; Pang et al., 2011)*. The EC50 doses for the cell lines treated with the ATM inhibitor are displayed in Appendix A.

Table 2.1. Details of Drug Treatment

Drug	**Stock Concentration in DMSO**	**Final Concentration**
KU-55933	20 mM	10 μM
Aphidicolin	2.5 mg/ml	5 μg/ml
Chk2 II inhibitor	20 mM	10 μM
Wortmannin	20 mM	10 μM
Cycloheximide	100 mg/ml	10 μg/ml
Leptomycin B	2 mM	2 nM
MG132	50 mM	25 μM
Neocarzinostatin	0.5 mg/ml	200 ng/ml
Adriamycin	2 mg/ml	1 μM
ICRF93	4 mg/ml	35 μM

2.4.4 Growth inhibition assay

The sulforhodamine B (SRB) technique (Skehan *et al.*, 1990) was used as a growth inhibition assay. Cells were plated on day 1 in a 96 well plate; for HCT116 2500 cells/well; for HCT116 p21-/- 5000 cells/well; for HCT116 p53-/- 2500 cells/well in a final volume of 150 μl of media. Cells were treated on day 2 with increasing doses of gamma ionising radiation (2.4.1). Following the IR treatment

cells were incubated for 72 h. Cells were fixed with 50 µl of 50 % trichloracetic acid and incubated for 1 h at 4°C; cells were washed ten times with tap water and air dried. Staining was undertaken by adding 50 µl of 0.4 % SRB dye (in 1 % acetic acid) for 30 min at room temperature. Excess dye was removed with four washes of 1 % acetic acid and air dried. Cell bound dye was redissolved by adding 150 µl of 10 mM Tris pH 10.5 with gentle agitation; plates were incubated for a further h at room temperature. Optical densities were measured at 540 nm with a Biohit BP-800 (Biohit, Helsinki, Finland). Growth inhibition curves were calculated as a percentage of untreated controls and analysed on Graphpad Prism 4 software (Graphpad Software, San Diego, CA).

2.4.5 Colony formation assay

The colony formation assay (clonogenic assay) was undertaken to determine the reproductive potential of cells following irradiation or drug treatment (Franken *et al.*, 2006). Treated cells were replated in triplicate at a density of 500–1000 cells per well in a 6 well plate in a final volume of 4 mls of complete media. Colonies were counted 10–14 days after seeding by fixing in 10 % TCA for 1 h at 4°C and staining with 0.4 % SRB dye. Vector quest image analysis software was used to count the colonies.

2.4.6 Transient transfection of small interfering RNA

Tissue culture cells were transfected with exogenous RNA using Dharmafect 1 transfection reagents (Dharmacon). CDC25A siGENOME siRNA D-003226–06 and siGENOME nontargeting siRNA pool #1 were used for target and nontarget siRNAs

respectively. Cells were plated at a density of 3×10^5 cells/well in a 6 well plate and allowed to adhere for 24 h in 4 mls of antibiotic free complete media at 37°C, 5 % $C0_2$ in a Hera $C0_2$ incubator. siRNA oligos were resuspended in 1 × siRNA buffer at a final concentration of 20 µM. In separate sterile 1.5 µl eppendorfs for each transfection 10 µl of siRNA oligo, 90 µl 1 × siRNA buffer and 100 µl OptiMEM I reduced serum media with GlutaMAX were combined and incubated for 5 min at room temperature. For mock treated cells 100 µl 1 ×siRNA buffer and 100 µl OptiMEM I reduced serum media with GlutaMAX were combined and incubated for 5 min at room temperature. In separate eppendorfs for each transfection 5 µl Dharmafect transfection reagent 1 and 195 µl of OptiMEM I reduced serum media with GlutaMAX were combined and incubated for 5 min at room temperature. Each siRNA solution was combined with one eppendorf of transfection reagent and incubated at room temperature for 20 min. During this incubation step media was aspirated from the 6-well plates and the cells were washed with 2 mls of PBS. The PBS was removed and 1 ml of antibiotic free complete media was added to each well. Following the siRNA/transfection reagent incubation; 600 µl of antibiotic free media was added and the 1 ml solution was added drop wise to the appropriate well with gentle agitation. To control cells 1 ml of media was added in a similar fashion. Each siRNa oligo or control was done in triplicate and incubated at 37°C, 5 % $C0_2$ in a Hera $C0_2$ incubator. Cells were harvested at the appropriate time.

2.5 Western Blotting

2.5.1 Cell lysis protocol

Cell pellets were recovered by either dissolving in ice cold urea lysis buffer and sonicated on ice for 10 s or resuspended in Tris lysis buffer incubated on ice for 15 min and cleared with centrifugation at 13000 rpm for 20 min at 4°C.

2.5.2 Protein quantification

Quantification of protein concentration in tissue lysates was determined with the bicinchoninic acid protein assay (BCA) Kit (Thermo Fisher Scientific, UK). Fifty parts BCA solution (1 ml) was combined with 1 part (20 µl) of copper sulphate solution to create the BCA reagent. An 8 point protein standard curve was generated by preparing a set of dilutions from 1 mg/ml bovine serum albumin (BSA) (1000, 750, 500, 350, 100, 75, 50 and 0 µg/ml) into sterile glass test tubes for a final volume of 50 µl. Five µl of each lysates sample was mixed with 45 µl of distilled water into sterile glass tubes. To each standard and unknown lysate sample 1 ml of BCA reagent was added and the samples were incubated in a water bath at 60°C for 30 min. Blank reagent was also incubated simultaneously, as a control. Following this incubation period 200 µl of blank reagent, standard samples and unknown lysates were loaded separately into a 96 well plate and absorbance of each was determined at 570 nm. A standard curve was generated from the known BSA concentration samples and the unknown lysates were determined by comparison to the standard curve.

2.5.3 Sodium dodecyl sulphate polyacrylamide gel electrophoresis

10–12 % sodium dodecyl sulphate (SDS) polyacrylamide gels were created using previously published recipes (Laemmlli *et al.* 1970) using Mini-Protean3™ (Biorad) gel casting equipment and Xcell *SureLock*™ mini cell tank (Novus). The separating gel was poured and overlayed with water saturated butanol. Once the gel had polymerised the butanol was removed and the stacking gel was poured in the presence of 10 or 12 well comb.

Lysate samples were prepared by aliquoting a volume containing 100 µg of protein into 500 µl eppendorfs and adding the appropriate volume of 5 × SDS sample loading buffer. Samples were denatured by heating to 95°C for 5 min and centrifuged briefly. Gels were loaded with required amount of protein and 10 µl of full range rainbow molecular weight marker (GE Healthcare) into the first lane and electrophoresed at 150 V for 60–120 min at room temperature in MOPS SDS running buffer.

2.5.4 Protein transfer

Proteins were transferred onto either Immobilon polyvinylidene difluoride (PVDF) membrane (Millipore Corp, Bedford, MA) or Hybond P nitrocellulose membrane (for Cdc25A) via electrophoresis at a constant current of 150 V for 60 min in ice cold Towbin buffer. Transfer was undertaken at 4°C in a Xcell *SureLock*™ mini cell tank (Novus) with an ice block. Following transfer membranes were stained in Ponceau red (Sigma) for 10 min to ensure even and efficient transfer of protein. Background stain was removed by rinsing several times in distilled water with agitation; the stain could be completely removed by continued washing.

2.5.5 Antibody incubation

Membranes were transferred to Perfect Western ® Containers with 10 mls blocking solution (5 % nonfat dried milk powder (w/v) (marvel, Nestle, UK) or 5 % BSA in tris-buffered saline tween (TBST) and placed on a shaker at room temperature for one h. Following blocking the appropriate primary antibody dilution was added to fresh blocking solution for a total volume of 5 mls. Membranes were incubated in the primary antibody overnight at 4°C. The primary antibody solution was drained off and the blot was rinsed three times for 5 min each in 10 mls of TBST at room temperature. Horseradish peroxidase (HRP)-conjugated secondary anti-mouse or anti-rabbit antibody (Santa Cruz Biotechnology, Santa Cruz, CA) was applied at a dilution of 1/4000 in blocking solution in TBST for 1 h at room temperature. Excess secondary antibody was removed by washing three times for 5 min each in 10 mls TBST. PBST was used as the for Cdc25A antibody.

Table 2.2. Details of Primary Antibodies

Protein	Supplier	Origin	Dilution
Actin AB1 JLA20	Calbiochem	Mouse	1/10000
ATM 5C2	Abcam	Mouse	1/500
ATM Y170	Abcam	Rabbit	1/500
ATM serine-1981	Abcam	Rabbit	1/500
ATM serine-1981	Cell Signalling	Mouse	1/1000
ATR	Abcam	Rabbit	1/400
Cdc25A F6	Santa Cruz	Mouse	1/200
Cdc2 tyrosine-15	Cell Signalling	Rabbit	1/1000

Cdk2 78B2	Cell Signalling	Rabbit	1/1000
Cdk tyrosine-15	Cell Signalling	Rabbit	1/1000
Cdk2 threonine-14	Epitomics	Rabbit	1/1000
Cdk2 threonine-160	Cell Signalling	Rabbit	1/1000
Chk1 G4	Santa Cruz	Mouse	1/10000
Chk1 serine-317	Cell Signalling	Rabbit	1/1000
Chk1 serine-345	Cell Signalling	Rabbit	1/1000
Chk2 A11	Santa Cruz	Mouse	1/200
Chk2 threonine-68	Cell Signalling	Rabbit	1/1000
Cyclin A	Abcam	Rabbit	1/200
Cyclin B	Abcam	Mouse	1/1000
E2F-1	Cell Signalling	Rabbit	1/1000
GAPDH	Cell Signalling	Rabbit	1/4000
Mre11 Clone18	BD Biosciences	Mouse	1/500
Mre11 12D7	Abcam	Mouse	1/500
NBS1	Abcam	Rabbit	1/400
NBS serine-343	Abcam	Rabbit	1/500
NBS serine-343	Cell Signalling	Rabbit	1/1000
p21	Calbiochem	Mouse	1/200
p53 AB-6 DO-1	Calbiochem	Mouse	1/200
p53 serine-15	Cell Signalling	Rabbit	1/200
p53 serine-20	Cell Signalling	Rabbit	1/1000
Rad50	Novus Biologics	Rabbit	1/200

2.5.6 Chemiluminescent signal detection

Immunoreactivity was detected using the Enhanced ChemiLuminescence (ECL) Plus® detection reagent (GE Healthcare, Little Chalfont, UK) or Super Signal West Femto ECL (Pierce) and autoradiography. Membranes were incubated in the corresponding solutions as per manufacturers' instructions for 2 min at room temperature. The blot was placed between two acetate transparencies and transferred to an X-ray film cassette. In the dark room the blot was overlaid with ECL™ Film (Hyperfilm ECL film, Amersham, Buckinghamshire, UK) for a period of 30 s to 5 min depending on signal intensity. Exposed films were developed using X-ray Imaging Equipment™, Fuji.

2.6 Immunofluorescence

Cells were seeded in chamber slides 48 h prior to analysis. For HCT116 wild-type cell line 1×10^5 cells and for HCT116 p21-/- 2×10^5 cells were required in a final volume of 2 mls of RPMI 1640 media containing 2 mM glutamine, 5 % foetal calf serum (Harlan) and 1 % penicillin/streptomycin. Medium was removed and the cells were washed twice with PBS. Cells were fixed with 1 ml of 2 % paraformaldehyde for 10 min at room temperature and rinsed twice in PBS for 10 min each. Cells were permeabilised with 0.1 % Triton X 100 in PBS for 15 min at room temperature. The triton X was removed and the cells were washed three times with PBS for 5 min each with gentle agitation. Cells were exposed to blocking solution (1 % BSA (BDH), 5 % goat serum (Jackson Laboratories. West Grove, PA)) in PBS for 1 h at room temperature. The blocking solution was discarded and an anti-phosphohistone H2AX primary antibody (Millipore, UK) was applied at a concentration of 1/1000 in 200ul of blocking solution overnight at 4°C. The following day the primary antibody is

rinsed with three times PBS washes 10 min each at room temperature with gentle agitation. Cells were exposed to 1/400 dilution of fluorescein isothiocyanate (FITC) Alexa Fluor 488 conjugated goat anti-mouse immunoglobulin G (IgG) antibody (Invitrogen, Paisley, UK) for 1 h in the dark at room temperature. The secondary antibody is removed and the cells are washed with PBS three times for 10 min each. The slides were mounted with Vectashield mounting medium. Images were captured with a Zeiss AxioPlanII fluorescence microscope equipped with a 100× Plan-Neofluar oil objective NA1.3, motorised filter wheels with Chroma 83000 filter set (Chroma Technology, Bellows Falls, Vermont), and Photometrics HQ CCD camera (Tucson, Arizona) controlled by IPLab software (Becton Dickinson). All images were captured with the same exposure time to allow comparison of results. Images were analysed using IPLab spectrum software. 4',6-diamidino-2-phenylindole (DAPI)-labelled nuclei were segmented on the basis of intensity and the segmentation mask was overlaid on the corresponding FITC image for analysis. The average FITC intensity per nucleus was calculated.

2.7 Flow Cytometric Cell Analysis

Nuclei were prepared as described by Vindelov *et al.* (Vindelov *et al.*, 1983). Briefly, cells were washed twice in ice cold PBS, trypsinised (0.05 % trypsin/0.02 %EDTA), counted (Beckton Dickson Coulter Counter) and a 5×10^5 aliquot was resuspended in 100 ul of citrate buffer and stored at -20°C prior to analysis. Each sample was digested by mixing with 450 ul of trypsin (0.003 %) and leaving for 1–2 min at room temperature. Trypsin inhibitor (0.05 % w/v) and RNAse A (0.01 % w/v) in a final volume of 375 µl were then added and left for further 10 min at room temperature. Finally the cells were stained on ice with propidium iodide (416 µg/ml) and spermine

tetrahydrochloride (1.61 µg/ml) in a final volume of 250 µl for 10 min. Analysis of 20,000 events was undertaken on a fluorescence-activated cell sorting (FACS) calibur (Becton Dickinson, Biosciences) flow cytometer at a of wavelength 564–607 nm using Cell Quest software. Fluorescence intensity histograms were gated (forward scatter (FSC) versus side scatter (SSC), FL2-A versus FL2-W) to exclude debris and doublets for analysis. Data was analysed using ModFit 2.0 program (Verity Software, Topsham, ME).

2.8 Coimmunoprecipitation Assay

Cells were grown in 10 cm^2 dishes until 70–80 % confluent and lysed in 150–200 µl of immunoprecipitation nonidet P40 (NP40) lysis buffer. 1 mg aliquots were placed into separate 1 ml eppendorfs and made up to 500 µl with immunoprecipitation NP40 lysis buffer. Samples were precleared by adding 5 µl of Rabbit IgG Agarose to each sample and incubating for 1 h at 4°C on an orbital rotator. Samples underwent a second preclearing step by adding 20 µl of Protein A Agarose and incubating for 1 h at 4°C on an orbital rotator. The rabbit IgG/Protein A beads was pelleted by centrifugation at 13000 rpm for 30 s at 4°C; the supernatant (precleared lysates) was transferred to a clean eppendorf tube. Immunoprecipitation was undertaken by adding 10 µl of Cdc Tyr15 (#9111) antibody to the precleared lysates; IgG control samples had an equivalent volume of rabbit IgG control added and blank samples had an equivalent volume of immunoprecipitation NP40 lysis buffer added. Samples were incubated overnight at 4°C on an orbital rotator. The following day 40 µl of Protein A agarose beads were added to each sample and incubated for 4 h at 4°C on an orbital rotator; 1 µl of IgG rabbit was added and samples were incubated for an h at 4°C on an orbital rotator. Beads were collected by centrifugation for 13000 rpm

for 30 s at 4°C and the supernatant was removed. Beads were washed 4 × in immunoprecipitation NP40 lysis buffer by vortexing briefly in 1 ml of buffer and centrifugation at 13000 rpm for 30 s at 4°C. Beads were finally washed in Lithium Chloride solution. 40 µl of 3 × SDS loading buffer was added to each sample to elute bound proteins from the beads and stored at -20°C. Samples were prepared by heating for 5 min at 95°C and spinning down briefly.

2.9 Cellular Fractionation

Cells were fractionated into soluble (cytoplasmic) and insoluble (nuclear) extracts using the following protocol. Cells were plated at a density of 2×10^6 cells/ml 48 h prior to being treated with 10 µM of KU-55933 or DMSO for 24 h. Cells were damaged with 5 Gy of IR or mock irradiated the following day and harvested at 2 h as 2.3.5. The pelleted cells were extracted in 500 µl of ice cold hypotonic buffer supplemented with complete® mini protease inhibitor tablet (Roche) and 1,4-dithiothreitol (DTT) to a final concentration of 1 mM. The suspension was micro centrifuged at 5000 rpm for 10 min at 4°C. The supernatant was collected as the soluble fraction. The nuclei were extracted from the remaining pellet with 150 µl of ice cold high salt buffer supplemented with complete® mini protease inhibitor tablet (Roche) and DTT to a final concentration of 1 mM on ice at 4°C with gentle agitation. The insoluble fraction was collected by micro centrifugation at 10000 rpm for 10 min at 4°C. Samples were mixed with gel loading buffer and heated for 5 min at 95°C.

2.10 mRNA Reverse Transcriptase Polymerase Chain Reaction

2.10.1 RNA extraction & quantification

Total RNA was extracted from cell lines with TRI Reagent following manufacturers' instructions. Briefly, cells were lysed with 1 ml of TRI reagent per 10 cm^2 of flask surface area and transferred into 13 ml polypropolene tubes. 200 µl of chloroform was added per ml of TRI reagent and incubated for 15 min at room temperature. The samples were separated by centrifugation at 10000 rpm using a SS34 rotor for 15 min at 4°C. The clear top layer was removed from the tubes, 500µl of isopropanol per ml of TRI reagent was added; samples were inverted and incubated at room temperature for 5 min and centrifuged for a further 10 min at 4°C. The supernatant was discarded and the pellet was resuspended in 7.5 mls of ice cold 70 % ethanol. The suspension was centrifuged at 10000 rpm for 10 min at 4°C. The ethanol was removed carefully by a Pasteur pipette and the samples were air dried before being finally resuspended in 100 µl distilled water. DNA was removed with DNAse treatment using Turbofree® DNAse Kit (Ambion, Huntingdon, UK). RNA was quantified by spectrophotometry at 260 nm using Nanodrop® ND-1000. 1 µl sample was placed onto the analysis platform and the concentration was determined by using the Nanodrop® software. RNA was prepared in a final concentration of 200 ng/µl and 5 µl aliquots were stored at -20°C.

2.10.2 Quantitative real time polymerase chain reaction

Standard PCR amplification of specific mRNA was performed using Quantitect SYBR Green quantitative real time PCR (RTPCR) kits (Qiagen, Crawley, UK). Forward and reverse primer sets for each transcript analysed are detailed below in

table. Primers were chosen from a number of options generated by Primer3, a web based primer design software program (http://fokker.wi.mit.edu/primer3/input.htm) using the mRNA sequence of the genes of interest deposited at the National Centre for Biotechnology Information (http://www.ncbi.nlm.nih.gov/). Primers specificity was checked using Blast search (http://www.ncbi.nlm.nih.gov/BLAST/Blast.cgi). The reaction was carried out using 40 ng RNA template and primers at a concentration of 20 μM; β-actin was used as the reference transcript to normalise the results. Reaction volumes of 15 μl were used and reactions were carried out in 0.5 ml thin walled microcentrifuge eppendorf tubes. All PCR reactions were set up as stated:

RNA template 1000 ng/	5 μl
(add 95 μl of ultra pure water)	4 μl
2× SYBR mix	7.5 μl
Primers 20 μM	0.375 μl
Reverse Transcriptase	0.15 μl
Water to a final volume of	2.975 μl

A master mix containing all of the above reagents was prepared on ice in an isolation hood and an appropriate volume added to each tube and 4 μl of the DNA template was added. The PCR cycle condition were as follows: reverse transcription step 50°C for 30 min, TAQ polymerase activation step 95°C for 15 min and 40 cycles of denaturation at 94°C for 10 s, reannealing at 57°C for 20 s and extension at 72°C for 20 s on a Rotor-Gene 3000 thermal cycler (Corbett Research, Cambridge, UK). After a final extension of 72°C for 60 s a PCR product melt curve was performed from 66–

99°C. Fluorescence signal was recorded on the 6-carboxyfluorescein channel (ExD470 nm, EmD510 nm) at the end of the reaction. PCR products were separated on 1.5 % agarose gels for quality control. Results were analysed on Rotor-Gene 6 software.

Table 2.3. Details of Reverse Transcriptase Polymerase Chain Reaction Primers

Gene	Forward Primer Reverse Primer
p21 (*CDKN1A*)	GAGCGATGGAACTTCGACTT CAGGTCCACATGGTCTTCCT
CDC25A	TAGATTCTCCTGGGCCATTG TCACAGGTGACTGGGGTGTA
CDK2	AAATTCATGGATGCCTCTGC CAGGGACTCCAAAAGCTCTG
Cyclin B1 (*CCNB1*)	GGCCAAAATGCCTATGAAGA CAAAATAGGCTCAGGCGAAA
Cyclin E (*CCNE1*)	CAGATTGCAGAGCTGTTGGA TCCCCGTCTCCCTTATAACC
Cyclin A (*CCNA1*)	ACCCCAAGAGTGGAGTTGTG GGAAGGCATTTTCTGATCCA
β-actin	GATGGAGCCGCCGATCCACACGG CTACGTCGCCCTGGACTTCGAGC

2.11 Quantification of DNA Synthesis

2.11.1 Exposure to radioactive nucleotides

Cells were plated two days before labelling in T75 flasks; at 60–80 % confluency they were exposed to 10 Ci/ml of [[14C]] thymidine for 24 h for labelling of basal DNA synthesis. Cells were washed twice with PBS, trypsinised and replated into 2 mls/well of radiation free media into 6-well dishes for a further 24 h. DNA damaged was induced by either exposing to irradiation treatments or incubation with drug containing media. At the required time points cells were pulse labelled with 2.5 Ci/ml of [[3H]] thymidine for 30 min. Radioactive medium was removed and the cell pellet was collected by washing twice in ice cold PBS and scraping from the plastic surface in the presence of 1 ml of ice cold PBS. The resultant suspension was centrifuged at 13000 rpm for 5 min at 4°C and the pellet frozen at -20°C.

2.11.2 Phenol:Chloroform extraction and ethanol precipitation of DNA

DNA extraction was undertaken by resuspending cell pellet in 100 µl of PBS and 400 µl of DNA lysis buffer supplemented with proteinase K for a final concentration of 300 µg/ml and incubating at 37°C overnight. An equal volume of Tris buffered Phenol:Chloroform:Isoamylalcohol (25;24:1; AMS Biotechnology) solution was added to the solution containing nucleic acid, gently vortexed and spun briefly at 13000 rpm for 5 min at 4°C. The upper aqueous phase was removed carefully to a clean tube and an equal volume of chloroform was added and the sample mixed and centrifuged as previously. The upper aqueous layer was placed into a clean tube and DNA was precipitated with 1/10th volume of 3 M sodium acetate (pH 5.5) and two volumes of ice cold 100 % ethanol on ice for 30 min at 4°C. The nucleic acid

precipitate was recovered by centrifuging for 15 min at 13000 rpm 4°C and the resultant pellet was washed with 70 % ethanol. After removal of the ethanol, the pellet was air dried at room temperature for 5 min.

2.11.3 Quantification of radioactivity

The air dried DNA was resuspended in 100 µl of ultra pure water and transferred into scintillation vials containing with 4 mls of Optiphase supermix scintillation cocktail to allow for radioactive assessment. Control sample contained 100 µl of ultra pure water dissolved into the scintillation cocktail. As [3H] and [14C] are both beta emitters but have different emission spectra, the proportion of [3H] to [14C] in the samples was assessed by scintillation using a Becton Coulter scintillation counter (Becton Coulter LS 6500, USA) and a dual label ([3H]/[14C]) quench curve as recommended by the manufacturer. Background radiation was subtracted from each sample. The degree of DNA synthesis during the 30 min pulse was proportionate with the [3H]/[14C] ratio, and the effect of irradiation was determined with reference to the [3H]/[14C] ratio in unirradiated controls.

2.12 Tissue Microarrays

2.12.1 Animal work

Animal experiments were carried (by Morwenna Muir) out using a project licence issued by the UK Home Office and UK Co-ordinating Committee on Cancer Research guidelines were adhered to rigorously. Xenografts of HCT116, HCT15, HCT-8, SW-620 and HT29 were established in immunodeficient C57/B16 nude mice (5-week old) by injecting subcutaneously 10 millions cells in suspension in RPMI

1640 or in RPMI 1640/Matrigel 50/50 (v/v). Xenografts were collected when the tumour volume measured of 100–200 mm3, dissected to remove mouse tissue and blood vessels and collected in formalin solution. The xenografts had not been treated with any DNA damage inducing drugs *in vivo* and were completely treatment naive.

2.12.2 Tissue microarray technology

Adequate evaluation of pathological tissue samples is often limited by specimen availability. A conventional paraffin-embedded tissue block will yield 200–300 sections, depending on the experience of processor (Bubendorf *et al.*, 2001). Tumour microarrays (TMA) are miniaturised platforms for the simultaneous assessment of multiple pathological tissue specimens (Kononen *et al.*, 1998). Such an approach reduces the variability introduced during sample preparation and subsequent processing (Rimm *et al.*, 2001a). To create microarrays, cored specimens from paraffin-embedded samples are taken from the *donor* block and assembled into the *recipient* TMA block. Multiple cores can be taken without disrupting the tissue architecture and tissue heterogeneity is optimally represented by at least three cores of 0.6 mm width per sample (Hoos *et al.*, 2001; Rimm *et al.*, 2001b). Goethals *et al.* (2006) used a virtual TMA with computer-generated images and suggested that four cores are more representative of tissue heterogeneity. As the amount of tissue sampled is small, it is recommended that multiple small cores be taken rather than larger cores (>2 mm) (Kallioniemi *et al.*, 2001). TMAs allow an assessment of tumour populations and are not intended for the detailed analysis of individual tumours. They are suited to immunohistochemistry, fluorescence *in situ* hybridisation (FISH) and RNA *in situ* hybridisation (RNA-ISH). Concordance rates of up to 95 %

have been demonstrated between TMA and conventional IHC single specimen analysis of MMR deficiency in HNPPC (Hendriks *et al.*, 2003).

One of the major concerns of using this technology is the issue of antigen preservation during tissue processing. Standard tissue processing is a robust mechanism for conserving tissue antigens but sectioning and subsequent deparaffinisation steps can render the tissue vulnerable to oxidative damage (Fergenbaum *et al.*, 2004). DiVito *et al.* (2004) assessed the impact of paraffin coating and storage of sectioned slides in a nitrogen desiccator on oestrogen receptor detection in a breast cancer TMA. This combination of treatments protected immunoreactivity for up to 3 months. We employed the approach of cutting TMA sections immediately before analysis (within 1–2 weeks). To reduce core loss during sectioning, it is advisable to use a tape-based transfer method. For this, an adhesive tape is applied to the TMA prior to sectioning; once sectioned, the tape is removed with the slice and applied to an adhesive-coated slide (Rimm *et al.*, 2001b). UV cross-linking the section to the slide allows the tape to be removed with a degreasing solution.

IHC staining of TMAs is used for the analysis of tissue populations and thus initial studies used a binary system of negative and positive staining as the only assessment tool (Rimm *et al.*, 2001b). More comprehensive evaluation can be achieved using the histoscore that grades the intensity of staining and the percentage of stained cells (McCarty *et al.*, 1986). Interindividual variability can be reduced using image analysis techniques for the interpretation of TMA slides (Cregger *et al.*, 2006). Histoscoring is a method of assessing the proportion of cells stained and the intensity

of IHC staining for a given antibody. Scores for the intensity of staining (0–3) and the proportion of cancer cells stained (0–100%) are combined to calculate a composite score, ranging from 0–300 (Cregger *et al.*, 2006; Vigo *et al.*, 1999). Three separate xenografts were available for each cell line and these were scored twice (Rimm *et al.*, 2001a); the resultant histoscore value was an average of six cores. The nuclei of the cells were scored independently by two people (S Din & E Gibson) and major discrepancies were resolved by discussion with the collaborating pathologist (Dr D. Faratian).

2.12.3 Xenograft tissue microarray

Xenografts were paraffin embedded using standard protocols (Division of Pathology, Queen Margaret Research Institute, Edinburgh). Blocks were at least 3 mm thick; slices were cut and stained with hematoxylin and eosin (H&E) to determine the architectural preservation during the preparation process and used as a guide to select the regions for sampling. A manual arrayer (Beecher Instrument, Sun Prairie, USA) was used to create duplicate microarrays of two cores 1 mm from each xenograft sample (triplicate samples of each xenograft line were used for analysis). The tissue micro-arrays (TMA) were placed in an oven at 56°C for 10 min to soften wax allowing cores to adhere more efficiently. Prior to sectioning the TMA were cooled on ice plates; 3 µm sections (Leica Rotary Microtome 2235) were placed onto silanised glass slides and baked in an oven overnight at 56°C.

2.12.4 Human colorectal tumour microarray

Ethical approval (Lotian Research Ethics Committee Reference 07/S1103/19) was granted for the assessment of treatment naïve human archival paraffin-embedded

colorectal cancers (CRC)(Bubb *et al.*, 1996). One hundred and seventy nine sporadic cancers were available for creation of the microarray (TMA was created by Euan Gibson). Normal colonic tissue was provided by Professor David Harrison from previous studies as comparative controls. Each CRC slide was sectioned and H&E stained to assess architectural preservation and select suitable tumour areas to be cored. Three × 0.6 mm cores of each colorectal cancer were placed into three separate microarray paraffin blocks using a Beecher instrument (Rimm *et al.*, 2001a; Rimm *et al.*, 2001b) to represent tissue heterogeneity. TMAs were placed in an oven at 56°C for 10 min to soften wax allowing cores to adhere more efficiently. Prior to sectioning the TMAs were cooled on ice plates; 3 µm sections (Leica Rotary Microtome 2235) were placed onto silanised glass slides and baked in an oven overnight at 56°C.

2.13 Histological Analysis

2.13.1 Immunohistochemistry

Paraffin embedment of tissue samples is a robust mechanism for preserving tissue antigens and architecture. However, the process creates interstrand cross-links between the paraffin and tissue which required to be disassociated before immunohistochemistry can be undertaken.

Slides were dewaxed by immersing in successive xylene solutions in glass jars for three times at 5 min each and rehydrated by immersing in 100 % ethanol for 5 min, 90 % ethanol for 2 min and 70 % ethanol for 2 min. Slides were rinsed in distilled water twice for 5 min and finally washed in PBS for 5 min with gentle agitation. Antigen retrieval was undertaken by heating 1 litre of 10 mM sodium citrate buffer pH6.0 in an 800 KW microwave for 15 min under pressure; the slides were

submerged and heated for a further 5 min in the microwave under pressure. The slides were then allowed to cool for 20 min and washed in PBS for 5 min. Endogenous peroxidise was blocked by incubating the sections in 3 % hydrogen peroxide for 10 min with gentle agitation at room temperature. Slides were rinsed first in distilled water for 5 min and then in PBS for five minutes. Sections were ringed with a DAKO pen and incubated with 100 µl of 5 % goat serum PBS or DAKO protein blocking solution for 1 h at room temperature. The blocking solution was run off and the section was incubated with primary antibody at the appropriate dilution in the blocking solution at 4°C overnight. The subsequent day the antibody was run off and the slides were washed in PBS for 5 min. Secondary antibody (Envision) was applied in a volume of 100 µl-200 µl for 30 min at room temperature. Signal was developed by applying 3,3'-diaminobenzidine (DAB) substrate for 10 min at room temperature and slides were washed in running water for 2 min. Counterstain was applied by immersing slides in Haematoxylin for 60 s, washed in running water and blued in Scotts tap water substitute for 10 s and finally rinsed in running water. Slides were dehydrated in successive ethanol submersions starting with 1 min in 70 % ethanol, 1 min in 90 % ethanol and 2 × 1 min in 100 % ethanol. Slides were dewaxed in xylene 3 times for 1 min each, mounted in dibutyl phthalate xylene (DPX) and protected with a coverslip.

2.13.2 Specificity of phospho-specific antibodies

Specificity of the Cell Signalling Chk2 threonine-68 phosphorylation rabbit polyclonal antibody was undertaking by performing competitive reactions with a Chk2 threonine-68 phosphorylation custom made peptide (Cell Signalling). The

antibody and the blocking peptide were incubated in a 1:5 (v/v) ratio for one h at room temperature and diluted to give the final antibody concentration before being applied to slides that had been non-specifically blocked as 2.12.1. Slides were then processed as the immunohistochemistry protocol.

2.14 Statistical Analysis

Continous data were analysed in GraphpadPrism software (version 4) to calculate standard deviations of the mean and the EC50 drug values for short term growth inhibition assays.

Standard Pearson correlation analysis for intraobserver agreement in analysing immunohistochemical data was analysed by the R foundation for Statistical Computing Services (Vienna, Austria) package.

2.15 Buffer Recipes

10 × Tris Buffered Saline pH7.5 (TBS)

0.5 M Tris Base,

1.5 M NaCl

1 × TBSTween

1/10 dilution of 10×TBS

0.001 % Tween

Urea Lysis Buffer

62.5 mM Tris pH 6.8

6 M urea

10 % v/v glycerol

2 % w/v SDS

Complete mini protease inhibitor tablet (Roche)

Tris Lysis Buffer

90 % 1× TBS

10 % NondietP40

0.01 % Protease inhibitor cocktail (Sigma P8340)

5× SDS Loading Buffer

30 % 0.3 M Tris pH 6.8

10 % 2-mercaptoethanol

40 % glycerol

20 % SDS

0.02 % Bromophenol blue

20 × MOPS SDS Running Buffer

1 M Tris

1 M MOPS

20.5 mM EDTA

2 % SDS

Towbin Transfer Buffer

25 mM Tris base

192 mM glycine

10 % methanol

FACS Citrate Buffer pH7.6

250 mM sucrose

45.6 mM trisodium citrate

5 % DMSO

NP40 Lysis Buffer pH8.0

65 mM TRIS

154 mMNaCL

1 % NP40

(to 10 ml of stock add one Protease inhibitor tablet (Roche) and 25 µL 400× PMSF)

Cellular Fractionation Hypotonic Buffer (25 mls)

500 µl 1 M Hepes

500 µl 10 % NP40

5 µl 0.5 M EDTA

23.95 mls distilled water

Cellular Fractionation Hypertonic Buffer (25 mls)

500 µl 1 M Hepes

500 µl 10 % NP40

2 mls 5 M NaCl

3 mls 100 % Glycerol

19 mls distilled water

DNA Lysis Buffer

10 mM Tris pH 7.4

50 mM EDTA

0.5 % SDS

Phosphatase buffers/stabilisers were not included in the cell lysis protocols in Chapter 5 for Cdc25A immunoblots as the phosphatase buffers inhibited the reaction with the Super Signal femto chemiluminescence. The cell pellets derived from these reactions were strictly subjected to Western blotting within 24 hours to limit protein degradation.

Chapter 3. Expression of DNA Damage Response Proteins in Sporadic Colorectal Cancers

3.1 Introduction

Colorectal cancer is a multistep process, progressing from an adenoma to a carcinoma by the accumulation of defects in genes that regulate cell survival and apoptosis (Lane and Crawford, 1979). Historically, there are two main types of genetic aberrations in colorectal cancer: chromosomal instability, which is commonest in sporadic cancers, and MSI, which occurs in over 90 % of hereditary nonpolyposis colon cancer (Lengauer *et al.*, 1998; Wheeler *et al.*, 2000) and up to 15 % of sporadic tumours (Lynch *et al.*, 1993). Constitutive activation of the ATM–Chk2–p53 pathway has been suggested to prevent disease progression from colonic adenoma to invasive carcinoma, highlighting that defects in these pathways may promote genetic instability and carcinogenesis (Bartkova *et al.*, 2005b). Activation of the DDR pathway can occur at various stages throughout the development of cancer, including chromatin alterations, generation of reactive radical species, senescence and telomere shortening (Bakkenist and Kastan, 2003; Bartkova *et al.*, 2005a; Bartkova *et al.*, 2005b; Herbig *et al.*, 2004).

The efficacy of conventional chemotherapy and radiotherapy is related to their ability to induce DNA damage (Norbury and Hickson, 2001). Inhibitors of the DDR and repair pathways have been shown to be (1) effective as single agents for treating cancers that have mutations in essential DNA repair genes and (2) a means of potentiating current cytotoxic and irradiation therapies (Bryant *et al.*, 2005; Farmer *et al.*, 2005; Hickson *et al.*, 2004). The *ATM* gene is mutated in the autosomal recessive

disorder AT that is characterised by extreme sensitivity to radiation (and other agents causing DSB) (Savitsky *et al.*, 1995) and, as such, supports the rational for using ATM inhibition to enhance the effects of radiation therapy (Hickson *et al.*, 2004). However, the effect of constitutive activation of the DDR in cancer cells may undermine the efficacy of such approaches (Madhusudan and Middleton, 2005) and this approach has not been studied in human (colorectal) cancers. Furthermore, the proportion of sporadic colorectal cancers that harbour defects within this signalling cascade is currently unknown. The majority of studies have evaluated expression of these proteins within hereditary nonpolyposis syndromes (Miquel *et al.*, 2007) and then extrapolated the findings to sporadic cancers with the MSI phenotype (Table 3.1). Therefore, a comprehensive analysis of the whole ATM pathway based on interrogating protein expression in sporadic cancers would be more informative and may perhaps predict patient response to current treatment modalities (Grabsch *et al.*, 2006; Madhusudan and Middleton, 2005). In this chapter I have analysed expression of the DDR proteins in 179 sporadic colorectal cancersof which 152 were microsatellite stable and 27 were microsatellite instable.

3.2 Results

3.2.1 Validation of antibody specificity

3.2.1.1 Western blotting

In order to undertake immunohistochemistry of complex tissue specimens, it is first necessary to validate antibody specificity. There is no accepted gold standard in IHC for assessing antibody specificity; however, certain biological methods can be used to provide evidence of specificity (Mandell, 2003). A simple method of assessing

antibody specificity (or cross-reactivity) is to immunoblot a positive control lysate sample that has been subjected to electrophoresis. This allows an assessment of the potential crossreactivity of the antibody with different protein bands. To reduce cross-reactivity, monoclonal antibodies (if available) are preferred to polyclonal antibodies (Bartkova *et al.*, 2005a). Although this method is commonly used, it should be noted that proteins are denatured during electrophoresis; in contrast, in immunohistochemistry, proteins are assessed in their native (folded) form. To test cross-reactivity of antibodies recognising DDR components, checkpoint-proficient osteosarcoma cells, U2OS, were irradiated with 5 Gy of ionising irradiation or 10 J/m^2 of UV irradiation to induce the ATM and ATR DDR pathways, respectively. Figures 3.1–3.4 show whole immunoblots depicting the range of antibodies used. An antibody was deemed specific if it detected induced band(s) of the predicted size on an immunoblot and was then considered appropriate for use in immunohistochemistry. For example, Figure 3.1 shows two Abcam anti-ATM antibodies: a poorly specific mouse monoclonal (5C2) antibody and a highly specific rabbit monoclonal (Y170) antibody. Similarly, the Mre11 clone 18 (BD Biosciences) antibody was deemed cross-reactive due to the detection of laddered bands (Figure 3.2) and Mre11 12D7 was considered more specific (Abcam). Four of the antibodies anti-Rad50; anti-Nbs1 phosphoserine 343, anti-Chk1 phosphoserine 317 and anti-Chk2 phosphothreonine 68 detected more than a single band however were considered suitable for IHC as it is likely that they are complexed with other proteins (resistant to separation with the lysate preparation) or have undergone further post translational modifications. The majority of the antibodies tested (Table 3.2) were found to be suitable for IHC and indeed had been used previously (Bartkova *et al.*,

2005a; Bartkova *et al.*, 2004; Bartkova *et al.*, 2005b; Gorgoulis *et al.*, 2005; Lukas *et al.*, 2001; Nuciforo *et al.*, 2007) on formalin-fixed paraffin-embedded human tissue specimens.

3.2.2 Xenograft tissue microarray

Xenograft tumours were also used to optimise antibodies for IHC analysis of formalin-fixed, paraffin-embedded tissues. These could be directly compared with lysate samples derived from monolayer cultures of the corresponding cell line analysed using the same antibodies. A tumour microarray was created from treatment naïve HCT-8, HCT15, HCT116, HT29 and SW-620 xenografts (Figure 3.5). Proteins involved in the DDR were assessed by IHC (Figure 3.6) using the antibodies described above and nuclear histoscores were calculated. A summary of the results is shown in Table 3.3.

The MRN complex is required to facilitate ATM activation after the formation of DNA DSB (Lee and Paull, 2005). The levels of Rad50 detected in the xenografts correlated well with immunoblot data from the corresponding cell lines (compare Figure 3.6 with Figure 6.5). Nbs1 staining was highest in the HCT116 xenograft; however, this contrasts with the immunoblot data. The Mre11 component of MRN is necessary for the stabilisation of both Nbs1 and Rad50 in cell culture models and HCT116 cells are reported to lack stabilisation of both these proteins (Takemura *et al.*, 2006).

No Chk2 staining is seen in HCT-8, HCT15 and HCT116 cells. Both HCT-8 and HCT15 are derived from the same primary tumour (Vermeulen *et al.*, 1998) and

HCT15 has been shown to have biallelic missense mutations in codon 145 (R145W) and codon 247 (A247D), resulting in the formation of an unstable Chk2 protein that is unable to undergo ATM-dependent phosphorylation at threonine-68 (see below) (Lee *et al.*, 2001). The antibody used to detect Chk2 protein was a mouse monoclonal directed against amino acids 1–300 of the human wild-type protein and should therefore be able to detect mutant Chk2 protein using both immunoblotting and IHC. However, data suggests that the R145W mutation alters the tertiary and quaternary structures of the resultant protein, which may explain the lack of detection by the antibody (Lee *et al.*, 2001). SW-620 and HT29 xenografts showed the highest levels of Chk2 staining. However, Chk2 threonine-68 staining was not present in HCT116, HCT-8 or HCT15 xenografts, which agrees with the immunoblot data (Figure 6.5) and provides supporting evidence that DDR pathways have not be activated. For the reasons outlined above, mutant Chk2 protein present in HCT-8 and HCT15 cells is unable to undergo phosphorylation at threonine-68 after DNA damage. SW-620 has the highest Chk2 threonine-68 staining, consistent with constitutive pathway activation. HT29 also has Chk2 threonine-68 nuclear staining, but this is mostly diffuse, which may reflect differences in tumour cell biology between monolayer cultured cells and xenografts.

p53 staining indicated the presence of stable mutant protein in HCT15, HT29 and SW-620 cells. Only SW-620 had a p53 serine 15 phoshorylation signal, albeit a very low level. p21 is a p53-inducible gene and p21 staining is highest in HCT116 xenografts, which contain wild-type p53.

In general, the level of nuclear IHC staining of DDR proteins in the majority of xenografts is in good agreement with data derived from immunoblots of the traditional western blotting of monolayer cell cultures (Figures 3.6 IHC and 6.4 immunoblots (see later))

3.2.3 Human colorectal Tissue Microarray

Ethical approval (Lothian Research & Ethics Committee 07/S1103/19) was granted for the assessment of human archival paraffin-embedded CRC. One hundred and seventy nine sporadic tumours were used to create the microarray: 152 CRC represented the MSS phenotype and 27 (15 %) the MSI phenotype. Microsatellite phenotyping had previously been undertaken by Bubb (1996). Each CRC slide was sectioned and H&E stained to assess architectural preservation and select suitable tumour areas to be cored. Three × 0.6 mm cores of each colorectal cancer were placed into three separate microarray paraffin blocks using a Beecher instrument (Figure 3.7) (Rimm *et al.*, 2001b). Core loss was between two and five (1–3 %) in MSI-negative cancers and between zero and one (0–3 %) in MSI-positive cancers.

The human colorectal TMA was interrogated using antibodies against proteins of the DDR signalling cascade, including ATM, Mre11, Nbs1 and Rad50 sensor proteins, Chk2 and Chk2 threonine-68 transducer proteins, and p53 and p21 effector proteins. Analysis was done by comparing data from microsatellite-stable tumours with data from microsatellite-unstable tumours. Representative staining patterns are depicted in Figure 3.8 for each antibody.

Nuclear staining of the cores was scored manually as low staining (0–100), moderate staining (101–200) or high staining grading (201–300); an example of p53 staining is

shown in Figure 3.9. The IHC data is descriptive data and does not test statistical significance between the staining intensity; the colorectal cancer series is small limiting the tests for statistical significance.

The specificity of phospho-specific antibodies can be assessed by peptide blocking and phosphatase treatment of the sample tissue. Following these treatments, no staining should occur with phospho-specific antibodies. Phosphospecificity of the anti-Chk2 threonine-68 antibody was assessed using a blocking peptide. Antibody incubation with the blocking peptide resulted in loss of tissue staining for the Chk2 threonine-68 antibody (Figure 3.10). These experiments validate the phosphospecificity of the Chk2 threonine-68 antibody.

3.2.3.1 ATM, Chk2 and Chk2 threonine-68 staining

Two-thirds (62 %) of MSS cancers and three quarters (74 %) of MSI cancers showed no or low ATM staining. High or moderate Chk2 staining was observed in 62 % of both MSS and MSI cancers.(Figure 3.11A) Certain mutant Chk2 proteins are more unstable than wild type; therefore, high staining levels may indicate the presence of wild-type protein, although this requires confirmation by genetic analysis. In all cancers, there was a positive correlation between ATM and Chk2 staining (P = 0.002). Chk2 threonine-68 staining was present in 22 % of microsatellite-stable tumours and in 33 % of tumours with the microsatellite instability phenotype.

3.2.3.2 p53 and p21 staining

Of the MSS cancers, 43 % had low levels of p53 immunostaining (suggesting the presence of wild-type protein) and 55 % had moderate-to-high p53 staining (suggesting that p53 was mutated). In contrast, 66 % of MSI cancers had low levels

of p53 staining and 23 % had moderate-to-high levels of p53 staining (Figure 3.11B). This data is consistent with the published literature (Midgley and Lane, 1997).

In human CRC, loss of p21 expression is associated with high p53 expression. Both MSI and MSS cancers had approximately 85 % low-grade p21 staining. Holland *et al.* reported that strong staining for p21 in the crypts of normal colon cells and correlated loss of staining or low staining with poorer survival (Holland *et al.*, 2001). In all cancers, there was an inverse correlation between p53 and ATM ($P = 0.023$) and an inverse correlation between p53 and p21 expression in MSS cancers ($P = 0.026$); these results are consistent with published data (Bukholm and Nesland, 2000).

3.2.3.3 MRN complex staining

Over 90 % of MSS cancers had no or low staining for Mre11 and Rad50; in contrast, 80% and 88% of MSI cancers had no or low staining of Mre11 and Rad50, respectively. The pattern of Nbs1 staining was different: 53 % of MSS cancers and 41 % of MSI cancers exhibited low Nbs1 staining. Moderate-to-high NBS staining was observed in 25 % and 42 % of MSS and MSI cancers, respectively.(Figure 3.12) There were no significant associations between the levels of different MRN component proteins. Therefore, alterations to MRN protein levels may be a late event in the development of colorectal cancer, following mutations in other genes.

3.2.3.4 p53 staining intensity and Chk2 threonine-68 detection

Activation of the DDR has been shown to precede the development of chromosomal instability (Bartkova *et al.*, 2005b). In this series of colorectal cancers, all cancers that were negative for p53 staining were also negative for Chk2 threonine-68

staining, although the numbers are too small to draw any definite conclusions. Chk2 threonine-68 was detected in cancers of both the MSI and MSS phenotypes, reflecting activation of the DDR, and levels of Chk2 threonine-68 expression correlated with p53 staining intensity (Figure 3.13); this correlation was statistically significant in the MSS cancers (Chi-squared test; $P = 0.041$). This observation supports the hypothesis that DDR activation precedes the development of chromosomal instability, including p53 mutations. A higher proportion of MSI cancers stained for phosphorylated Chk2, which may reflect the increased burden of genetic instability created by mismatch repair-deficiency. Alternatively, it may reflect the activation of compensatory DNA repair processes.

3.3 Discussion

TMA are miniature platforms for the assessment of defined sets of tumour samples, as opposed to conventional immunohistochemistry which analyses single specimens. In this cohort of 186 cancer samples, 71 cancers had previously been IHC assessed for p53 using conventional single specimen processing and binary analysis of staining. Conventional IHC assessment of p53 was either low/normal or negative in 32 cancers, and this correlated well with TMA-generated histoscores; the majority of tumours (27/32; 84 %) had a histoscore of less than 100. Positive or high staining was previously demonstrated in 39 of the colorectal cancers and was also seen in 72 % (28/39) of TMA specimens. Differences in antigen retrieval and antibody specificity were not further considered in this analysis. Thus, TMA technology is a robust and reliable method for analysing tissue populations.

An activated ATM dependent DDR is considered to be present when phosphorylated proteins such as ATM serine1981, H2AX serine 139 (γH2AX), Chk2 threonine 68, and p53 serine 15 are present. In the original articles Chk2 threonine 68 was used as a marker of an activated ATM DDR as it is not often mutated in cancer unlike p53 and is not inherently overexpressed.

A previous study (Oka *et al.*, 2010) analysed DDR activation by assessing ATM serine-1981, Chk2 threonine-68 and γ-H2AX phosphorylation in 55 surgically resected adenomas and colorectal cancers; they reported that 6 %, 1 % and 8 % of cells had positively nuclear staining, respectively, for these phosphoproteins. However, it is unclear whether all of the specimens showed evidence of a DDR. There was evidence of an activated DDR in advanced cancers compared with normal tissues; however, no data was presented for commonly associated genetic mutations. In this study, treatment naïve cancers (Bubb *et al.*, 1996) were used to create the TMA to inform of activation of the DDR. Limited data were available to asses the impact of an activated DDR on the site of lesion, treatment response or survival. Nevertheless, analysis of all cancers revealed that ATM expression positively correlated with Chk2 expression and inversely with p53 staining. This suggests that high ATM (and Chk2) expression is associated with low p53 (or wild-type) expression. ATM downregulation correlated with high p53 levels, perhaps reflecting a more stabilised protein or mutant p53 status. In response to DNA damage, ATM and p53 function in a linear pathway. Thus, inactivation of p53 and reduced ATM expression could be considered as “two hits” in the same pathway; this may explain resistance to chemotherapy exhibited both by the inability to sense and repair DNA damage and to undergo apoptosis. Knappskog *et al.* (2012) reported that resistance to

DNA damaging agents significantly associated with low ATM expression or p53 and/or Chk2 mutations in breast cancer. However, they did not report any defects in the DSB DNA repair pathway (i.e., BRCA). Therefore, it is unclear whether the chemoresistance may be due to attenuation of the ATM–p53 apoptotic pathway or to ATM-independent p53 cell cycle arrest.

In this study, the majority of sporadic colorectal cancers exhibit the MSS phenotype and approximately 55 % of these cancers demonstrated moderate-to-high p53 staining, suggesting that a large proportion of these cancers harbour mutant p53. IHC assessment of p53 staining is a valid surrogate marker of p53 mutational status when done using strict criteria (Nyiraneza *et al.*, 2011). Using p53 staining as a prognostic and predictive marker has led to conflicting results, partly due to the use of homogeneous patient groups and the absence of a validated framework in which to assess staining patterns. p53 mutation is a late event in the development of microsatellite-stable cancers and reflects chromosomal instability at 17p (Hollstein *et al.*, 1991). The negative association between p53 and p21 levels confirms the biological role of p21 as a p53 target gene (Deng *et al.*, 1995; el-Deiry *et al.*, 1994). Although evidence suggests that DNA DSB can result in chromosomal instability, it is less clear whether this leads to activation of the DDR in colorectal cancers (Li *et al.*, 2004; Raynaud *et al.*, 2008a). Chromosomal instability is a major molecular feature of the autosomal recessive condition ataxia telangiectasia, suggesting that defective ATM signalling is a key feature of this phenotype (Shiloh, 2003). Robust activation of the DDR pathway has been described in precancerous lesions, which appear to be reduced longitudinally as cancer develops. Bladder cancers that demonstrate high levels of genomic instability have variable staining for Chk2

threonine-68 (Bartkova *et al.*, 2004) compared with cancers with lower genomic instability. This presumably reflects increased molecular and genetic heterogeneity as the cancer develops, resulting in varying degrees of (in)activation of the DDR. Chk2 threonine-68 phosphorylation is considered a surrogate marker for activation of the DDR signalling pathway and is present in approximately one fifth of microsatellite-stable cancers. The absence of an activated DDR pathway in the majority of microsatellite-stable cancers suggests that these cancers circumvent the response and repair of DNA damage, which may reflect an aggressive cancer phenotype and a poorer prognosis following DNA damage-inducing therapy. Alternatively, activation of the ATM-dependent DDR and high levels of chromosomal instability may represent a dependency on the DNA repair machinery; however, this effect was not further evaluated in the current study.

In contrast, the majority (66 %) of microsatellite-unstable cancers exhibit low p53 staining, reflecting the distinct molecular characteristics of these cancers. Low, restricted nuclear p53 staining has been significantly associated with MSI-H cancers (Nyiraneza *et al.*, 2011). Although MSI-positive cancers have a less aggressive phenotype, they do demonstrate resistance to particular therapies as the toxic DNA lesion is not recognised by the defective MMR machinery. MSI-H cancers have been shown to be resistant to 5-fluorouracil therapy, partly due to the defective mismatch repair proteins and to high levels of the enzyme thymidylate synthase, which 5-fluorouracil competitively inhibits (Carethers *et al.*, 2004; Ribic *et al.*, 2003; Ricciardiello *et al.*, 2005; Wang *et al.*, 2004a). Activation of DDR, indicated by Chk2 threonine-68 phosphorylation, was demonstrated approximately one-third of these cancers. Nbs1 protein expression was higher in MSI cancers compared with the

MSS cancers. These results suggest that different pathways are activated in the MSI-H cancers. Brown *et al.* (2003) reported physical interactions between MLH1 and ATM and between MSH2 and Chk2, suggesting that these associations are required to induce an effective DNA damage S-phase arrest. Luo *et al.* (2004) reported that hMLH1-dependent nuclear localisation of the MMR proteins, hPMS1 and hPMS2, augmented the DNA damage- and ATM-induced p53 stabilisation and activation. The identification of the MMR complexes in DNA damage-induced foci also suggests that the MMR components may have a role in modulating the DDR (Wang *et al.*, 2000). Thus, activation of DDR in MSI cancers may reflect a compensatory response to defective MMR.

Robust activation of the DDR pathway has been described in precancerous lesions, and adaptation leads to mutations in downstream genes. Constitutive activation of the DDR in cancers may represent replication stress (i.e., unscheduled DNA synthesis), telomere shortening, DNA repair or a persistent signal to induce cellular apoptosis or senescence (Bartkova *et al.*, 2005b; Cangi *et al.*, 2008; Chen *et al.*, 2005a; Chen *et al.*, 2005b; Osborn *et al.*, 2002; Raynaud *et al.*, 2008a; Raynaud *et al.*, 2008b) It remains unclear as to whether constitutive activation of the DDR in cancerous lesions predicts treatment response, allowing the development of a rational approach to cancer therapy.

Table 3.1. Summary of DNA damage response proteins currently assessed in colorectal cancer cell lines and human tumour samples

Protein	Cell Lines	MSS CRC	MSI CRC	Hereditary CRC
ATM/ATR	***Ejima 1999***	***Beggs 2012*** ***Bartkova 2005***	***Lewis 2007*** ***Lewis 2005***	***Kim 2007***
MRN	***Gianni 2002***	***Wang 2004***	***Gianni 2004*** ***Miquel 2007***	***Alemaheyu 2007***
Chk2	***Takemura 2006***	***Williams 2006*** ***Bartkova 2005***		***Lee 2001***
Chk1	***Lewis 2005***		***Kim 2007*** ***Lewis 2007***	***Kim 2007***
p53	***O'Connor 1997*** ***Gayet 2001***	***Gervaz 2002*** ***Bartkova 2005***	***Bubb 1996***	***Vahteristo 2001***

Sources: (Alemayehu and Fridrichova, 2007; Bartkova *et al.*, 2005b; Beggs *et al.*, 2010; Bubb *et al.*, 1996; Ejima *et al.*, 2000; Gayet *et al.*, 2001; Gervaz *et al.*, 2002; Giannini *et al.*, 2004; Giannini *et al.*, 2002; Kim *et al.*, 2007; Lee *et al.*, 2001; Lewis *et al.*, 2007; Lewis *et al.*, 2005; Miquel *et al.*, 2007; O'Connor *et al.*, 1997; Takemura *et al.*, 2006; Vahteristo *et al.*, 2001; Wang *et al.*, 2004b; Williams *et al.*, 2006).

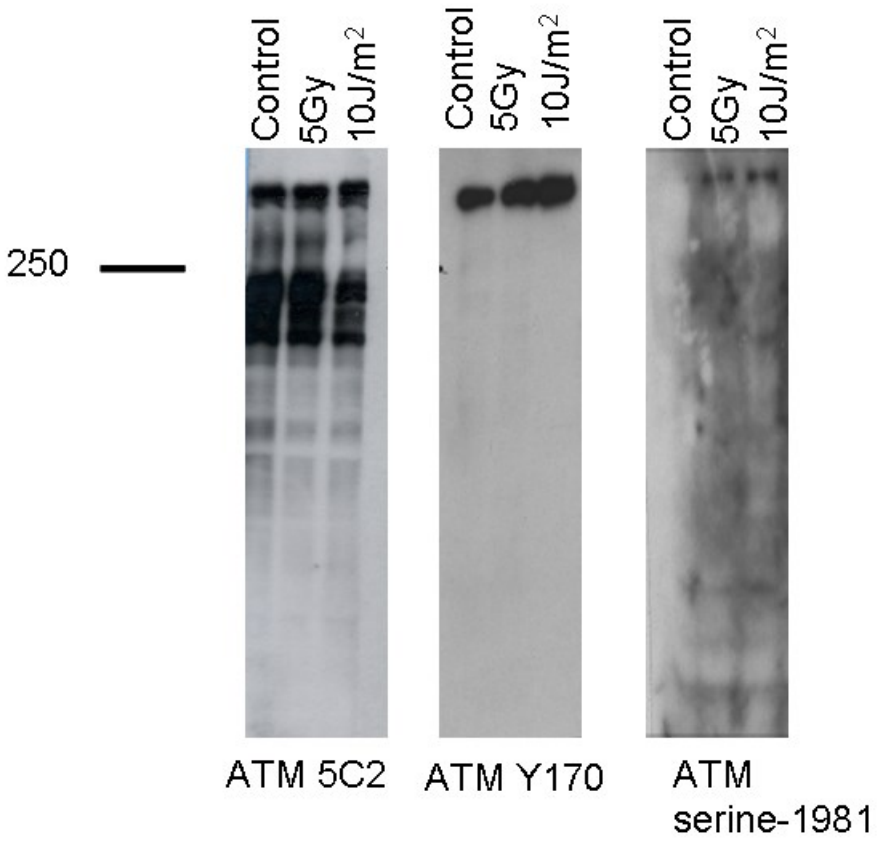

Figure 3.1. DNA damage induction of the 350 kDa ATM protein in U20S osteosarcoma cells. Cells were treated with 5 Gy IR or 10 J/m^2 ultraviolet radiation and harvested after 2 h. Equal amounts of cell lysate was analysed by immunoblotting (75 μg/lane). Membranes were probed with ATM 5C2, ATM Y170 and ATM serine-1981 antibodies. A protein band is induced above the 250 kDa marker following DNA damage.

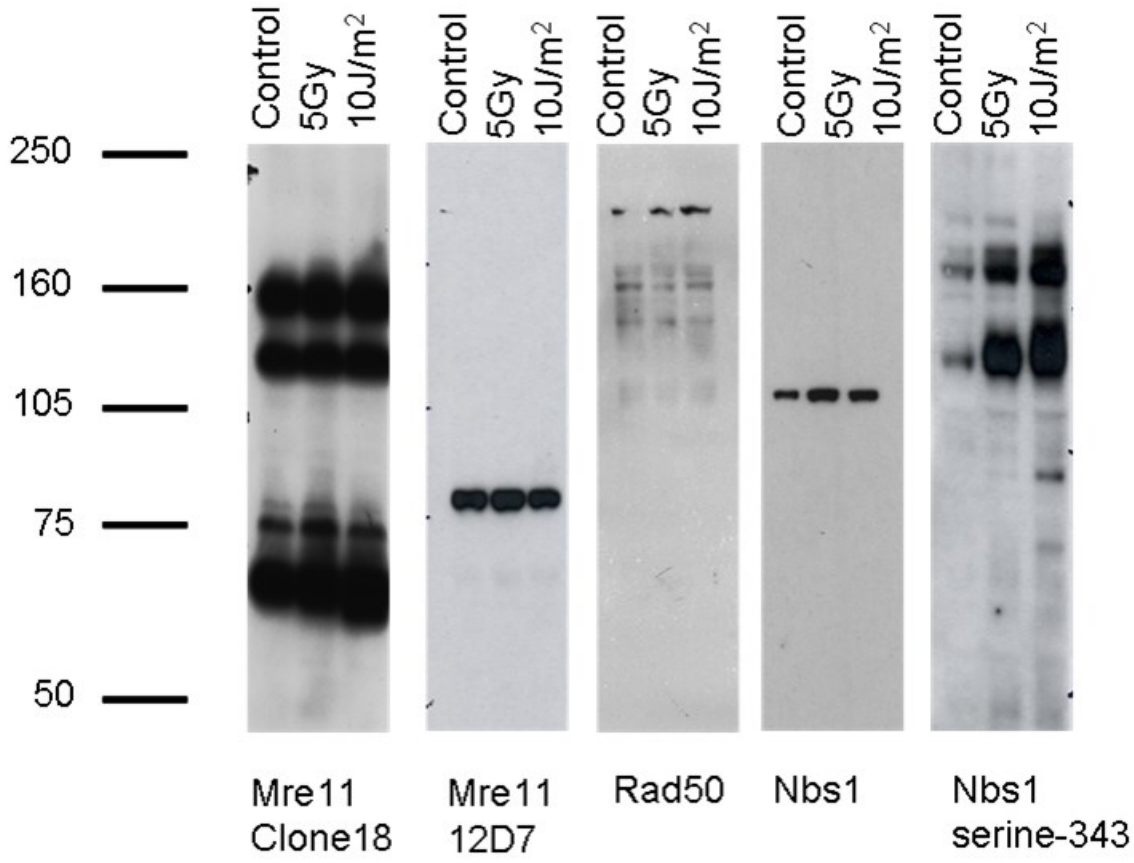

Figure 3.2. DNA damage induction of the MRN complex in U20S osteosarcoma cells.

Cells were treated with 5 Gy IR or 10 J/m^2 ultraviolet radiation and harvested at 2 h. Equal amounts of cell lysate was analysed by immunoblotting (75 µg/lane). Membranes were probed with Mre11 clone18, Mre11 12D7, Nbs1, Nbs1 serine-343, and Rad50 antibodies. A protein band is induced above the 105 kDa marker following DNA damage.

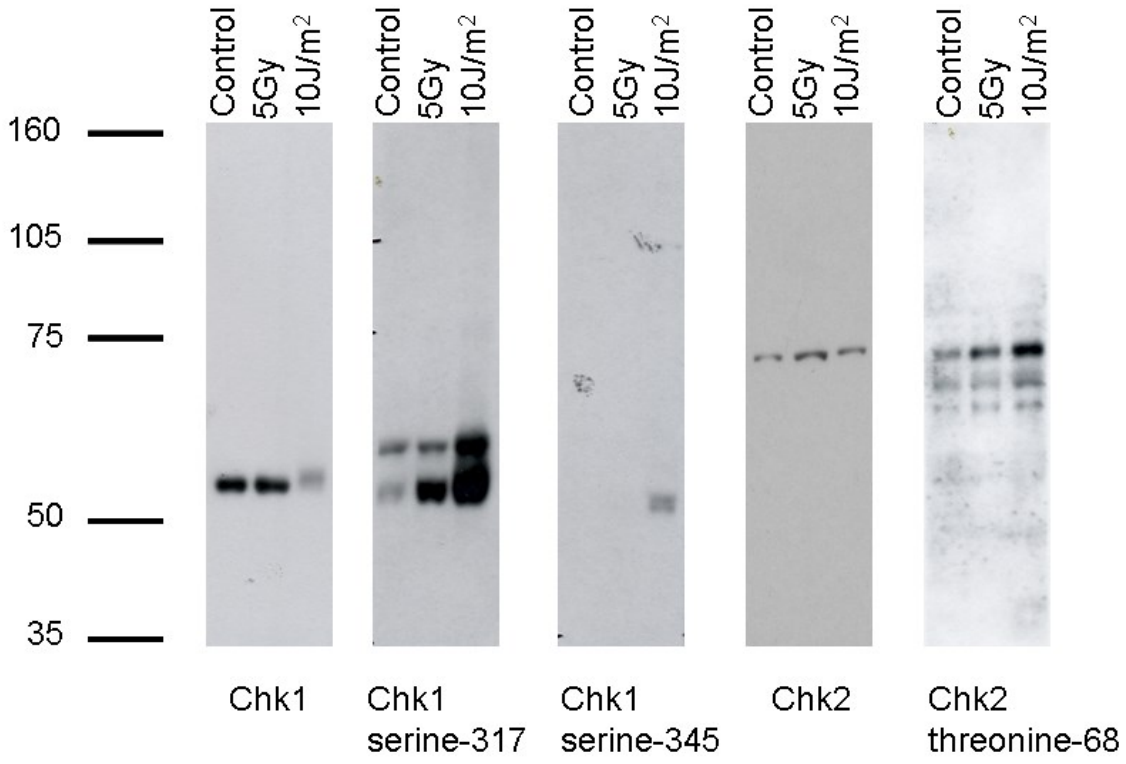

Figure 3.3. DNA damage induction of checkpoint kinase proteins in U20S osteosarcoma cells. Cells were treated with 5 Gy IR or 10 J/m^2 ultraviolet radiation and harvested at 2 h. Equal amounts of cell lysate was analysed by immunoblotting (75 μg/lane). Membranes were probed with Chk1, Chk1 serine-317, Chk1 serine-343, Chk2 A11 and Chk2 threonine-68 antibodies. A protein band is induced above the 50 kDa marker following DNA damage.

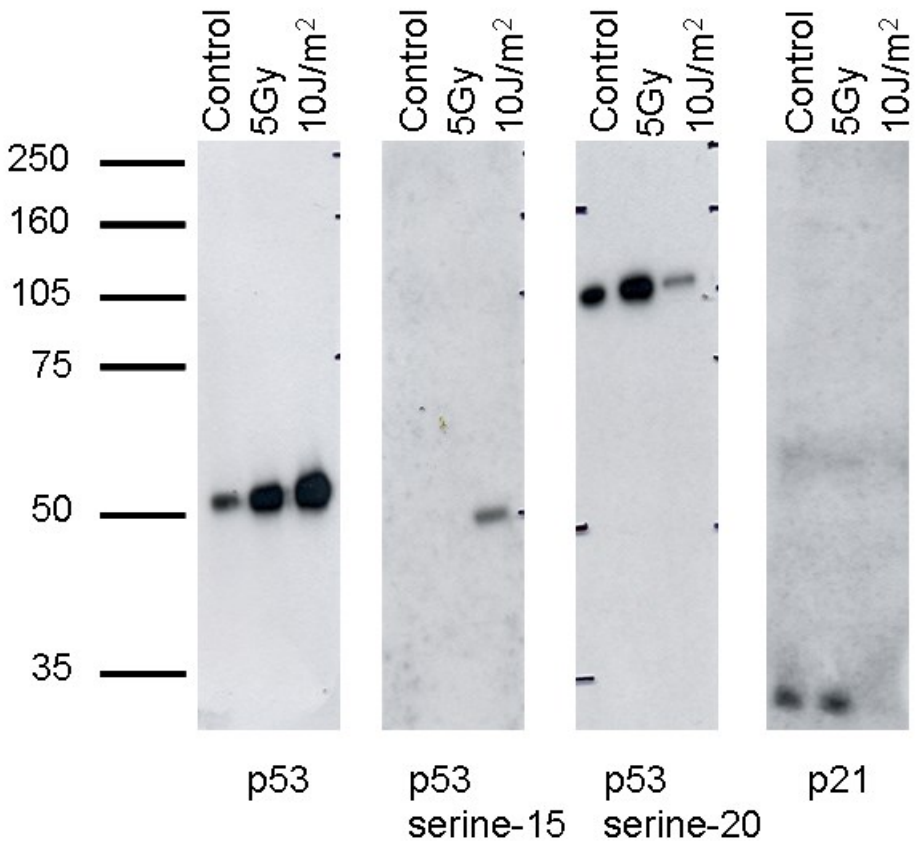

Figure 3.4. DNA damage induction of p53 and p21 proteins in U20S osteosarcoma cells.
Cells were treated with 5 Gy IR or 10 J/m^2 ultraviolet radiation and harvested at 2 h. Equal amounts of cell lysate was analysed by immunoblotting (75 μg/lane). Membranes were probed with p21, p53, p53 serine-15 and p53 serine-20 antibodies. A protein band is induced above the 50 kDa marker following DNA damage.

Table 3.2. Summary of antibody specificity for immunohistochemistry

Protein	Size (KDA)	Antibody	Origin	Immunoblot	IHC
ATM 5C2	350	Abcam	Mouse monoclonal	Multiple bands	No
ATM Y170	350	Abcam	Rabbit monoclonal	Single band	Yes
ATM serine-1981	350	Abcam 2888	Rabbit polyclonal	Single band	Yes
Mre11 clone18	79	BD Biosciences	Mouse IG1	Multiple bands	No
Mre11 12D7	79	Abcam	Mouse monoclonal	Single band	Yes
Rad50	153	Novus biologicals	Rabbit polyclonal	Multiple bands	Yes*
Nbs1	95	Abcam 398	Rabbit polyclonal	Single band	Yes
Nbs1 serine-343	95	Abcam 15088	Rabbit polyclonal	Multiple bands	Yes*
Chk1 G4	56	Santa Cruz	Mouse monoclonal	Single band	Yes
Chk1 serine-317	56	Cell Signaling Technology	Rabbit polyclonal	Two bands	Yes*
Chk1 serine-345	56	Cell Signaling Technology	Rabbit polyclonal	Single band	Yes
Chk2 A11	62	Santa Cruz	Mouse monoclonal	Single band	Yes
Chk2 threonine-68	62	Cell Signaling Technology	Rabbit polyclonal	Multiple bands	Yes*
p53 D01	53	Calbiochem	Mouse monoclonal	Single band	Yes
p53 serine-15	53	Cell Signaling Technology	Rabbit polyclonal	Single band	Yes
p53 serine-20	53	Cell Signaling Technology	Rabbit polyclonal	No signal	No
p21	21	Calbiochem	Mouse monoclonal	Single band	Yes

Tabulated summary of Figures 3.1–3.4, describing the antibodies used, the predicted molecular weight, and antibody specificity and suitability for immunohistochemistry (IHC). *Although these antibodies recognise more than a single band; it is likely that the protein remains in a complex (not disrupted by the lystate preparation) with other proteins or has undergone further post translational modifications as detected at similar predicted size.

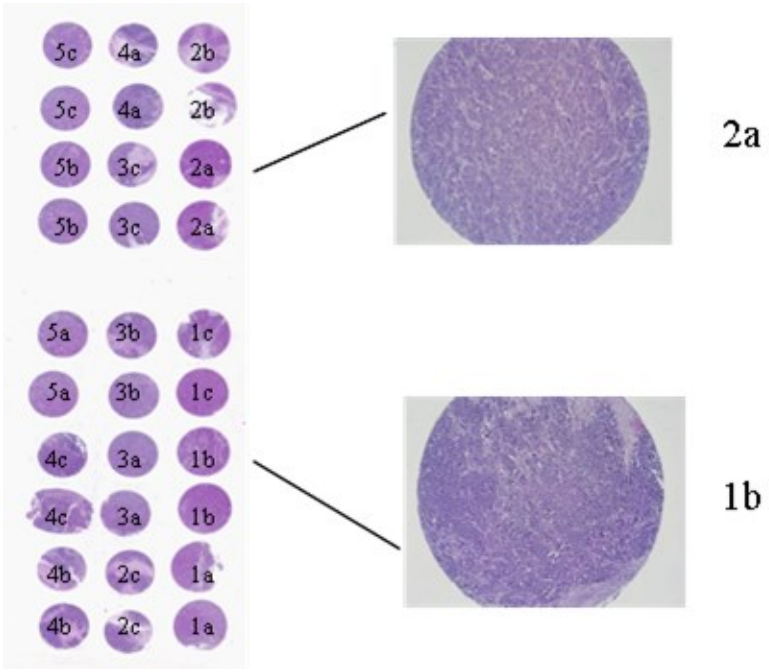

Figure 3.5. Xenograft tissue microarray.

Xenograft tissue microarray was created using 2 × 1 mm cores from triplicate xenografts (a-c) derived from HCT116 (1), HCT-8 (2), HCT15 (3), SW-620 (4) and HT29 (5) colorectal cancer cell lines. Images 1b and 2a are high power field views of the corresponding cores.

A

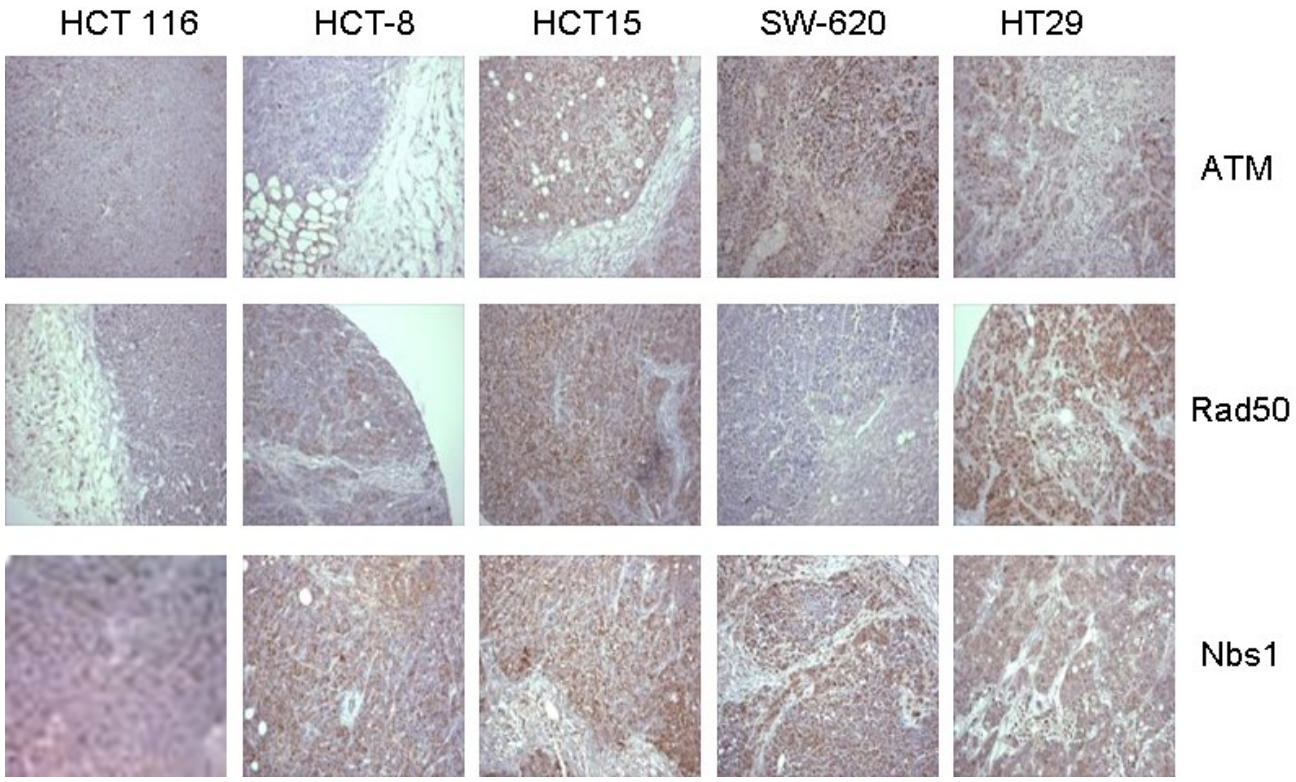

Figure 3.6. DDR protein expression in xenograft models.

The expression of the DNA damage response proteins was assessed immunohistochemically using (*A*) ATM, Nbs1 and Rad50 antibodies and (*B; next page*) Chk2, Chk2 threonine-68, p53, p53 serine-15 and p21 antibodies. Representative cores of each xenograft stained with selected antibodies are shown.

B

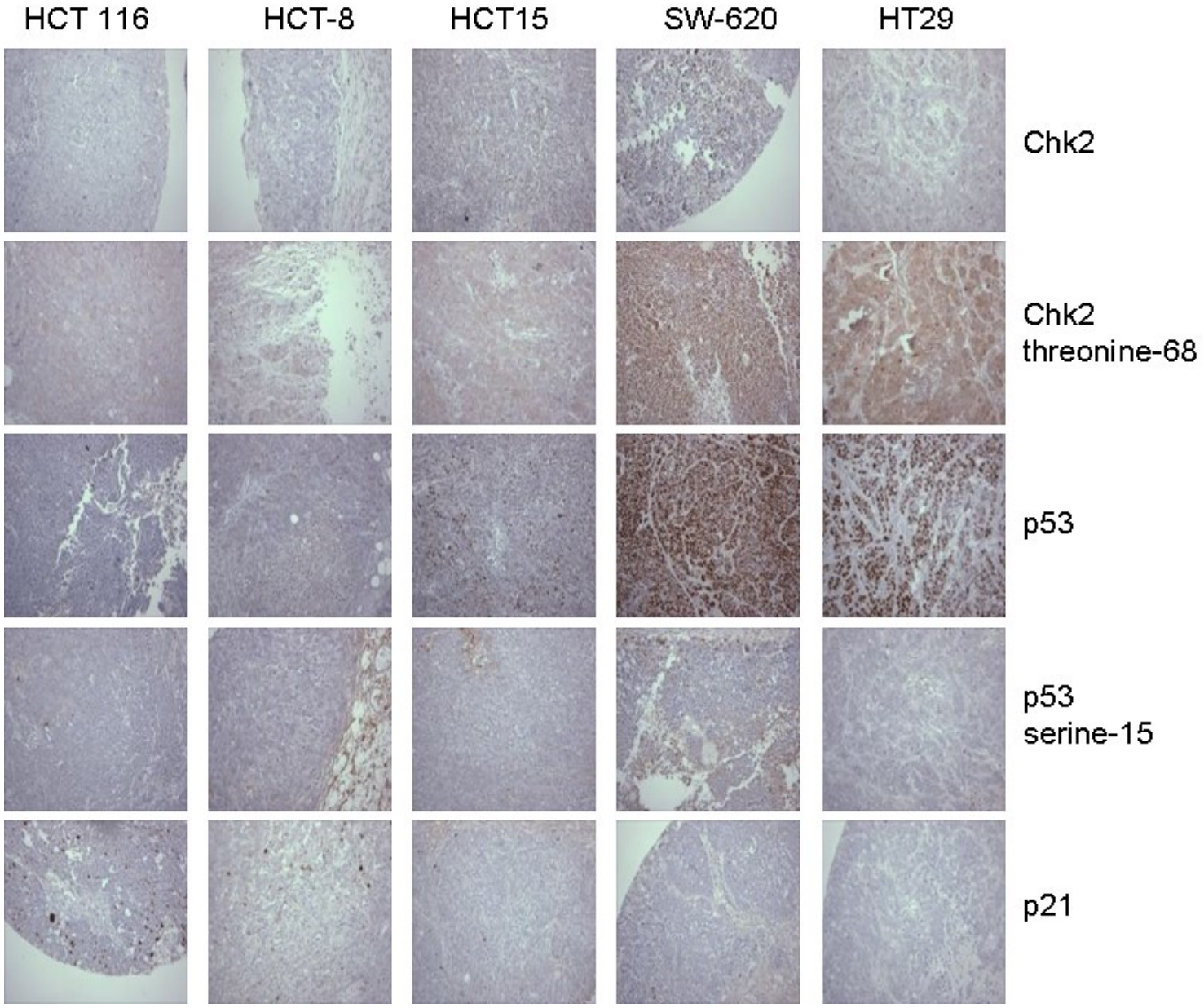
HCT 116
HCT-8
HCT15
SW-620
HT29
Chk2
Chk2
threonine-68
p53
p53
serine-15
p21

Table 3.3. Nuclear histoscores generated by scoring xenograft tumour microarrays by two observers

A

Antibody	**HCT116**		**HCT-8**		**HCT15**		**SW-620**		**HT29**	
Histoscore	A	B	A	B	A	B	A	B	A	B
ATM	45	42.5	76	83	140	126	66	72.5	116	112
Rad50	0	3	150	108	200	253	57	20	247	280
Nbs1	190	200	90	102	58	100	122	93	80	92
Chk2	0	0	0	0	0	0	42	31	37	50
Chk2 threonine-68	0	0	0	0	0	0	165	177	170	123
p53	3	2	0	0	35	33	210	240	173	205
p53 serine-15	0	0	0	0	0	0	1	15	0	0
p21	33	58	13	17	2	7	1	0	0	0

B

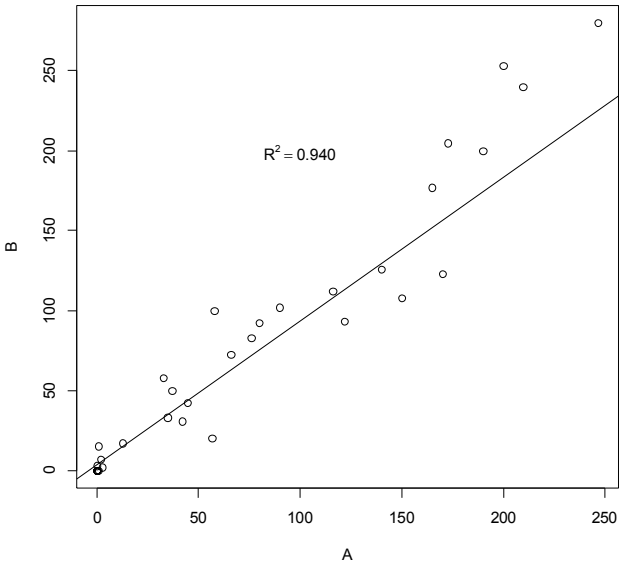

Histoscore is a composite scoring method based on assessing the proportion of cells stained and the intensity of antibody staining. (*A*) Two independent individuals (A & B) analysed and histoscored the nuclear antibody staining. (*B*) Intra-observer agreement was analysed by the $R^2 = 0.94$).

Figure 3.7. Colorectal cancer tumour microarray.

Each CRC slide was sectioned and H&E stained to assess architectural preservation of tumour tissue and select suitable areas to be cored. Three × 0.6 mm cores of each colorectal cancer sample were placed into individual microarray paraffin blocks using a Beecher instrument.

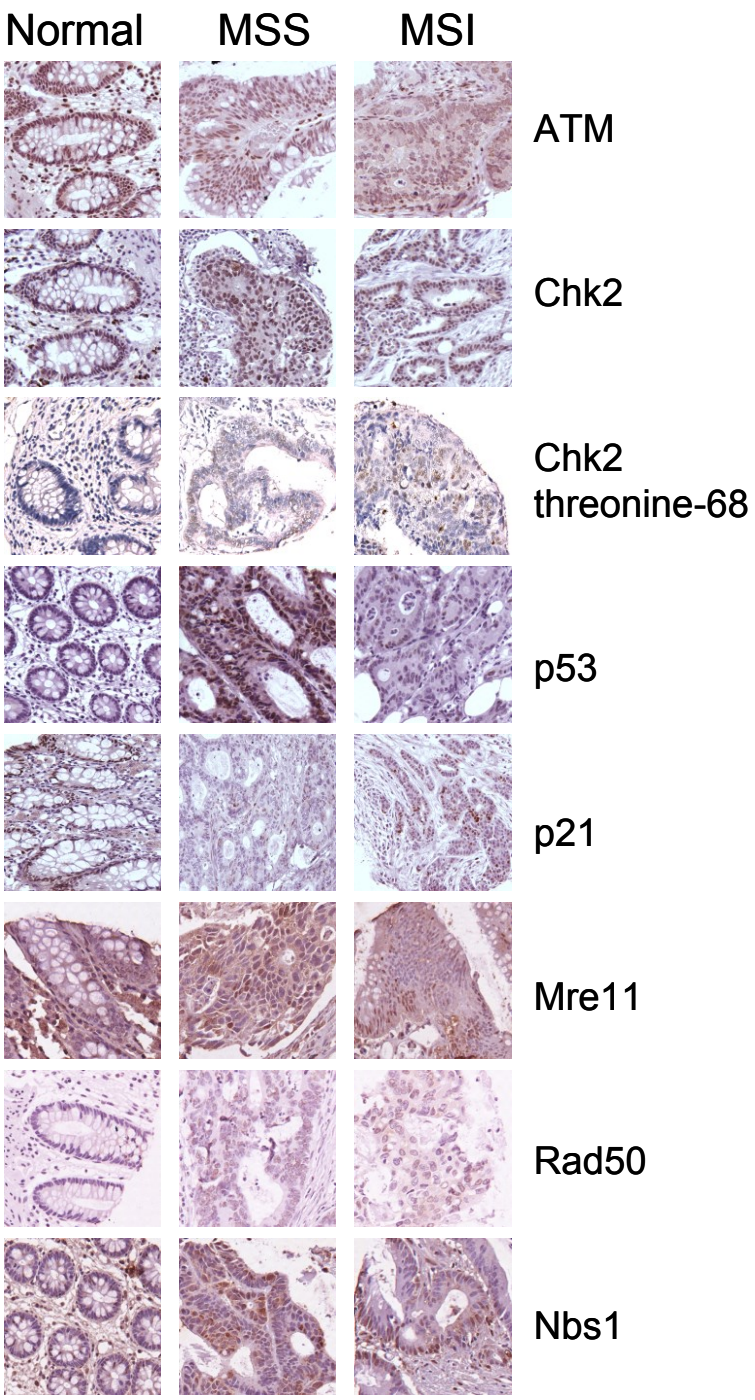

Figure 3.8. DDR protein expression on human colorectal tumour microarray.

The expression of the DNA damage proteins was assessed immunohistochemically using the antibodies described above. Representative cores of each cancer were stained using ATM, Chk2, Chk2 threonine-68, p21, p53, Mre-11, Nbs1 and Rad50 antibodies. MSI, Microsatellite instability; MSS, Microsatellite stable.

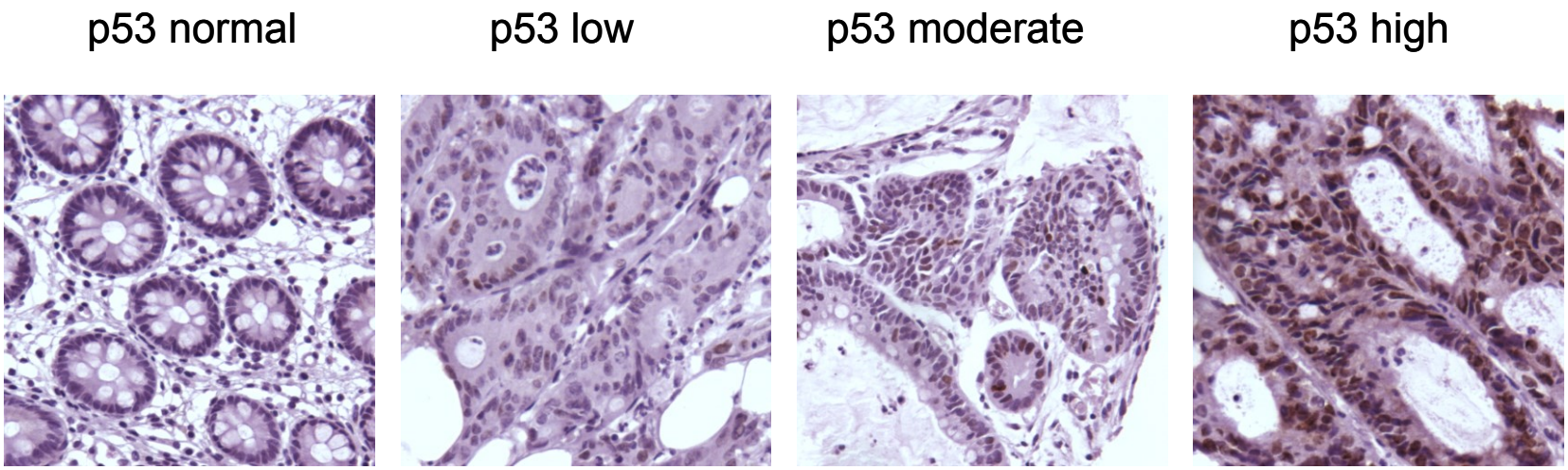

Figure 3.9. Analysis of p53 immunostaining in colorectal cancer cores.

p53 immunostaining was undertaken and staining intensity and the proportion of cancer cells stained were used to calculate the histoscore. Low staining, histoscore 0–100; moderate staining, histoscore 101–200; high staining, histoscore 201–300.

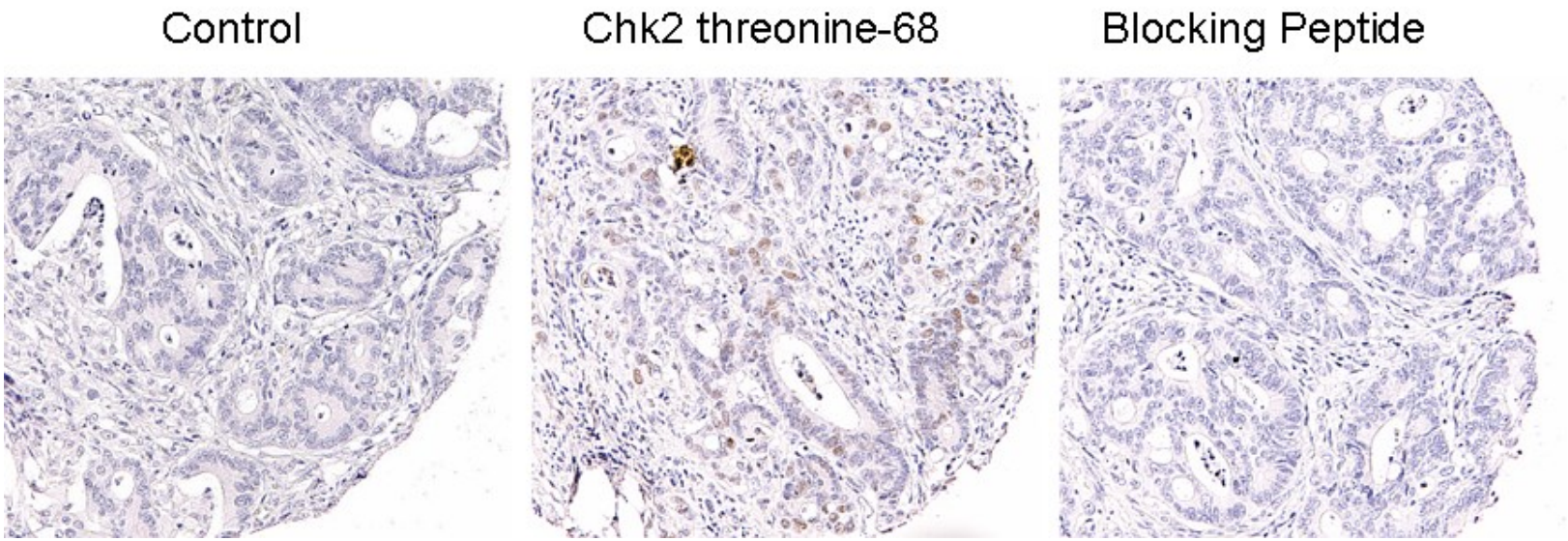

Figure 3.10. Phosphospecificity of Chk2 threonine-68 antibody.

Phosphospecificity of the Chk2 threonine-68 antibody was assessed using competitive peptide blockade. Antibody incubation with the blocking peptide prevents Chk2 threonine-68 staining in the same tumour core.

A

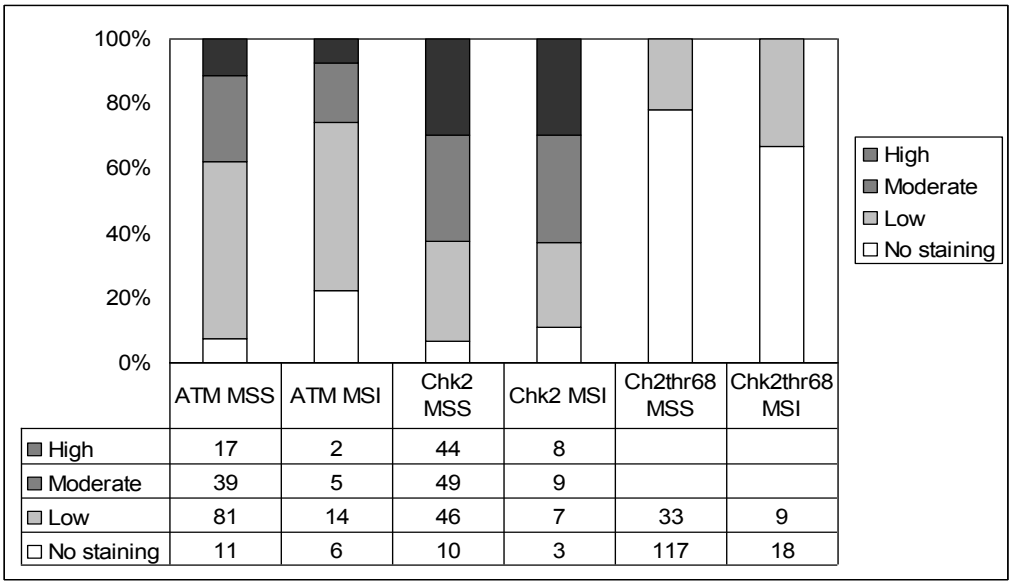

	ATM MSS	ATM MSI	Chk2 MSS	Chk2 MSI	Ch2thr68 MSS	Chk2thr68 MSI
High	17	2	44	8		
Moderate	39	5	49	9		
Low	81	14	46	7	33	9
No staining	11	6	10	3	117	18

B

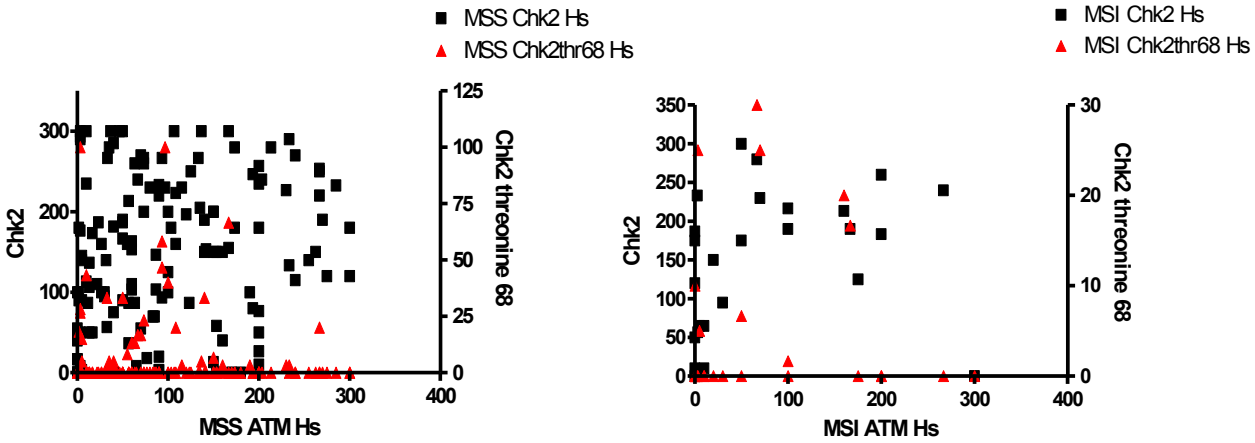

Figure 3.11. ATM, Chk2 and Chk2 threonine 68 protein expression in a human colorectal tumour microarray.

(*A*). ATM, Chk2 and Chk2 threonine-68 staining (Chk2thr68) staining were evaluated according to type of colorectal cancer. Staining was absent (white); or detected at low (light grey), moderate (dark grey) or high (black) levels. (B) Scatter plots depicting association between staining patterns. MSI, Microsatellite instability; MSS, Microsatellite stable.

A

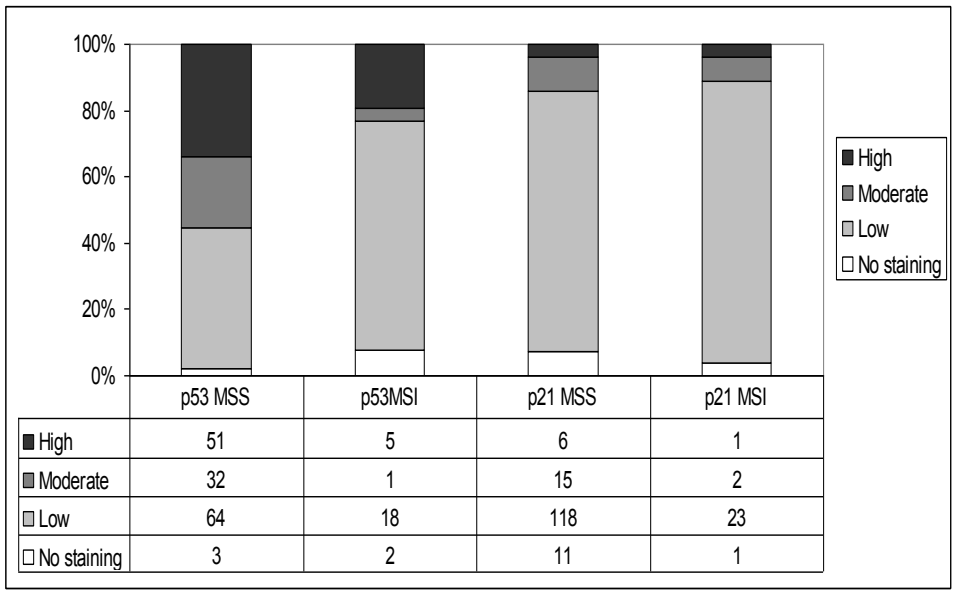

	p53 MSS	p53MSI	p21 MSS	p21 MSI
High	51	5	6	1
Moderate	32	1	15	2
Low	64	18	118	23
No staining	3	2	11	1

B

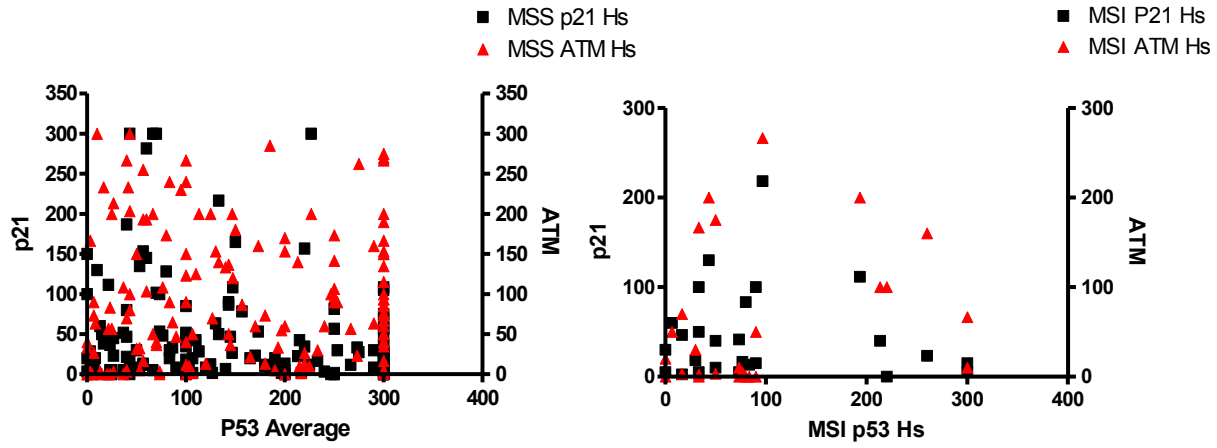

Figure 3.12. p53-p21 axis and ATM protein expression in a human colorectal tumour microarray.

(*A*). p53, and p21 staining were evaluated according to type of colorectal cancer. Staining was absent (white); or detected at low (light grey), moderate (dark grey) or high (black) levels. (*B*) Scatter plots depicting association between staining patterns of p53, p21 and ATM. MSI, Microsatellite instability; MSS, Microsatellite stable.

A

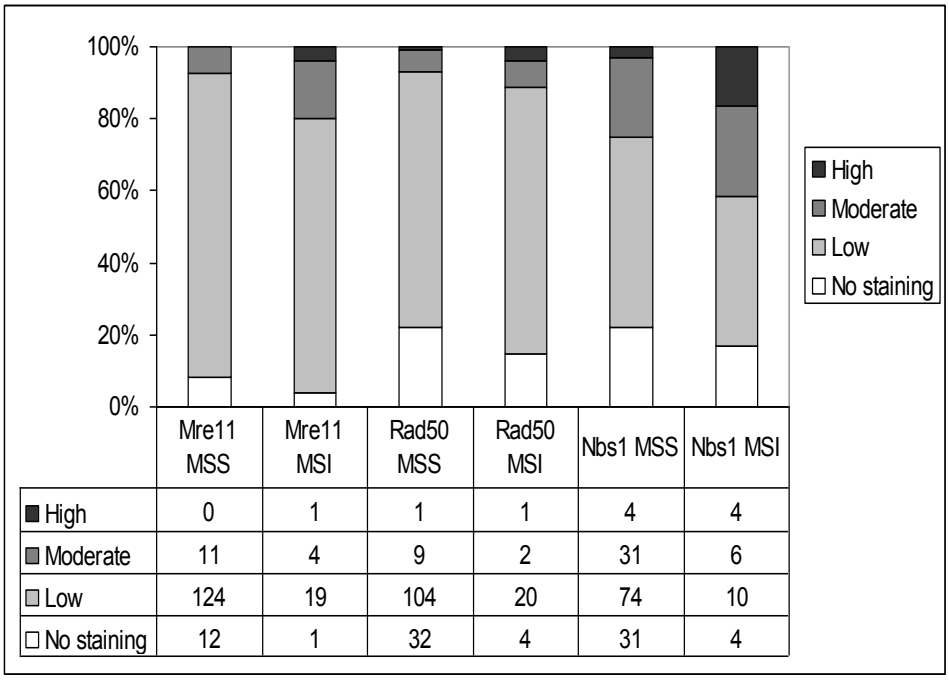

	Mre11 MSS	Mre11 MSI	Rad50 MSS	Rad50 MSI	Nbs1 MSS	Nbs1 MSI
High	0	1	1	1	4	4
Moderate	11	4	9	2	31	6
Low	124	19	104	20	74	10
No staining	12	1	32	4	31	4

B

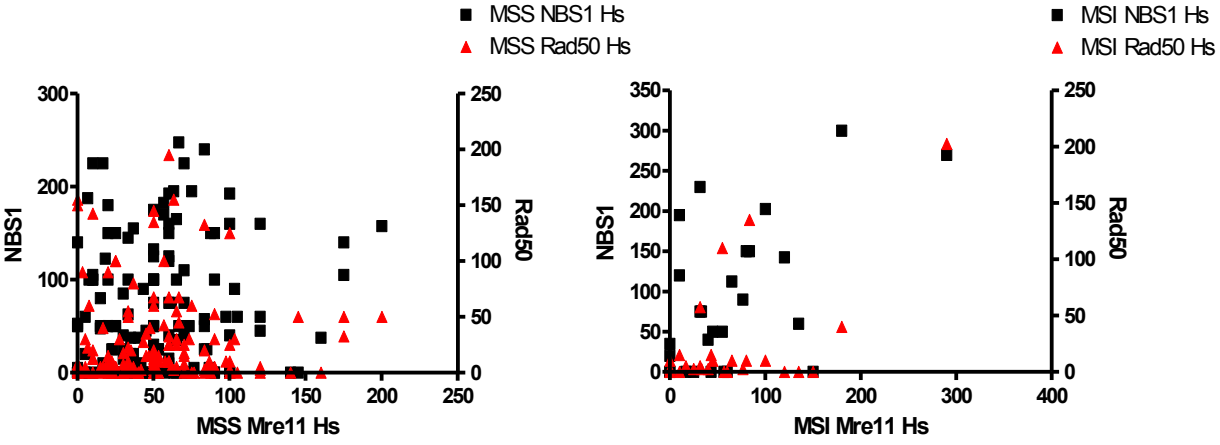

Figure 3.13. MRN component expression in a human colorectal tumour microarray.

Summary of Mre11, Rad50 and Nbs1 staining, classified by type of colorectal cancer. Staining was absent (white); or detected at low (light grey), moderate (dark grey) or high (black) levels. MSI, Microsatellite instability; MSS, Microsatellite stable. (*B*) Scatter plots depicting association between staining patterns of p53, p21 and ATM.

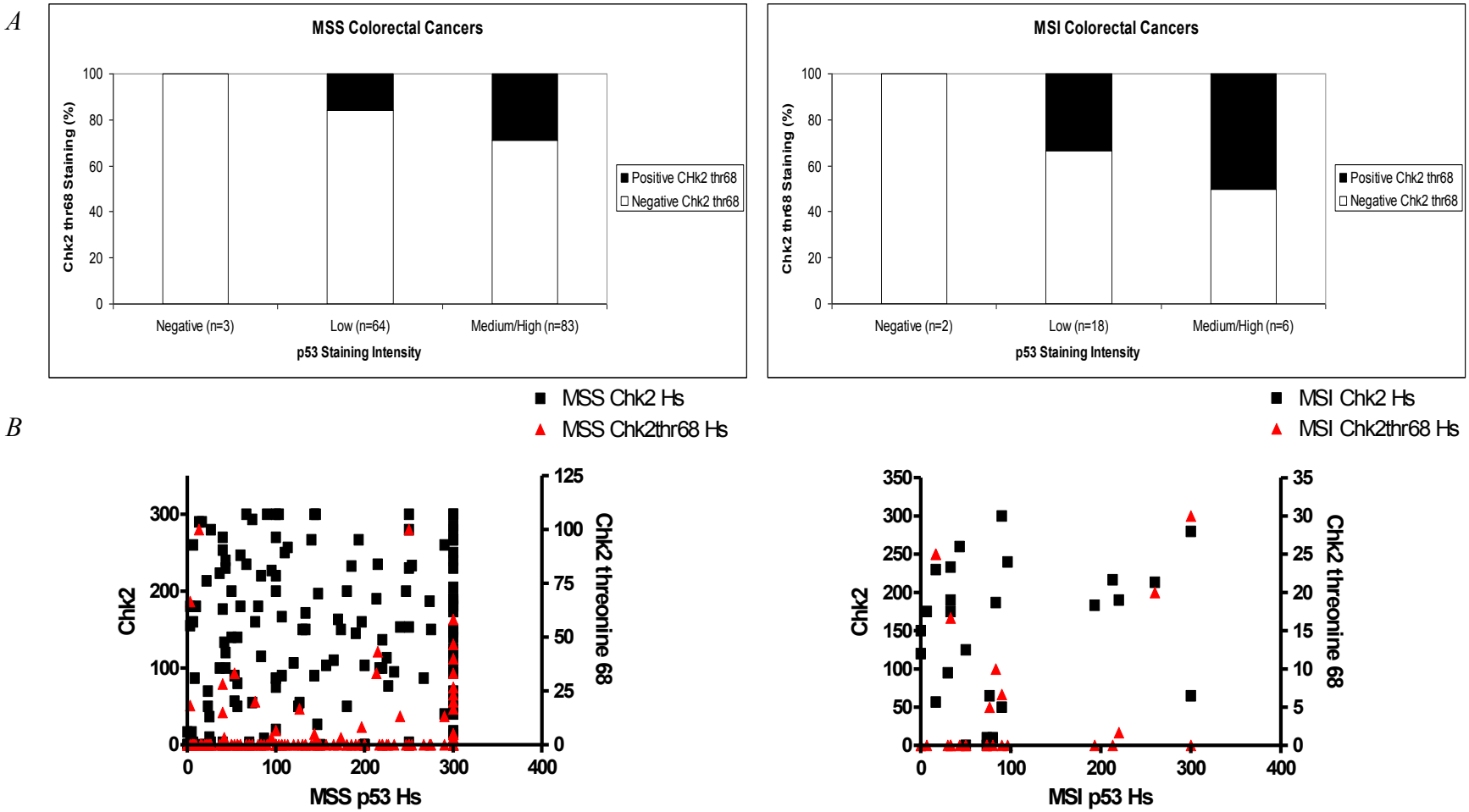

Figure 3.14. Relationship between p53 staining intensity and Chk2 threonine-68 staining.

For both (*A*). microsatellite stable (MSS) and microsatellite instable (MSI) colorectal cancers, Chk2 threonine-68 (Chk2 thr68) staining became more positive as p53 staining intensity increased. The overall proportion of Chk2 threonine-68 staining in MSI colorectal cancers was higher than in MSS cancers, presumably reflecting a higher burden of genetic instability or compensatory repair function. Chk2 threonine-68 staining is shown as absent (white) or positive (black). (*B*) Scatter plots of all data MSS and MSI data. MSI, Microsatellite instability; MSS, Microsatellite stable.

Table 3.4. Comparison of conventional single specimen immunohistochemistry and tissue microarray-generated histoscores for p53 immunostaining.

	TMA Hs <100	**TMA Hs 101-200**	**TMA Hs 201-300**
Normal/Negative	27	5	0
Positive/High	11	8	20

Seventy-one colorectal samples were previously analysed as single specimens using p53 immunostaining. Cancers derived from the same individuals were then formatted into a tissue microarray (TMA) and assessed for p53 immunostaining in this platform. Histoscore, Hs.

Chapter 4. p21-Null Cells Display Radioresistant DNA Synthesis

4.1 Introduction

The cytotoxic effect of current therapies for the treatment of cancer is related to their ability to induce DNA damage. The type of damage created depends on the particular treatment modality but may include altered bases, single- and double-strand breaks, inter strand cross-links and the formation of bulky DNA adducts (Norbury and Hickson, 2001). DSB are a particularly detrimental form of DNA damage, which can be caused by endogenous processes (Carney *et al.*, 1998; Dasika *et al.*, 1999) and as a therapeutic consequence of cytotoxics that create stalled replication forks, interstrand cross-links and other similar structural modifications. (Kuzminov, 2001b; Sancar *et al.*, 2004). The inherent ability to sense and repair different forms of DNA damage may undermine the efficacy of such approaches. Inhibition of key molecules within this network is an attractive approach that may potentiate the effects of radiotherapy and chemotherapy and overcome resistance to current cytotoxics (Madhusudan and Hickson, 2005).

Ataxia-telangiectasia mutated (ATM) is a nuclear protein kinase that has been implicated in orchestrating the response to DNA DSB by coordinating cell cycle arrest, DNA repair and apoptosis. In response to IR, DNA DSB are sensed by a number of proteins, including TRF2 and the Mre11–Rad50–Nbs1 complex. These subsequently recruit ATM and additional kinases, resulting in the phosphorylation of multiple substrates, including Nbs1, H2AX, p53, Chk2, Chk1. Upon DNA damage, cells in G1 phase are able to undergo a prolonged arrest through activation of the ATM–Chk2–p53–p21 pathway, thus retarding progression into S phase (Brugarolas

et al., 1995; Brugarolas *et al.*, 1999; Deng *et al.*, 1995; el-Deiry *et al.*, 1994; el-Deiry *et al.*, 1993). However, it can take several hours before p21 is transcriptionally upregulated and this pathway is induced. DNA synthesis can therefore be inhibited at the G1/S transition and during S phase by the rapid degradation of Cdc25A, induced by the ATM–Chk2/1–Cdc25A (or the ATR–Chk1–Cdc25A) pathway (Bartek *et al.*, 2004; Bartek and Lukas, 2003; Falck *et al.*, 2001; Mailand *et al.*, 2000) and by ATM-dependent activation of Nbs1, which appears to function exclusively in S phase (Heffernan *et al.*, 2002; Kastan and Lim, 2000; Shiloh, 2003). Degradation of the Cdc25A dual specificity protein phosphatase results in increased inhibitory phosphorylation on Cdk2 threonine-14 and tyrosine-15, thus inactivating the Cdk2/cyclin E and Cdk2/cyclin A complexes. A sharp decline in DNA synthesis occurs as new replication origins are inhibited (Kastan and Lim, 2000; Painter and Young, 1980), which is reinforced by full engagement of p21–Cdk2–Rb-dependent G1 arrest. p21 can also inhibit DNA synthesis by binding to proliferating cell nuclear antigen (PCNA), a subunit of DNA polymerase delta. The G2/M checkpoint serves to repair DNA damage accumulated during DNA synthesis prior to mitosis and to prevent segregation of damaged chromosomes during mitosis (Dasika *et al.*, 1999). Chk1 (and Chk2), a nuclear serine/threonine kinase, has a major role in this cell cycle phase by preventing premature mitotic entry following IR (Matsuoka *et al.*, 1998). p21 is also required to sustain G2/M arrest and allow exit from the cell cycle (Bunz *et al.*, 1998).

The *ATM* gene, located on chr11q22.3, is mutated in the autosomal recessive disorder ataxia telangiectasia that is characterised by extreme sensitivity to radiation (and other agents causing DSBs) and susceptibility to the development of

malignancies, especially those of lymphoid origin (Savitsky *et al.*, 1995). Cells from AT patients are defective in DSB processing and DNA damage checkpoint controls (Shiloh, 2003). In ATM deficiency, S-phase checkpoints are defective, which allows cells to continue synthesising DNA in the presence of DNA damage, a phenomenon termed radioresistant DNA synthesis; this is an established characteristic of AT cells. This phenotype has prompted investigation into the inhibition of ATM to increase the therapeutic effect of irradiation and DSB-inducing chemotherapies.

The HCT116 colorectal cancer cell line containing wild-type p53 is a suitable model for assaying DDR inhibitors as it demonstrates competent G1/S and G2/M checkpoints. In addition, the cell line has specific isogenic derivatives lacking checkpoint proteins that allows comparative assessments (Bunz *et al.*, 1998; Waldman *et al.*, 1995). HCT116 and its isogenic derivatives HCT116 p53-/- and HCT116 p21-/- (lacking the p53 and p21 proteins, respectively) have differing sensitivities to a variety of potential therapeutic agents that target different points of the cell cycle (Hayward *et al.*, 2003; Hayward *et al.*, 2005; Hill *et al.*, 2008a; Hill *et al.*, 2008b; Pietenpol *et al.*, 1994). The p53 and p21 proteins are downstream of ATM and have been shown to play important roles in cell cycle arrest following DNA damage. Disruption of the p21 gene *CDKN1A* results in constitutive activation of DDR pathways (Hill *et al.*, 2008a; Hill *et al.*, 2008b; Pang *et al.*, 2011). A constitutively activated DDR pathway would be fundamentally expected to have a robust checkpoint response to additional exogenous genotoxins. Conversely, the data presented here suggests that constitutive activation of the DDR represents a deregulated pathway that is unable to induce the downstream expected DNA damage induced checkpoint responses. This chapter describes a novel defect in the DNA

damage induced ATM-dependent intra-S-phase checkpoint in the absence of p21 and suggests that p21 may positively regulate ATM.

4.2 Results

4.2.1 HCT116 p21-/- cells display constitutive activation of the ATM-dependent DNA damage response and radioresistant DNA synthesis

In the absence of exogenous DNA damage, wild-type HCT116 cells have undetectable levels of ATM serine-1981, Chk2 threonine-68, Chk1 serine-317 and p53 serine-15 phosphorylation; these sites are all known targets of activated ATM (Figure 4.1). Phosphorylation at these sites is also absent in unstressed HCT116 p53-/- cells. In contrast, HCT116 p21-/- cells demonstrated basal phosphorylation at ATM serine-1981, Chk2 threonine-68 and p53 serine-15, but not at Chk1 serine-317 (Figure 4.1). Chk1 has been previously shown to be more robustly phosphorylated by the related protein, ATR, in response to replication-associated DSB (Takemura *et al.*, 2006). In addition, basal levels of Chk1, Chk2, and p53 proteins appeared to be higher in p21-null cells than in wild-type cells. These results suggest that the DDR pathway is constitutively activated in unstressed p21-null cells. To determine whether this is as a result of ATM activation, p21-null cells were treated with a specific ATM inhibitor, KU-55933 (a gift from KUDOS Pharmaceuticals). A dose of 10 μM has previously been demonstrated to inhibit ATM kinase activity in wild-type HCT116 cells (Pang *et al.*, 2011). Wild-type and p21-null HCT116 cells were incubated with 10 μM and harvested after 1, 2, 4, 12 and 24 h (Figure 4.2). There appeared to be a reduction in the overall expression of Chk2 and p53 proteins in wild-type cells after 2 h and after 24 h in the p21-null cell line. In wild-type cells, there was no detectable Chk2 threonine-68 or p53 serine-15 phosphorylation, as

demonstrated previously (Figure 4.1). In contrast, p21-null cells showed increased Chk2 threonine-68 and p53 serine-15 phosphorylation (Figure 4.1). Following addition of the ATM inhibitor, Chk2 threonine-68 phosphorylation was reduced after 1 h and undetectable thereafter, and p53 serine-15 phosphorylation was reduced after 4 h and undetectable at 12–24 h (Figure 4.2). Protein phosphorylation often results in stabilisation; therefore, treatment with kinase inhibitor may lead to dephosphorylation and proteins may therefore become destabilised, resulting in reduced expression. Loss of phosphorylation at Chk2 threonine-68 and p53 serine-15 and a reduction in total protein levels in the presence of a specific ATM inhibitor would confirm that the ATM kinase is constitutively active in these cells.

Constitutive activation of the DDR pathway has previously been shown to be a consequence of endogenous DNA damage resulting from oxidative and DNA replication stress (Lee and Paull, 2004; Schultz *et al.*, 2000). In p21-null cells, it is possible that a lack of p21 results in precocious Cdk/cyclin activity or an inability to regulate PCNA activity, thus resulting in unscheduled DNA synthesis generating high levels of replication and/or oxidative stress. In mammalian cells, the phosphorylated histone γ-H2AX is a sensitive surrogate marker for DNA damage, which localises to sites of DSB (Bekker-Jensen *et al.*, 2006; Gorgoulis *et al.*, 2005; Lukas *et al.*, 2004b). To determine whether constitutive activation of the ATM pathway is associated with increased levels of DNA damage in the absence of p21, both wild-type and p21-null HCT116 cells were analysed immunochemically for γ-H2AX staining (Figure 4.3A). γ-H2AX staining intensity was similar in both cell lines (Figure 4.3B), suggesting that increased levels of DNA damage may not be responsible for basal activation of the DDR in the absence of p21. To determine

whether the p21-null cells are responsive to exogenous DNA damage, cells were irradiated with 5 Gy, an inducer of the DDR pathway through the generation of DNA DSB, and harvested over a 24-h time course (Figure 4.4). In the parental HCT116 cell line, Chk2 threonine-68, p53 serine-15 and p53 levels were maximal after 2 h and Chk2 was stabilised at 12 h. Cdc25A was degraded at 2 h in the wild-type cells and recovered after 4–12 h (Figure 4.4). The absence of Cdc25A at 24 h most likely represents a second wave of DNA damage induced degradation or inhibition at the (epi) genetic or mRNA level enforcing and maintaining the G1 and G2/M arrests. As, anticipated, there was no detectable Chk1 serine-317 activation and Chk1 levels remained unchanged. In the wild-type cells p53 was able to induce p21 at 2 h and maximal at 24 h. These results would reflect an appropriate induction of the ATM-Chk2-p53-p21 and ATM–Chk2–Cdc25A DNA damage response pathway in the wild-type HCT116 cells. HCT116 p21-/- cells demonstrate basal phosphorylation of Chk2 threonine-68 and p53 serine-15 (Figure 4.1). In response to additional cellular stress Chk2 threonine-68 levels were further induced at 2 h and maximal at perhaps 12 h post-gamma irradiation. The Chk2 protein appeared to become more stable over the time course. The basal phosphorylation on p53 serine-15 was further induced at 2 h but there was no further increase in the p53 protein level. The Chk1 protein levels remained constant; however, Chk1 serine-317 was induced at 12–24 h, suggesting either accumulation of DNA damage and activation of additional upstream kinases such as ATR. As expected, no p53 induction of p21 was detected in p21-/- cells. In p21-/- cells, the overabundant Cdc25A is degraded after 2 h, but not as effectively as in the wild-type cells (Figure 4.4). Cdc25A levels recover at 4–24 h, suggesting that these cells continue to progress through G1/S transition phase and undergo DNA

synthesis. Vigneron *et al.* (2006) also reported that after treatment with DNA damaging agents Cdc25A levels remain elevated at 12–48 h in the p21-null derivatives compared with wild-type HCT116 cells. Using chromatin immunoprecipitaion, they provided evidence that ectopic expression of p21, was associated with the *CDC25A* promoter region complexed with STAT1 and E2F1 transcription factors suggesting a potential role in *CDC25A* transcriptional regulation. HCT116 p21-/- cells are therefore unlikely to induce an effective G1/S and intra-S-phase cell cycle arrest following DNA damage. These results suggest that the radiation-induced DDR pathway is attenuated in p21-null cells.

ATM is activated in response to DNA DSB resulting in delayed progression through the cell cycle by temporary arrest at the G1/S and S-phase checkpoints. Cell lines derived from individuals with the inherited condition ataxia telangiectasia (AT), in which the ATM protein is mutated and/or absent, display a defect in the IR-induced intra-S-phase checkpoint, termed radioresistant DNA synthesis (Houldsworth and Lavin, 1980; Painter and Young, 1980). To ascertain whether constitutively active ATM DDR represents a functional pathway in p21-null cells, DNA synthesis was assessed following 5 Gy irradiation. For this, asynchronously growing cells were first labelled for 24 h with [14C] thymidine for basal DNA synthesis analysis and then pulse labelled for 30 min with [3H] thymidine to assess DNA synthesis at the indicated time points following 5 Gy IR. An AT-derived fibroblast cell line was used as an internal control; these cells demonstrated no reduction in DNA synthesis 30 min after irradiation but do have a reduction at 2 hours, consistent with previous reports (Figure 4.5) (Houldsworth and Lavin, 1980; Painter and Young, 1980; Young and Painter, 1989). The ATM independent reduction in DNA synthesis at 2 hours in

the AT cells may represent DNA repair related inhibition of DNA synthesis at the origins of replication (replicon) (Houldsworth and Lavin, 1980). Wild-type HCT116 cells underwent a rapid initial reduction in DNA synthesis, which occurred to a lesser extent in p21-null cells (Figure 4.5). The rapid initial reduction in DNA synthesis is due to inhibition of the initiation of new origins of replication. Subsequent reductions in DNA synthesis are most likely to be due to inhibition of DNA chain elongation and enforcement of the G1 arrest, which prevents cells from entering S phase. In addition, in wild-type cells DNA synthesis continued to be reduced throughout the time course, whereas in the absence of p21 DNA synthesis increased over the time course. However, this was not as marked as in the AT cell line. Surprisingly, this data demonstrates that constitutive activation of the ATM-dependent DDR in the absence of p21 is associated with attenuation of DNA synthesis following DNA damage. In comparison with wild-type HCT116 cells, the p21-null counterparts display an intermediate radioresistant DNA synthesis phenotype. Brown *et al.* (2003) demonstrated that the mismatch repair system is required for the appropriate induction of S-phase arrest and that the HCT116 cell line undergoes radioresistant DNA synthesis. They reported that low levels of IR (1–5 Gy) were unable to activate the ATM–Chk2–Cdc25A response; however, complementation with MLH1 restored the wild-type response. Takemura (Takemura *et al.*, 2006) reported defective activation of the S-phase checkpoint in HCT116 cells in response to low dose camptothecin treatment, due to MMR-associated genetic attenuation of *MRE11A*. Complementation of *MRE11A* in HCT116 cells resulted in increased reduction in DNA synthesis following camptothecin treatment. Both of these studies suggested that low levels of DNA DSB require amplification of the DNA damage signal to

enable an effective S-phase response; indicating that a threshold level of DNA damage is required for robust activation of the ATM–Chk2–Cdc25A cascade.

4.2.2 p21-deficient cells have a defective IR-induced S-phase checkpoint that is independent of alterations to the cell cycle following irradiation damage.

In response to gamma irradiation-induced DNA damage, p21 arrests cell cycle progression at the G1 checkpoint in a p53-dependent manner (Deng *et al.*, 1995; Dulic *et al.*, 1994; el-Deiry *et al.*, 1994; Macleod *et al.*, 1995; Ohtsubo *et al.*, 1995). HCT116 p21-/- cells have an IR-induced RDS phenotype, which may be secondary to quantitative changes in the cell cycle profile and an inefficient G1 DNA damage checkpoint. Asynchronous cells were harvested using the method of Levack *et al.* (1987) and flow cytometric DNA analysis was undertaken. In wild-type HCT116 cells, approximately two-thirds of the cells were in G1 phase, one-fifth in S phase and the remainder were in G2/M phase (Figure 4.6). In the absence of p21, the cell cycle profile was altered dramatically: most cells were in S-phase (up to 45 %), one-third were in the G1 phase and one-fifth in G2/M phase. Asynchronous p21-null cells had a higher proportion of cells in S phase compared with the parental cell line (Figure 4.6), which may explain the reduced inhibition of DNA synthesis after IR (Figure 4.5). Previous reports have demonstrated that the p53–p21 pathway plays an important role in negatively regulating G1/S transition in response to a variety of cellular stresses. To confirm this, wild-type and p21-null cells were irradiated with 5 Gy and their cell cycle profiles were analysed over 24 h. As expected, following DNA damage wild-type HCT116 cells induced the G1/S and G2 checkpoints (Figure 4.7); no cells entered S phase at 2, 4, 12 or 24 h and the S-phase cell population encountered a G2/M block after 24 h. In contrast, HCT116 p21-/- cells continued to

progress through the cell cycle with no apparent block (Figure 4.7; compare both cell types at 4, 12 and 24 h). Despite Chk1 activation, as demonstrated by Chk1 serine-317 phosphorylation after 12 and 24 h (Figure 4.4), p21-/- cells were unable to sustain the G2 DNA damage checkpoint. This suggests that following DNA damage p21-null cells continue to progress through the cell cycle (at least for the time points analysed), unlike wild-type cells. This result concurs with previously published data and confirms the integrity of the genetic p21 deletion. Therefore, the intermediate radioresistant DNA synthesis phenotype in the absence of p21 (Figure 4.5) may be explained by the higher proportion of cells being present in S phase (Figure 4.6) and/or a failure in G1/S and G2 DNA damage checkpoints following IR (Figure 4.7). To delineate whether p21 loss results in a genuine defect in the IR-induced S-phase checkpoint despite constitutive activation of the ATM–Chk2–p53 pathway, it was necessary to overcome the alterations to the cell cycle profile described above. Cells were synchronised at the G1/S transition by a double blockade method involving culture in reduced serum for 24 h followed by treatment with aphidicolin (5 μg/ml), a DNA polymerase alpha inhibitor (Huberman, 1981) in the presence of serum-containing media. This protocol effectively blocked the majority of the cells at the G1/S boundary, committing them to undergo DNA synthesis once released from the aphidicolin block (Figure 4.8A and B). The aphidicolin block was more effective in wild-type HCT116 cells than in p21-null cells (Figure 4.8B). Cells were released from aphidicolin blockade by washing twice with serum-containing media. They were then allowed synchronised entry into S phase before being irradiated with 5 Gy IR. Cell cycle profile and DNA synthesis were then analysed. The synchronisation process enabled cells to traverse the G1/G0 restriction checkpoint at the time of IR

treatment; therefore, both the wild-type and p21-null cells were committed to continue to cycle through S phase regardless of irradiation (Figure 4.9A and B). In wild-type cells, the aphidicolin blockade did not appear to result in activation of the G2/M checkpoint, and at 12 h cells returned to a normal cell cycle profile (compare Figure 4.9A with Figure 4.6). Irradiation-induced DNA damage and forced passage through S phase resulted in G2/M arrest in wild-type cells (compare cell cycle profiles at 12 h; Figure 4.9A). HCT116 p21-null cells have a slower passage through S phase than do wild-type cells (Figure 4.9B), which suggests activation of additional DNA damage response cascades. Next, wild-type and p21-null HCT116 cells were synchronised and DNA synthesis was assayed following irradiation damage to ascertain whether p21 loss results in a defective irradiation-induced S-phase checkpoint. AT-derived fibroblasts were used as a control; they demonstrated radioresistant DNA synthesis irrespective of the radiation dose (Figure 4.10). Wild-type HCT116 cells retain a fast ATM-dependent decrease in DNA synthesis after IR (at 30 min; Figure 4.10A). When cells were treated with increasing doses of IR (Figure 4.10B), wild-type HCT116 cells rapidly suppressed DNA synthesis (at 30 min) in a dose-dependent fashion. HCT116 p21-/- cells were unable to suppress DNA synthesis as effectively as were wild-type cells (Figure 4.10A); p21-null cells demonstrated no reduction in DNA synthesis 30 min after 5 or 10 Gy, but suppressed DNA synthesis after the higher dose of 15 Gy (Figure 4.10B). Therefore, the absence of p21 results in a defective IR-induced S-phase checkpoint that is not attributable to a perturbed cell cycle profile and is independent of G1/S-phase arrest (which is compromised in p21-null cells). Even at low doses, aphidicolin creates DSB at sites of DNA synthesis and it's possible that this results in activation of additional DNA

damage response pathways (no immunoblot data is available to assess this effect); as such, this data may not wholly represent an effect of the ATM DDR. However, when unirradiated cell cycle profiles are assessed (Figure 4.9), p21-null cells are seen to cycle more slowly than wild-type cells. To overcome this possible confounding factor, cells were cultured in serum-free media for 12 h to allow synchronisation at the G0/G1 boundary. Next, cells were grown in the presence of serum for 2 h to allow mobilisation, before being irradiated and analysed after 30 min and 2, 4 and 8 h. HCT116 cells demonstrated a reduction in DNA synthesis at 30 min, which was absent in p21-null cells (Figure 4.11). Interestingly, the changes in DNA synthesis observed in wild-type cells are also seen in the absence of p21, but are exaggerated. On analysing the both sets of cell cycle profiles, it appears that serum starvation is much less successful in p21-null cells than in wild-type cells, thus suggesting a role for p21 in the G0/G1 restriction checkpoint (Figure 4.12A and B). Serum starvation of cells p21-null cells also exit S phase much more quickly than do wild-type cells (Figure 4.12A and B; compare the 8 h time points). Collectively, these data suggest that constitutive activation of ATM-dependent DDR associated with the absence of p21 cannot induce an effective S-phase checkpoint, which would result in a reduction in DNA synthesis. Consequently, p21-null cells continue to progress inappropriately through S phase and undergo DNA synthesis despite the presence of IR-induced DNA damage.

4.2.3 p21-null cells are hypersensitive to ionising irradiation.

In the absence of p21, the constitutively active ATM DDR pathway cannot induce an effective IR-induced S-phase arrest. The failure to induce appropriate G1/S and G2

checkpoints (Figure 4.7) and S-phase arrest (Figure 4.10) following DNA damage led me to predict that HCT116 p21-/- cells should demonstrate less inhibition, compared with the parental cell line, in a growth inhibition assay. The SRB assay is used to measure cell proliferation over a short period; the amount of dye-bound protein is proportional to the final cell density. This assay was used to measure IR-induced growth inhibition in HCT116 cells of different genotypes. Both p53-/- and p21-/- HCT116 cells were more resistant than wild-type cells to IR induced growth inhibition (Figure 4.13). This confirms that p21-/- cells continue to undergo division, in contrast to wild-type cells, in the presence of IR-induced DNA damage. This data is in contrast to previous studies which have demonstrated that HCT116 p21-/- cells are hypersensitive to certain cytotoxic agents (Hayward *et al.*, 2005; Hill *et al.*, 2008a; Hill *et al.*, 2008b). The short-term SRB assay may not accurately reflect cell line radiosensitivity/replicative potential and therefore the conventional clonogenic survival assay was undertaken (Banasiak *et al.*, 1999). Wild-type, p53-/- and p21-/- HCT116 cells, as well as AT cell lines, were treated with increasing doses of IR and their clonogenic survival was analysed. p53-/- HCT116 cells appeared slightly more resistant than wild-type cells to IR (Figure 4.14); neither of these cell lines showed basal activation of the ATM DNA damage response pathway (Figure 4.1). In contrast, p21-null cells were more sensitive than both wild-type and p53-null cells to IR (Figure 4.14). The radiosensitivity/reduction in colony formation of p21-null cells was similar to that of a cell line derived from an individual with AT, in which the ATM protein is mutated and/or absent. This supports previous results described in this chapter and by others that ATM and p21 are components of a common signal transduction pathway.

p21-null cells displayed constitutive activation of the DDR pathway, as demonstrated by Chk2 threonine-68 phosphorylation in cycling cells (Figure 4.1) and are able to induce the DDR response following IR (Figure 4.4). However, they also display a defect in the IR induced S phase arrest termed radioresistant DNA synthesis (Figures 4.5, 4.10, 4.11) indicating an uncoupling of the damage signal and downstream effects. Basal levels of Cdc25A also appear to be elevated compared with parental HCT116 cells. Following treatment with 5 Gy IR, most Cdc25A was degraded in the HCT116 parental cell line but less degradation occurred in p21-null cell line (Figure 4.4). This inefficient degradation of Cdc25A may explain why p21-null cells display a radioresistant DNA synthesis phenotype.

4.3 Discussion

The efficacy of conventional chemotherapy and radiotherapy is related to their ability to induce DNA damage (Shiloh, 2003). DSB comprise one of the most detrimental forms of DNA damage and therefore cells have developed a complex network of signalling pathways to maintain genetic integrity (Shiloh, 2006). The ATM-driven DDR pathway orchestrates the response to DNA DSB, resulting in the induction of cell cycle arrest (Bartkova *et al.*, 2005b) and the coordination of DNA repair and apoptosis. After DNA damage, the MRN complex (Mre11–Rad50–Nbs1) activates ATM, which in turn activates transducers such as the Chk1 and Chk2 checkpoint kinases, Nbs1 and p53. These proteins activate downstream effectors such as Cdc25A or p21, thereby inducing cell cycle arrest to allow DNA repair or, if necessary, inducing apoptosis (Bryant *et al.*, 2005; Farmer *et al.*, 2005; Hickson *et al.*, 2004). Constitutive activation of the ATM–Chk2–p53 pathway has been suggested to prevent disease progression from precancerous lesions to invasive

carcinoma, thus highlighting that defects in these pathways promote genetic instability and tumorigenesis (Madhusudan and Middleton, 2005). However, activation of the ATM DNA damage response pathway has also been demonstrated in normal human tissues such as the bone marrow and adult testis, where V(D)J recombination and meiotic recombination occur, respectively. ATM pathway activation has also been demonstrated in breast, colon and lung cancers (Bartkova *et al.*, 2005b; DiTullio *et al.*, 2002; Tort *et al.*, 2006), urinary bladder cancers (Bartkova *et al.*, 2004) and prostate cancers (Fan *et al.*, 2006). Certain cytotoxic therapies that induce senescence of (G2/M-arrested) human cancer cells also demonstrate activated ATM/ATR kinases.

Inhibitors of the DNA damage response and repair pathways have been shown to be effective single agents for treating cancers that have mutations in essential DNA repair genes, as well as a means of potentiating current cytotoxic and irradiation therapies (Grabsch *et al.*, 2006; Madhusudan and Middleton, 2005). However, constitutive activation of DDR in cancer cells may reduce the efficacy of such approaches and this phenomenon is unstudied in human cancers. Assessing the functional status of the DNA damage response pathway may be important for developing personalised anti-cancer therapies and may also predict the patient response to current treatment modalities. Data shown in this chapter has demonstrated that constitutive activation of the ATM dependent DDR pathway has a defect in the IR induced S phase checkpoint in the absence of p21 and highlighted a novel role for p21 in regulating the intra-S-phase checkpoint.

p21 has important roles in G1/S-phase arrest, DNA synthesis and apoptosis downstream of ATM. Following DNA damage at the G1/S-phase, mammalian cells have previously demonstrated a temporary reduction in DNA synthesis, which appears to be independent of p53; however, conclusive evidence that inhibition of DNA synthesis is also independent of p21 is lacking (see later in discussion) (Falck *et al.*, 2001; Mailand *et al.*, 2000). Following inhibition of DNA synthesis, a prolonged G1 arrest occurs, which has been shown to be mediated by the ATM–Chk2–p53–p21 pathway. Many human cancers have a defective G1 arrest response through inactivation or mutation of p53 and reduced expression of Rb. In the absence of p21, there are high basal levels of ATM serine-1981, Chk2 threonine-68 and p53 serine-15 phosphorylation (Figure 4.1). Incubation with a specific ATM inhibitor resulted in loss of the phosphorylation at Chk2 threonine-68 and p53 serine-15, and reduction in total Chk2 and p53 protein levels (Figure 4.2); confirming that the ATM kinase is active in HCT116 cells in the absence of p21. In the absence of exogenous DNA damage, I speculated that loss of p21 may have resulted in unscheduled DNA synthesis due to uncontrolled Cdk/cyclin activity, unopposed PCNA activity and transcriptional upregulation of S-phase proteins, thus generating a DNA damage response. However, γ– H2AX staining intensity in asynchronous control cells was similar in both p21-null and wild-type cells, suggesting that comparable levels of DNA damage foci are present in both cell types (Figure 4.3). The detection of similar levels of γ– H2AX contrasts with that of Hill *et al.* (2008a), who demonstrated activation of kinases other than ATM, including ATR, p38 and AKT, along with increased levels of γ– H2AX. My results reflect more closely data reported by Pang *et al.* [2011] and may represent further genetic alterations in the HCT116 MMR-

deficient cell line. Activation of the DDR in HCT116 p21-/- may also represent DNA repair. This was not studied in this report, as p21 has not been shown to have a major role in directing DNA repair and the role of ATM directed DNA repair was elusive during the time of this PhD.

Recovery from the various DNA damage responses is an equally important mechanism that allows the cell cycle to continue. Following DNA damage, checkpoint recovery is mediated by several phosphatases, of which wild-type p53-induced phosphatase 1 is important. If cells are unable to undergo checkpoint recovery, then it's conceivable that they may develop checkpoint adaption, i.e., continued progression through the cell cycle despite activation of DNA damage responses. When DNA damage responses are permanently activated, additional DNA damage may not enhance the activity of downstream effectors. Data presented here show that after 5 Gy IR there is an increase in Chk2 threonine-68 phosphorylation and less efficient degradation of Cdc25A in p21-null cells. Although there is an increase in p53 serine-15 phosphorylation, levels of the p53 protein remain unchanged and p21 is not induced, as seen in wild-type cells (Figure 4.4). These data are in line with previous reports that the G1/S and G2/M DNA damage checkpoints are abrogated in the absence of p21 and, crucially, also demonstrate a novel role for p21 in the regulation of the intra-S-phase checkpoint. The radioresistant DNA synthesis seen in p21-null HCT116 cells (Figure4.5) indicates that p21 probably augments the downstream effects of ATM activation. Synchronisation of the cells at the G1/S transition or at the G0/G1 restriction point confirms that the radioresistant phenotype occurs independently of alterations to the cell cycle profile and of an incompetent G1/S-phase arrest (Figures 4.9-4.12). An earlier report by Guo *et al.*

(1999) using the same isogenic cell lines concluded that the radiation-induced intra-S-phase checkpoint is independent of p21. However, there are several key differences between their study and the data presented here. In the study of Guo *et al.*, cells were synchronised at the G1/S boundary by exposure to a high concentration of thymidine followed by hydroxyurea, a DNA chain elongation inhibitor similar to aphidicolin. Hydroxyurea was then removed and cells were grown in complete media for 2 h before being irradiated with 10 Gy IR and pulse labelling with [3H] thymidine to assess changes in DNA synthesis. Incorporation of [3H] thymidine into DNA was measured using a liquid scintillation counter and results were displayed as a percentage of non-irradiated controls. The experimental method used in this study differs in three ways. Firstly, cells were prelabelled with [14C] thymidine to quantitate basal DNA synthesis and results were shown as a ratio of [3H] / [14C] incorporation for each sample. This method improves reproducibility, reduces standard deviation and corrects for variations in the amount of DNA recovered from cells. In contrast, single labelling of cells is a semi-quantitative method of assessing DNA synthesis. Secondly, Guo *et al.* irradiated cells 2 h after synchronisation, which may have resulted in the assessment of late S-phase cells that mainly undergoing chain elongation as opposed to initiation of replication at origins following synchronisation; in contrast, in this study cells were irradiated immediately after aphidicolin removal. The cell cycle profiles of unirradiated controls demonstrated that aphidicolin treatment did not induce DNA damage, which could have confounded measurements in both wild-type and p21-null cells. Thirdly, a dose of 5 Gy was used in this study and 10 Gy was used by Guo *et al.* The higher dose may have activated additional DNA damage response pathways, thus masking subtle

difference that may have arisen between the parental and p21-null cells. There are additional limitations of each synchronisation method used and this can be improved by using non-pharmacological/non-mitogen restriction methods such as cell separation by centrifugal force or flow cytometric sorting (Rosner *et al.*, 2013). The RDS phenotype demonstrated in the p21-null HCT116 cells suggests that both the ATM–Chk2–Cdc25A and the ATM-Chk2-p53 pathways are attenuated in the absence of p21. Checkpoint abrogation and radioresistant DNA synthesis are two of the hallmarks of ataxia-telangiectasia. Cells derived from patients with AT show extreme sensitivity to irradiation, which correlates with radioresistance; in addition, new data suggests that radioresistance may also reflect an inability to repair DNA damage. In HCT116 cells, the absence of p21 results in abrogation of the three major ATM-dependent DNA damage induced checkpoints; the strongest indicator that p21 augments the effects of ATM activation. Abrogation of these checkpoints may also explain why this study (Figures 4.13-4.14) and others have demonstrated that p21-null cells display increased sensitivity to DNA damaging agents compared with both wild-type and p53-null HCT116 isogenic cells (Bataller *et al.*, ; Hayward *et al.*, 2003; Hayward *et al.*, 2005; Hill *et al.*, 2008a; Pang *et al.*, 2011). Waldman (1996) demonstrated uncoupling of DNA synthesis and the mitotic phase in the HCT116 p21 null cells following DNA damage. Despite retaining their ability to arrest temporarily in G2/M following DNA damage, p21 null cells were unable to effectively inhibit DNA synthesis, resulting in the formation of cells with greater than 4N DNA, thus prompting apoptosis. Wang *et al.* (1997) reported increase in radiation sensitivity in the gut epithelium of ATM/p21 double knockout mice and concluded that ATM and p21 cooperated to reduce radiation-induced apoptosis. This

was not seen in mice lacking p21 alone. Abrogation of DNA synthesis and escape from G2 arrest DNA damage checkpoints closely correlate with increased sensitivity towards DNA damaging agents. Loss of p21 in a large series of colon cancer cases was found to be independently associated with increased survival of patients ≥ 60 years, but with reduced survival of patients <60 years of age. These data presumably reflect a more aggressive cancer phenotype in younger patients (Ogino *et al.*, 2009). This was confirmed by Noske *et al.*, who reported significantly improved outcomes of p21−/p53+ sporadic colorectal cancers in both recurrence-free and overall patient survival following adjuvant chemotherapy (Noske *et al.*, 2009).

In this chapter, loss of p21 resulted in constitutive activation of the ATM dependent DDR yet surprisingly also displayed a RDS phenotype. This novel data implicates a role for p21 in the DNA damage induced S phase checkpoint. Uncoupling of the ATM-Chk2-Cdc25A would result in abrogation of the three major DNA damage induced cell cycle checkpoints resulted in increased sensitivity to IR, similar to cells derived from AT patients; providing further evidence that p21 and ATM act in a common pathway. In this situation where cells are extremely sensitive to DNA damage treatment with an ATM inhibitor to abrogate all three DNA damage induced checkpoints would have no additional effect clinically on reduction in cancer size or prognosis in patients.

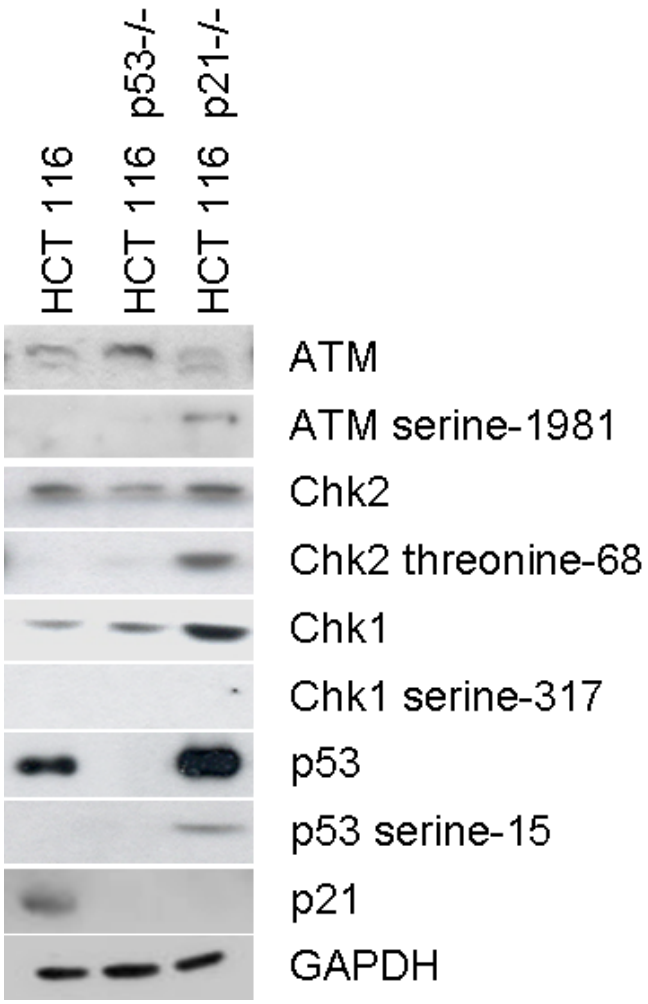

Figure 4.1. Targeted disruption of the p21 protein results in constitutive activation of the DNA damage response pathway in the absence of exogenous DNA damage.

HCT116 parental, p53-null and p21-null whole cell lysates (10 µg) were resolved by SDS-PAGE. Proteins were immunoblotted using the following antibodies ATM, ATM serine-1981, Chk2, Chk2 threonine-68, Chk1, Chk1 serine-317, p53, p53 serine-15, p21 and GAPDH. GAPDH was used as a loading control.

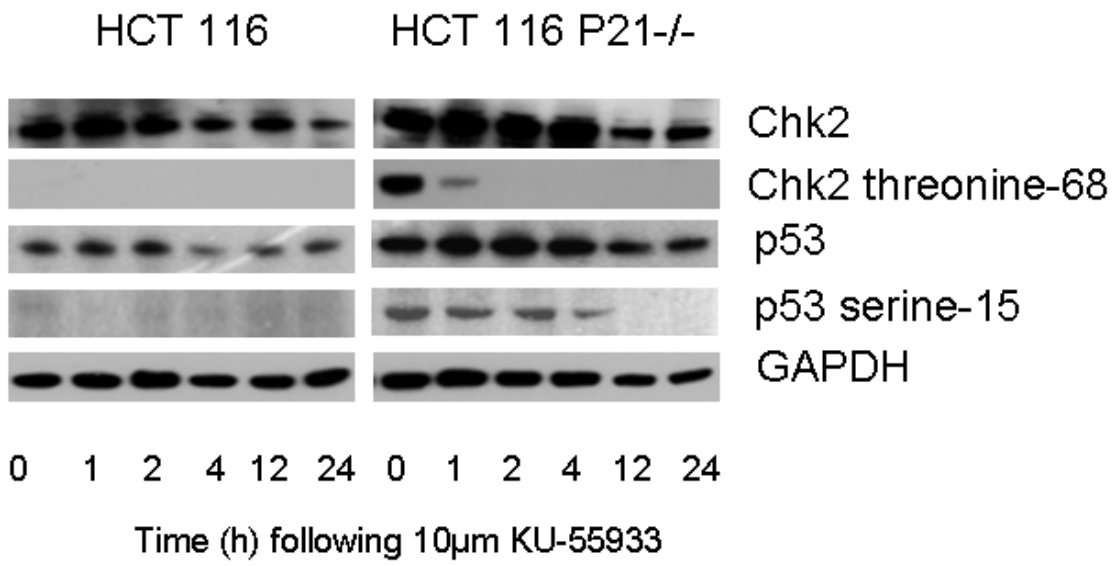

Figure 4.2. Constitutive activation of the DNA damage response pathway in the absence of p21 is ATM dependent.

Wild-type and p21-null (p21-/-) HCT116 cells were incubated with 10 µM KU-55933 and harvested at the indicated time points; 0 time point is control cells i.e. no exposure to inhibitor. Treatment with a specific ATM inhibitor abolishes basal Chk2 threonine-68 and p53 serine-15 phosphorylation in p21-null cells. Protein lysates (20 µg) were analysed by immunoblotting. GAPDH was used as a loading control.

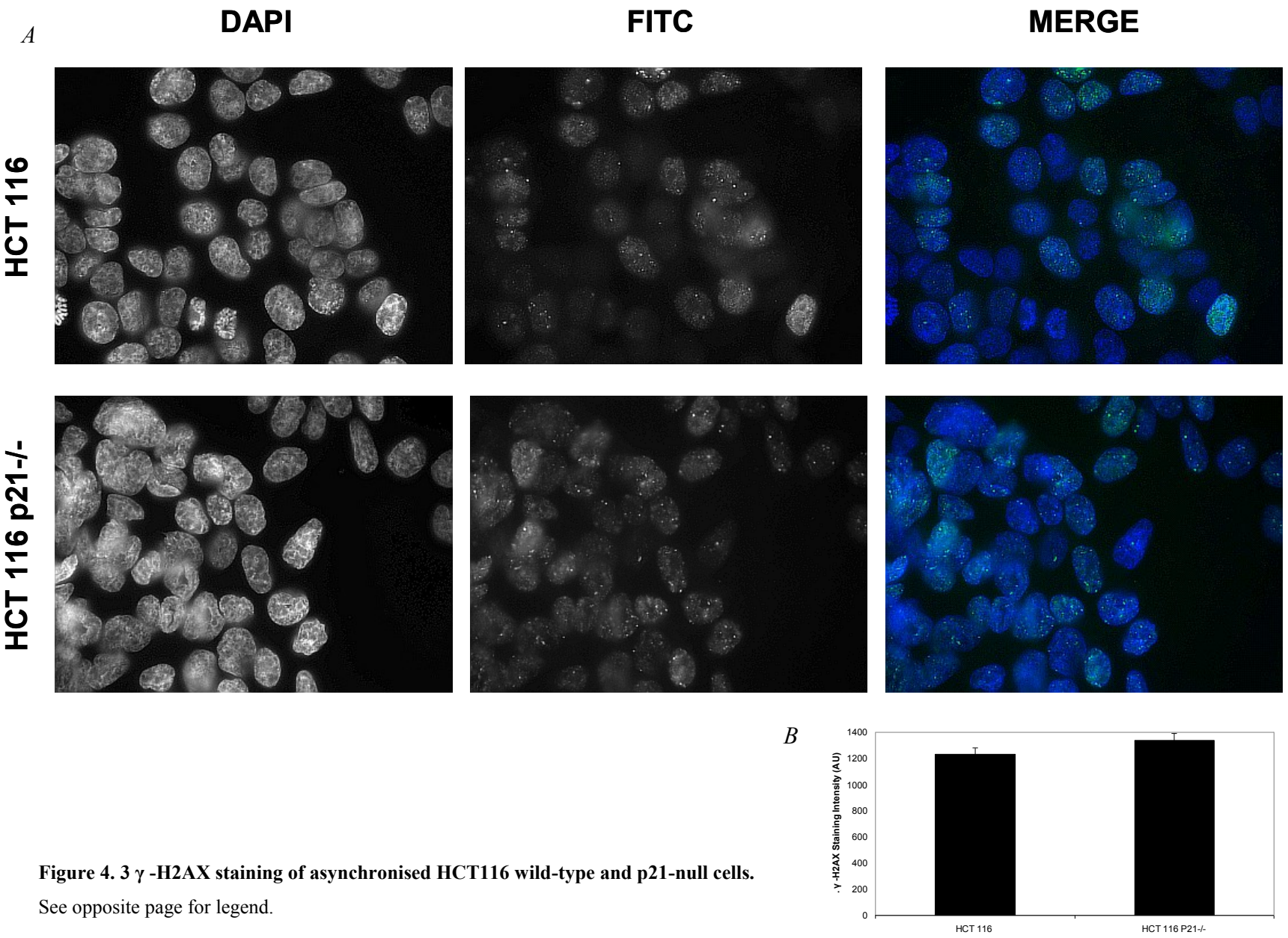

Figure 4. 3 γ -H2AX staining of asynchronised HCT116 wild-type and p21-null cells.

See opposite page for legend.

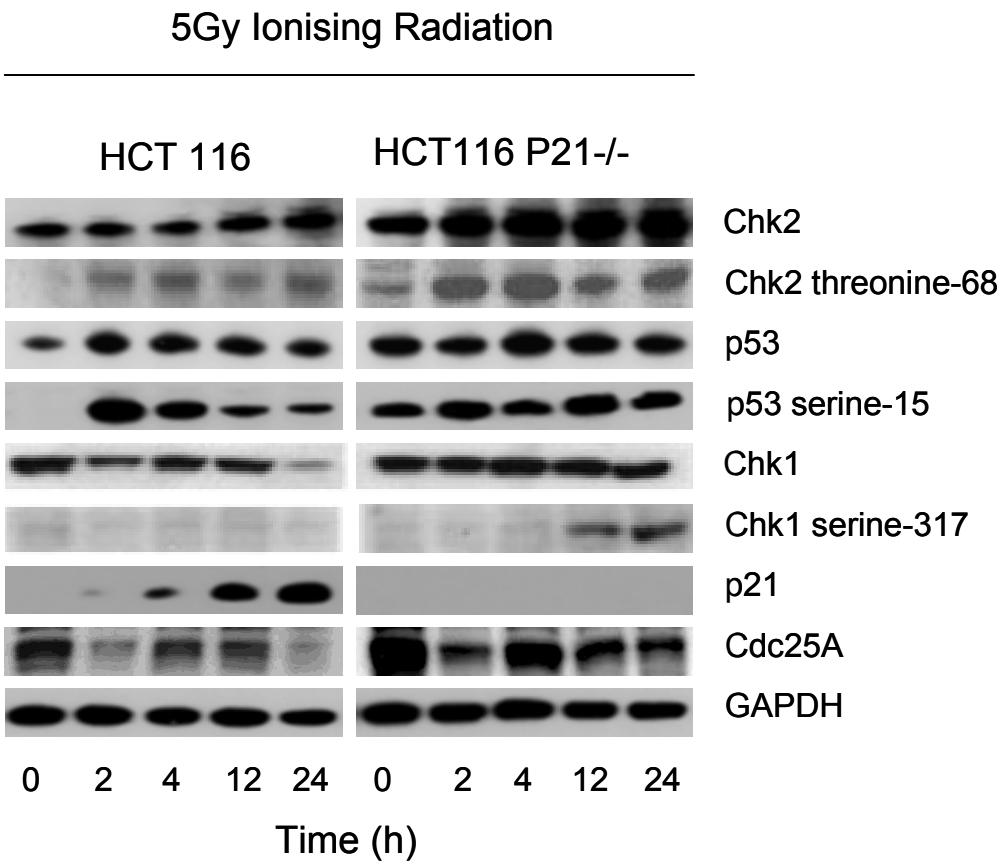

Figure 4.4 The constitutively active ATM DNA damage response pathway is induced following DNA damage.

Wild-type and p21-null (p21-/-) HCT116 cells were treated with 5 Gy irradiation and harvested over a 24 h time course. Whole cell lysates (20 μg) were analysed by immunoblotting. GAPDH was used as a loading control.

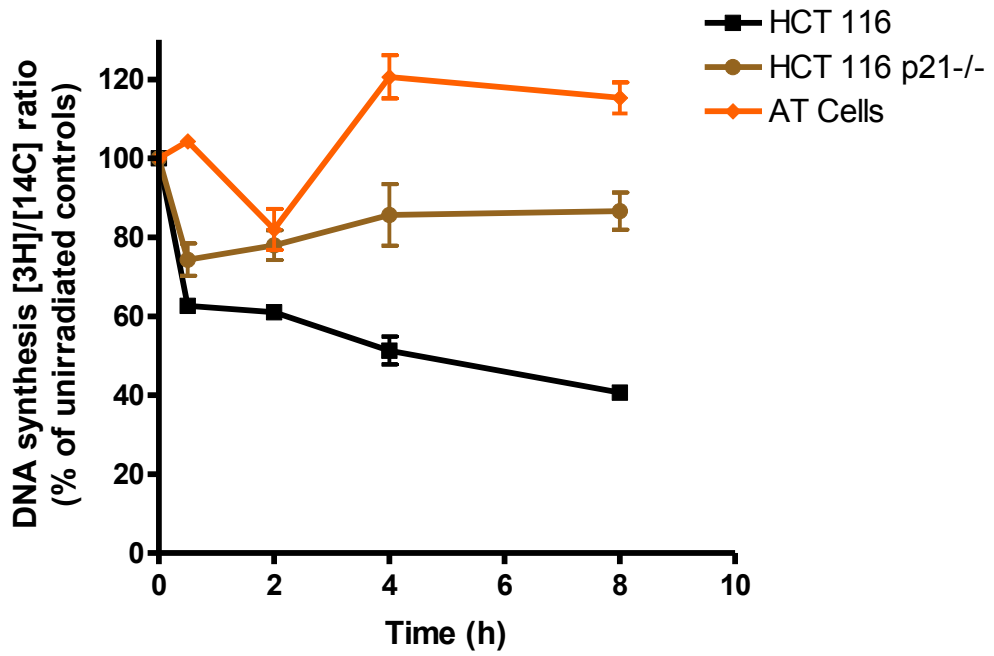

Figure 4. 5 Loss of p21 induces an intermediate radioresistant DNA synthesis phenotype following gamma irradiation, despite a constitutively active ATM DDR.

Compared with the parental cell line, p21-null HCT116 cells display a less marked reduction in DNA synthesis following DNA damage. Asynchronously cycling cells were labelled with [14H] thymidine for 24 h to assess basal DNA synthesis, followed by a 24 h washout period. Triplicate cell samples were then irradiated with 5 Gy and pulse labelled for 30 min with [3H] thymidine. Cells were harvested at 0.5, 2, 4 and 8 h time points and DNA was extracted. Radioactive incorporation was analysed using a liquid scintillation counter. DNA synthesis is expressed as a ratio of [3H]/[14C] over unirradiated controls; error bars represent standard deviation of the mean. Results are representative of three individual experiments. Ataxia-telangectasia (AT) cells were used as an internal control.

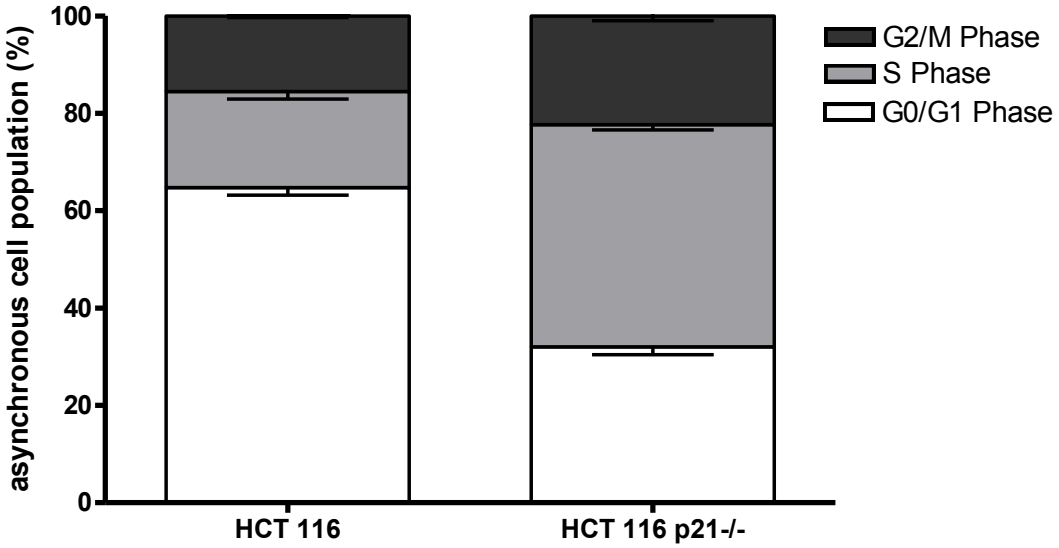

Figure 4. 6 p21 loss results in an aberrant cell cycle profile in asynchronous HCT116 cells.
Most wild-type HCT116 cells are in G1 phase and most p21-/- HCT116 cells are in S phase. The cell cycle profiles of asynchronous cells were analysed by flow cytometry using ModFit 2.0 (Verity Software). The relative proportions of cells in the G0/G1, S and G2/M phases of the cell cycle are shown. Results represent the mean of triplicate samples and error bars represent standard deviation of the mean.

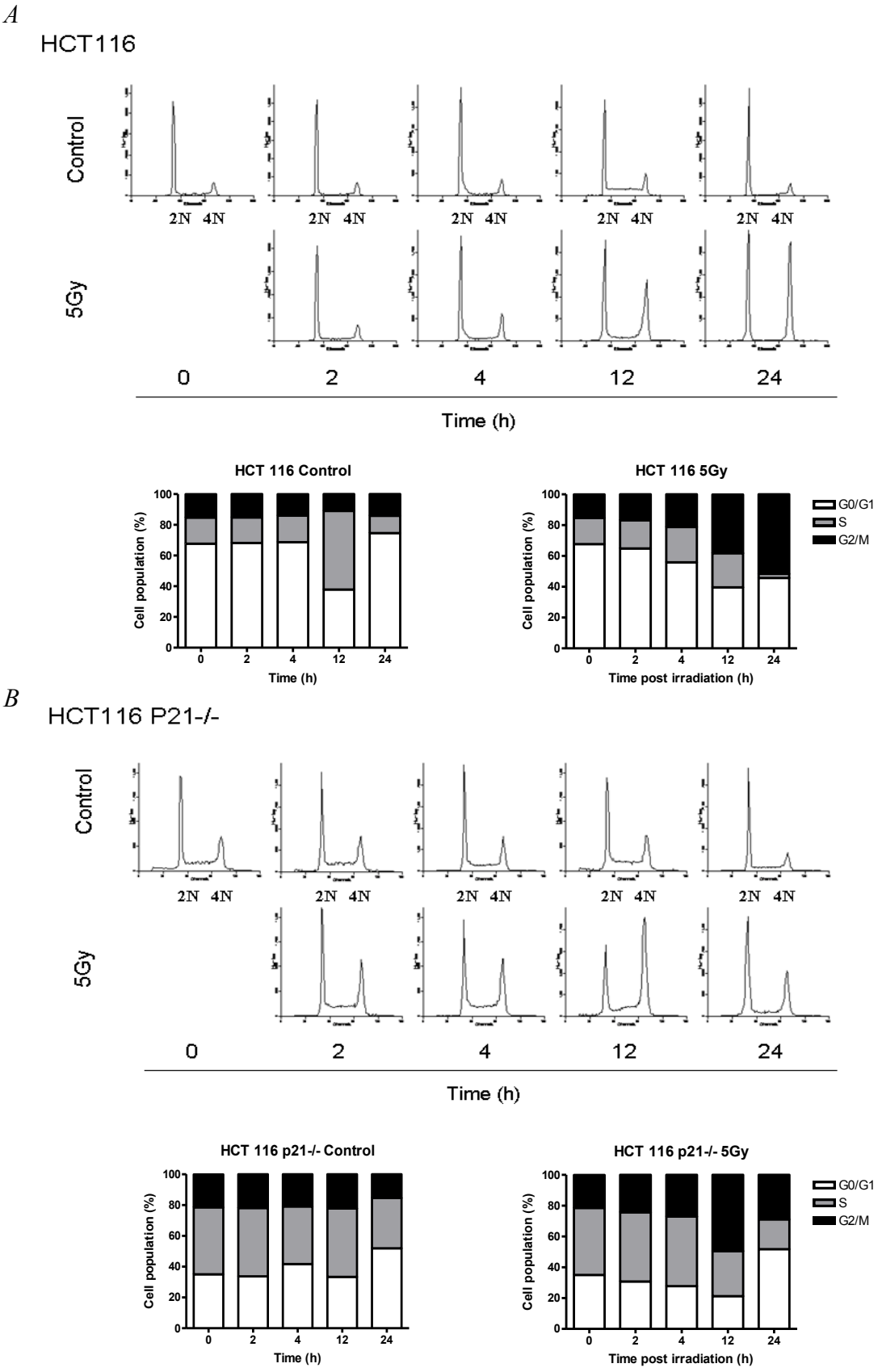

Figure 4. 7 p21 loss results in abrogation of the G1 and G2 DNA damage checkpoints following 5 Gy irradiation. See opposite page for legend details.

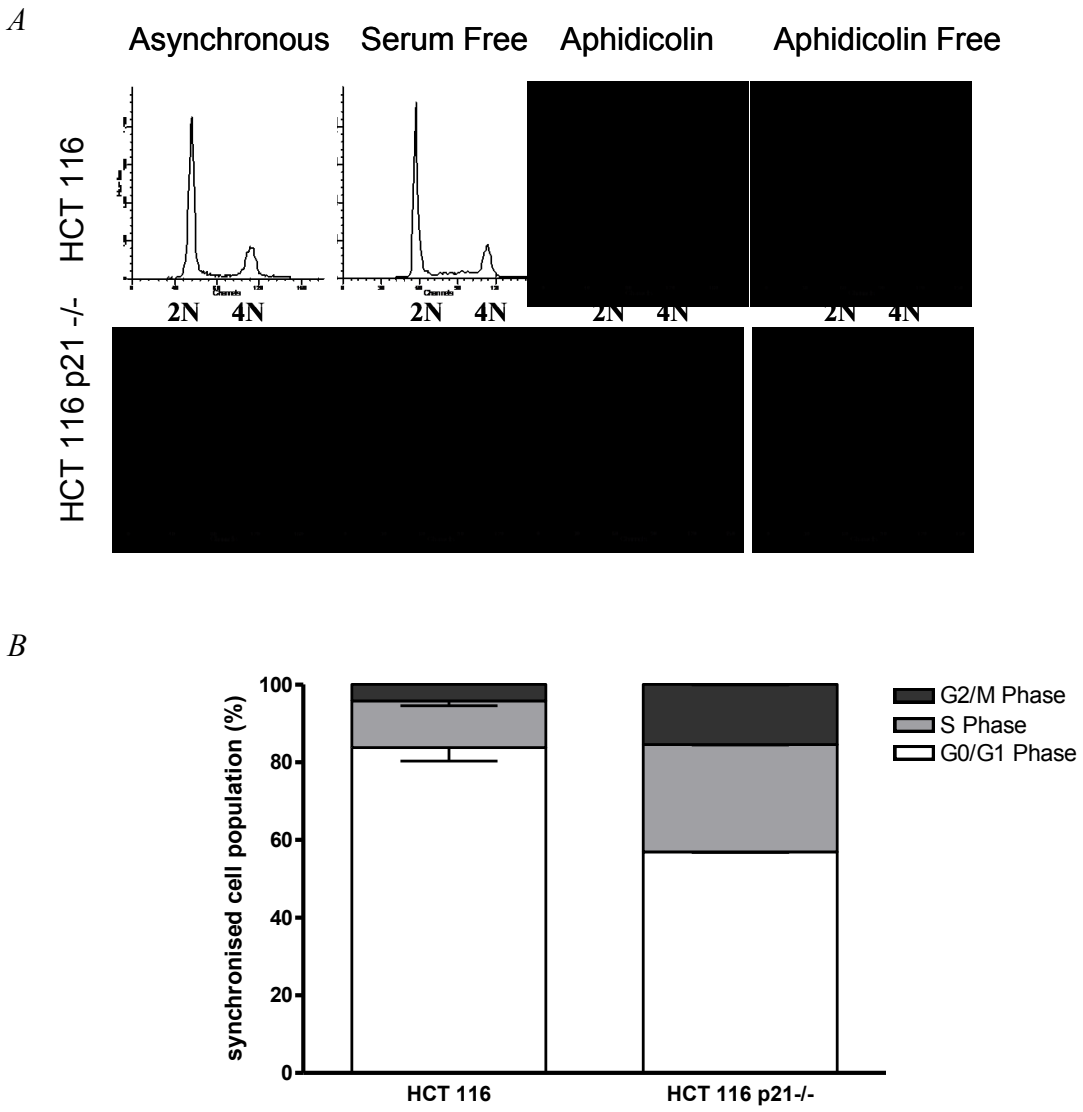

Figure 4.8. Synchronisation arrests the majority of cells at the G1/S boundary.

Wild-type (WT) and p21-null (p21-/-) HCT116 cells were synchronised at the G1/S phase by culture in reduced serum followed by aphidicolin blockade. (*A*). Release of the aphidicolin blockade allowed cells to enter S phase. Asynchronous (controls); Serum Free (24 h culture in of reduced serum conditions), Aphidicolin (treatment with 14 μm aphidicolin and serum replacement) and Aphidicolin off (aphidicolin removed). (*B*). Histogram depicting cell cycle profiles prior to the removal of aphidicolin blockade. The synchronisation method was more successful in wild-type cells than in p21-null counterparts. The x axis represents propidium iodide staining i.e., DNA content; 2N, diploid chromosomes; 4N, tetraploid chromosomes. The experiments were done in replicates of three at least twice. Error bars represent standard deviation of the mean.

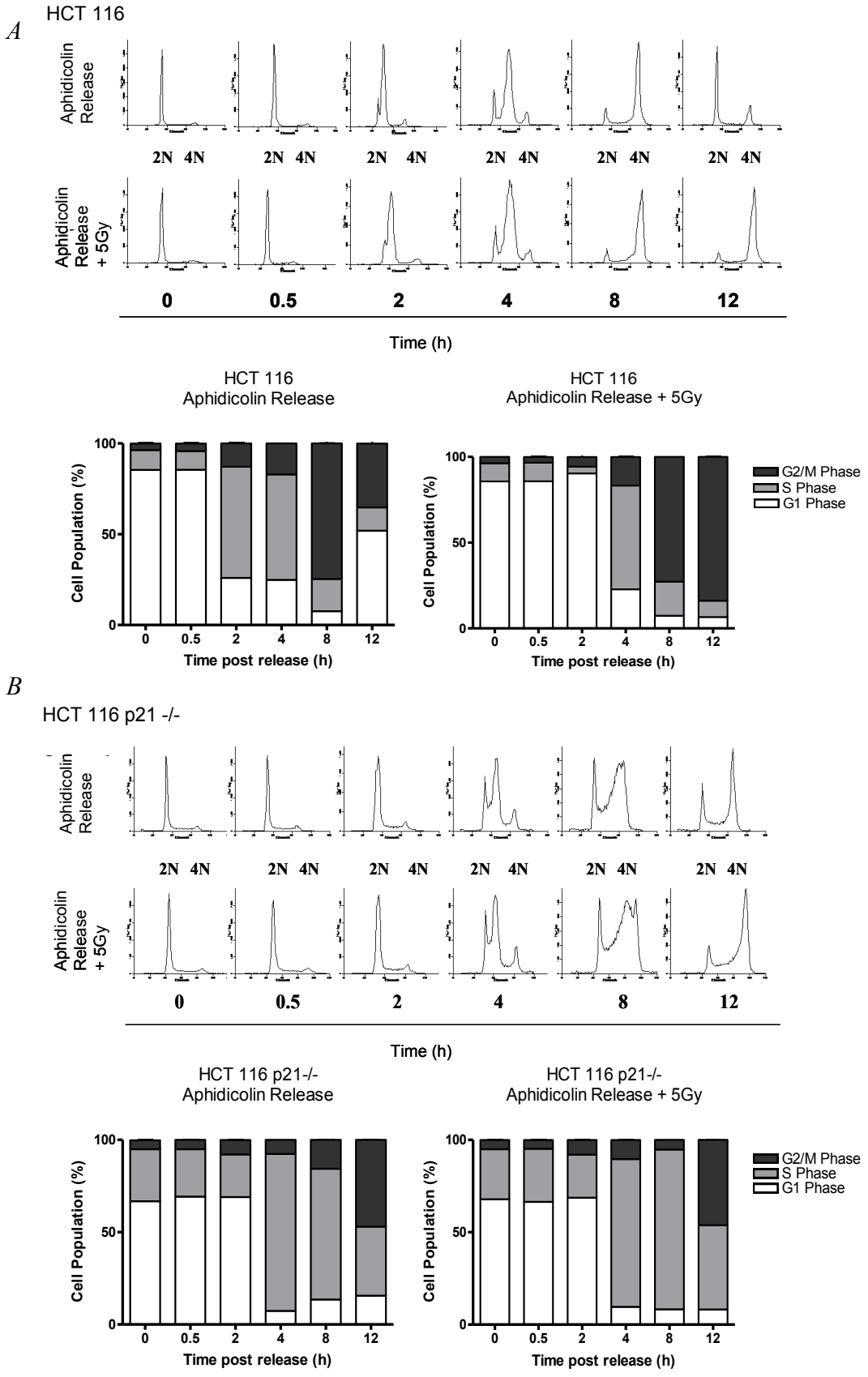

Figure 4.9. Synchronisation allows assessment of the post-G1 cell cycle progression after 5 Gy irradiation. See opposite page for legend details.

A

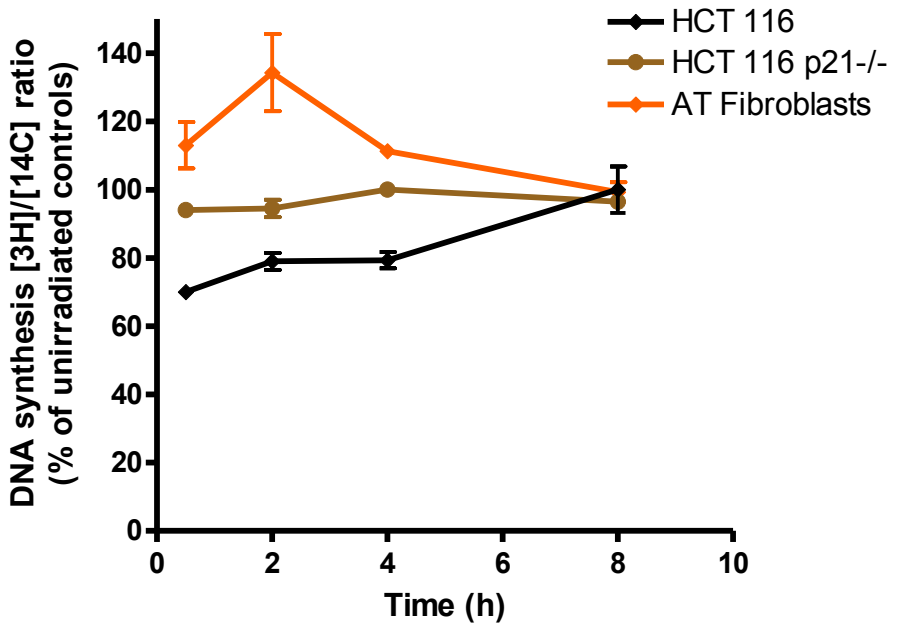

B

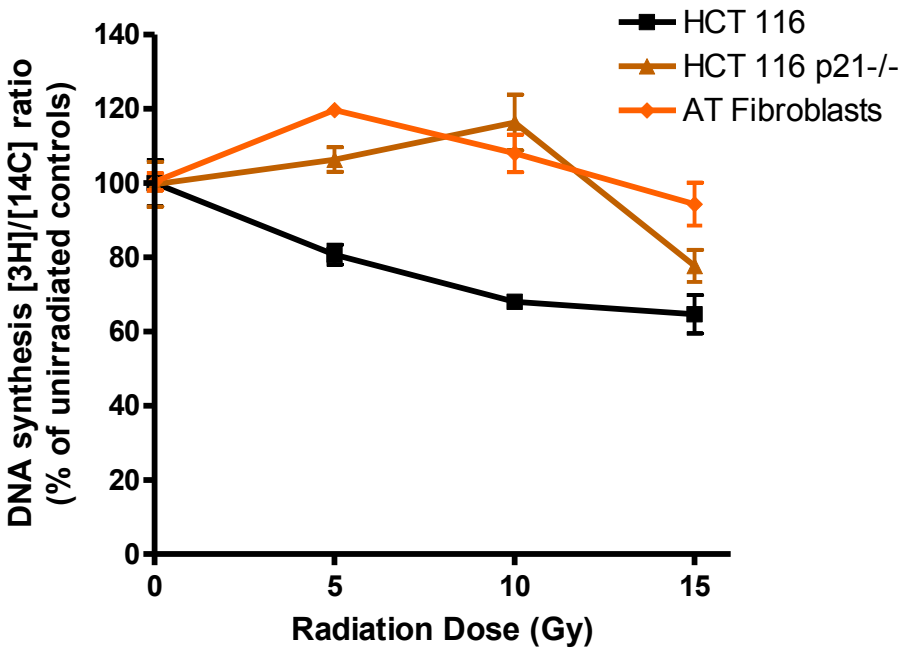

Figure 4.10. p21 loss results in a defective IR-induced S-phase checkpoint, termed radioresistant DNA synthesis.

(*A*).Synchronised cells were subjected to 5 Gy of irradiation and DNA synthesis was analysed after 0.5, 2, 4 and 8 h. Compared with parental cell, p21-null cells display a less marked reduction in DNA synthesis following DNA damage. (*B*). Loss of p21 abrogates the IR-induced S-phase checkpoint after 5 and 10 Gy but not after 15 Gy. DNA synthesis was assessed 30 min after irradiation. Synchronised AT cells were used as controls. Error bars represent standard deviation of the mean.

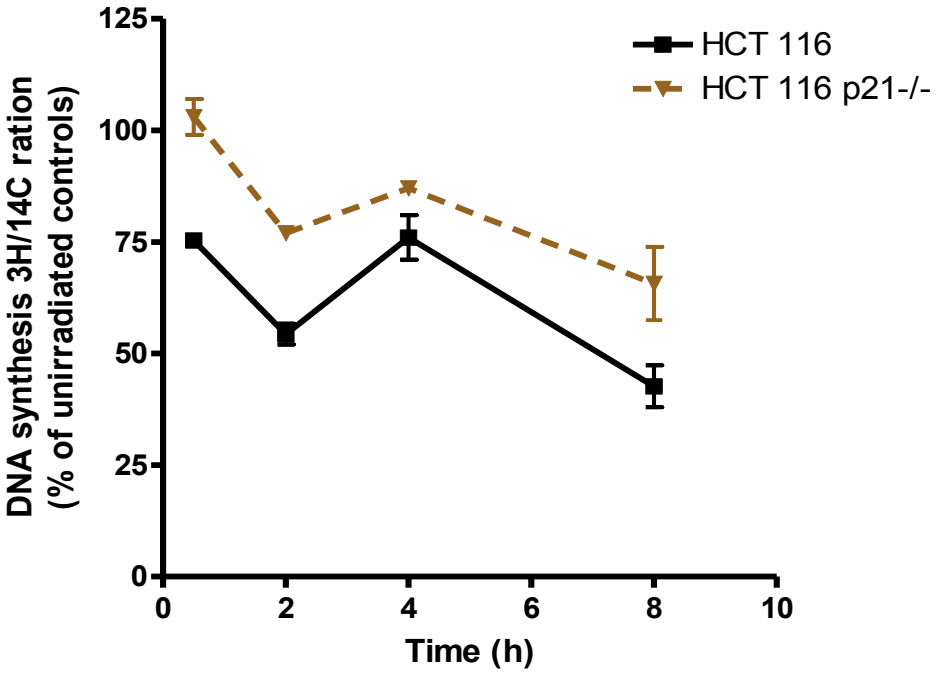

Figure 4.11. HCT116 p21-/- cells undergo radioresistant DNA synthesis when synchronised by serum-free culture.

Compared with parental cells, p21-null cells display a less marked reduction in DNA synthesis following DNA damage. Synchronised cells were subjected to 5 Gy ionising radiation and DNA synthesis was analysed after 0.5, 2, 4 and 8 h, as described in Figure 4.10.

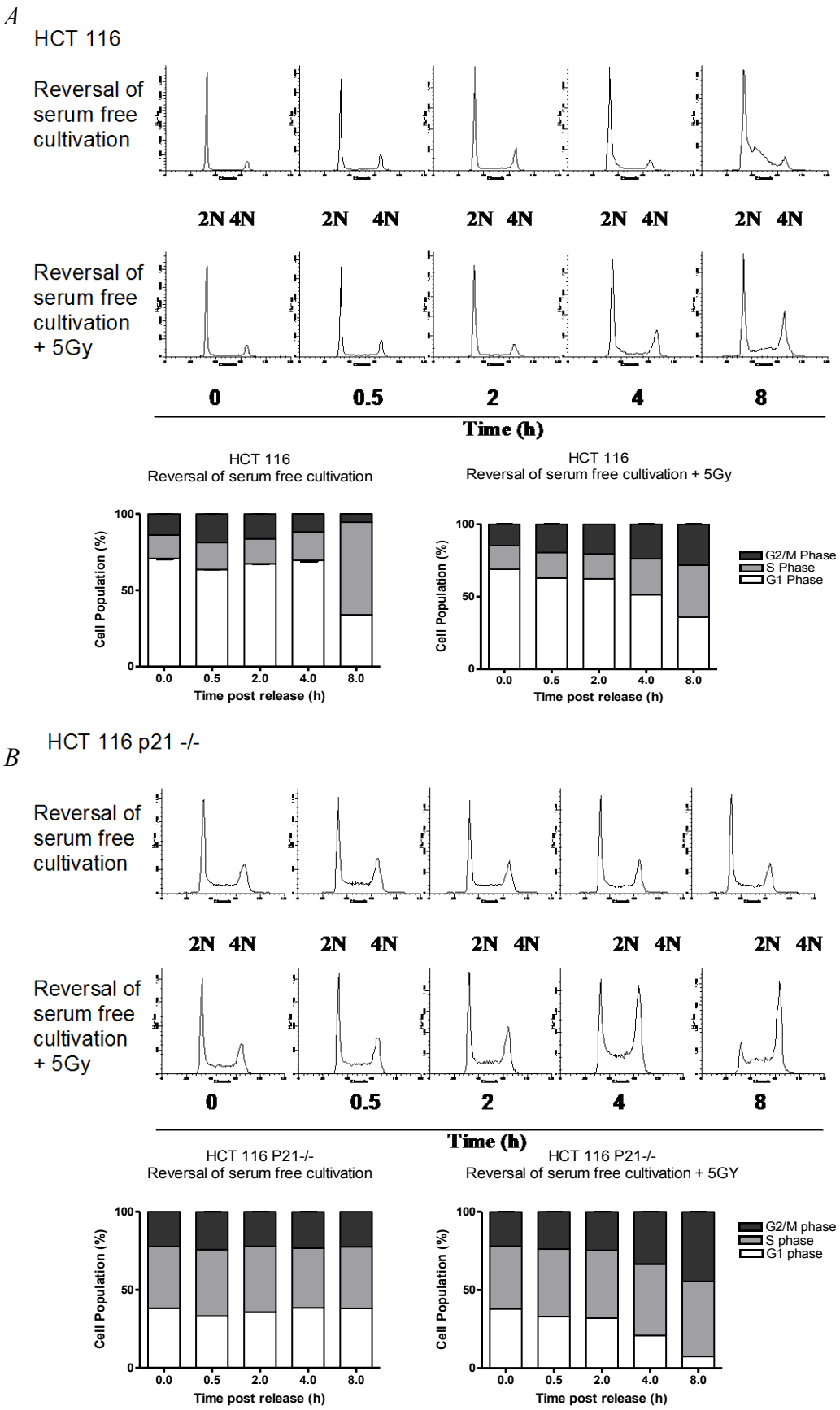

Figure 4.12. Cell Cycle profiles of wild-type and p21-null HCT116 following synchronisation by serum starvation. See opposite page for legend details.

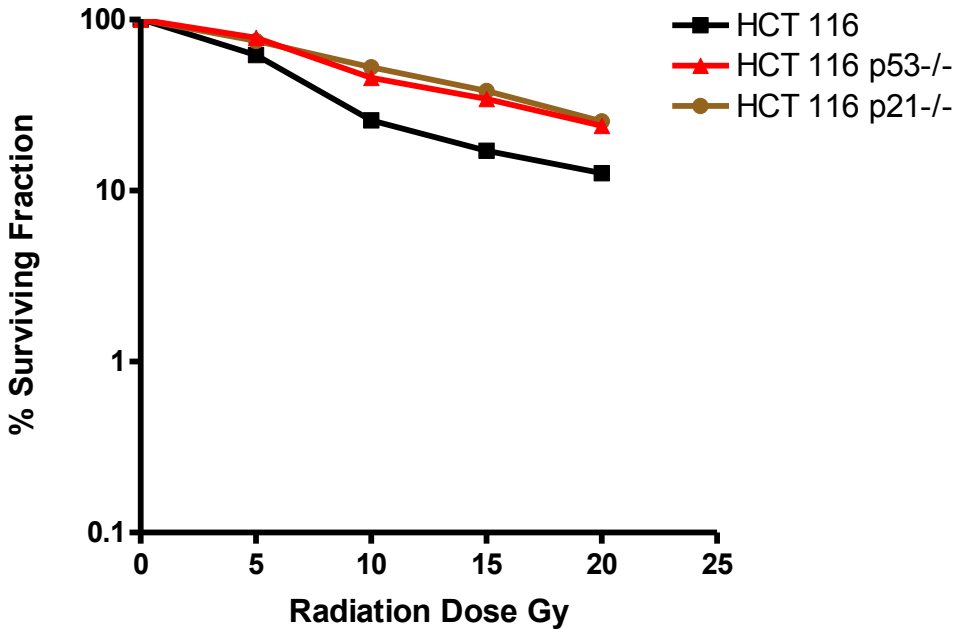

Figure 4.13. HCT116 p21-/- cells display radioresistance in a short-term growth inhibition assay. HCT116 p21-/- cells are more radioresistant than their wild-type counterparts. Cell lines were irradiated with the indicated dose of ionising radiation and replated in triplicate into 6-well dishes for assessment of colony formation. Results represent the mean of three independent experiments and error bars represent standard deviation of the mean.

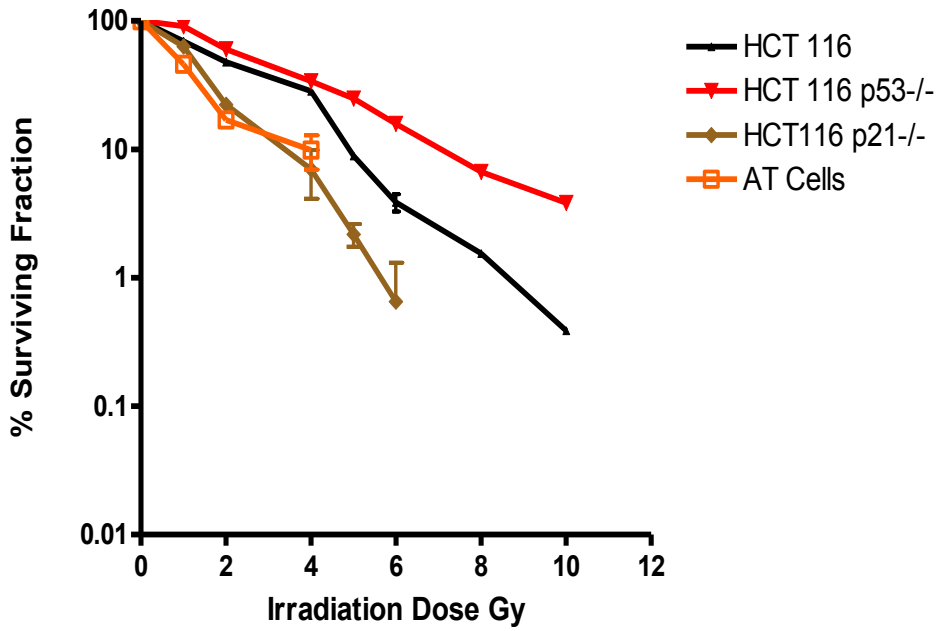

Figure 4.14. HCT 116 p21-/- cells display radiosensitivity similar to that of AT cells.
p21-null HCT116 cells (p21-/-) are more radiosensitive than their wild-type counterparts. Cell lines were irradiated with the indicated dose of ionising radiation and replated in triplicate into 6-well dishes for assessment of colony formation. Results represent the mean of three independent experiments and error bars represent standard deviation of the mean.

Chapter 5. p21 Regulates DNA Damage-Induced Cdc25A Degradation

5.1 Introduction

p21 levels are low under physiological conditions, facilitating progression of the cell cycle. p21 is targeted for proteasomal degradation by Cdk2/cyclin E at the G1/S transition and by interaction with the anaphase promoting complex/cyclosome (ANAPC/C) complex at G2 phase (Lu and Hunter, 2010). It is therefore unclear whether absence of p21 would result in unscheduled DNA synthesis through the premature activation of Cdk/cyclin complexes and lack of PCNA binding (a subunit of DNA polymerase delta). Certainly, in normal human cells p21 exists in a quaternary structure with cyclin/Cdk and PCNA, and basal p21 levels appear to promote the correct assembly, activation and nuclear localisation of the cyclin D/Cdk4 complex (Cheng *et al.*, 1999; LaBaer *et al.*, 1997). Sequestration of free p21 by cyclin D-associated kinases is also considered to be crucial for full activation of Cdk2 at the G1/S transition. However, p21 does not appear to be crucial for cyclin D/Cdk4 function, as Cdk complexes can still phosphorylate Rb in p21 and p27 double null mouse embryonic fibroblasts (MEF). Cheng *et al.* (1999) proposed that in nontransformed cells binding of p21 (and p27) positively regulates the assembly, stability, activity and nuclear localisation of D-type cyclins. Cdk2-associated cyclin complexes are inhibited by p21 and, in the absence of p21, Cdk2/cyclin activity compensates for loss of cyclin D-dependent kinase activity. Such a paradigm could allow fine-tuning of Cdk activity and cell cycle progression, but would also prime Cdk/cyclin complexes for DNA damage-induced inhibition by p21. Collectively, this

data suggest that Cdk2 activity is enhanced in the absence of p21, resulting in Rb hyperphosphorylation and the release of E2F transcription factors. p21 has also been shown to directly associate with E2F transcription factors, thereby influencing the level of E2F target genes, including *cyclin A*. Homozygous p21-null mice undergo normal development (Brugarolas *et al.*, 1995; Deng *et al.*, 1995) but lack a DNA damage-induced G1 arrest The mice do not appear to develop spontaneous malignancies compared with p53 deficient controls.

The dual specificity phosphatase Cdc25A is regulated through cytoplasmic sequestration (Chen *et al.*, 2003) and ubiquitin-dependent proteasomal degradation (Donzelli *et al.*, 2002). During G2/M phase, Cdc25A degradation is regulated by Chk1 and mediated by the ANAPC/C^{cdh1} multiprotein complex (Donzelli *et al.*, 2002; Zhao *et al.*, 2002). DNA damage-induced Cdc25A degradation at the G1/S-phase transition and during S phase is orchestrated through Chk2/Chk1-dependent phosphorylation (Sorensen *et al.*, 2003; Xiao *et al.*, 2003; Zhou and Elledge, 2000) and SCFβ^{TRCP} ubiquitin-mediated degradation (Busino *et al.*, 2004; Busino *et al.*, 2003). Over expression of Cdc25A has been detected in 47 - 60% of paired colorectal and normal tissue samples (Hernandez *et al.*, 2001; Takemasa *et al.*, 2000) and with an aggressive disease phenotype in cancers (Kristjansdottir and Rudolph, 2004). Over expression of Cdc25A protein *in vitro* results in a reduced ability to downregulate DNA synthesis following genotoxic treatments (Mailand *et al.*, 2000). Overexpression of Cdc25A was evident in HCT 116 p21-/- cells from the previous results and may be important in the sensitivity of the p21 null cells to genotoxic agents. This chapter demonstrates that the S-phase checkpoint is deregulated at the

level of S-phase-promoting proteins Cdc25A and Cdk2 due to p21 loss and Chk2 mislocalisation despite an inducible DDR.

5.2 Results

5.2.1 Specific inhibition of the ATM-Chk2 pathway abrogates the S-phase checkpoint in wild-type but not p21-null HCT116 cells.

In HCT116 cells, loss of p21 resulted in constitutive activation of the ATM-dependent DNA damage response pathway, as demonstrated by phosphorylation of ATM serine-1981, Chk2 threonine-68 and p53 serine-15 (Figures 4.1 and 4.2). Despite this, p21-null cells demonstrated a defect in the IR-induced S-phase checkpoint, similar to that of AT cells, that was not attributable to a perturbed cell cycle profile and was independent of G1 and G2 arrest, which are compromised in these cells (Figure 4.9). In the absence of p21, constitutive activation of the ATM DDR pathway is uncoupled from its ability to induce an effective IR-induced reduction in DNA synthesis. This radioresistant phenotype can arise as a result of deregulation of any of the components involved in the ATM–Chk2/Cdc25A–Cdk2 (or ATM–Nbs1–SMC1) S-phase DNA damage checkpoint. To delineate which specific pathway component is deregulated, chemical inhibitors were employed as molecular tools. For example, cell treatment with a specific ATM inhibitor would be expected to abrogate the S-phase checkpoint. Asynchronous cells were exposed for 1 h to KU-55933 and then treated with 5 Gy IR. DNA synthesis was then analysed. ATM inhibition led to S-phase checkpoint abrogation in wild-type HCT116 cells at 0.5, 2 and 4 h; there was no effect at 8 h (Figure 5.1A), which most likely reflects activation of additional kinases or accumulation of cells at the G2/M transition. In contrast, p21-nulls showed no abrogation of the S-phase checkpoint at any time

points (Figure 5.1B). An AT-derived fibroblast cell line was used as a control as it demonstrates no abrogation of DNA synthesis following ATM inhibition (Figure 5.1C).Immunoblot analysis of proteins over a similar time frame demonstrated abrogation of ATM-dependent Chk2 threonine-68 phosphorylation at all time points examined, and no degradation of Cdc25A after 2 h, in wild-type cells (Figure 5.2); however, Cdc25A is absent at both 12 and 24 h. This result agrees the DNA synthesis data shown in Figure 5.1A. p53 serine-15 phosphorylation occurs at 12–24 h, but with no induction of p21. Interestingly, Chk1 serine-317 becomes phosphorylated after 2 h in wild-type cells; in contrast, Chk1 serine-317 becomes phosphorylated following ATM inhibition in the absence of p21. In p21-/- cells, ATM-dependent Chk2 threonine-68 phosphorylation is attenuated upon ATM inhibition, although p53 serine-15 phosphorylation persists. These data suggest that ATM inhibition induces additional DNA damage-related kinase pathways after 12 h in wild-type cells, but that this occurs almost immediately in p21-null cells. In the wild-type cell line, activation of an ATR-dependent pathway is likely, as ATR can phosphorylate both p53 serine-15 and Chk1 serine-317. Activation of this parallel pathway also coincides with loss of Cdc25A, but without p21 induction. In the absence of p21, activation of an additional kinase-dependent signalling network appears to occur rapidly following ATM inhibitor treatment, as Chk1 serine-317 becomes phosphorylated and basal p53 serine-15 phosphorylation levels remain unchanged. Despite this, robust degradation of Cdc25A does not occur; in fact, the data are very similar to those shown in Figure 4.4, where cells were irradiated with 5 Gy in the absence of ATM inhibition. In p21-null cells, there appears to be more phosphorylation of Chk2 threonine-68 and p53 serine-15 after 24 h, which does

coincide with loss of Cdc25A, suggesting hyperactivation of a DNA damage response pathway. This data confirms that ATM function is attenuated in the absence of p21, and suggest that p21 may be a positive regulator of the ATM-dependent DDR. It also supports the hypothesis that ATM and p21 are components of a common pathway.

In response to DNA damage, ATM phosphorylates Chk2 on threonine-68; therefore, a specific Chk2 inhibitor was used to determine whether the p21-dependent IR induced RDS phenotype was caused by misregulation of Chk2 protein. Asynchronous cells were exposed to 10 μM Chk2 inhibitor II (Sigma) and then treated with 5 Gy IR. DNA synthesis was assessed after 30 min. HCT15 cells, which harbour biallelic inactivation of Chk2 (Lee *et al.*, 2001), were used as negative controls; ATM-dependent phosphorylation of Chk2 threonine-68 is absent in this cell line (Wu *et al.*, 2001). The positive controls were provided by the wild type HCT 116 cell line. As expected, the Chk2 inhibitor does not increase DNA synthesis (Figure 5.3) in HCT15 cells after 30 min. In contrast, pre-exposure of wild-type HCT116 cells to the Chk2 inhibitor II resulted in incomplete abrogation of the IR-induced reduction in DNA synthesis after 30 min, but this did not occur in the p21-null background (Figure 5.3). It is likely that DNA synthesis was not completely abrogated in HCT116 cells due to activation of additional kinases, i.e., Chk1. This data confirms that the constitutively active ATM-Chk2 pathway cannot effectively activate the IR-induced S-phase checkpoint in p21-null HCT116 cells. The inability to increase the level of DNA synthesis with either an ATM inhibitor or a Chk2 inhibitor suggests that the pathway is deregulated downstream of these components in the absence of p21. If this is correct, then treatment with a nonspecific PIKK

inhibitor should also fail to increase the level of DNA synthesis in HCT116 p21-null cells following DNA damage. To test this, HCT116 p21-null cells were treated with wortmannin, a fungal metabolite that has been shown to inhibit ATM, DNA-PK and, to a lesser extent, ATR in cultured cells, resulting in radiosensitisation (Sarkaria *et al.*, 1998). Cells were exposed to wortmannin, followed by 5 Gy IR. Wortmannin treatment did not induce any additional DNA synthesis following 5 Gy IR (Figure 5.4). Similarly, caffeine, a nonselective PIKK inhibitor, is reported to be unable to potentiate the effects of IR in an AT-derived homozygote lymphoblastoid cell line (Bebb *et al.*, 1998).

Collectively, ATM and Chk2 inhibitors cannot abrogate the IR-induced S-phase checkpoint in the absence of p21, suggesting that the radioresistant phenotype of these cells may be attributable to elevated Cdc25A and/or Cdk activity.

5.2.2 S-phase cyclins are transcriptionally upregulated in the absence of p21.

p21 was initially described as a DNA damaged-induced p53-dependent Cdk inhibitor that inactivates cyclin-associated cyclin-dependent kinases in the G1 phase (i.e., Cdk4–Cdk6–cyclinD1 and Cdk2–cyclin E complexes), thereby preventing hyperphosphorylation of the Rb protein and the release of E2F transcription factors (Hatakeyama *et al.*, 1994; Lundberg and Weinberg, 1998; Mittnacht *et al.*, 1994; Sherr and Roberts, 1995). p21 can also directly inhibit E2F-dependent transcription in a Cdk/pRb-independent manner (Delavaine and La Thangue, 1999). In the absence of p21, it is conceivable that DNA synthesis is promoted, as E2F1 transcriptional upregulation of S-phase-promoting proteins such as cyclin E, cyclin A and Cdc25A would be unopposed (Vigo *et al.*, 1999). The level of E2F1 expression was similar in

wild-type and p21-null HCT116 cells (Figure 5.5A). In comparison with the wild-type cell line, HCT116 p21-/- cells display transcriptional upregulation of cyclin A, cyclin E and Cdc25A, but not of Cdk2 or cyclin B1 (Figure 5.5B &C). Cyclin A expression is increased approximately 7-fold, cyclin E is increased 4-fold and Cdc25A is only slightly increased. Vigneron (2006) has also demonstrated that Cdc25A mRNA basal levels are similar between wild-type HCT116 and the isogenic p21-null derivative. However, increased gene expression does not necessarily correlate with increased protein level and activity. The levels of Cdc25A, cyclin A and Cdk2 proteins appear more abundant in the p21-null cell line compared with the parental cell line (Figure 5.5D). Cyclin B levels remained unchanged in the absence of p21. As described previously, initiation of DNA synthesis requires the appropriate activation of Cdk2-associated cyclins. Cdc25A is essential for embryonic development and for activation of Cdk4/cyclin D and Cdk2/cyclin E (Hoffmann *et al.*, 1994; Jinno *et al.*, 1994). Cdc25A overexpression can result in the removal of wee1- and myt1-dependent inhibitory phosphorylation at threonine-14 and tyrosine-15, resulting in increased Cdk2 activity (Blomberg and Hoffmann, 1999). Although there is no difference in Cdk2 mRNA expression (Figure 5.5C), protein levels are approximately doubled in the absence of p21 (Figure 5.5D). Intriguingly, there is an increase in Cdk tyrosine-15 phosphorylation in the absence of p21, but a decrease in threonine-14 phosphorylation (Figure 5.6A). In contrast, there is no change in phosphorylation at the threonine 160 activation site, which is regulated by CAK. Differences in the inhibitory phosphorylation patterns can be explained by antibody specificity. The Cdk2 threonine-14 antibody is a specific rabbit monoclonal antibody, but the antibody used to detect Cdk tyrosine-15 (rabbit polyclonal

antibody; Cell Signalling #9111) also detects Cdc2/CDK1 tyrosine-15, CDK2 tyrosine-15 and CDK5 tyrosine-15. The use of a specific antibody that detects only Cdc2/CDK1 tyrosine-15 (rabbit monoclonal antibody 10A11; Cell Signalling #4539) phosphorylation suggests that most tyrosine phosphorylation is attributable to Cdc2/CDK1 in the p21-null cell line (Figure 5.6B). This suggests that the G2/M checkpoint is activated in these cells. Next, immunoprecipitation experiments were undertaken to clarify whether differences in Cdk tyrosine-15 phosphorylation exist between the parental and p21-null cell lines. Cdk tyrosine-15 was immunoprecipitated from wild-type and p21-null cells (using #9111) and probed with the Cdk2 antibody. Tyrosine phosphorylation appeared to be higher in wild-type HCT116 cells than in p21-null cells (Figure 5.6C). A slower migrating form of Cdk2 was observed in the parental cell line, suggesting that Cdk2 may be hyperphosphorylated and/or is subject to additional post-translational modifications in these cells. Collectively, these results suggest that Cdk2 has less inhibitory phosphorylation on threonine-14 and tyrosine-15 in the absence of p21, perhaps as a result of increased Cdc25A protein expression. Cdc25A protein overexpression, unscheduled activation of Cdk2 and overabundant cyclin A are all consistent with the promotion of radioresistant DNA synthesis in the p21-null cell line.

5.2.3 Basal Cdc25A levels and DNA damage-induced degradation are affected by the loss of p21.

The rapid reduction of DNA synthesis following low dose IR-induced DNA damage is primarily due to activation of the ATM-Chk2 pathway, which results in the degradation of the dual specificity phosphatase Cdc25A (Falck *et al.*, 2001; Mailand

et al., 2000). Basal levels of Cdc25A are higher in the p21-null cells than in the HCT116 parental cell line (Figure 5.5C). Increased Cdc25A protein expression may be due to increased genetic transcription, altered mRNA processing, increased protein stability due to post translational modifications or reduced protein degradation by the proteosome. Cdc25A mRNA transcript expression was only slightly increased in the absence of p21 (Figure 5.5A). *CDC25A* gene expression is under the control of the myc proto oncogene and E2F (Galaktionov *et al.*, 1996; Vigo *et al.*, 1999) transcription factors. In addition, p21 has been reported to repress *MYC* and *CDC25A* transcription upon DNA damage (Vigneron *et al.*, 2006). As p21 is upregulated later in the DNA damage response cascade (Figure 4.4), it may be responsible for transcriptional repression of Cdc25A at the 12 h time point, resulting in the reduction of Cdc25A protein seen in the wild-type cell line but not in p21-null cells (Figure 4.4). To determine whether the increase in Cdc25A protein was due to increased protein stability, the protein stability of Cdc25A was analysed using cycloheximide, a protein synthesis inhibitor. Exponentially growing cells were treated with 10 μg/ml cycloheximide and harvested at ten minute intervals. Although p21-null cells contained approximately three–four times more Cdc25A protein than did wild-type cells, the half-life of Cdc25A was shorter than in the parental cell line (Figure 5.7). Cdc25A levels are low following mitosis and increase gradually throughout G1, peaking in early S phase upon mitogenic stimuli. The basal turnover of Cdc25A is dependent on Chk1-dependent phosphorylation on serine-76 that targets the protein for ubiquitination by ANAPC/C^{cdh1} ubiquitin ligase complex, resulting in proteasome-mediated degradation (Donzelli *et al.*, 2002; Zhao *et al.*, 2002). Degradation of Cdc25A following DNA damage is dependent on the SKP1-

CUL1-F-box protein (SCF)β–TRCP E3 ubiquitin ligase -mediated complex that targets phosphorylated Cdc25A for degradation by the proteasome (Busino *et al.*, 2003; Donzelli *et al.*, 2004; Jin *et al.*, 2003). To determine whether there is a specific defect in DNA damage-induced Cdc25A degradation in p21-null cells, both wild-types and p21-null cells were treated with 5 Gy IR and then with cycloheximide. Cdc25A was degraded within 10 min in the HCT116 parental cell line, but DNA damaged-induced degradation was delayed in p21-null cells (Figure 5.8). Pre-incubation with an ATM inhibitor prevents DNA damage-induced Cdc25A degradation in wild-type HCT116 cells and in p21-/- cells (Figure 5.8) Damage-induced Cdc25A degradation involves many steps, including Chk2 phosphorylation, recognition by ubiquitin ligases, nuclear export and proteasomal degradation. Leptomycin B inhibits Exportin 1, a nuclear export factor that mediates nuclear export signal-dependent protein transport. Leptomycin B treatment blocked DNA damage-induced degradation of Cdc25A in wild-type cells and, to a lesser extent, in p21-null cells (Figure 5.9). Cdc25A is degraded by the proteasome. Indirect analysis of proteasome function was undertaken using the specific proteasome inhibitor MG132. In both wild-type and p21-null cells, damage-induced Cdc25A degradation was blocked by proteasome inhibition, suggesting that the failure to degrade Cdc25A in the absence of p21 is not due to decreased proteasome activity (Figure 5.9). Cdc25A levels were analysed over a 24 h time course following 5 Gy IR in wild-type HCT116 cells and p21-/- cells without cycloheximide treatment. In wild-type cells, Cdc25A was biphasic: protein was degraded after 2 h, levels recovered after 4–12 h, and degradation again occurred after 24 h. In p21-/- cells, there was only a partial reduction in Cdc25A protein levels at 2 h, which recovered at 4–24 h. Thus, DNA

damage regulation of Cdc25A is altered in the absence of p21. Furthermore, pretreatment of cells with the ATM inhibitor prevented Cdc25A degradation in wild-type HCT116 cells at 2 h (Figure 5.2), but this was less effective in p21-null cells, which is consistent with the radioresistant phenotype (Figure 5.1), supporting previous evidence that constitutive activation of the ATM–Chk2 pathway is unable to effectively induce S-phase arrest. Mechanistically, the overexpression and delayed reduction in DNA damage-induced Cdc25A degradation forms the basis for the radioresistant phenotype.

Although not further examined in this study, enhanced Cdc25A stability may also influence the failure to arrest at G2/M in these cells (Busino *et al.*, 2004; Mailand *et al.*, 2002; Zhao *et al.*, 2002).

5.2.4 DNA damage-induced Cdc25A degradation is reduced in the p21-null background.

To examine whether the reduced degradation of Cdc25A that occurs in the absence of p21 is specific to IR, other DNA damaging agents were also examined. Neocarzinostatin is a radiomimetic drug that induces similar types of DNA damage as ionising radiation. Asynchronous cells were exposed to 200 ng/ml neocarzinostatin, and DNA synthesis and Cdc25A levels were analysed in combination with cycloheximide. In the wild-type cells, there was a steep decline in DNA synthesis, which stabilised after 4 h (Figure 5.10A); this was accompanied by Cdc25A degradation at 30 minutes (Figure 5.10B,C). In contrast, in the absence of p21 there is a minimal reduction of DNA synthesis after 30 min, although DNA synthesis is reduced thereafter, thus demonstrating a partial radioresistant phenotype.

In p21 null cells (Figure 5.10C) Cdc25A degradation appears to occur at a faster rate but the abundant Cdc25A protein is able to promote DNA synthesis in the presence of DNA damage. Altenatively, the overexpressed cyclinA (Figure 5.5) and uninhibited cdk2 (Figure 5.6) may also promote unscheduled DNA synthesis.

p21-/- cells show basal Cdc25A overexpression. Following 5 Gy IR, Cdc25A levels remained high despite rapid Chk2 threonine-68 phosphorylation and Chk1 serine-317 phosphorylation occurring at later time points (Figure 4.4). UV-induced DNA damage has been shown to preferentially activate the ATR–Chk1 pathway, resulting in Cdc25A degradation. Therefore, p21-null cells are expected to continue undergoing radioresistant DNA synthesis in the presence of UV damage. To test this, cells were subjected to 10 J/m^2 UV radiation and assayed for both DNA synthesis and Cdc25A levels. Wild-type HCT116 cells showed a reduction in DNA synthesis throughout the time course (Figure 5.11A), accompanied by Cdc25A degradation (Figure 5.11B). However, in the absence of p21, there was no immediate (within 30 min) reduction in DNA synthesis or although the degradation profile of Cdc25A was similar in the first 20 minutes (Figure 5.11A and B). However, DNA synthesis was reduced sharply thereafter. The degradation profile at 30 minutes between the cell lines may be explain the apparent lack of reduction in DNA synthesis in the HCT 116 p21-/- cell line compared with the wild type cell line.

As different forms of DNA damage are unable to degrade Cdc25A as effectively in the absence of p21, these data provide additional evidence that the S-phase checkpoint is defective at the level of S-phase-promoting proteins.

DNA topoisomerases are enzymes involved in resolving the DNA helical structure, thus enabling DNA synthesis. Type 1 topoisomerases cut one strand of the DNA helix to allow relaxation of supercoiled and reannealing. Type II topoisomerases cut both strands of DNA, which allows another double-strand of DNA to pass through, before religation (Bower *et al.*, 2010b). Adriamycin is a DNA intercalator that has different effects depending on the concentration used. Its effect on S phase is dependent on the dosing schedule and tissue type. Low doses of adriamycin stabilise (or poison) the topoisomerase II–DNA complex after cleavage of the first strand, thereby trapping the enzyme, preventing cutting of the second strand and inhibiting DNA unwinding for replication, which therefore inhibits DNA synthesis. High doses of adriamycin intercalate with DNA, thus altering the molecular structure and preventing topoisomerase II from relieving DNA supercoils to allow DNA replication (Pommier *et al.*). This latter mode of action has been shown to generate DNA DSB (Bower *et al.*, 2010a). Both wild-type and p21-null HCT116 cells were treated with 1 μM adriamycin (low dose). Interestingly, a DNA synthesis assay demonstrated similar time-dependent reductions in DNA synthesis following exposure to this dose of adriamycin, which correlated with Cdc25A accumulation in both cell lines (Figure 5.12). This suggests that adriamycin-induced reduction in DNA synthesis is independent of Cdc25A degradation. In order to clarify whether direct topoisomerase inhibitors delay DNA synthesis independently of Cdc25A (and DNA damage checkpoint activation), another more specific topoisomerase inhibitor was utilised. ICRF-193 inhibits the catalytic site of topoisomerase, trapping the enzyme on the DNA in a noncleavable complex (Fasulo *et al.*), and is associated with G2/M arrest (Chene *et al.*, 2009). Topoisomerase II catalytic inhibitors have

been shown to prevent topoisomerase II-associated cleavage of DNA complexes and therefore appreciable numbers of DNA strand breaks (Bower *et al.*, 2010a). Therefore, any reduction seen in DNA synthesis should occur after completion of S phase and reflects G2 arrest. Consequently, no changes in Cdc25A protein level are expected. In wild-type HCT116 cells, exposure to 10 μM ICRF-193 for 12 h did not activate a robust checkpoint response, which may be related to the low amount of DNA damage sustained. HCT116 cells have a functional deficiency of the MRN trimeric complex, which is necessary for the recognition of low levels of DNA damage (Lossaint *et al.*, 2011). An alternative mechanism has been described by Bower *et al.* (2010b), in which ICRF-93 inhibition of topoisomerase induces ATM-dependent phosphorylation of Chk2 and p53, mediators of the G2/M arrest independent of DNA damage as no γ–H2AX was detected. I therefore exposed wild-type and p21-null HCT116 cell to 35 μm ICRF-193 and analysed DNA synthesis and Cdc25A levels, as previously described. Regardless of p21 status, normal levels of DNA synthesis took place up to 4 h following with drug treatment and only decreased at after 8 h; no acceleration in Cdc25A degradation was observed at these time points (Figure 5.13). Cell cycle profiles would clarify that the reduction in DNA synthesis represents accumulation of cells at the G2/M phase. These data confirm that ICRF 193 does not activate a DNA damage checkpoint in S phase but is more likely to activate the decatenation checkpoint prior to entry into mitosis by promoting the cytosolic sequestration of Cdk1/Cyclin B1(Deming *et al.*, 2001). The decatenation checkpoint delays entry into mitosis until newly synthesised daughter DNA are released by DNA topoisomerase II and is distinct from the mitotic spindle

checkpoint that delays anaphase and telphase until metaphase has been completed (Andreassen *et al.*, 2001; Deming *et al.*, 2001).

Measurement of DNA synthesis and Cdc25A levels after treating the HCT116 p21 null cells with different types of DNA damage has clarified that the RDS phenotype of p21-null cells is associated with the less effective DNA damage-induced Cdc25A degradation. Ponceau stained membranes confirm that the differences in Cdc25A levels are not due to unequal protein loading (Figure 5.14).

5.2.5 SiRNA-mediated Cdc25A knockdown leads to a reduction in DNA synthesis

In the absence of p21, cells exhibit heightened Cdk activity and therefore short-term knockdown of Cdc25A was used to determine whether Cdc25A overexpression is indeed the reason for the radioresistant phenotype of p21-null cells. Short-term siRNA-mediated Cdc25A knockdown in p21-null cells leads to an increase in inhibitory phosphorylation of Cdk2 at threonine-14 (Figure 5.15A). There is very little enhancement in Cdc25A degradation following 5 Gy IR in siRNA-treated cells (Figure 5.15A; compare Cdc25A and Cdc25A irradiated), in line with my previous data (Figure 4.4). DNA synthesis is reduced in Cdc25A siRNA treated samples, confirming efficient knockdown of Cdc25A (Figure 5.15B). In line with previous data, there are no differences in Cdc25A levels and DNA synthesis between unirradiated and irradiated samples (Figure 5.15). DNA synthesis can be reduced in the p21-null cell line by a reduction in Cdc25A expression; confirming that the RDS phenotype seen in p21-null cells is secondary to Cdc25A overexpression (resulting from an inability to degrade Cdc25A), as opposed to overactive Cdk/cyclin complexes.

5.2.6 Chk2 is differentially localised in the absence of p21.

Following DNA damage, Cdc25A degradation is mediated by the checkpoint kinases, Chk1 and Chk2. Cells deficient in ATM or Chk2 demonstrate a delay in Cdc25A degradation. However, Chk2 is not essential for this purpose, as Chk1 can compensate when Chk2 is depleted from wild type HCT116 cells (Jin *et al.*, 2008) . The correct spatial organisation of DDR proteins is important for transducing the damage signal to downstream effectors (Lukas *et al.*, 2004b). I therefore examined the possibility that p21 directly or indirectly influences the localisation of DDR proteins. Whole cell lysates were fractionated according to differential solubility of cell components in Triton X-100, and both soluble (cytoplasmic) and insoluble (nuclear) materials were collected by centrifugation. GAPDH is an abundant soluble protein, which was used to confirm the efficiency of cell fractionation (Figure 5.16). The soluble proteins were collected after lysing the cell membrane without disrupting the nuclear compartment. The insoluble fraction contained chromatin bound proteins. In untreated (control) wild-type HCT116 cells, Chk2 is present in the soluble fraction and treatment with 5 Gy IR, ATM inhibition for 24 h or a combination of both does not lead to a change in localisation. Cdc25A levels in the insoluble fraction appear to be reduced after 5 Gy IR with or without ATM inhibition. p53 stability is increased in the insoluble fraction in response to DNA damage, but this is reversed in the presence of ATM inhibition. In comparison, HCT116 p21-null cells express a slower migrating form of Chk2 in the soluble fraction and a small pool of faster migrating Chk2 in the insoluble chromatin compartment. Following 5 Gy IR, the amount of Chk2 in the insoluble fraction is unchanged, suggesting that it is not released from chromatin under these circumstances. The inability of p21-null cells to release a

small but significant pool of Chk2 from chromatin may partly explain the inefficient degradation of Cdc25A following DNA damage and subsequent radioresistant DNA synthesis. Incubation of p21-/- cells for 24 h with the ATM inhibitor leads to a loss of Chk2 from the insoluble compartment; this suggests that activation of additional upstream kinases leads to Chk2 release from chromatin. Combined treatment of cells with ATM inhibition and 5 Gy IR appears to lead a reduction in soluble Chk2 but not in insoluble Chk2. The reason for this difference is unclear but may represent unequal protein transfer. Cdc25A levels remain unchanged, regardless of treatment and the amount of insoluble p53 protein increased after 5 Gy IR. The GAPDH signal is slightly lower in p21-null compared with wild-type HCT116 cells, suggesting higher protein concentrations in the wild type HCT116 cells compared with the p21 null cells. However, this does not detract from the observed differences, as no Chk2 signal is apparent in the insoluble fraction in wild-type HCT116 cells.

5.3 Discussion

IR induced radioresistant DNA synthesis can arise from a deficiency in upstream DNA damage-dependent kinases or overexpressed and/or mutated forms of downstream S-phase-promoting proteins. The specific ATM inhibitor, KU-55993, abrogated the DNA damage-induced S-phase checkpoint in wild-type HCT116 cells (Figure 5.1); this effect was not observed in either the AT cell line (due to the lack of ATM) or the p21-null cell line. Furthermore, following irradiation, there was no reduction in Cdc25A protein levels in the wild-type HCT116 cell line, as was seen previously (compare Figure 5.2 with Figure 2.1). Inhibition of ATM for 1 h in the p21-null cell line resulted in Chk1 phosphorylation at serine-317; this was also apparent after 2 h in the wild-type cell line. This result suggests that additional

kinases are activated in p21-null cells upon ATM inhibition. ATM directly phosphorylates Chk2 at threonine-68, leading to activation. Activated Chk2 phosphorylates Cdc25A on serine-134; however phosphorylation at this site has not been shown to be a prerequisite for ubiquitin-mediated degradation (Busino *et al.*, 2003; Donzelli *et al.*, 2004; Jin *et al.*, 2008). Inhibition of neither ATM nor Chk2 in p21-/- HCT116 cells attenuated the S-phase checkpoint; this suggests that the IR induced radioresistant DNA synthesis (RDS) phenotype is caused by factors downstream of these kinases. The inability to degrade Cdc25A appropriately in response to DNA damage has previously been shown to result in RDS (Falck *et al.*, 2001; Zhao *et al.*, 2002). Basal Cdc25A turnover did not appear to be defective, although damage-induced degradation was slowed in the absence of p21. This response was specific to agents that induce the DNA damage-dependent S-phase checkpoint, including IR, neocarzinostatin and UV irradiation. DNA damage-induced degradation of Cdc25A is dependent on checkpoint kinases and associated with phosphorylation on serine-76; additional phosphorylation at serines 82 and 88 promote $SCF\beta^{TRCP}$-mediated degradation (Donzelli *et al.*, 2002; Jin *et al.*, 2008). Inhibition of topoisomerase II enzymes led to a reduction in DNA synthesis but there was no appreciable change in the levels of Cdc25A. Reasons for the delayed degradation of Cdc25A include mislocalisation of checkpoint kinases, kinase mutation and inactivation, Cdc25A mutation (Busino *et al.*, 2003; Mailand *et al.*, 2000), Cdc25A overexpression (Falck *et al.*, 2001), loss of protein ubiquitination and defects in ubiquitin/proteasome complex components (Busino *et al.*, 2003)

Cdc25A is considered to be an oncogene, with cancer-promoting properties that are linked to its role in sustaining progression through the cell cycle. Cdc25A

overexpression has been demonstrated in a variety of human cancers, including breast, colorectal, endometrial, liver and oesophageal cancers, and non-Hodgkin lymphomas (Boutros *et al.*, 2007; Kristjansdottir and Rudolph, 2004), due to increased protein stability (Loffler *et al.*, 2003); however, evidence for a specific role for Cdc25A in colorectal cancer is sparse. Cell culture models have identified Cdc25A downregulation in response to mesalazine therapy, which forms a protective mechanism against the development of inflammatory bowel disease-associated colorectal cancer (Stolfi *et al.*, 2008).

Mislocalisation of Chk2 may explain the reduced degradation of Cdc25A in p21-null cells. A slower migrating form of Chk2 was observed in the soluble fraction; this was absent in the insoluble chromatin-bound fraction in wild-type cells. This result suggests that soluble Chk2 protein is hyperphosphorylated or has undergone additional post-translational modification. In the absence of p21, there was a small pool of Chk2 associated with chromatin, which was unaffected by treatment with 5 Gy IR but was lost after 24 h incubation with the ATM inhibitor. Li *et al.* (2005) demonstrated that a small pool of chromatin-associated hypophosphorylated Chk2 is activated and released from chromatin in response to DNA damage; in the presence of ionising irradiation, this is ATM dependent. Chk2 mobility is necessary for transducing the damage signal, and forced immobilisation at sites of double-strand breaks reduces p53 activation and subsequent p53 dependent transcription (Lukas *et al.*, 2004b). Likewise, chromatin-associated viral proteins that bind to and sequester Chk2, thus hindering its release from chromatin, cannot induce an appropriate DNA damage response (Gupta *et al.*, 2007). Notably, Jin *et al.* (2008) demonstrated that Cdc25A degradation in HCT116 cells is dependent on Chk1, but not on Chk2, in

response to 10 Gy IR. However, it is possible that the higher dose of irradiation has masked a subtle Chk2-mediated effect on Cdc25A degradation. In p21-/- cells, it is surprising that Chk1 cannot compensate for such a mechanism, suggesting that Chk2 may be an important cofactor or directly responsible for Cdc25A degradation in this cell line. Alternatively, Chk1 may be inappropriately associated with chromatin, which may explain the similar profile in Cdc25A degradation following UV treatment (Figure 5.11).

Protein overexpression or delayed degradation may be a global phenomenon in the p21-null background. Certainly, Cdc25A, Cdk2, Chk1, Chk2, and cyclin A and p53 all appear to be overexpressed and/or more stable in p21-null cells. Cangi *et al.* (2008) showed that Cdc25A overexpression in primary human mammary epithelial cells results in unscheduled S phase entry and multiple firing of DNA replication origins within a single cell division cycle. Although, p21 has been shown to directly regulate the level and activity of S-phase proteins, such as PCNA (Guo *et al.*, 1999) I was unable to confirm a direct role in the DNA damage induced intra-S-phase checkpoint. Equally surprising is the apparent mislocalisation of Chk2 in HCT116 p21-null cells.

In the HCT116 p21 null cells abrogation of the DNA damage induced checkpoints, overexpression of S phase promoting proteins, reduced DNA damage induced degradation of Cdc25A and protein mislocalisation all contribute to the IR induced RDS phenotype. Further detailed investigation is required in non-transformed cells to directly asses the relationship of p21 and the DNA damage induced intra-S-phase checkpoint.

A

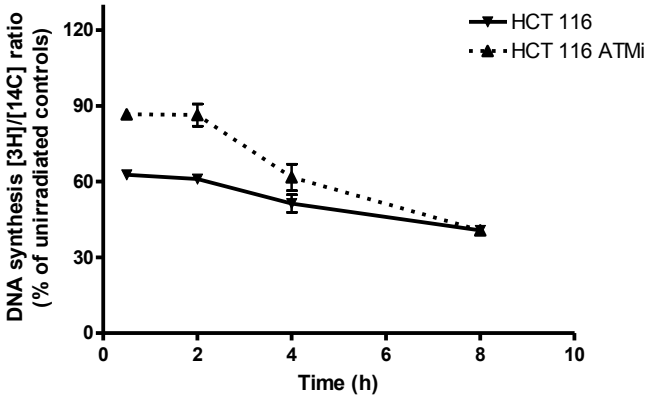

B

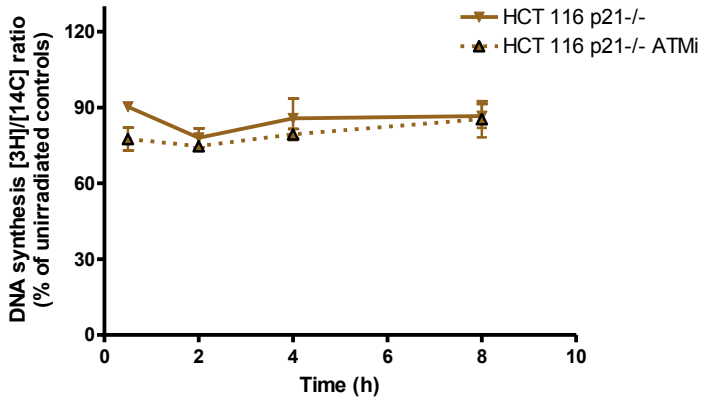

C

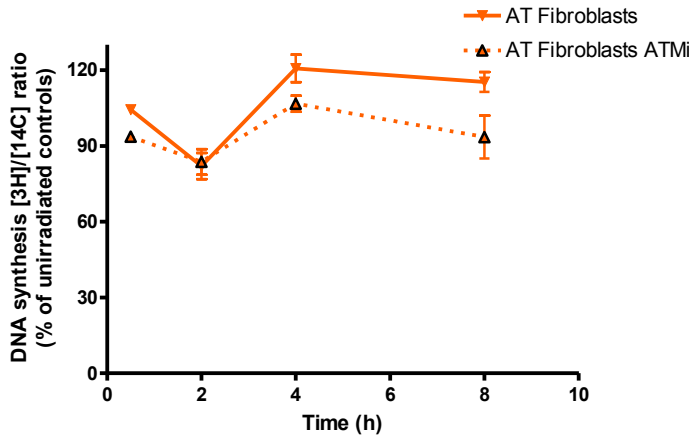

Figure 5.1. ATM inhibition abrogates the S-phase checkpoint in wild-type HCT116 cells but not in isogenic p21-null cells.

(*A*). Wild-type HCT116 cells pretreated with the ATM inhibitor (ATMi; broken line) demonstrate increased DNA synthesis following treatment with 5 Gy IR, compared with IR alone (solid line). This effect was not seen in (*B*) isogenic p21-null cells or (*C*) in AT cells. DNA synthesis was assayed as previously described. Error bars indicate standard deviation of the mean.

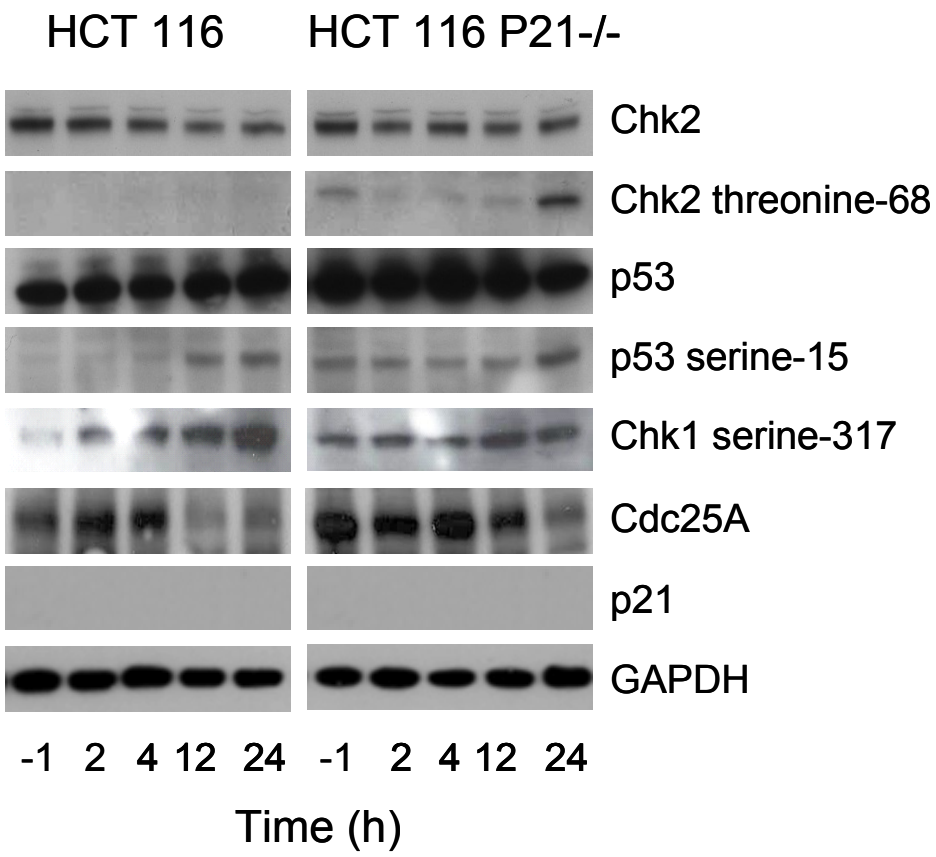

Figure 5.2. KU-55933 treatment abrogates the ATM-dependent DNA damage response in wild-type HCT116 cells.

Abrogation of the ATM-dependent DDR occurred in wild-type HCT116 cells but was less efficient in p21-null cells. Cells were exposed to 10μM of the ATM inhibitor KU-55933 for 1 h (-1 time point) and then treated with 5 Gy ionising radiation and harvested over a 24-h time course. Equivalent amounts of protein (40μg/lane) were analysed by immunoblotting on the same blot. GAPDH was used as a loading control. Antibodies were described in Figure 3.4.

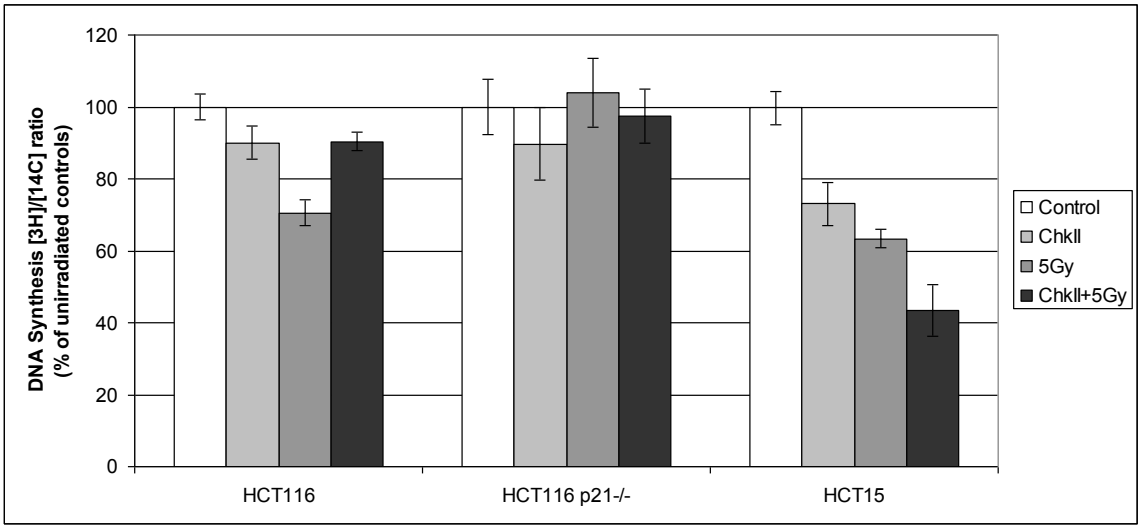

Figure 5.3. Chk2 inhibition abrogates the IR-induced S-phase checkpoint in wild-type but not in p21-null HCT116 cells.

Wild-type HCT116 cells pretreated with a Chk2 inhibitor (Chk II) demonstrate increased DNA synthesis 30 min after treatment with 5 Gy. This effect was not seen in p21-/- HCT116 or HCT15 cells. DNA synthesis was analysed as previously described. Experiments were done in triplicate and error bars indicate standard deviation of the mean.

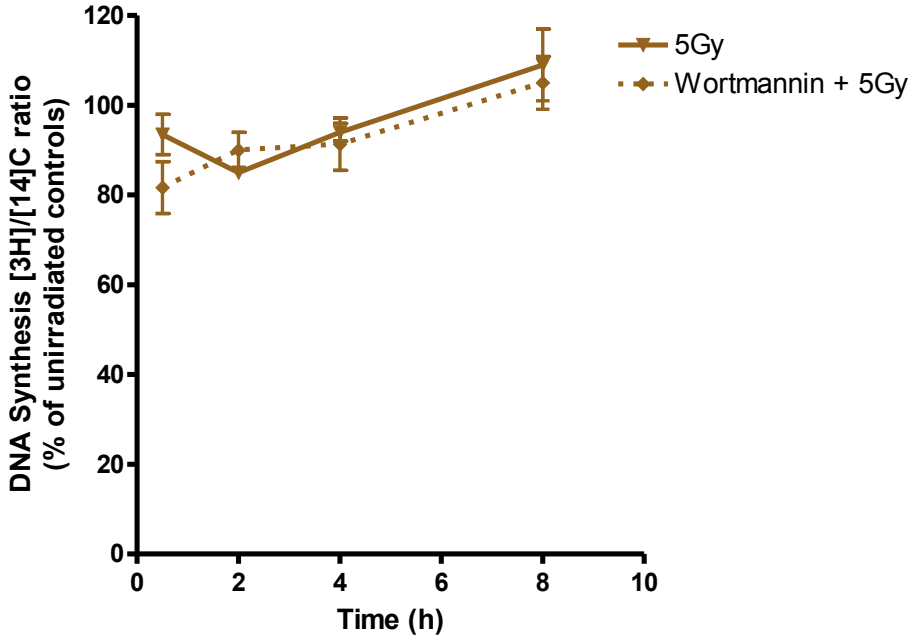

Figure 5.4. The radiosensitising agent, wortmannin, is unable to abrogate DNA synthesis in p21-/- HCT116 cells.

Asynchronous cells were pretreated with 10 μM wortmannin and then exposed to 5 Gy ionising radiation. DNA synthesis was assessed at the indicated time points. Limited amount of drug precluded the same experiment in wild type cells. Experiments were done in triplicate and error bars indicate standard deviation of the mean.

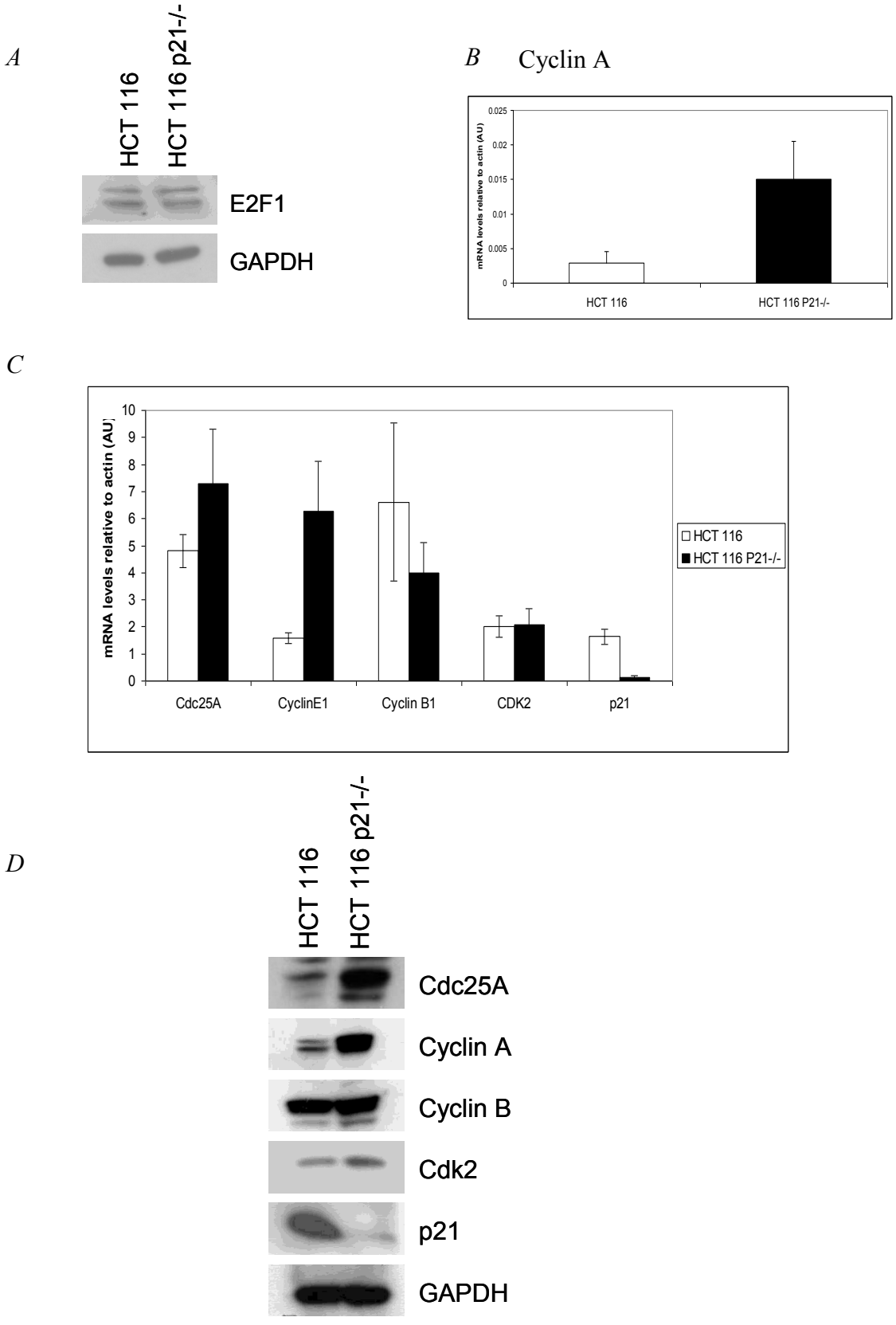

Figure 5.5. S-phase cyclins are transcriptionally upregulated in the absence of p21 and show a corresponding increase in protein levels. See opposite page for legend details.

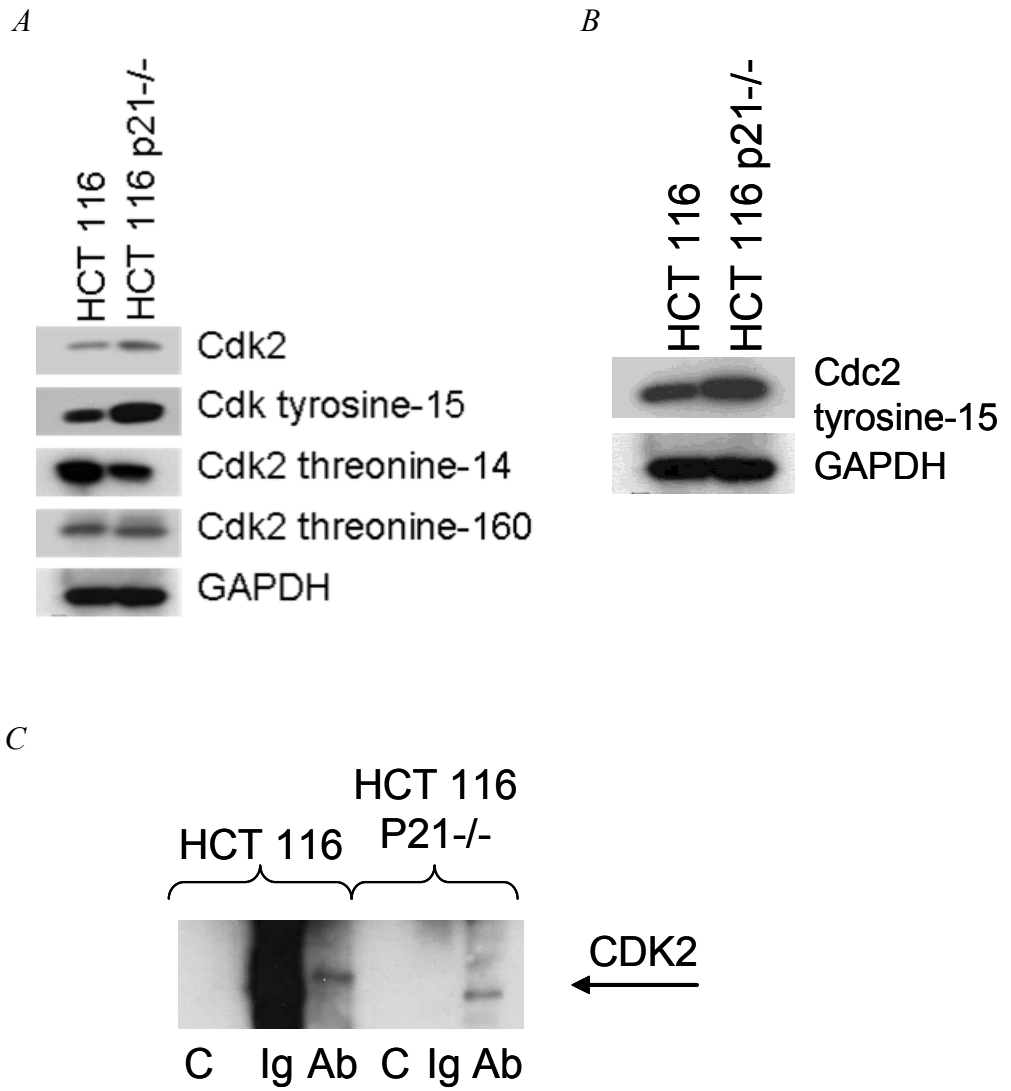

Figure 5.6. Reduction in inhibitory phosphorylation in CDK2 under basal conditions.

(*A*). HCT116 p21-nulls display a reduction in the Cdk2 phosphorylation at the inhibitory threonine-14 site. (*B*) Inhibitory phosphorylation on Cdc2 tyrosine-15 appears to be increased, but this may reflect poor antibody specificity (see text for details). (*C*) Cdk tyrosine-15 immunoprecipitated from cell lysates was probed with an antibody recognising total Cdk2. Equivalent amounts of protein (40 µg/lane) were analysed by immunoblotting. GAPDH was used as a loading control. Antibody, Ab; Control, C; Immunoglubulin control, Ig.

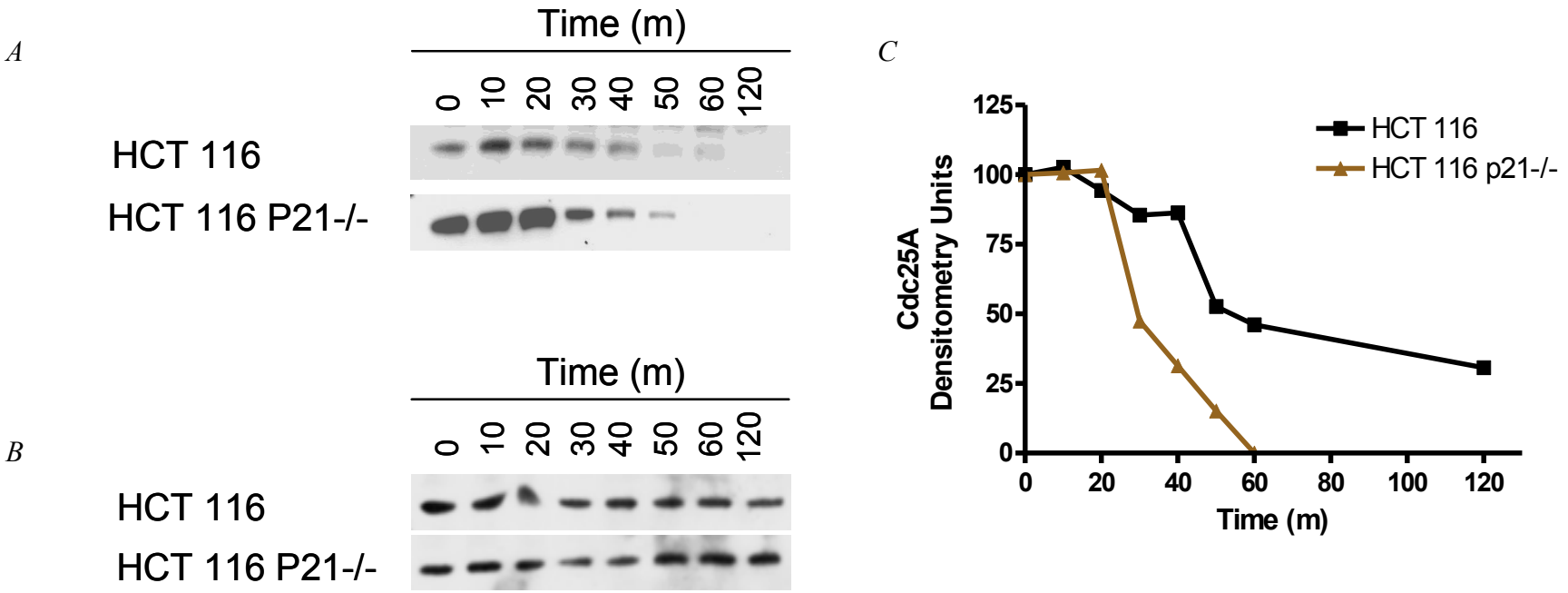

Figure 5.7. High basal Cdc25A expression in p21-/- HCT116 cells is not due to increased stabilisation.

Loss of p21 does affect the half-life of Cdc25A (*A*)**.** Lysates were prepared from wild-type and p21-/- HCT116 cells at ten minute intervals following treatment with 10µg/ml cycloheximide. Equivalent amounts of protein (40µg/lane) were analysed by immunoblotting with an anti-Cdc25A antibody. (*B*) A cross-reacting band used as a loading control. (*C*) Cdc25A is degraded more rapidly in HCT 116 p21-/- cells compared with wild type cells despite the higher abundance.

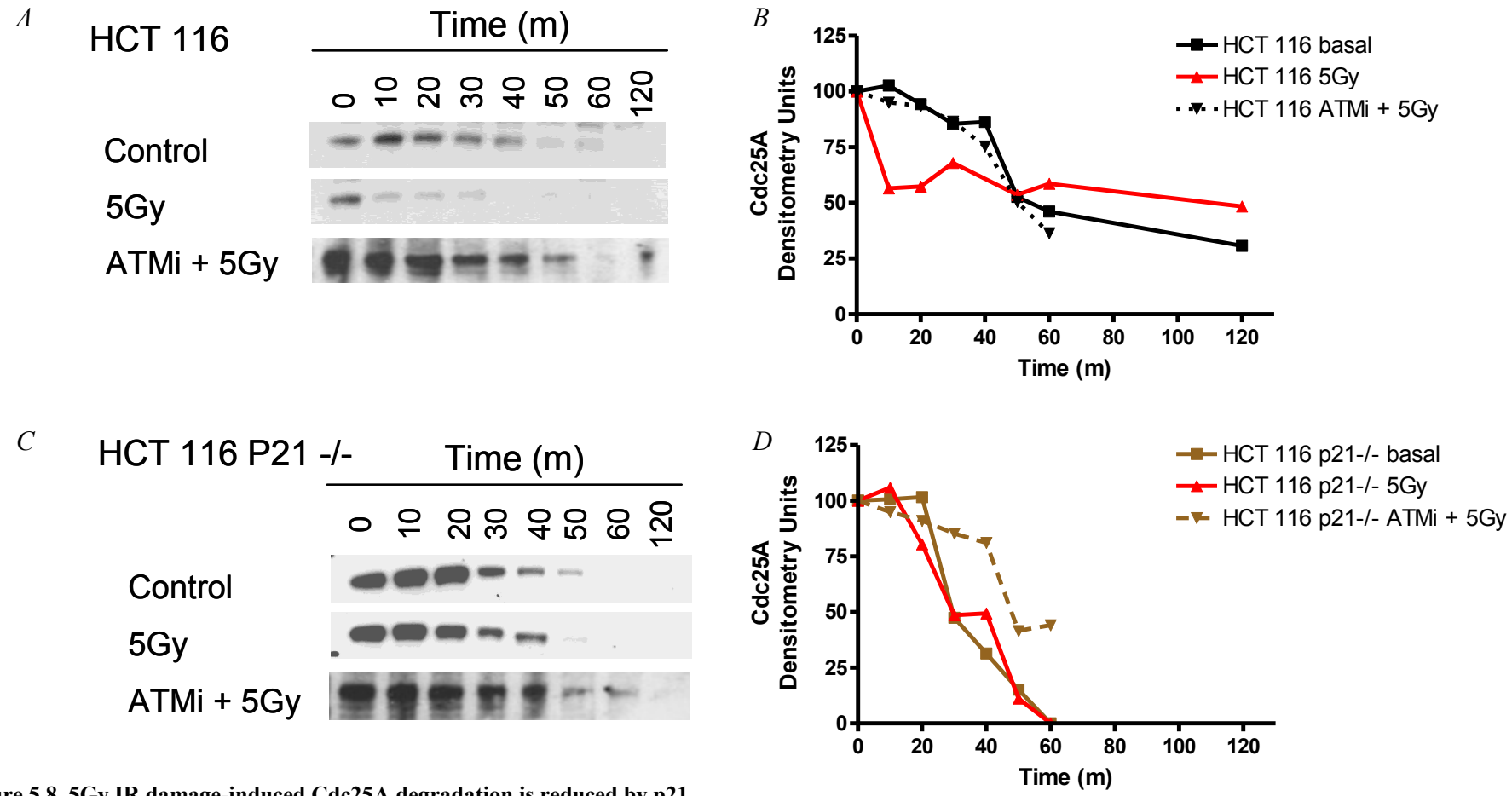

Figure 5.8. 5Gy IR damage-induced Cdc25A degradation is reduced by p21.

HCT116 p21-/- cells are unable to increase the degradation of Cdc25A after 5Gy IR. (*A*) Wild-type and (*C*) p21-/- HCT116 cells were treated with 5 Gy ionising radiation, 10 μg/ml cycloheximide, and harvested at 10 min intervals (solid red line). ATM inhibition delays Cdc25A degradation in both cell lines (broken line). (*B,D*)T he densitometry line graphs represent Cdc25A degradation over time in each cell line, respectively. Equivalent amounts of protein (40 μg/lane) were analysed by immunoblotting with an anti-Cdc25A antibody.

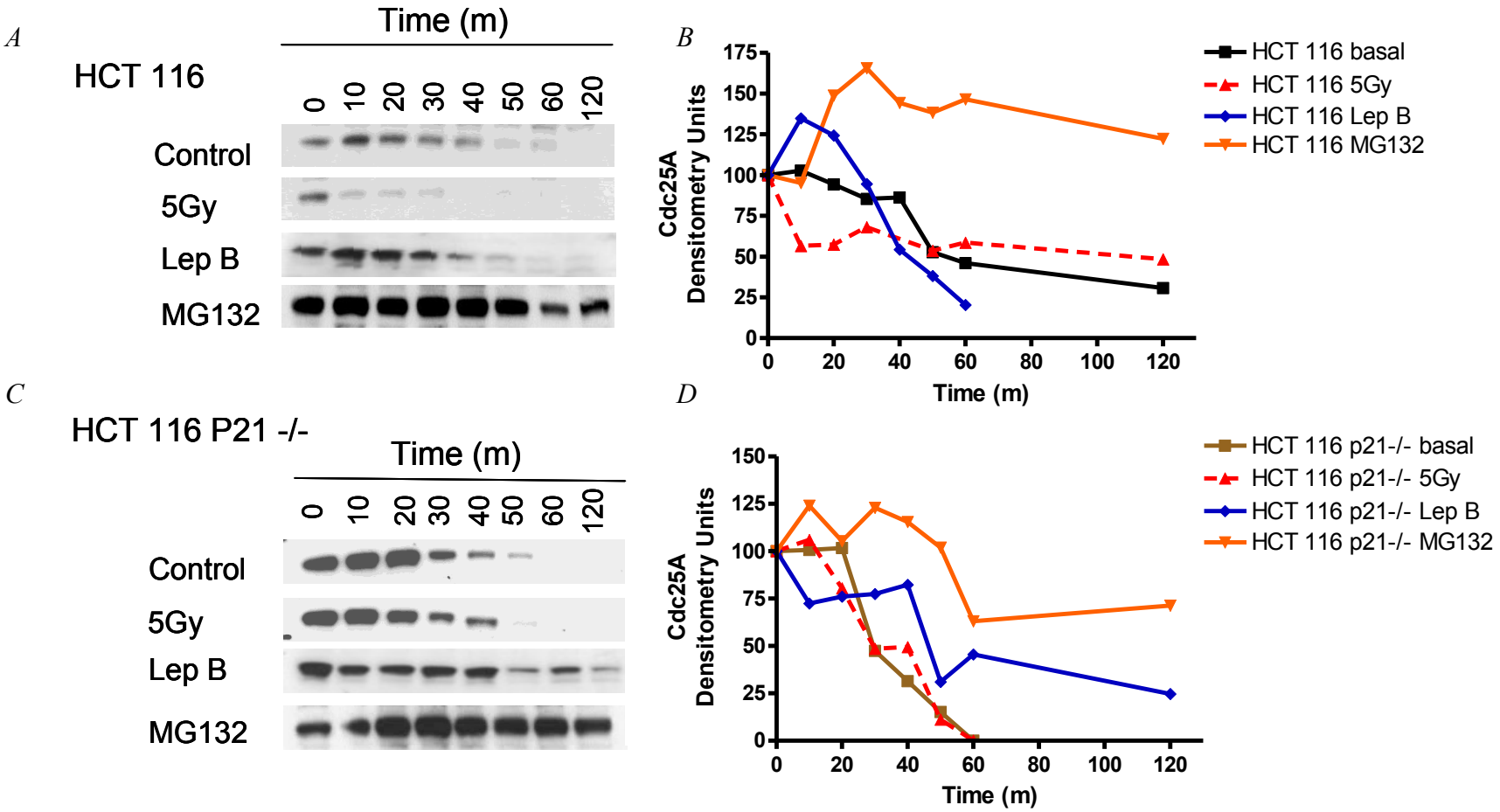

Figure 5.9. Nuclear export and proteasomal degradation of Cdc25A is unaffected by the loss of p21.

Inhibiting damage-induced nuclear export and proteasome activity recovers Cdc25A in both wild-type and p21-null cells. (*A*) Wild-type and (*C*) HCT 116 p21-/- cells were treated with 5 Gy ionising radiation, followed by 10 µg/ml cycloheximide and either 2 nm leptomycin B or 25 µM MG132. (*B,D*) The densitometry line graphs represent Cdc25A degradation over time in each cell line, respectively.

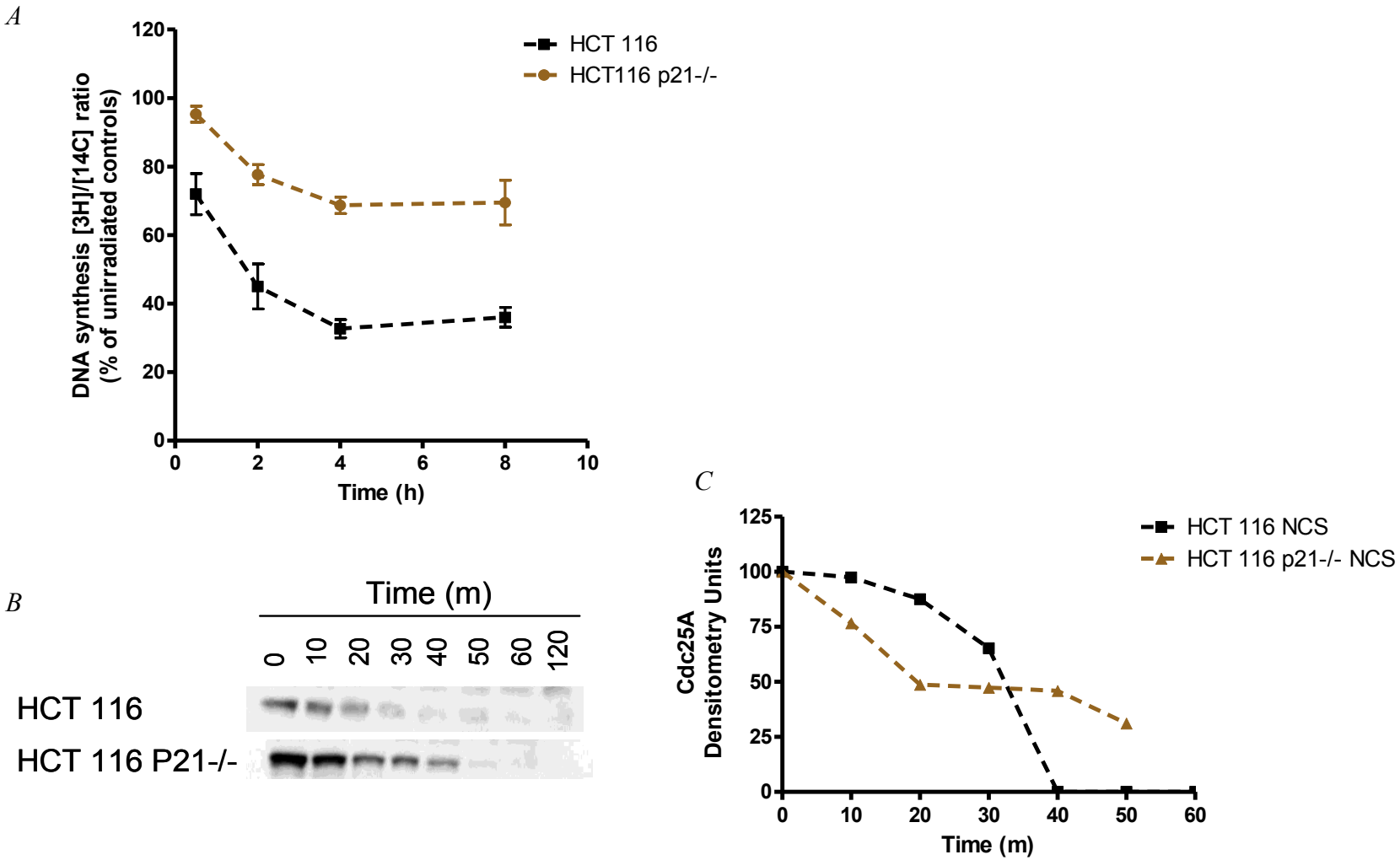

Figure 5.10. HCT 116 p21-/- cells demonstrate a partial radioresistant phenotype in the presence of 200ng/ml neocarzinostatin.

(*A*) Wild-type HCT 116 cells can suppress DNA synthesis and degrade Cdc25A. In the absence of p21, cells are less able to inhibit DNA synthesis and (*B*) degrade Cdc25A less effectively. Cells were treated with 200 ng/ml neocarzinostatin (NCS); DNA synthesis was measured as described previously and cells harvested at 10 min intervals in the presence of 10 μg/ml cycloheximide. (*C*) The densitometry line graphs calculated from *(B)* represent Cdc25A degradation over time.

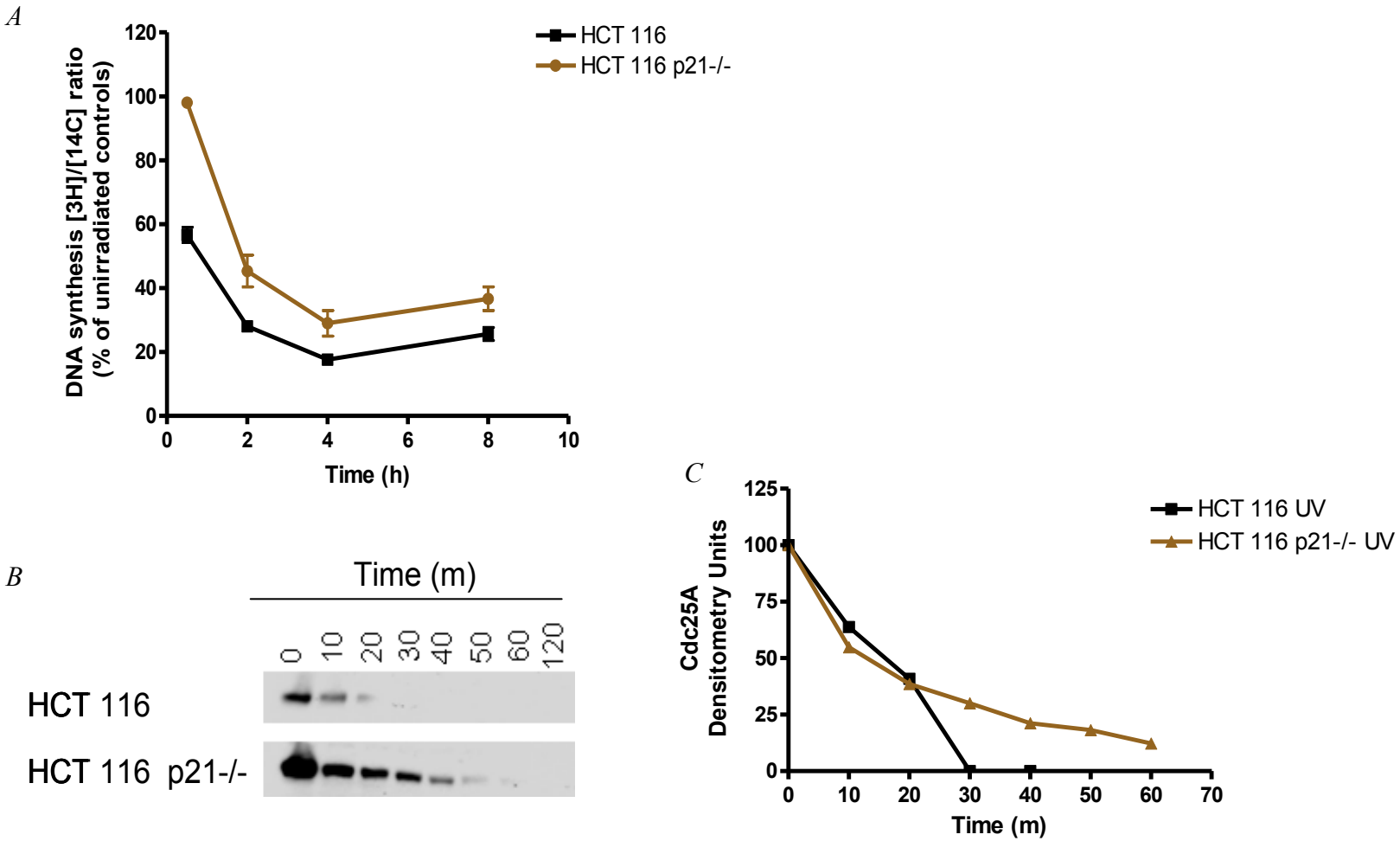

Figure 5.11. HCT116 p21-null cells demonstrate a partial radioresistant phenotype following treatment with 10 J/m^2 ultraviolet radiation.

(*A*) Wild-type HCT116 cells can suppress DNA synthesis appropriately and (*B*) induce degradation of Cdc25A following ultraviolet radiation damage. These responses were attenuated in the absence of p21. Cells were treated with 10 J/m^2 ultraviolet radiation; DNA synthesis was measured as described previously and harvested at 10 min intervals in the presence of cycloheximide 10 µg/ml. (*C*) The densitometry line graphs calculated from *(B)* represent Cdc25A degradation over time.

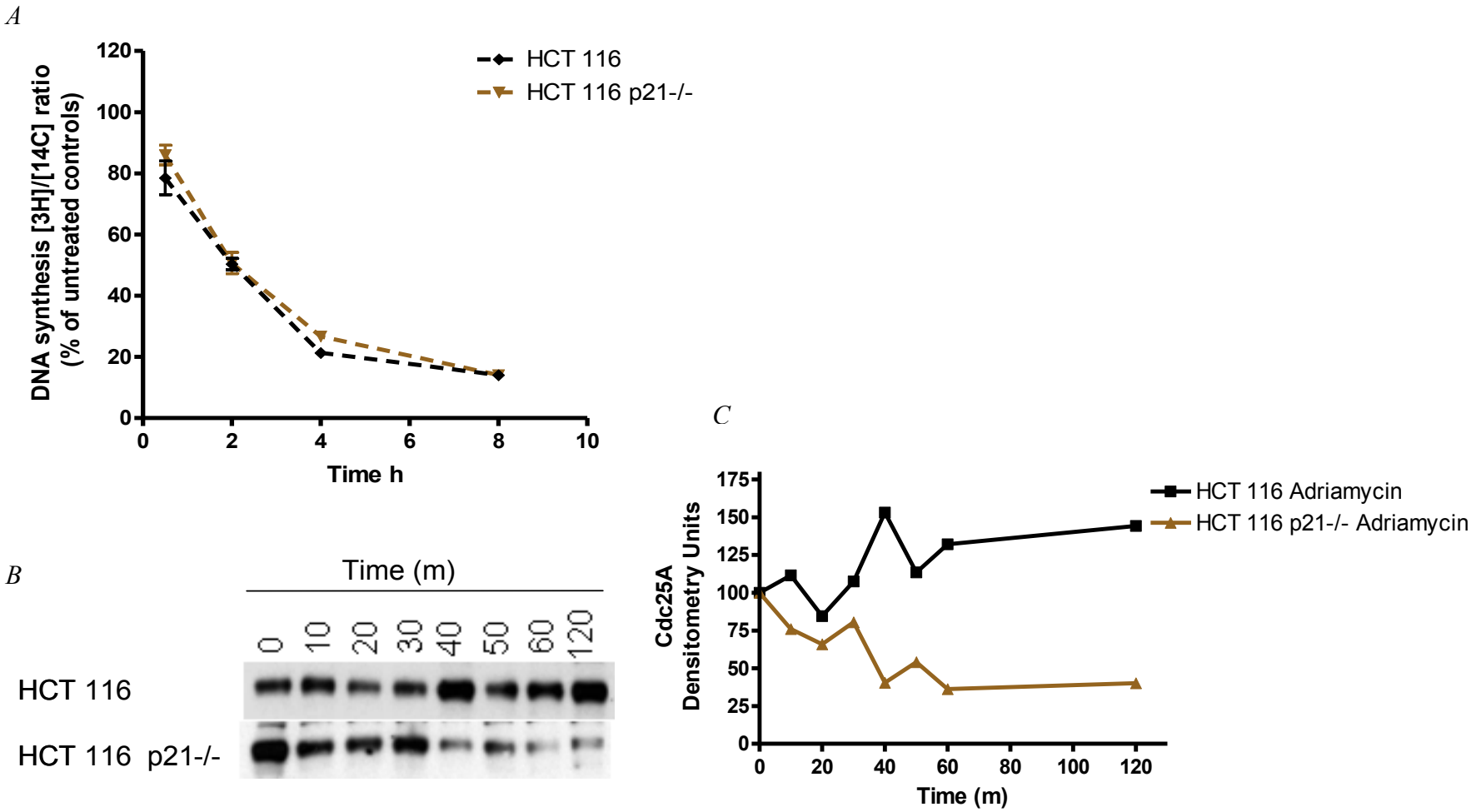

Figure 5.12. 1 µM Adriamycin-induced reduction in DNA synthesis is independent of Cdc25A degradation.

Cells were treated with adriamycin to induce DNA damage. No difference (*A*) in the reduction of DNA synthesis was observed between cell lines and (*B,C*) the kinetics of Cdc25A degradation were not accelerated in either cell line. Cells were treated with 1 µM adriamycin: DNA synthesis was measured as described previously and harvested at 10 min intervals in the presence of cycloheximide 10 µg/ml.

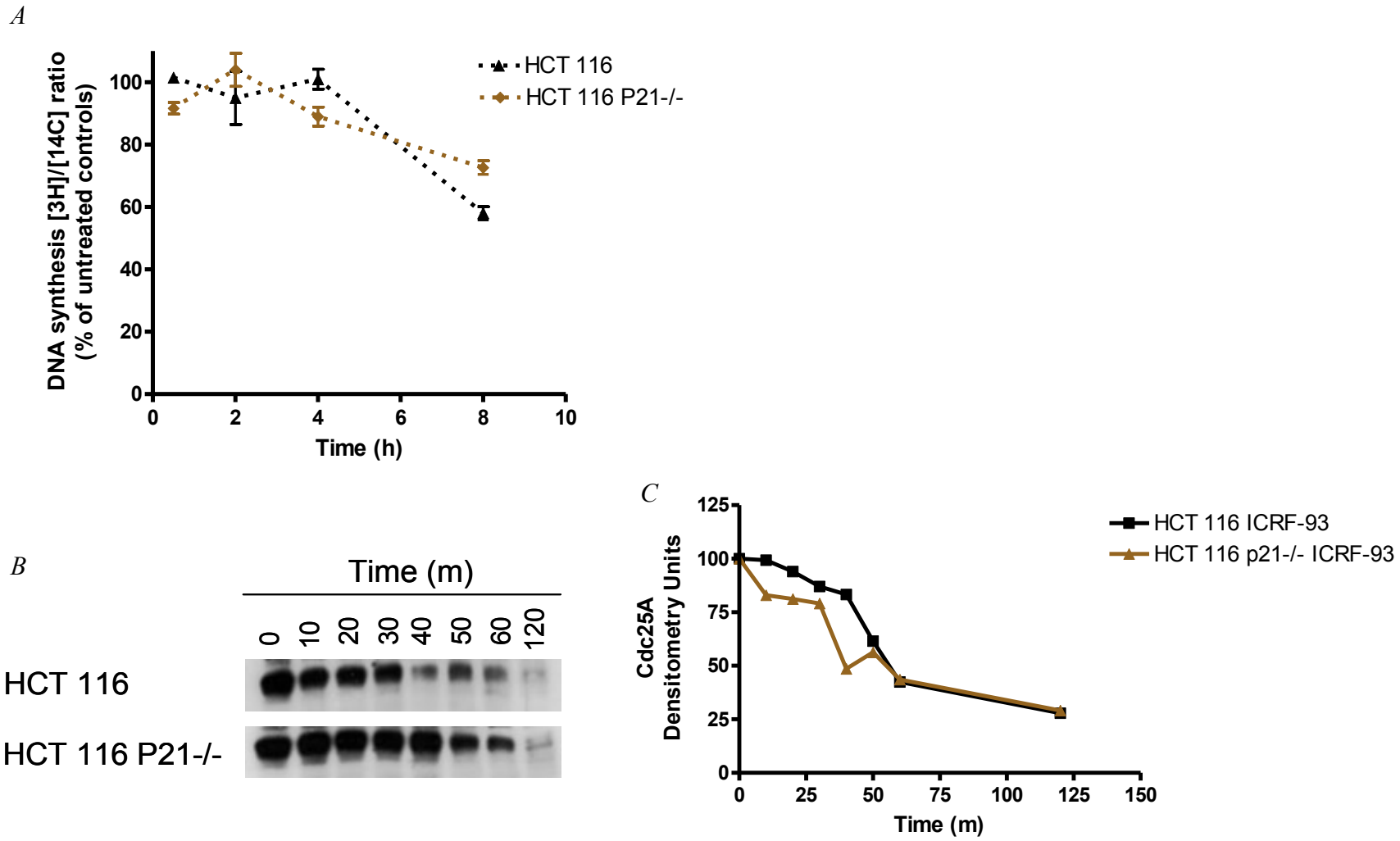

Figure 5.13. 35 µM The ICRF-193-induced reduction in DNA synthesis is independent of Cdc25A degradation

Cells were treated with the ICRF-193 topoisomerase II catalytic inhibitor. There was no difference in (*A*) the reduction of DNA synthesis between cell lines and (*B,C*) no acceleration in the rate of Cdc25A degradation in either cell line.

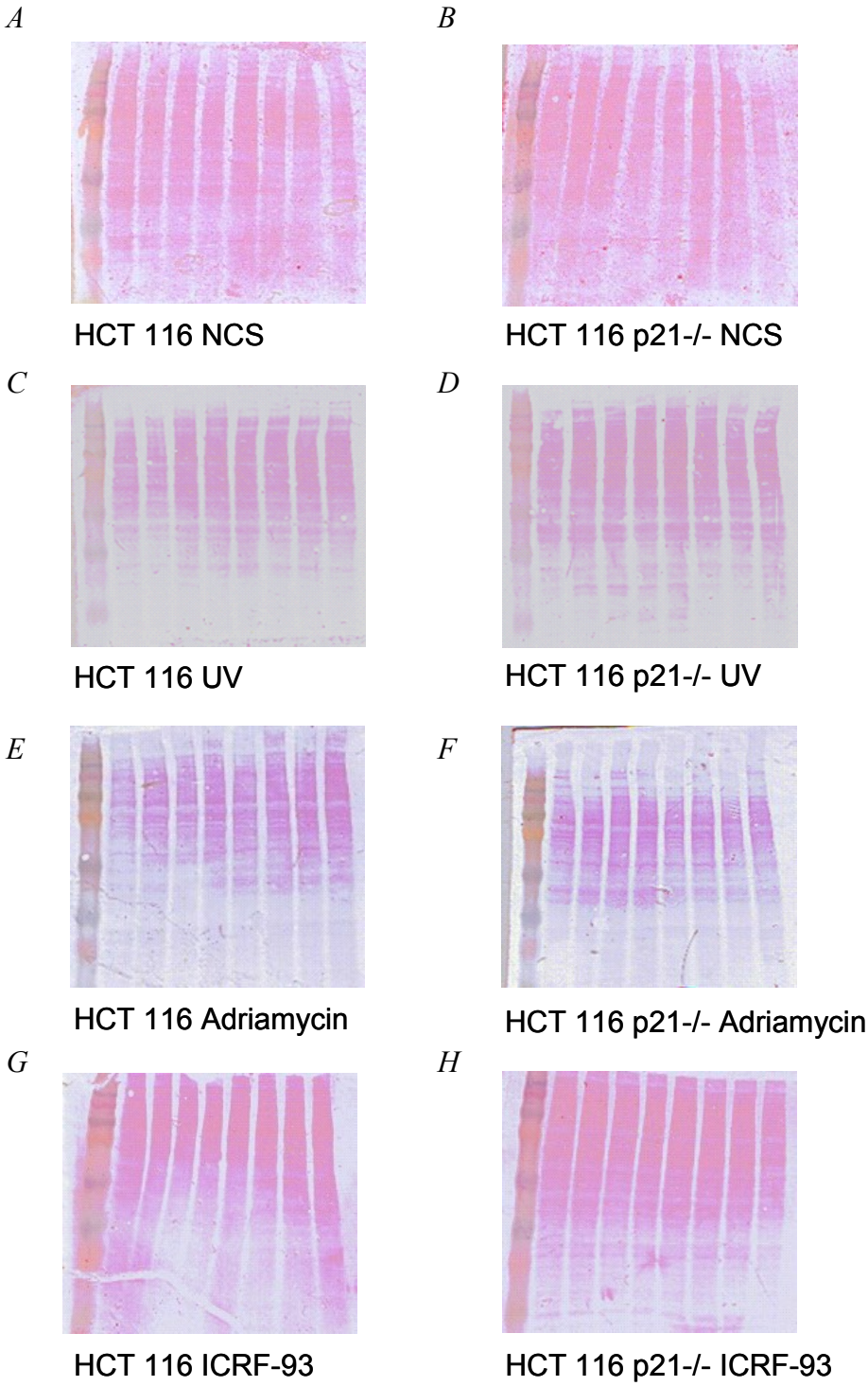

Figure 5.14 Ponceau-stained membranes corresponding to Figures 5.10–5.13.

Ponceau-stained membranes showing comparable protein loading between wild-type and p21-null cell lines following (A-B) neocarzinostatin, NCS; (C-D) ultraviolet, UV; (E-F) Adriamycin and (G-H) ICRF-93 treatment of wild type HCT116 and p21 null cells.

A

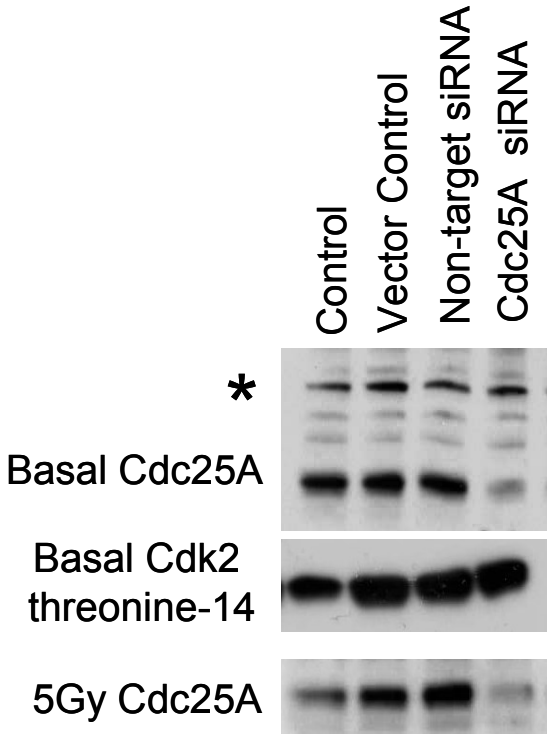

B

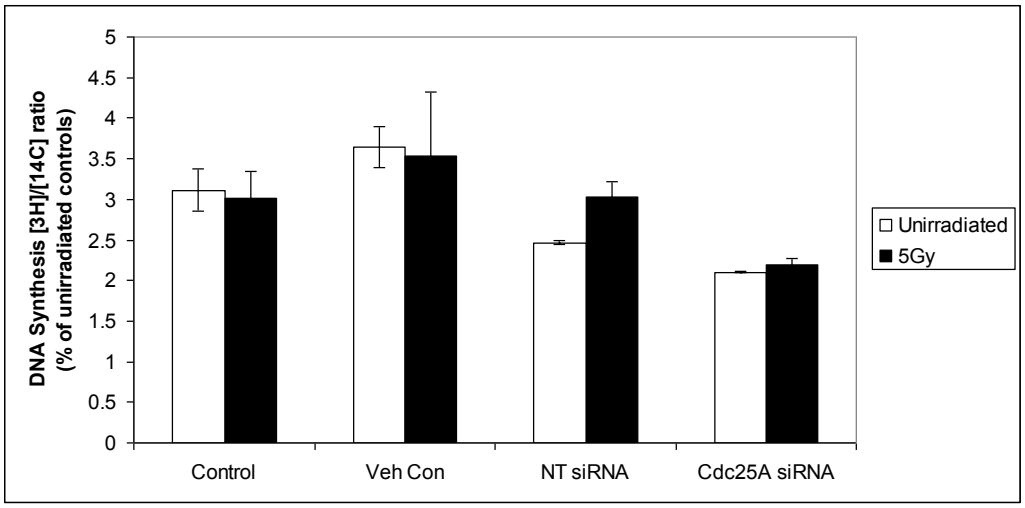

Figure 5.15. Cdc25A siRNA inhibits DNA synthesis in p21-null cells.

(*A*) HCT116 p21-/- cells were treated with Cdc25A siRNA or control siRNA for 48 h and then with 5 Gy; (*B*) Treatment with Cdc25A siRNA reduces DNA synthesis. Equivalent amounts of protein (40μg/lane) were analysed by immunoblotting. *, a cross-reacting band was used as loading control. Antibodies used have been described elsewhere. DNA synthesis was 30 min after treatment with 5Gy.

A

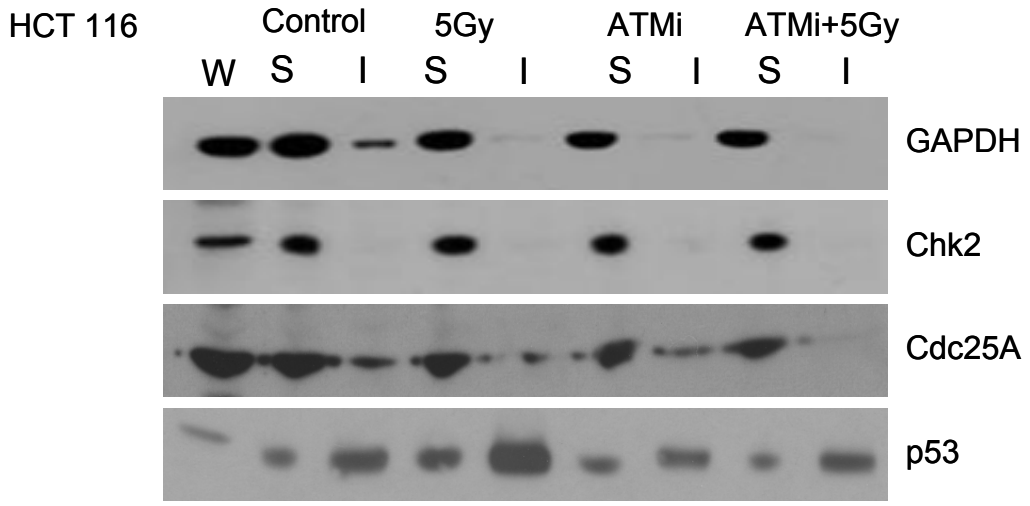

B

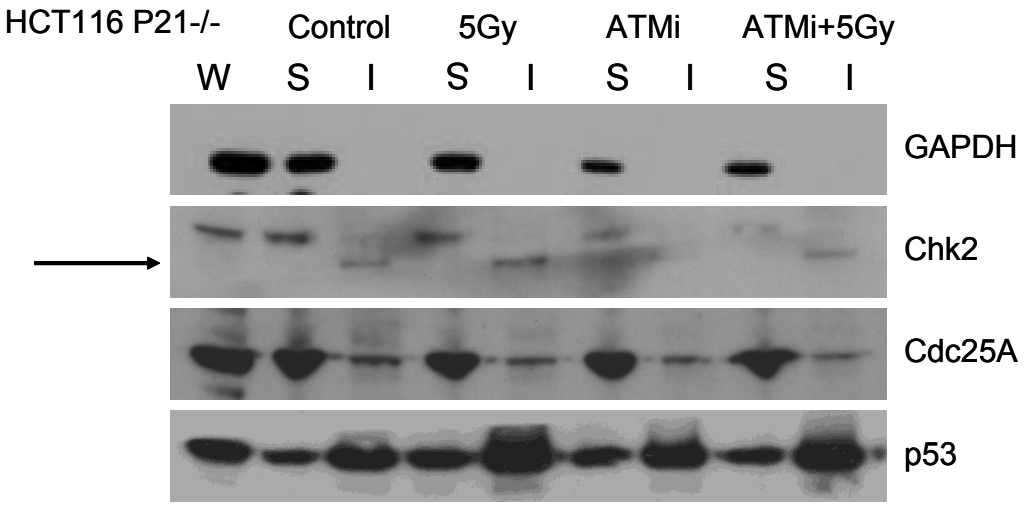

Figure 5.16. Differential localisation of Chk2 in HCT116 p21-null cells.

Cells were treated with 5 Gy ionising radiation, an ATM inhibitor for 24 h or a combination of treatments and harvested after 2 h. For (*A*) wild-type cells, 10 µl of the soluble (cytoplasmic) fraction and 15 µl of the insoluble (nuclear) fraction were loaded; for (*B*) p21-null cells, three times as much sample was loaded. W, whole cell lysate; S, soluble fraction; I, insoluble fraction.

Chapter 6. Constitutive Activation of the ATM-Dependent DNA Damage Response is a Negative Predictor of Successful ATM Inhibitor Therapy

6.1 Introduction

The *ATM* gene, located on chr11q22.3, is mutated in the autosomal recessive disorder ataxia-telangiectasia (AT), which is characterised by extreme sensitivity to radiation (and other agents causing DSB) and susceptibility to developing malignancies especially those of lymphoid origin (Savitsky *et al.*, 1995). Cells from AT patients are defective in the processing of DSB and in DNA damage checkpoint controls (Shiloh, 2003). This phenotype has prompted investigations into the use of ATM inhibition to increase the therapeutic effect of irradiation and DSB-inducing chemotherapy. Hickson *et al.* (2004) identified a specific small molecule ATM inhibitor, KU-55933, which sensitises U20S osteosarcoma cancer cells to camptothecin (a topoisomerase I inhibitor), etoposide (a topoisomerase II inhibitor), doxorubicin and ionising radiation. However, this inhibitor had no appreciable effect on the response to alkylating (cisplatin, melphalan, chlorambucil) and cross-linking (mitomycin B) agents. There is a reduction in IR-induced phosphorylation of CHK1, H2AX, Nbs1 and SMC1 (known targets of ATM) in the presence of KU-55933 and cells accumulate in G2-M phase, similar to ATM-deficient cells. In addition, KU-55933 was also able to additionally sensitise DNA-PK-deficient cells to etoposide. However, AT cells (lacking ATM protein) showed no significant increase in radiosensitivity when exposed to the specific ATM inhibitor, suggesting that ATM expression and activation is necessary for ATM inhibitor activity. Cowell *et al.*

(2005) demonstrated a reduction in breast cancer cell survival (in a colony formation assay) after ionising radiation therapy (1–5 Gy) in cells pretreated with the same compound. Mukhopadhyay *et al.* (2005) used short hairpin siRNAs to down regulate *ATM* and reported increased sensitivity of prostate cancer cells containing mutant p53 to the DNA damaging agent, doxorubicin. Disruption of the G2 checkpoint by ATM inhibition in cells containing mutant p53 is thought to render cells more sensitive to DNA damage (Eastman, 2004; Guha *et al.*, 2000; Shiloh, 2003). Importantly, reducing *ATM* gene expression in normal human fibroblasts does not appear to increase the cytotoxicity of doxorubicin; suggesting competent parallel pathways and/or checkpoints will prevent damage to normal cells. Antisense gene therapy and small interference RNA silencing against ATM has also been successfully used to increase the radiosensitivity of brain tumour cell lines (Guha *et al.*, 2000), human cervical cancer cells (Li *et al.*, 2006) and prostate cancer cell lines (Collis *et al.*, 2003).

Normal cells have multiple overlapping processes that serve to sense and repair DNA damage. If a cancer is defective in some checkpoint controls and/or repair mechanisms, then inhibiting the remaining functional pathways may be sufficient to trigger the apoptotic machinery or promote mitotic catastrophe. This could be an effective method of increasing the specificity of treatments for cancer cells, thus reducing the cytotoxic effect on normal tissues. Selective targeting of cancer cells by taking advantage of somatic mutations that occur in DNA damage repair pathways during cancer development is an attractive concept and could create a significant therapeutic index for ATM inhibitors (Bartek and Lukas, 2007; Bartek *et al.*, 2007). However, to date no criteria have been established that allow the rational use of this

novel approach in human cancers. Similarly, no pharmacodynamic or therapeutic endpoints have been developed to assess the efficacy of small molecule inhibitors of the DNA damage response and repair pathways.

This chapter shows that basal Chk2 threonine-68 phosphorylation may be a marker for the deregulated ATM DNA damage response. As such, the use of an ATM inhibitor in an ATM-deficient background may have limited efficacy in cancer treatment.

6.2 Results

6.2.1 Functional ATM DDR is a pre-requisite for successful ATM inhibitor therapy

Robust activation of the DNA damage response pathway has been demonstrated in precancerous lesions and becomes attenuated during cancer progression. The presence of an activated DDR in human cancers may represent continuous DNA damage signalling or persistently activated DNA repair mechanisms. However, a constitutively active ATM DDR pathway, in the absence of p21, represents a nonfunctional or ineffective pathway, as cells with this defect display IR induced radioresistant DNA synthesis. The radioresistant phenotype is likely to be due to activation of Cdk/cyclin complexes in the absence of p21, increased expression of the dual specificity phosphatase Cdc25A and its delayed degradation following DNA damage. Cdc25A is targeted for degradation upon phosphorylation by Chk2 and Chk1 in response to the ATM and ATR kinases. AT cells treated with the ATM inhibitor and 5 Gy IR demonstrated no change in cell cycle profile (Figure 6.1A) and no increase in radiosensitivity (Figure 6.1B). These data suggest that a functionally active ATM kinase is required for the ATM inhibitor to be efficacious.

Pretreatment of wild-type HCT116 cells for 1 h with the ATM inhibitor resulted in abrogation of Chk2 threonine-68 phosphorylation following 5 Gy IR (Figure 6.2). DNA damage-induced Cdc25A degradation is rescued after a further 2 h (compare with Figure 4.4). p53 serine-15 phosphorylation and increase p53 protein expression are inhibited for the first 4 h; thereafter, p53 serine-15 phosphorylation and increased p53 protein are evident. However, these changes do not result in p21 induction, suggesting that ATM activity is also required. Interestingly, Chk1 becomes robustly phosphorylated at serine-317 after 2 h when cells are damaged in the presence of ATM inhibition; however, there is a delay in Cdc25A degradation until the 12 h time point. This suggests that following DNA damage a threshold level of Chk1 activity must be reached before Cdc25A degradation is induced when the ATM–Chk2 axis is inhibited. Collectively, this suggests that an ATM-independent mechanism of p53 and Chk1 phosphorylation exists, which results in Cdc25A degradation after 12–24 h. Importantly, this result also indicates that cells can adapt to ATM inhibition by inducing the activity of another kinase. Wild-type HCT116 cell cycle analysis demonstrates that abrogation of the G1 and S-phase checkpoint occurs after 12–24 h; cells appear to accumulate in G2 phase of the cell cycle (Figure 6.3A). Presumably, activation of Chk1 enforces the G2 arrest when ATM is inhibited. Prolonged DNA damage-induced G2 arrest in cancer cells is associated with reduced survival. When cell survival is examined following ATM inhibition in the presence of 5 Gy IR, wild-type cells demonstrate a reduced number of colonies after 2–4 h of ATM inhibition and a complete absence of colonies at later time points (Figure 6.3B).

In the absence of p21, pretreated with the ATM inhibitor for 1 h leads to Chk1 phosphorylation at serine-317 in the absence of DNA damage; Chk2 threonine-68

and p53 serine-15 phosphorylation are also present, as described previously (Figure 5.2). ATM inhibition in combination with 5 Gy IR resulted in loss of Chk2 threonine-68 phosphorylation after 2, 4 and 12 h, but a reappearance after 24 h; this coincided with Cdc25A degradation. p53 serine-15 phosphorylation and protein expression were unaffected by ATM inhibition. Despite rapid Chk1 serine-317 phosphorylation, Cdc25A is not effectively degraded at the early time points. This suggests that an additional upstream kinase is responsible for phosphorylation of Chk1, Chk2 and p53 and the subsequent Cdc25A degradation. Wild-type HCT116 cells treated with the ATM inhibitor resulted in abrogation of the S-phase checkpoint (Figure 5.1A), which correlated with the reduced degradation of Cdc25A. In p21-null cells, there was no abrogation of DNA synthesis (Figure 5.1B), reflecting unchanged Cdc25A protein expression.

In the absence of p21, the G1 checkpoint is compromised and this is enhanced by ATM inhibition for 12 h (Figure 6.4A). The G2 checkpoint is also compromised 24 h following 5 Gy IR in the p21-null cell line; however, this appears to be restored in the presence of the ATM inhibitor and may represent a Chk1- or p53-dependent function. Lossaint *et al.* (2011) provided evidence that p21 and Chk1 cooperate in nontransformed cells to induce G2 arrest following DNA damage. When p21 was depleted, DNA damage-induced Chk1 phosphorylation increased but was unable to induce G2 arrest. These findings confirm that the ATM inhibitor is capable of abrogating the G1- and S-phase DNA damage-induced checkpoints in wild-type HCT116 cell line; this function is partially lost in the p21-null cell line. Phosphorylation of Chk1 serine-317 and p53 serine-15 and induction of a G2 arrest in both wild-type and p21-null background suggest that the activation of additional

kinases can compensate for ATM inhibition. p21-null cells are extremely radiosensitive compared with wild-type cells (Figure 4.10); they are also hypersensitive to other forms of DNA damage. In contrast, there is no additional effect of ATM inhibition on IR-induced colony formation in the absence of p21 (Figure 6.4B). This suggests that ATM and p21 are components of a linear pathway and that the phenotype of the HCT116 p21-/- lineage resembles that acquired by ATM inhibition in wild-type HCT116 cells.

ATM inhibitor therapy was developed as a mean of increasing the radio/chemosensitivity of current therapeutic agents. As such, ATM inhibitor therapy may have a limited role in cancers that are already sensitive to DNA damage-inducing treatments and/or have a deregulated DDR pathway. Abrogation of the G1- and S-phase DNA damage checkpoints and prolonged G2 arrest appear to correlate with radiosensitivity. A RDS phenotype may aid in the prediction of response to ATM inhibitor therapy.

6.2.2. Multiple modes of deregulation of the DNA damage response in colorectal cancer

Cancers are inherently heterogeneous and it may be necessary to assess the functionality of the DNA damage response pathway in individual tumours prior to using therapy that targets components of these ubiquitous systems. Takemura *et al.* (2006) reported that many of the commonly used cancer cells lines are defective in Chk2 activation following replication-associated DSB. The expression and activity of specific components of the ATM DDR pathway were profiled in commonly used cell lines (Figure 6.5). HCT116 cells are MMR-deficient and have reduced levels of

the MRN complex; consequently, this leads to a less effective but not altogether absent Chk2 activation in response to IR. This phenotype is similar in the p53-null cells, but the opposite is seen in p21-null cells: p21-null cells exhibit basal phosphorylation of ATM serine-1981, Chk2 threonine-68 and p53 serine-15, yet display radioresistant DNA synthesis. Evidence presented in the previous chapter indicates that this may be due to an inability to dissociate chromatin-bound Chk2, the overexpression and delayed degradation of the Cdc25A protein in response to DNA damage, and increased Cdk activity. HCT-8 and HCT15 cells are also MMR-deficient; however, levels of the MRN proteins are comparable with those of the HCT116 p21-null derivative. These cell lines express a truncated, mutant, labile Chk2 protein. Wu *et al.* (2001) demonstrated that low levels of mutant Chk2 in HCT15 cells fail to undergo ATM-dependent phosphorylation. In addition, HCT-8 harbours wild-type p53 protein, whilst p53 is mutated in HCT15. SW-620 is the metastatic lineage of SW480 cells; these cells are MMR proficient and express high levels of the MRN complex and low levels of Chk2 protein. SW-620 cells have reduced levels of the DNA repair enzyme, MGMT (O-6-methylguanine DNA methyltransferase), which is necessary for the removal of the toxic methylation adduct, 06-meGua. This phenotype renders SW-620 cells highly sensitive to the toxic adducts N-methyl-N-nitrosourea and *N*-Methyl-*N*'-Nitro-*N*-Nitrosoguanidine. Finally, HT29 cells express detectable levels of MRN complex components and Chk2 protein, as well as mutated p53 protein.

To assess the functionality of the ATM DNA damage response, these commonly used cell lines, including the HCT116 isogenic panel, were irradiated with 20 Gy IR and analysed after 2 h (Figure 6.6). The dose of 20Gy (and not 5Gy) was used to

overcome any cell line specific deficiencies that may prevent activation of the ATM DDR pathway at low doses. Wild-type HCT116 cells demonstrated IR-induced phosphorylation of ATM serine-1981, Chk1 serine-317, Chk2 threonine-68, NBS serine-343 and p53 serine-15, and no p21 induction was observed at this early time point. The NBS serine-343 phosphorylation signal was less pronounced than that observed with the other proteins. The HCT116 p53-null derivative differed from the wild type only by a failure to induce p53 serine-15 phosphorylation and elevated basal p21. The HCT116 p21-null cell line exhibited basal phosphorylation of ATM, Chk2 and p53, as described previously. There was no increase in the ATM serine-1981 signal following IR, but there was an increase in Chk2 threonine-68 and p53 serine-15 phosphorylation after 2 h. As expected, no p21 was detected. HCT-8 and HCT15 cell lines have inactivating mutations of the Chk2 protein resulting in a labile protein; therefore no Chk2 threonine-68 signal is detected. The other proteins showed similar phosphorylation to that of wild-type cells, with robust phosphorylation of NBS serine-343 suggesting the presence of a compensatory mechanism. The SW480 and SW-620 cell lines are derived from the same adenocarcinoma lineage. Both cell lines have a missense mutation in codon 273 in the *p53* gene (Liu and Bodmer, 2006) and yet SW480 appear to retain DNA damage induced p53 functions (Rochette *et al.*, 2005) whilst SW-620 cells are unable to induce the p53 mediated DDR (O'Connor *et al.*, 1997). Interestingly, SW-620 displays basal Chk2 threonine-68 phosphorylation, which is increased after IR, similar to the HCT116 p21-null cell line. It also shows prominent NBS serine-343 phosphorylation, similar to HCT-8 and HCT15 cells that lack functional Chk2. This increase in NBS serine-343 may be functionally important when Chk2 is inactivated.

HT29 is an adenocarcinoma cell line that harbours the same p53 mutation as SW-620, which results in the expression of a stable mutant protein. This cell line does not show basal phosphorylation in any of the proteins examined; in response to IR, normal levels of ATM, Chk1, Chk2 and p53 are seen, although there is a reduction in Nbs phosphorylation (Figure 6.6).

Despite MRN deficiency, HCT116 cells can induce a DNA damage response at the doses of IR used in this study. Clearly, the p53-dependent DDR is defective in HCT116 p53-/- cells and data has been presented that supports deregulation of the DDR in p21-/- HCT116 cells. HCT-8 and HCT15 cells lack Chk2, a main effector of the DDR, and basal levels of Chk2 threonine-68 phosphorylation in SW-620 cells suggest that the DRR is deregulated. Therefore, SW480 and HT29 may be the only cell lines in this study considered to have an intact ATM–Chk2-dependent DDR in response to IR.

6.2.3. Constitutive Chk2 threonine-68 phosphorylation represents a deregulated DNA damage response

In the HCT116 p21-null cell line, basal Chk2 threonine-68 phosphorylation reflects deregulation of the ATM-dependent DDR pathway and the inability to abrogate the S-phase DNA damage checkpoint using ATM inhibitor therapy. This model predicts that the ATM–Chk2 axis is deregulated in cells in which basal Chk2 threonine-68 is detected. Furthermore, ATM inhibition will be unable to abrogate the ATM dependent intra-S-phase checkpoint. SW-620 and HT29 cell lines harbour the same p53 missense mutation in codon 273 (O'Connor *et al.*, 1997). Previous reports suggested that Chk2 is less functional in SW-620, which appears to rely on the Chk1

protein to execute DDR roles (Parsels *et al.*, 2004). SW-620 cells were irradiated with 5 Gy IR and DNA synthesis was assessed as described in Chapter 4. In response to IR damage, SW-620 cells downregulate DNA synthesis in a time-dependent manner. However, pretreatment with the ATM inhibitor does not abrogate the S-phase checkpoint (Figure6.7A). This result suggests that the reduction in DNA synthesis demonstrated in SW-620 cells is independent of ATM–Chk2 axis. In contrast, the ATM inhibitor treatment abrogates DNA damage-induced inhibition of DNA synthesis in the HT29 cell line (Figure 6.7B). Combined ATM inhibition and IR therapy is more efficacious in reducing colony formation in HT29 cells compared with SW-620 cells (Figure 6.8).

6.3 Discussion

Constitutive activation of the DDR and repair pathways has been demonstrated in various solid tumours. Previous reports have hypothesised that this may reduce the efficacy of conventional cancer therapies and that inhibition may improve therapeutic outcomes. In this chapter, evidence has been presented to suggest that basal Chk2 threonine-68 phosphorylation may reflect a deregulated ATM DNA damage response, checkpoint adaption or engagement of DNA repair processes essential for cancer survival. ATM orchestrates a G1- and S-phase cell cycle arrest directly through the ATM–Chk2–p53–p21 and the ATM–Chk2–Cdc25A pathways respectively, and indirectly augments G2/M arrest through upregulation of p53-dependent genes. The DNA synthesis process is precisely regulated to permit DNA replication only once and with high fidelity in each cell cycle. Each origin of replication is initiated only once at specific nucleotide sites, termed replicons, and eukaryotic DNA has many individual replicons per chromosome. Following DNA

damage, DNA synthesis is inhibited, initially by inhibiting replicon initiation and subsequently by inhibiting DNA chain elongation. The inability to inhibit DNA synthesis within an hour of experiencing DNA damage is termed radioresistant DNA synthesis and occurs when the upstream components of the ATM DDR pathway are inhibited through various mechanisms or when S-phase proteins are overexpressed and/or contain activating mutations. The radioresistant phenotype represents a spectrum which can be complete or partial. Classically, cells from patients with the inherited condition ataxia telangiectasia, in which the ATM protein is mutated, demonstrate complete radioresistance, whereas deregulation of components downstream of ATM causes partial radioresistance. In such a situation, inhibition of ATM is unlikely to lead to an additional increase in radiosensitivity, as demonstrated when AT cells are treated with caffeine, wortmannin or a specific ATM inhibitor (as in this study). ATM inhibition and gamma irradiation combined treatment in parental HCT116 cells resulted in ablation of the ATM–Chk2–Cdc25A and ATM–Chk2–p53–p21 signalling cascades (Figure 6.1), radioresistant DNA synthesis (Figure 5.1), abrogation of G1 cell cycle arrest (Figure 6.2) and reduced colony formation (Figure 6.4). However, at later time points, these combined treatments also induced ATM-independent Chk1 serine-317 and p53 serine-15 phosphorylation, Cdc25A degradation and G2/M arrest. This indicates the activation of additional kinases targeting ATM substrates and is reminiscent of cells derived from patients with ataxia-telangiectasia, thus confirming the specificity of the ATM inhibitor. In radiosensitive p21-null derivative cells, combination therapy reduced ATM-dependent Chk2 threonine-68 phosphorylation (Figure 6.1) and enhanced the compromised G1 arrest response (Figure 6.3), but had no effect on radioresistant

DNA synthesis (Figure 5.1) or radiosensitivity (Figure 6.4). In this situation, there is an uncoupling of the DDR signal generated and downstream effects on DNA synthesis and supports previous evidence that radiosensitivity is associated with IR induced radioresistant DNA synthesis. Activation of additional kinases related to ATM was also apparent in p21-null cells, resulting in Chk1 serine-317, Chk2 threonine-68 and p53 serine-15 phosphorylation, and degradation of Cdc25A in the presence of an ATM inhibitor. Interestingly, the compromised DNA damage-induced G2/M arrest was also restored by ATM inhibition (Figure 6.3A bottom panel). Despite the latter, the radiosensitivity phenotype was not rescued, indicating the importance of p21 expression for sustained G2/M arrest and/or senescence. It is likely that treatment with ATM inhibitors may be more effective in cancers that have a functional ATM–Chk2–Cdc25A DDR and a parallel defect in the DNA repair machinery. Jiang *et al*. (2009) have proposed a framework for selecting patients for treatment with ATM inhibitors, based on ATM protein expression and p53 status. Using ARF- and p53-deficient murine embryonic fibroblasts, they reported chemosensitisation to doxorubicin and cyclophosphamide by ATM downregulation or chemical inhibition. They concluded that in a p53-deficient background cancer cell survival following DNA damage is dependent on ATM-directed cell cycle arrest. Hence, ATM inhibition abrogates cell cycle arrest, forcing the cells towards mitotic catastrophe. In contrast, suppression of ATM or Chk2 in p53-proficient MEFs treated with cisplatin or doxorubicin conferred a survival advantage by preventing p53-dependent apoptosis. They validated this data in different cell lines and xenograft models. Based on this framework, the wild-type HCT116 and the LoVo (wild-type p53) cell line (Hickson *et al.*, 2004) should not be sensitive to ATM inhibition;

however, Hickson *et al.* and this thesis show increased radiosensitivity with IR-induced DNA damage and ATM inhibition. Both HCT116 and LoVo cell lines have defects in the DNA MMR machinery, affecting hMLH1 and hMSH2, respectively; indicating that these cell lines depend on ATM-directed DNA repair mechanisms. The results generated using HT29 and SW-620 cell line harbouring the same p53 mutation support the proposed Jiang framework to some extent. HT29 cells treated with a combination therapy comprising IR and ATM inhibition show a reduction in colony formation, but this effect is lower in SW-620 cells. SW-620 cells demonstrate IR induced radioresistant DNA synthesis, a mutant p53 status and a reduced level of the MGMT DNA repair enzyme. This may constitute an ATM- and p53-deficient cancer, which may benefit from inhibiting ATM-independent DNA repair pathways (such as the DNA-PK pathway, as suggested by the authors) in combination with DNA damage-inducing therapies.

Previous reports have proposed that the cancer-limiting properties of the DDR is circumvented during the development of cancer and therefore that assessment of the ATM DDR would have to be integrated into a framework for recommending inhibitor therapy. Two cell lines that exhibit basal Chk2 threonine-68 phosphorylation, HCT116 p21-/- and SW-620, were unable to abrogate the S-phase checkpoint when treated with an ATM inhibitor, thus confirming a IR induced RDS phenotype. p21-/- HCT116 cells display abrogation of all three DNA damage checkpoints and are extremely sensitive to all forms of DNA damage. Pang (Pang *et al.*, 2011) demonstrated that p53 is functionally inactivated (Aneja *et al.*, 2007) in the HCT116 p21-null cell line due to cellular mislocalisation and that SW-620 cells contain mutant p53 protein. Collectively, this indicates that p53 mutations or

functionally inactivated p53 are associated with constitutive activation of the ATM-dependent DDR pathway. However, it may be difficult to ascertain whether (1) DDR activation resulted in a selective pressure for p53 mutations/genetic instability and cancer progression or (2) functionally inactivated p53 resulted in activation of the DDR through replication stress. What is clear, though, is that the cancer has been able to overcome these complex constraining signals and progress despite activation of the DDR. In the SW-620 cell line, Chk2 is expressed at low levels and there is some additional evidence to suggest that S-phase checkpoint is independent of Chk2 and Chk1 in this particular cell line. Falck (Falck *et al.*, 2002) reported that two parallel pathways regulate the intra-S-phase checkpoint: ATM–Chk2–Cdc25A and ATM–NBS. Interestingly, HCT-8 and HCT15 have a mutant labile Chk2 and SW-620 cells in which the ATM-Chk2 axis appears to be deregulated, demonstrate more pronounced phosphorylation of Nbs serine-343, suggesting that compensatory activation of this pathway may occur. HT29 cells, which harbour the same p53 mutation as SW-620 cells, do not display basal Chk2 threonine-68 phosphorylation and ATM inhibition results in abrogation of the IR-induced reduction in DNA synthesis. Zoppoli *et al.* (2012) interrogated the National Cancer Institute 60 cell line panel using Chk2 genomic and proteomic assays. They revealed that Chk2 threonine-68 phosphorylation is associated with p53 inactivation, and downregulation of proteins involved in HR and Fanconi repair proteins. p21-/- HCT116 cells are defective in MMR due to silencing of the *MLH1* gene and SW-620 express low levels of the MGMT enzyme responsible for removing toxic 06-methyl Guanine adducts. Constitutive activation of the ATM DDR may therefore represent a deregulated ATM DDR and compensatory DNA repair mechanisms. Exploiting

cancer-dependent DNA repair pathways may allow selective targeting of cancer by ATM inhibitors; normal tissues will be protected by a full complement of redundant DNA repair processes.

A predictive model is proposed that integrates functionality of the ATM–Chk2 axis, p53 mutation status and defects in DNA repair pathways when considering ATM inhibitor therapy. Assessing the functionality of the ATM DDR pathway is essential for maximising the therapeutic potential of ATM inhibition. The functional status of the ATM pathway can be determined by dividing human biopsy (and/or resection) specimens and treating one part with IR (or chemotherapeutic drugs) *ex vivo*, while leaving the other as an untreated control; both treated and control samples should be paraffin-embedded and assayed for Chk2 threonine-68 phosphorylation, γ-H2AX and/or other DNA damage markers (Nuciforo *et al.*, 2007). This type of *ex vivo* treatment and analysis of cancer tissue will also retain the cancer–stromal interaction, which is often lost in homogenised tissue samples. Evaluating differential staining between the control and treated samples will allow an assessment of functionality of the ATM DDR. Simultaneously, p53 IHC staining (with strict criteria for reporting the staining pattern) and/or genetic analysis can inform the p53 mutation status. Analysis of DNA repair proteins can be dictated by the type of cancer studied, e.g., BRCA for breast cancers and MMR proteins for right-sided colon cancers.

Cancers that have both a functional ATM DDR and p53 mutations will benefit from ATM inhibitor therapy (e.g., HT29 and MSS colorectal cancers), although this may promote genetic instability in normal tissues which retain wild-type p53. Cancers that have both a functional ATM DDR and a wild-type p53 status may benefit from

ATM inhibitor therapy if other DNA repair pathways are deregulated (e.g., HCT116, LoVo and MSI colorectal cancers). ATM inhibitor therapy would not be recommended for cancers that have a functional ATM DDR and wild-type p53 status, as the potential for inducing genetic instability maybe far greater than the potential benefit.

If the ATM DDR is defective, p53 status becomes less important and targeting ATM-independent DNA repair pathways may provide greater benefit. Such an approach would be more powerful if other DNA repair pathways were deregulated in addition to ATM.

It is conceivable that ATM inhibitors may be used to potentiate the effects of chemoradiotherapy at all stages of disease and this combination will have to be tested in preclinical models.

For example, in this study using Chk2 threonine 68 staining as a biomarker of a deregulated ATM DDR identified 22% of MSS and 33% of MSI colorectal cancers who would not benefit from ATM inhibitor therapy. This means that 78% of MSS and 67% of MSI cancers have a functional ATM-Chk2 pathway and will potentially benefit from ATM inhibitor therapy alongside adjuvant chemotherapy. Further stratification of the 78% (118) MSS cancers will identify 57 patients who are likely to have wild type p53 for whom this therapy is not recommended and 61 patients who are likely to have p53 mutational status (Figure 6.9A). The latter patient cohort accounts for 40% of the MSS cancers who have a functional ATM-Chk2 axis and p53 mutations that will benefit from the use of an ATM inhibitor. Similarly, MMR deficient cancers may be inherently sensitive to inhibitors of ATM directed DNA

repair therefore potentially all of these patients would benefit from combination therapy of an ATM inhibitor and chemoradiotherapy regimens. If the predictive model was utilised 9 patients would be immediately excluded as the cancer is positive for Chk2 threonine 68 staining. Of the remaining 18 patients all could benefit from ATM inhibitor therapy but perhaps those with higher p53 staining would benefit the most (Figure 6.9B).

In this chapter, the predictive model based on preclinical data allows a framework to be established whereby potential outcomes of therapy can be modelled integrating genetic and functional array analysis from murine models or large scale human cancer collaborations. This will become more challenging as our understanding of the underlying pathogenesis of cancer and response to therapy are discovered.

A

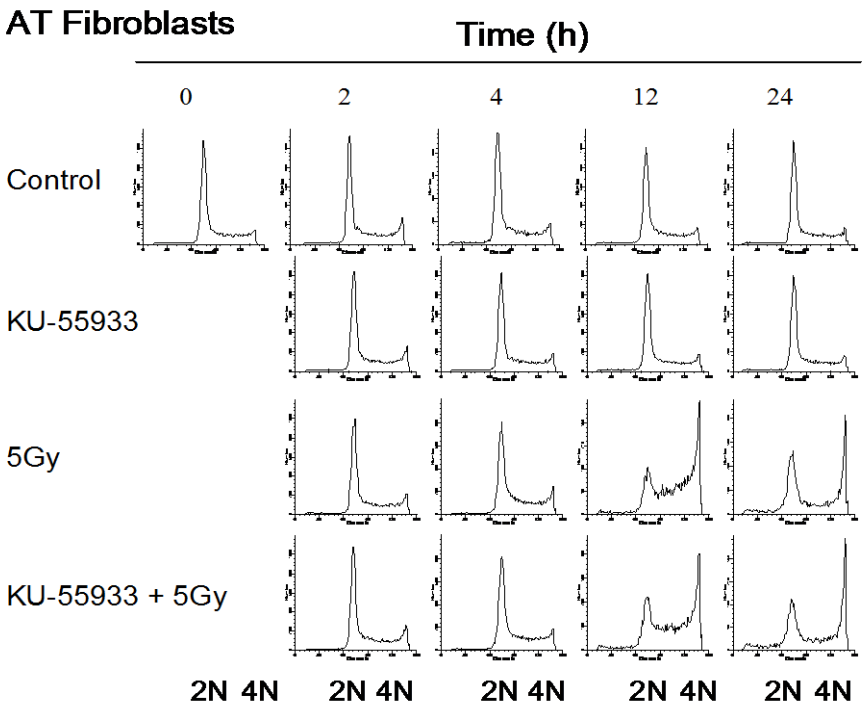

B

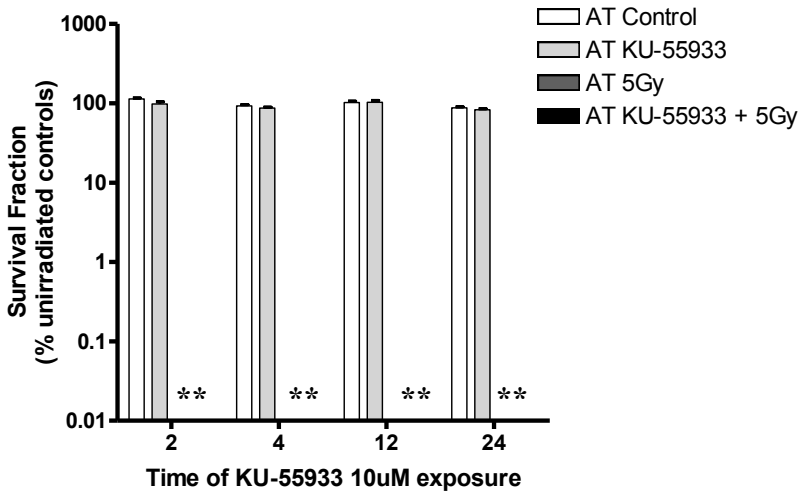

Figure 6.1. Cell cycle analysis of AT fibroblasts following combination therapy of KU-55933 and 5 Gy ionising radiation.

ATM inhibitor therapy (KU-55933) has no effect on the (*A*) cell cycle profile or (*B*) colony formation in AT fibroblasts, either alone or in combination therapy with ionising radiation. The x axis (*A*) represents propidium iodide staining i.e., DNA content; 2N, diploid chromosomes; 4N, tetraploid chromosomes. Error bars indicate the standard deviation of the mean. Cells were preexposed for 1 h to KU-55933, irradiated with 5 Gy in the presence of KU-55933 and harvested at the indicated time points. **No colonies survived after 5Gy and KU-55933 + 5Gy treatment.

A

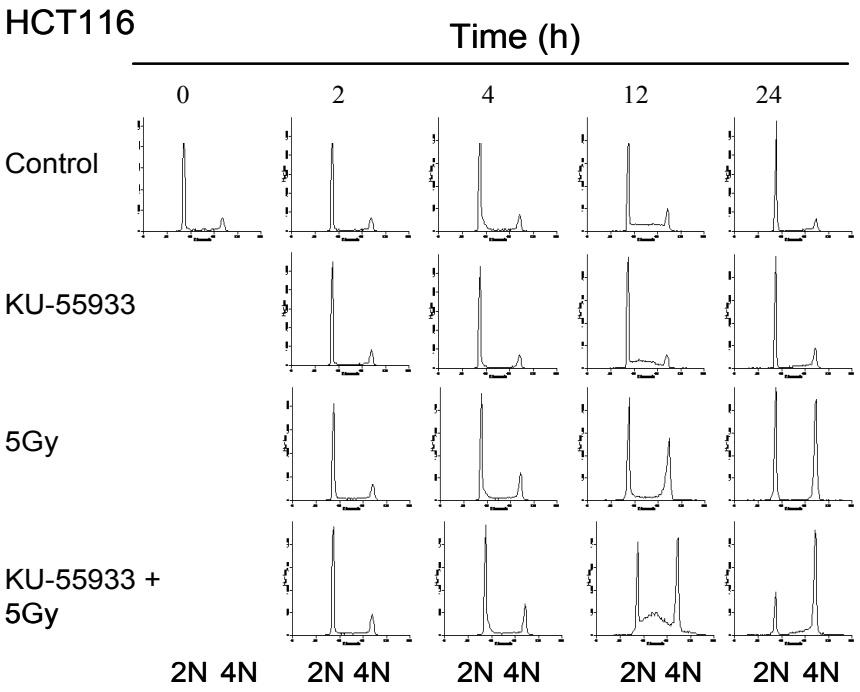

B

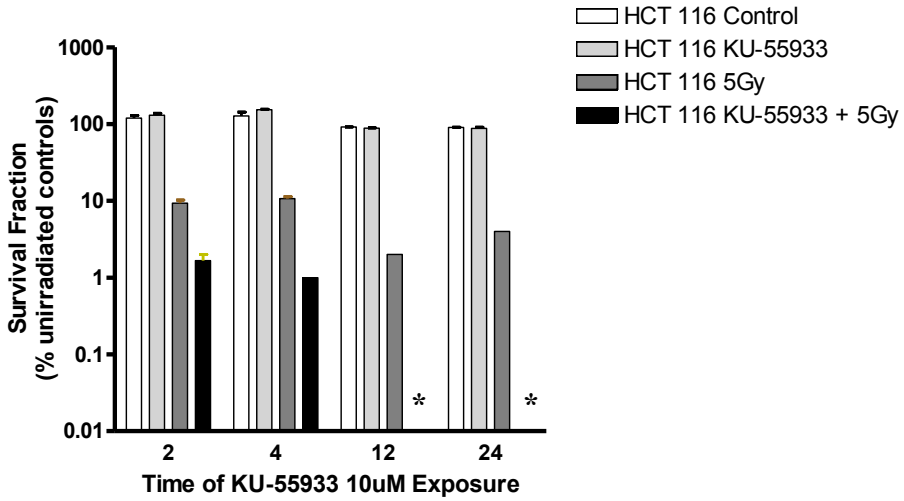

Figure 6.2. ATM inhibition (KU-55933) abrogates DNA damage-induced checkpoints in wild-type cells and reduces colony formation.

(*A*) ATM inhibitor therapy (KU-55933) abrogates the G1 and S-phase checkpoint in wild-type HCT116 cells and induces a G2/M arrest. The x axis represents propidium iodide staining i.e., DNA content; 2N, diploid chromosomes; 4N, tetraploid chromosomes. Error bars indicate the standard deviation of the mean.

(*B*). Colony survival is reduced following ATM inhibitor/ionising radiation combination therapy Cells were preexposed for 1 h to KU-55933, irradiated with 5 Gy ionising radiation in the presence of KU-55933 and analysed at the indicated time points. *No colonies survived.

A

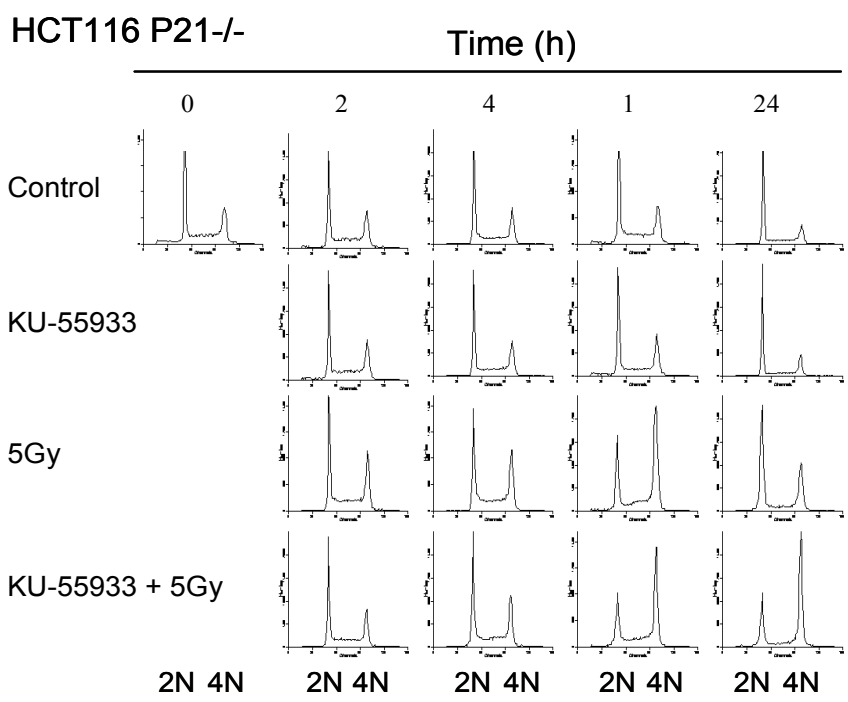

B

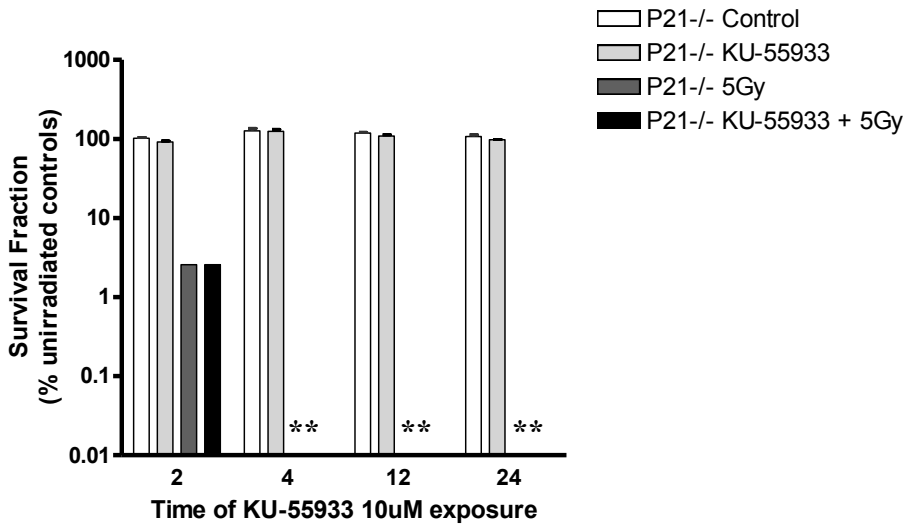

Figure 6.3. ATM inhibition (KU-55933) restores the G2/M arrest in the p21-null cells but does not enhance the radiosensitive phenotype.

(*A*) ATM inhibition (KU-55933) enhances the defective G1 arrest in p21-null cells but (*B*) has no additional effect on cell survival**.** Cells were treated as described in Figure 5.3. **No colonies survived for assessment.

Table 6. 1. Summary of DNA damage response and DNA repair characteristics of colorectal cancer cell lines

Cell Line	**ATM-Chk2 axis**	**p53 Status**	**DNA Repair Defect**
HCT116	Normal	Normal	MMR MLH1
HCT116 p53-/-	Normal	Absent	MMR MLH1
HCT116 p21-/-	Abnormal	Inactive	MMR MLH1 *
HCT-8	Abnormal	Normal	MMR MSH2
HCT15	Abnormal	Mutated	MMR MSH2 *
SW480	Normal	Normal	_
SW-620	Abnormal	Mutated	↓MGMT *
HT29	Normal	Mutated	_

Summary of the DNA damage response and DNA repair characteristics of commonly used colorectal cancer cell lines. *, cell lines that have defects in all three components of DDR and DNA repair. Sources: (Giannini *et al.*, 2002; Takemura *et al.*, 2006; Wheeler *et al.*, 1999) (Branch *et al.*, 1995; Gayet *et al.*, 2001; O'Connor *et al.*, 1997; Pang *et al.*, 2011; Zoppoli *et al.*, 2012)

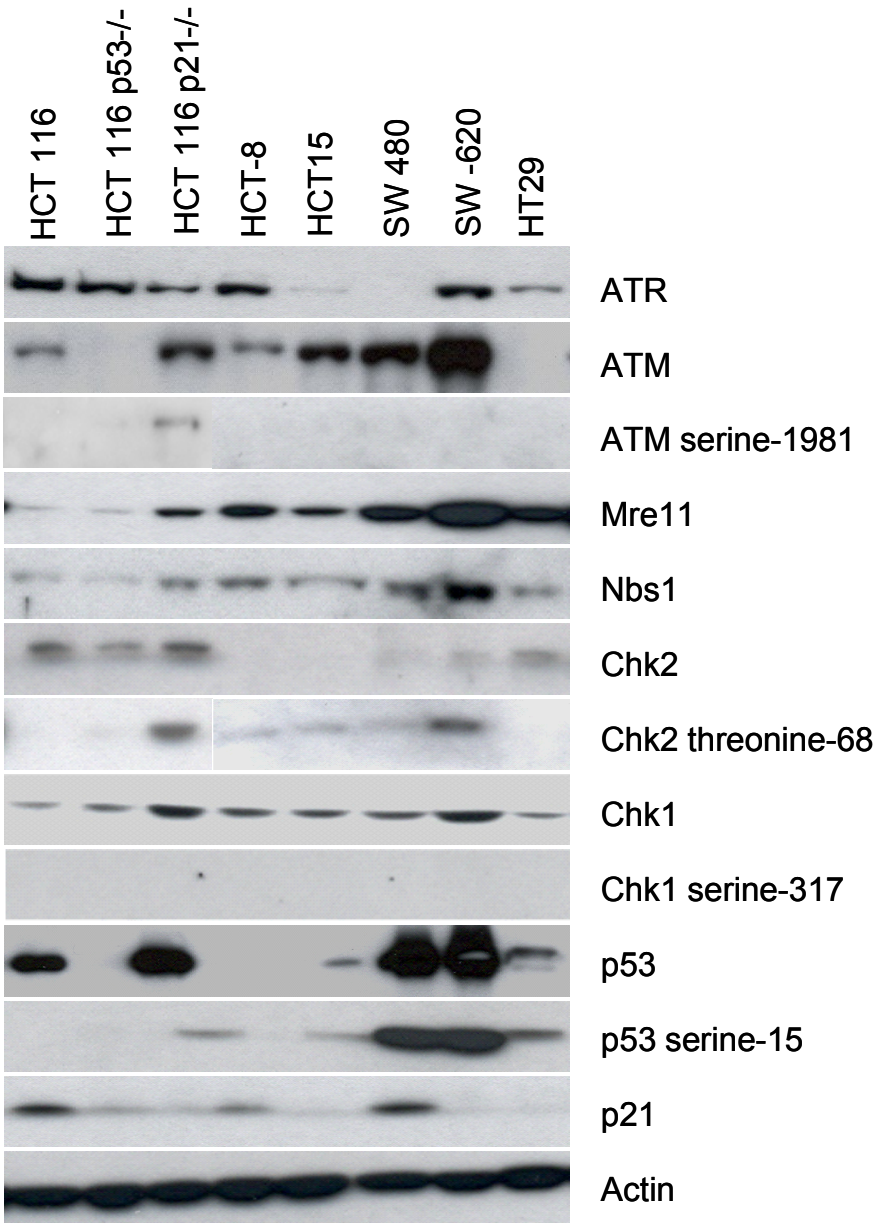

Figure 6.4. Characterisation of the DNA damage response proteins in colorectal cancer cell lines.

Lysates from exponentially growing cells were analysed by electrophoresis. Equivalent amounts of protein (20 μg/lane) were analysed by immunoblotting and actin was used as a loading control. Antibodies used have been are described in the Materials and methods chapter.

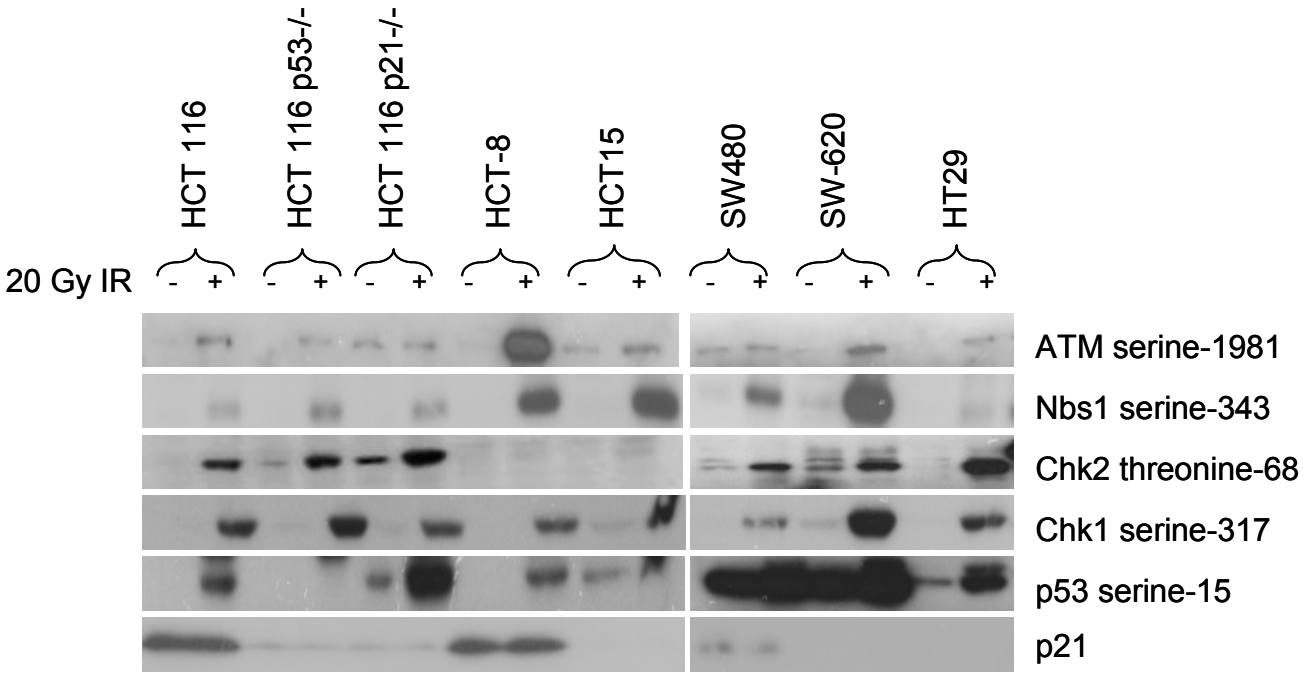

Figure 6.5. Induction of the DNA damage response pathway following treatment of a panel of commonly used colorectal cancer cell lines with 20 Gy ionising radiation.

HCT116 p21-null and SW-620 cells display constitutive Chk2 threonine-68 phosphorylation. Exponentially growing cells were treated with 20 Gy ionising radiation (IR) and harvested after 2 h. Equivalent amounts of protein (20 μg/lane) were analysed by immunoblots.

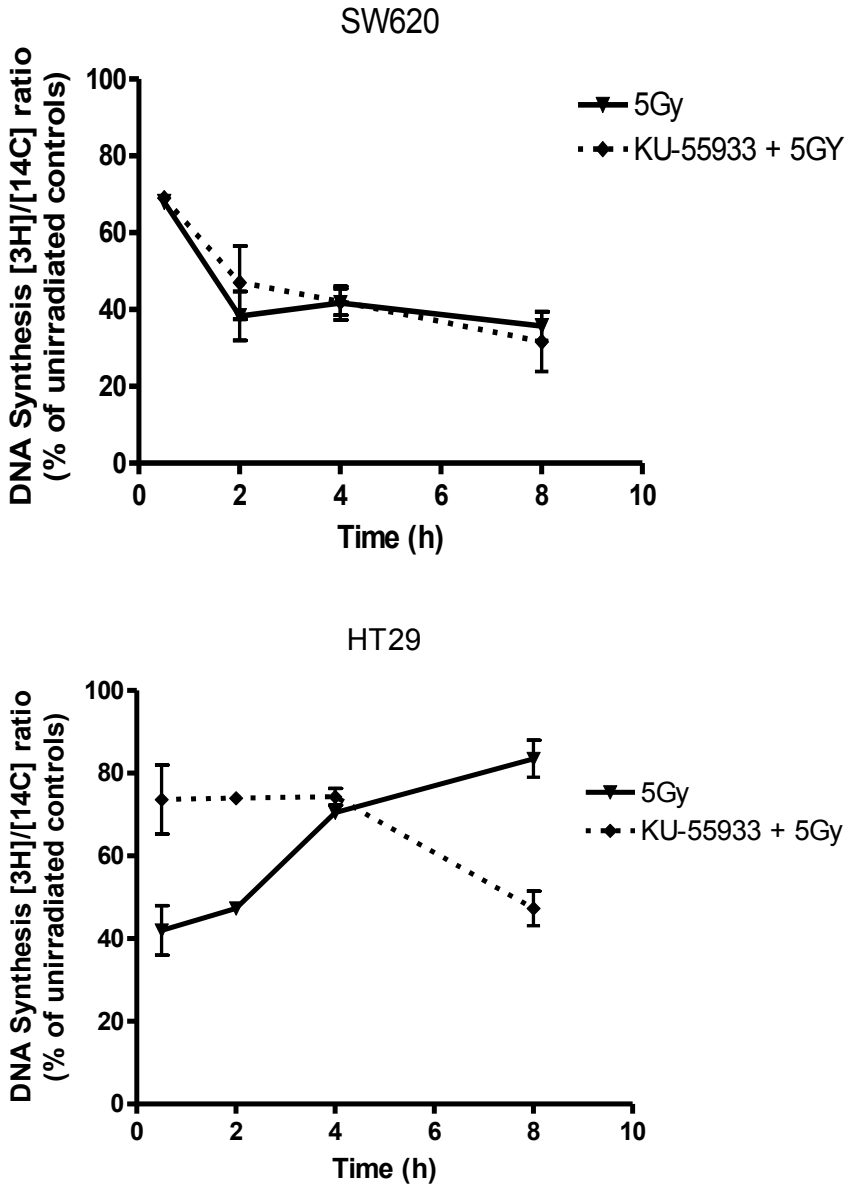

Figure 6.6. Basal Chk2 threonine-68 phosphorylation is associated with an inability to abrogate the DNA damage-induced reduction in DNA synthesis by ATM inhibition.

(*A*) ATM inhibition is unable to abrogate DNA damage-induced reduction in DNA synthesis in SW-620 cells that display basal Chk2 threonine-68 phosphorylation. (*B)*ATM inhibition abrogates DNA synthesis in HT29 cells. The DNA synthesis assay was described previously.

A

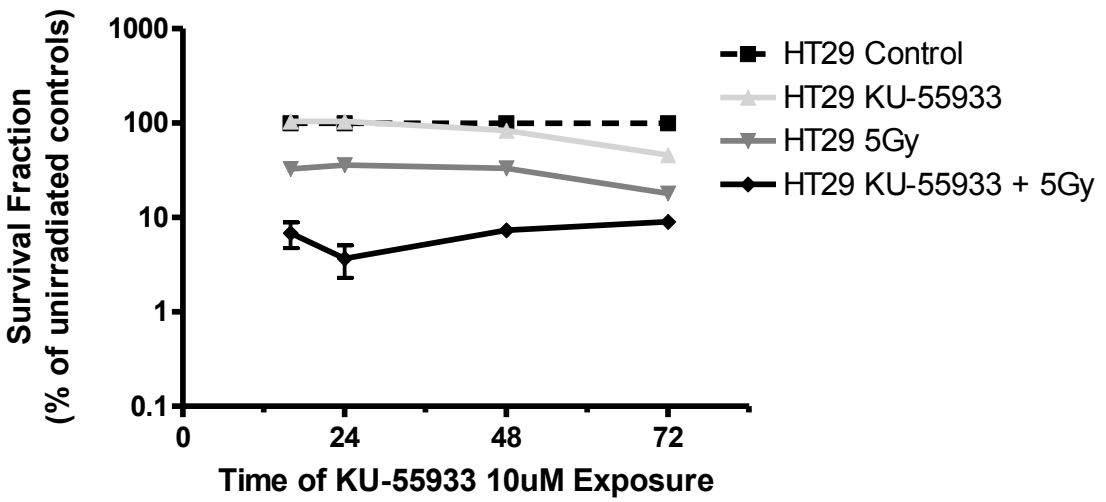

B

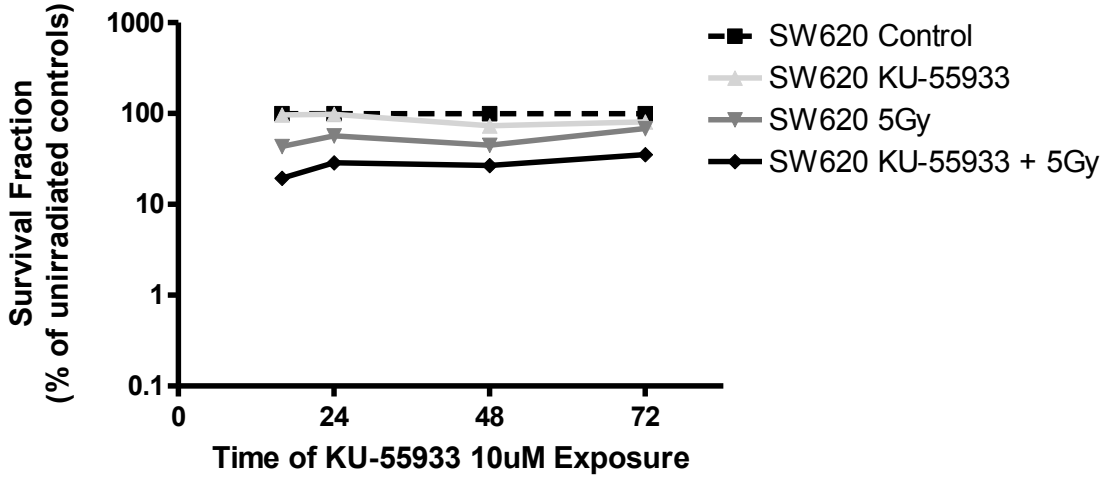

Figure 6.7. Colony formation in HT29 and SW-620 cells following combination therapy of ionising radiation and ATM inhibition (KU-55933).

Combination therapy (ATM inhibitor/5 Gy ionising radiation) reduces colony formation in HT29 cells but has a limited effect in SW-620 cells. Cells were treated as described in Figure 5.7 and replated for the assessment of colony formation. Error bars represent standard deviation of the mean.

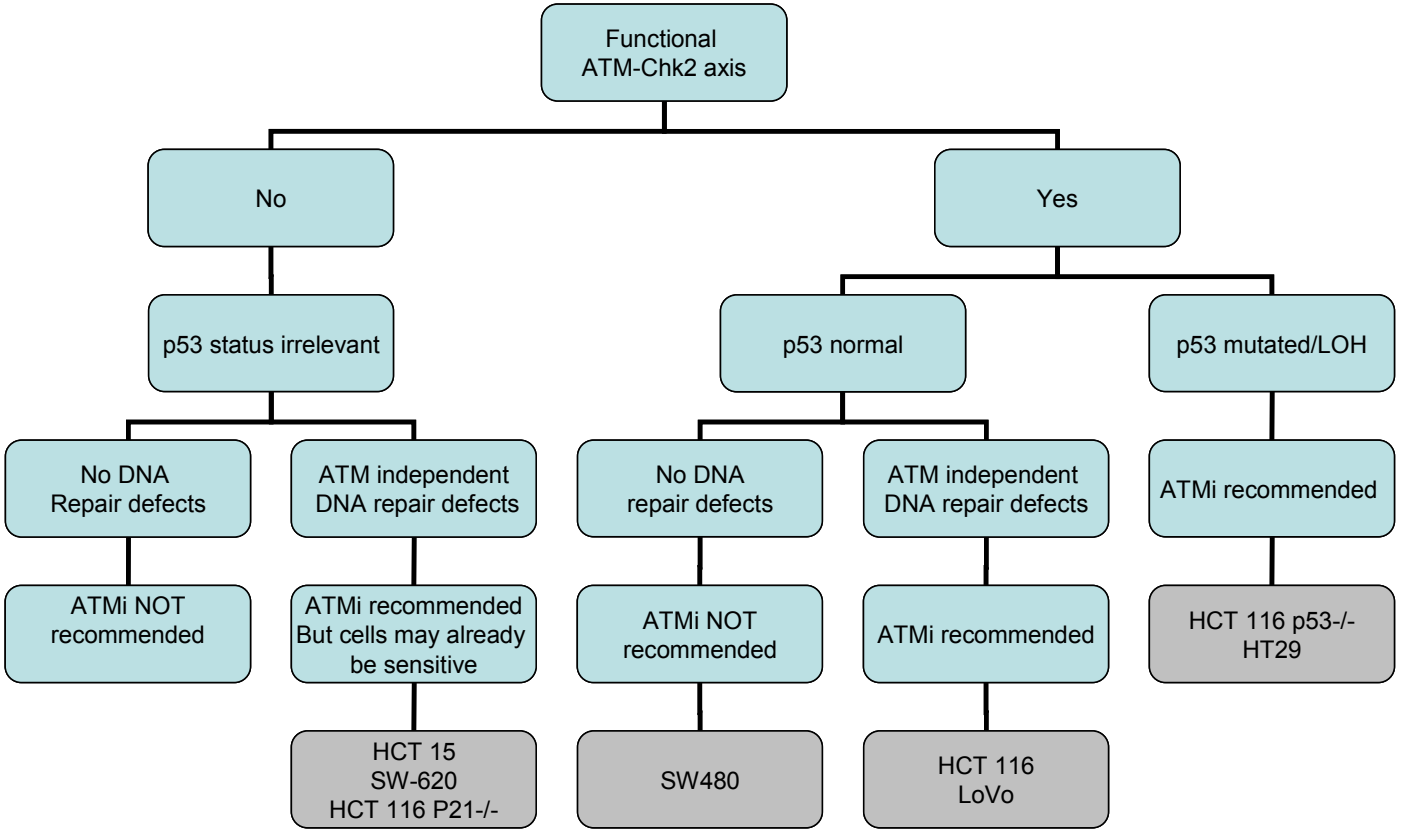

Figure 6.8. Framework for rationalising ATM inhibitor therapy.

A framework was constructed for rationalising ATM inhibitor therapy with reference to p53 status and the function of DNA repair mechanisms in tumours. See text for detailed discussion.

Table 6. 2. TNM staging for colorectal cancer.

AJCC stage	TNM stage	2010 7th edition TNM stage criteria for colorectal cancer
Stage 0	Tis N0 M0	Tis: Tumor confined to mucosa; cancer-*in-situ*
Stage I	T1 N0 M0	T1: Tumor invades submucosa
Stage I	T2 N0 M0	T2: Tumor invades muscularis propria
Stage II-A	T3 N0 M0	T3: Tumor invades subserosa or beyond (without other organs involved)
Stage II-B	T4 N0 M0	T4: Tumor invades adjacent organs or perforates the visceral peritoneum
Stage III-A	T1-2 N1 M0	N1: Metastasis to 1 to 3 regional lymph nodes. T1 or T2.
Stage III-B	T3-4 N1 M0	N1: Metastasis to 1 to 3 regional lymph nodes. T3 or T4.
Stage III-C	any T, N2 M0	N2: Metastasis to 4 or more regional lymph nodes. Any T.
Stage IV	any T, any N, M1	M1: Distant metastases present. Any T, any N.

The 7th edition of the TNM staging for colorectal cancer proposed by the American Joint Committee for Cancer (Edge and Compton, 2010).

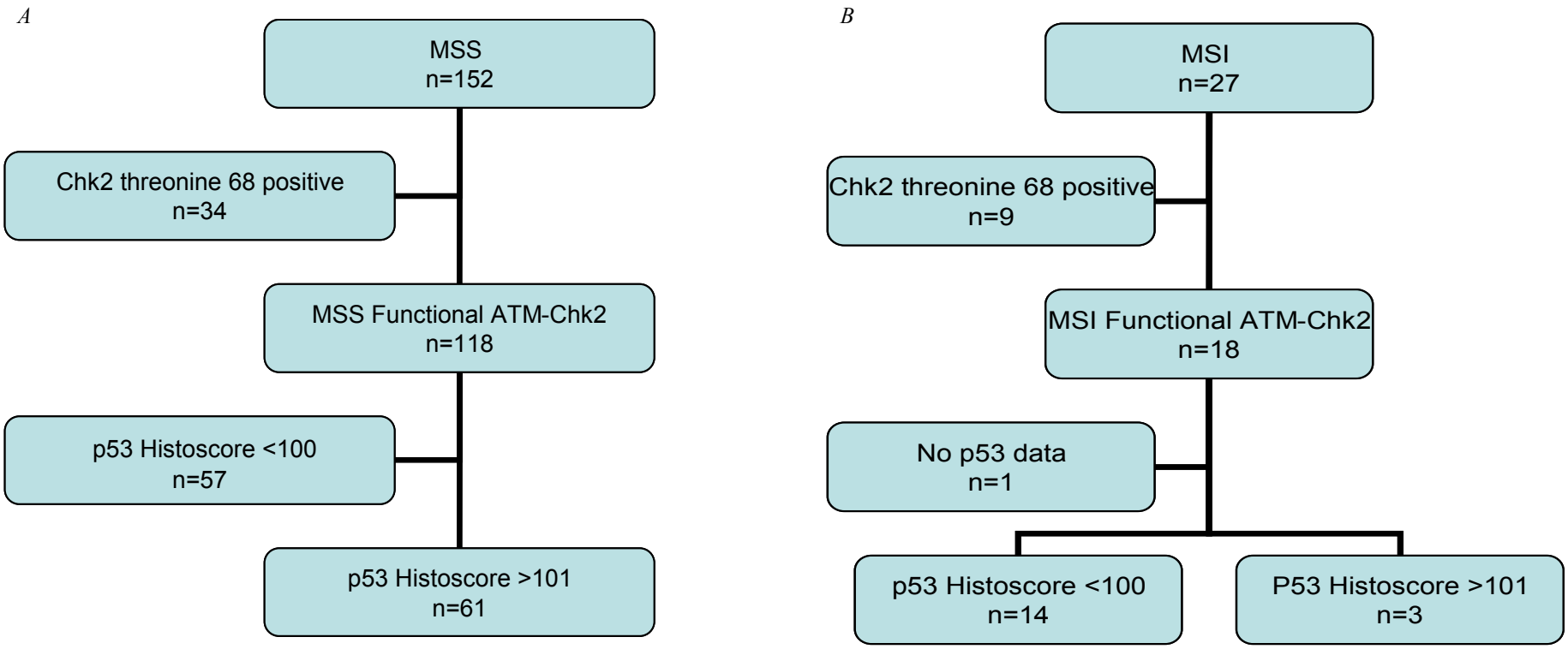

Figure 6.9. Stratification of human colorectal cancers from Chapter 3 by proposed predictive model.

The predictive model was used to stratify the colorectal cancers studied in Chapter3; (A) MSS cancers and (B) MSI cancers. .

Chapter 7. Discussion and Further Work

7.1 Deregulation of DNA Damage Response in Colorectal Cancer

DNA damage response pathways are considered to be anti-cancer barriers: cancer develops and progresses by circumventing these constraining mechanisms. The inherent ability of cells to sense and repair DNA damage is deregulated in cancer; however, knowledge of these abnormal signalling networks can be exploited to improve cancer therapeutics. An elegant example is the killing of BRCA-deficient cells with PARP inhibitors, demonstrating the concept of synthetic lethality, whereby cancer-specific defects result in dependency on the remaining redundant processes.

DNA damage response signalling cascades, which confer the ability to sense and repair DNA damage, are deregulated in colorectal cancer. MSI and chromosomal instability appear to be mutually exclusive during the early stages of colorectal cancer development. Activation of the ATM-dependent DDR, as assayed by Chk2 threonine-68 phosphorylation, was found in a higher proportion of sporadic colorectal cancers harbouring MSI than in MSS colorectal cancers. This is not surprising as, conversely, a higher proportion of MSS cancers exhibit p53 stabilisation, reflecting the expression of mutant p53 protein. This may reflect the increased burden of genomic instability or activation of compensatory DNA repair processes in MSI cancers. Bartkova *et al.* (2005b) demonstrated that the DDR becomes attenuated (or circumvented) as the level of genomic instability increases, as shown by genetic mutation or loss of heterozygosity in the ATM–Chk2–p53 axis. The data presented in this thesis support this observation, i.e., the DDR increased with increasing p53 expression. Improvements in our ability to monitor and assess

DDR activation in human cancer samples using conventional IHC and proteomic/genomic arrays will complement our understanding of cancer development, an essential prerequisite for designing tailored therapies. An analysis of cancer biopsy and resection specimens *ex vivo* for basal activation and induction of the DDR cascade will identify potential molecular targets for improving chemo/radio therapy. This could be done by dividing tissue specimens and then treating one part with DNA damaging agents and monitoring the DNA damage response with specific markers including γ-H2AX and RAD foci, as well as phosphorylated forms of Chk2 and Chk1 proteins. Examination of cancer samples *ex vivo* will also preserve the surrounding tissues, thus providing important information on cancer–stromal interactions which is often lost when analysing retrospective stored samples. For example, a microarray analysis of fresh colorectal cancer stromal tissue identified two novel microRNAs that downregulated target genes involved in cytokine interaction and cellular adhesion promoting cancer progression (Iwaya *et al.*, 2012; Nishida *et al.*, 2012; Yamashita *et al.*, 2012). In addition to dissecting the pathogeneisis of cancer-stromal interactions, novel therapeutic targets can also be identified. In a recent report, the production of angiogenesis promoting interleukin 6 (IL6) by fresh human colon cancer fibroblasts was confirmed. The investigators then proceeded to inhibit IL6 function by a targeted antibody to IL6 receptor on stromal cells and demonstrated greater anti-tumour activity than targeting the IL6 receptor on the colon cancer cells(Nagasaki *et al.*, 2014).

7.2 ATM–p21 Interaction

The ATM protein has a pivotal role in implementing the DNA damage response and repair networks by controlling the activity of effectors that coordinate cell cycle

arrest, DNA repair, apoptosis and cellular senescence. The p21 protein is an important molecule in this signalling cascade, which executes GI/S-phase arrest by inhibiting and modulating S-phase-promoting proteins and directly contributing to G2/M arrest. In cancer, attenuated p21 function is usually associated with p53 deficiencies; indeed, a negative association was confirmed between p53 and p21 expression levels in this study. p21 loss of function studies support a tumour suppression role, although this is specific to both tumour type and tissue type. p21 deficiency results in an incompetent G1/S-phase arrest and an inability to sustain G2 arrest after DNA damage. The role of p21 in the S-phase arrest is poorly defined. This report has identified a radioresistant DNA synthesis phenotype using an established isogenic colorectal cancer cell line panel. Although the direct molecular mechanism by which p21 contributes to the phenotype remains undefined, it may be related to the aberrant Chk2 localisation contributing to inefficient DNA damage-induced degradation of the abundant Cdc25A protein. Pang *et al.* (2011) demonstrated that p53 is aberrantly localised and transcriptionally inactivated in the same isogenic cell panel. Abrogation of all three DNA damage-induced cell cycle checkpoints by p21 deficiency provides further evidence that ATM and p21 are components of a single pathway and resembles the AT phenotype. Complementation of p21 in the p21-/- HCT116 cell line and siRNA-mediated p21silencing in the wild-type HCT116 cell line would clarify whether this is a direct effect of loss of p21. Further validation of this effect in a noncancer cell model would further clarify the specific role of p21 in DNA damage-induced inhibition of DNA synthesis. Murine embryonic fibroblasts in which p21 has been genetically disrupted are available;

analysis of the IR-induced S-phase checkpoint in these cells would confirm whether p21 has a direct role in regulating both Chk2 localisation and Cdc25A protein levels.

The loss of p21 appears to stimulate the ATM DDR, although it is unclear whether this predominantly reflects the sensing of continuous DNA damage or the active repair of damaged DNA. Gamma (γ-)H2AX is a sensitive marker of an acute DNA damage response and numbers of γ-H2AX foci this were similar in both wild-type and p21-/- backgrounds; however, γ-H2AX is downregulated during of cancer progression. Combined with the inability to reduce DNA synthesis, this may primarily reflect DNA repair in the p21-null cells. In cells displaying constitutive activation of the ATM-dependent DDR, I was unable to abrogate IR-induced S-phase arrest using the ATM inhibitor; suggesting deregulation of the ATM–Chk2–Cdc25A axis. In HCT116 colorectal cancer cells, Cdc25A is overexpressed and Chk2 is mislocalised in the absence of p21. Further work should be undertaken to determine the mechanism of Cdc25A overexpression. Cdc25A transcription is slightly upregulated in the absence of p21, which may reflect unopposed activation of the c-myc and E2F transcription factors. Despite Cdc25A overexpression, I was unable to identify a role for p21 in promoting basal protein degradation, suggesting that Chk1-mediated ANAPC/C^{cdh1}ubiquitin-mediated degradation was unaffected by p21 status. A more striking abnormality was the delay in degradation of Cdc25A following DNA damage in the absence of p21. In response to low dose IR, this is primarily an ATM-Chk2-dependent process. I identified potential aberrant localisation of Chk2 in p21-/- HCT116 cells, but not of Cdc25A. Mislocalisation of Chk2 may be more clearly defined using more precise methods of separating the cellular compartments. If Chk2 is immobilised onto chromatin, then micronuclease treatment of cells may be

able to restore Cdc25A degradation in p21-null cells following IR. The studies presented in this thesis have been undertaken in an *in vitro* model which will not account for any additional contributions by the cancer microenvironment. This could be investigated by using *in vivo* models of cancer in the form of xenografts or tissue specific murine cancer models. An exciting development is the organoid tissue culture which may improve on the inherent difficulties of both *in vivo* and *in vitro* models of studying disease.

7.3 Implications for Inhibitors of the DNA Damage Response

Activation of the DDR machinery has been identified in precancerous lesions and appears to be attenuated during the progression to invasive cancer. As the DDR signalling cascade is considered to be an anti-cancer barrier, inhibition of these components in isolation may promote tumorigenesis when applied during the early stages of cancer development. Therefore, therapeutic strategies combining DNA damaging agents and/or DDR inhibition maybe more efficacious in these circumstances. Chk2 threonine-68 is a surrogate marker for activation of the ATM-dependent DDR pathway and reflected an IR induced RDS phenotype in both cancer cell lines analysed (p21-/- HCT116 and SW-620). No additional abrogation of DNA damage-induced S-phase arrest was induced by the use of a specific ATM inhibitor. However, p53 status may have influenced the outcome: p21-/- HCT116 cells express transcriptionally attenuated p53 and SW-620 express mutant p53. In the two cell lines that lack basal Chk2 threonine-68 phosphorylation (HCT116 and HT29), abrogation of the IR-induced reduction in DNA synthesis was possible following ATM inhibition, which resulted in a further reduction in colony formation compared with IR therapy alone. This effect was independent of p53 status, but may have been

mediated by a defective MMR system in the HCT116 cells. The role of the MMR system can be tested by complementation of human MLH1 to the HCT 116 wild type cells (Brown *et al.*, 2003). Confirmation of these effects can be undertaken using xenograft models of the cancer cell lines in nude mice. This would permit an *in vivo* assessment of the effects of ATM inhibition in cancers that display constitutive activation of the ATM-dependent DDR.

A framework for rationalising the use of ATM inhibitors was constructed, which incorporates an assessment of ATM-Chk2 axis functionality, p53 mutational status and DNA repair defects (Figure 6.8). This framework requires to be validated integrating molecular markers of response to therapy. ATM inhibitor therapy could potentially exploit the concept of synthetic lethality when used in combination with standardised drug regimens (discussed in section 1.5.2) in cancers that harbour p53 mutations or mismatch repair defects. Controversially, they could also be used following DNA damage induced senescence to force senescent cells to re-enter the cell cycle. The latter regimen is not without risk as it may unwittingly promote cancer progression.

7.4 Conclusion

Cancer is caused by deregulation of an intricate network of signalling cascades, resulting in uncontrolled cellular proliferation. Attenuation of cellular DNA damage response mechanisms is necessary for the development of cancer. Targeting DNA damage response pathways will only be therapeutically beneficial if these pathways are essential for cancer cell survival. This study has discovered that p21 loss results in radioresistant DNA synthesis, despite constitutive activation of the ATM–Chk2

DDR. The RDS phenotype is related to Cdc25A overexpression. Constitutive activation of the DDR in cancers may represent deregulated DDR or DNA repair, limiting the efficacy of therapies targeting DDR proteins. Analysis of the DDR pathway function in cancers will help to tailor specific therapies to individual patients, thus allowing a rational approach to personalised therapy and limiting toxicity to normal tissues.

References

Abraham, R. T. (2004) The ATM-related kinase, hSMG-1, bridges genome and RNA surveillance pathways. *DNA Repair (Amst)* **3**(8-9), 919-925

Abraham, R. T. (2001) Cell cycle checkpoint signaling through the ATM and ATR kinases. *Genes Dev* **15**(17), 2177-2196

Adamsen, B. L., Kravik, K. L., and De Angelis, P. M. (2011) DNA damage signaling in response to 5-fluorouracil in three colorectal cancer cell lines with different mismatch repair and TP53 status. *Int J Oncol* **39**(3), 673-682

Ahn, J. Y., Schwarz, J. K., Piwnica-Worms, H., and Canman, C. E. (2000) Threonine 68 phosphorylation by ataxia telangiectasia mutated is required for efficient activation of Chk2 in response to ionizing radiation. *Cancer Res* **60**(21), 5934-5936

Akiyama, Y., Sato, H., Yamada, T., Nagasaki, H., Tsuchiya, A., Abe, R., and Yuasa, Y. (1997) Germ-line mutation of the hMSH6/GTBP gene in an atypical hereditary nonpolyposis colorectal cancer kindred. *Cancer Res* **57**(18), 3920-3923

Alemayehu, A., and Fridrichova, I. (2007) The MRE11/RAD50/NBS1 complex destabilization in Lynch-syndrome patients. *Eur J Hum Genet* **15**(9), 922-929

Andreassen, P. R., Lohez, O. D., Lacroix, F. B., and Margolis, R. L. (2001) Tetraploid state induces p53-dependent arrest of nontransformed mammalian cells in G1. *Mol Biol Cell* **12**(5), 1315-1328

Aneja, R., Ghaleb, A. M., Zhou, J., Yang, V. W., and Joshi, H. C. (2007) p53 and p21 determine the sensitivity of noscapine-induced apoptosis in colon cancer cells. *Cancer Res* **67**(8), 3862-3870

Assenmacher, N., and Hopfner, K. P. (2004) MRE11/RAD50/NBS1: complex activities. *Chromosoma* **113**(4), 157-166

Bai, A. H., Tong, J. H., To, K. F., Chan, M. W., Man, E. P., Lo, K. W., Lee, J. F., Sung, J. J., and Leung, W. K. (2004) Promoter hypermethylation of tumor-related genes in the progression of colorectal neoplasia. *Int J Cancer* **112**(5), 846-853

Bakkenist, C. J., and Kastan, M. B. (2003) DNA damage activates ATM through intermolecular autophosphorylation and dimer dissociation. *Nature* **421**(6922), 499-506

Banasiak, D., Barnetson, A. R., Odell, R. A., Mameghan, H., and Russell, P. J. (1999) Comparison between the clonogenic, MTT, and SRB assays for determining radiosensitivity in a panel of human bladder cancer cell lines and a ureteral cell line. *Radiat Oncol Investig* **7**(2), 77-85

Bartek, J., Lukas, C., and Lukas, J. (2004) Checking on DNA damage in S phase. *Nat Rev Mol Cell Biol* **5**(10), 792-804

Bartek, J., and Lukas, J. (2003) Chk1 and Chk2 kinases in checkpoint control and cancer. *Cancer Cell* **3**(5), 421-429

Bartek, J., and Lukas, J. (2007) DNA damage checkpoints: from initiation to recovery or adaptation. *Curr Opin Cell Biol* **19**(2), 238-245

Bartek, J., Lukas, J., and Bartkova, J. (2007) DNA damage response as an anti-cancer barrier: damage threshold and the concept of 'conditional haploinsufficiency'. *Cell Cycle* **6**(19), 2344-2347

Bartkova, J., Bakkenist, C. J., Rajpert-De Meyts, E., Skakkebaek, N. E., Sehested, M., Lukas, J., Kastan, M. B., and Bartek, J. (2005a) ATM activation in normal human tissues and testicular cancer. *Cell Cycle* **4**(6), 838-845

Bartkova, J., Guldberg, P., Gronbaek, K., Koed, K., Primdahl, H., Moller, K., Lukas, J., Orntoft, T. F., and Bartek, J. (2004) Aberrations of the Chk2 tumour suppressor in advanced urinary bladder cancer. *Oncogene* **23**(52), 8545-8551

Bartkova, J., Horejsi, Z., Koed, K., Kramer, A., Tort, F., Zieger, K., Guldberg, P., Sehested, M., Nesland, J. M., Lukas, C., Orntoft, T., Lukas, J., and Bartek, J. (2005b) DNA damage response as a candidate anti-cancer barrier in early human tumorigenesis. *Nature* **434**(7035), 864-870

Bartkova, J., Rezaei, N., Liontos, M., Karakaidos, P., Kletsas, D., Issaeva, N., Vassiliou, L. V., Kolettas, E., Niforou, K., Zoumpourlis, V. C., Takaoka, M., Nakagawa, H., Tort, F., Fugger, K., Johansson, F., Sehested, M., Andersen, C. L., Dyrskjot, L., Orntoft, T., Lukas, J., Kittas, C., Helleday, T., Halazonetis, T. D., Bartek, J., and Gorgoulis, V. G. (2006) Oncogene-induced senescence is part of the tumorigenesis barrier imposed by DNA damage checkpoints. *Nature* **444**(7119), 633-637

Bataller, M., Mendez, C., Salas, J. A., and Portugal, J. Cellular response and activation of apoptosis by mithramycin SK in p21(WAF1)-deficient HCT116 human colon carcinoma cells. *Cancer Lett* **292**(1), 80-90

BDWG. (2001) Biomarkers and surrogate endpoints: preferred definitions and conceptual framework. *Clin Pharmacol Ther* **69**(3), 89-95

Bebb, D. G., Steele, P. P., Warrington, P. J., Moffat, J. A., and Glickman, B. W. (1998) Caffeine does not potentiate gamma-radiation induced DNA damage in ataxia telangiectasia lymphoblastoid cells. *Mutat Res* **401**(1-2), 27-32

Beggs, A. D., Domingo, E., McGregor, M., Presz, M., Johnstone, E., Midgley, R., Kerr, D., Oukrif, D., Novelli, M., Abulafi, M., Hodgson, S. V., Fadhil, W., Ilyas, M., and Tomlinson, I. P. (2010) Loss of expression of the double strand break repair protein ATM is associated with worse prognosis in colorectal cancer and loss of Ku70 expression is associated with CIN. *Oncotarget*

Bekker-Jensen, S., Lukas, C., Kitagawa, R., Melander, F., Kastan, M. B., Bartek, J., and Lukas, J. (2006) Spatial organization of the mammalian genome surveillance machinery in response to DNA strand breaks. *J Cell Biol* **173**(2), 195-206

Ben-Porath, I., and Weinberg, R. A. (2005) The signals and pathways activating cellular senescence. *Int J Biochem Cell Biol* **37**(5), 961-976

Bennetzen, M. V., Larsen, D. H., Bunkenborg, J., Bartek, J., Lukas, J., and Andersen, J. S. (2010) Site-specific phosphorylation dynamics of the nuclear proteome during the DNA damage response. *Mol Cell Proteomics* **9**(6), 1314-1323

Bensimon, A., Schmidt, A., Ziv, Y., Elkon, R., Wang, S. Y., Chen, D. J., Aebersold, R., and Shiloh, Y. (2010) ATM-dependent and -independent dynamics of the nuclear phosphoproteome after DNA damage. *Sci Signal* **3**(151), rs3

Bernstein, J. L., Seminara, D., and Borresen-Dale, A. L. (2002) Workshop on The Epidemiology of the ATM Gene: Impact on Breast Cancer Risk and Treatment, Present Status and Future Focus, Lillehammer, Norway, 29 June 2002. *Breast Cancer Res* **4**(6), 249-252

Blomberg, I., and Hoffmann, I. (1999) Ectopic expression of Cdc25A accelerates the G(1)/S transition and leads to premature activation of cyclin E- and cyclin A-dependent kinases. *Mol Cell Biol* **19**(9), 6183-6194

Boland, C. R., Thibodeau, S. N., Hamilton, S. R., Sidransky, D., Eshleman, J. R., Burt, R. W., Meltzer, S. J., Rodriguez-Bigas, M. A., Fodde, R., Ranzani, G. N., and Srivastava, S. (1998) A National Cancer Institute Workshop on Microsatellite Instability for cancer detection and familial predisposition: development of international criteria for the determination of microsatellite instability in colorectal cancer. *Cancer Res* **58**(22), 5248-5257

Boutros, R., Lobjois, V., and Ducommun, B. (2007) CDC25 phosphatases in cancer cells: key players? Good targets? *Nat Rev Cancer* **7**(7), 495-507

Bower, J. J., Karaca, G. F., Zhou, Y., Simpson, D. A., Cordeiro-Stone, M., and Kaufmann, W. K. (2010a) Topoisomerase IIalpha maintains genomic stability through decatenation G(2) checkpoint signaling. *Oncogene* **29**(34), 4787-4799

Bower, J. J., Zhou, Y., Zhou, T., Simpson, D. A., Arlander, S. J., Paules, R. S., Cordeiro-Stone, M., and Kaufmann, W. K. (2010b) Revised genetic requirements for the decatenation G2 checkpoint: the role of ATM. *Cell Cycle* **9**(8), 1617-1628

Boyer, J. C., Umar, A., Risinger, J. I., Lipford, J. R., Kane, M., Yin, S., Barrett, J. C., Kolodner, R. D., and Kunkel, T. A. (1995) Microsatellite instability, mismatch repair deficiency, and genetic defects in human cancer cell lines. *Cancer Res* **55**(24), 6063-6070

Branch, P., Hampson, R., and Karran, P. (1995) DNA mismatch binding defects, DNA damage tolerance, and mutator phenotypes in human colorectal carcinoma cell lines. *Cancer Res* **55**(11), 2304-2309

Brown, E. J., and Baltimore, D. (2003) Essential and dispensable roles of ATR in cell cycle arrest and genome maintenance. *Genes Dev* **17**(5), 615-628

Brown, K. D., Rathi, A., Kamath, R., Beardsley, D. I., Zhan, Q., Mannino, J. L., and Baskaran, R. (2003) The mismatch repair system is required for S-phase checkpoint activation. *Nat Genet* **33**(1), 80-84

Brugarolas, J., Chandrasekaran, C., Gordon, J. I., Beach, D., Jacks, T., and Hannon, G. J. (1995) Radiation-induced cell cycle arrest compromised by p21 deficiency. *Nature* **377**(6549), 552-557

Brugarolas, J., Moberg, K., Boyd, S. D., Taya, Y., Jacks, T., and Lees, J. A. (1999) Inhibition of cyclin-dependent kinase 2 by p21 is necessary for retinoblastoma protein-mediated G1 arrest after gamma-irradiation. *Proc Natl Acad Sci U S A* **96**(3), 1002-1007

Bryant, H. E., and Helleday, T. (2004) Poly(ADP-ribose) polymerase inhibitors as potential chemotherapeutic agents. *Biochem Soc Trans* **32**(Pt 6), 959-961

Bryant, H. E., and Helleday, T. (2006) Inhibition of poly (ADP-ribose) polymerase activates ATM which is required for subsequent homologous recombination repair. *Nucleic Acids Res* **34**(6), 1685-1691

Bryant, H. E., Schultz, N., Thomas, H. D., Parker, K. M., Flower, D., Lopez, E., Kyle, S., Meuth, M., Curtin, N. J., and Helleday, T. (2005) Specific killing of BRCA2-deficient tumours with inhibitors of poly(ADP-ribose) polymerase. *Nature* **434**(7035), 913-917

Brzoska, K., and Szumiel, I. (2009) Signalling loops and linear pathways: NF-kappaB activation in response to genotoxic stress. *Mutagenesis* **24**(1), 1-8

Bubb, V. J., Curtis, L. J., Cunningham, C., Dunlop, M. G., Carothers, A. D., Morris, R. G., White, S., Bird, C. C., and Wyllie, A. H. (1996) Microsatellite instability and the role of hMSH2 in sporadic colorectalcancer. *Oncogene* **12**(12), 2641-2649

Bubendorf, L., Nocito, A., Moch, H., and Sauter, G. (2001) Tissue microarray (TMA) technology: miniaturized pathology archives for high-throughput in situ studies. *J Pathol* **195**(1), 72-79

Bukholm, I. K., and Nesland, J. M. (2000) Protein expression of p53, p21 (WAF1/CIP1), bcl-2, Bax, cyclin D1 and pRb in human colon carcinomas. *Virchows Arch* **436**(3), 224-228

Bunz, F., Dutriaux, A., Lengauer, C., Waldman, T., Zhou, S., Brown, J. P., Sedivy, J. M., Kinzler, K. W., and Vogelstein, B. (1998) Requirement for p53 and p21 to sustain G2 arrest after DNA damage. *Science* **282**(5393), 1497-1501

Burma, S., Chen, B. P., and Chen, D. J. (2006) Role of non-homologous end joining (NHEJ) in maintaining genomic integrity. *DNA Repair (Amst)* **5**(9-10), 1042-1048

Burma, S., and Chen, D. J. (2004) Role of DNA-PK in the cellular response to DNA double-strand breaks. *DNA Repair (Amst)* **3**(8-9), 909-918

Burrell, R. A., McClelland, S. E., Endesfelder, D., Groth, P., Weller, M. C., Shaikh, N., Domingo, E., Kanu, N., Dewhurst, S. M., Gronroos, E., Chew, S. K., Rowan, A. J., Schenk, A., Sheffer, M., Howell, M., Kschischo, M., Behrens, A., Helleday, T., Bartek, J., Tomlinson, I. P., and Swanton, C. (2013) Replication stress links structural and numerical cancer chromosomal instability. *Nature* **494**(7438), 492-496

Busino, L., Chiesa, M., Draetta, G. F., and Donzelli, M. (2004) Cdc25A phosphatase: combinatorial phosphorylation, ubiquitylation and proteolysis. *Oncogene* **23**(11), 2050-2056

Busino, L., Donzelli, M., Chiesa, M., Guardavaccaro, D., Ganoth, D., Dorrello, N. V., Hershko, A., Pagano, M., and Draetta, G. F. (2003) Degradation of Cdc25A by beta-TrCP during S phase and in response to DNA damage. *Nature* **426**(6962), 87-91

Byun, T. S., Pacek, M., Yee, M. C., Walter, J. C., and Cimprich, K. A. (2005) Functional uncoupling of MCM helicase and DNA polymerase activities activates the ATR-dependent checkpoint. *Genes Dev* **19**(9), 1040-1052

Cangi, M. G., Piccinin, S., Pecciarini, L., Talarico, A., Dal Cin, E., Grassi, S., Grizzo, A., Maestro, R., and Doglioni, C. (2008) Constitutive overexpression of CDC25A in primary human mammary epithelial cells results in both defective DNA damage response and chromosomal breaks at fragile sites. *Int J Cancer* **123**(6), 1466-1471

Canman, C. E., Lim, D. S., Cimprich, K. A., Taya, Y., Tamai, K., Sakaguchi, K., Appella, E., Kastan, M. B., and Siliciano, J. D. (1998) Activation of the ATM kinase by ionizing radiation and phosphorylation of p53. *Science* **281**(5383), 1677-1679

Carethers, J. M., Smith, E. J., Behling, C. A., Nguyen, L., Tajima, A., Doctolero, R. T., Cabrera, B. L., Goel, A., Arnold, C. A., Miyai, K., and Boland, C. R.

(2004) Use of 5-fluorouracil and survival in patients with microsatellite-unstable colorectal cancer. *Gastroenterology* **126**(2), 394-401

Carney, J. P., Maser, R. S., Olivares, H., Davis, E. M., Le Beau, M., Yates, J. R., 3rd, Hays, L., Morgan, W. F., and Petrini, J. H. (1998) The hMre11/hRad50 protein complex and Nijmegen breakage syndrome: linkage of double-strand break repair to the cellular DNA damage response. *Cell* **93**(3), 477-486

Carson, C. T., Schwartz, R. A., Stracker, T. H., Lilley, C. E., Lee, D. V., and Weitzman, M. D. (2003) The Mre11 complex is required for ATM activation and the G2/M checkpoint. *Embo J* **22**(24), 6610-6620

Cerosaletti, K., and Concannon, P. (2004) Independent roles for nibrin and Mre11-Rad50 in the activation and function of Atm. *J Biol Chem* **279**(37), 38813-38819

Chapman, J. R., Taylor, M. R., and Boulton, S. J. (2012) Playing the end game: DNA double-strand break repair pathway choice. *Mol Cell* **47**(4), 497-510

Chehab, N. H., Malikzay, A., Appel, M., and Halazonetis, T. D. (2000) Chk2/hCds1 functions as a DNA damage checkpoint in G(1) by stabilizing p53. *Genes Dev* **14**(3), 278-288

Chen, C., Shimizu, S., Tsujimoto, Y., and Motoyama, N. (2005a) Chk2 regulates transcription-independent p53-mediated apoptosis in response to DNA damage. *Biochem Biophys Res Commun* **333**(2), 427-431

Chen, C. R., Wang, W., Rogoff, H. A., Li, X., Mang, W., and Li, C. J. (2005b) Dual induction of apoptosis and senescence in cancer cells by Chk2 activation: checkpoint activation as a strategy against cancer. *Cancer Res* **65**(14), 6017-6021

Chen, L., Gilkes, D. M., Pan, Y., Lane, W. S., and Chen, J. (2005c) ATM and Chk2-dependent phosphorylation of MDMX contribute to p53 activation after DNA damage. *Embo J* **24**(19), 3411-3422

Chen, M. S., Ryan, C. E., and Piwnica-Worms, H. (2003) Chk1 kinase negatively regulates mitotic function of Cdc25A phosphatase through 14-3-3 binding. *Mol Cell Biol* **23**(21), 7488-7497

Chene, P., Rudloff, J., Schoepfer, J., Furet, P., Meier, P., Qian, Z., Schlaeppi, J. M., Schmitz, R., and Radimerski, T. (2009) Catalytic inhibition of topoisomerase II by a novel rationally designed ATP-competitive purine analogue. *BMC Chem Biol* **9**, 1

Cheng, M., Olivier, P., Diehl, J. A., Fero, M., Roussel, M. F., Roberts, J. M., and Sherr, C. J. (1999) The p21(Cip1) and p27(Kip1) CDK 'inhibitors' are essential activators of cyclin D-dependent kinases in murine fibroblasts. *Embo J* **18**(6), 1571-1583

Cimprich, K. A., and Cortez, D. (2008) ATR: an essential regulator of genome integrity. *Nat Rev Mol Cell Biol* **9**(8), 616-627

Cliby, W. A., Roberts, C. J., Cimprich, K. A., Stringer, C. M., Lamb, J. R., Schreiber, S. L., and Friend, S. H. (1998) Overexpression of a kinase-inactive ATR protein causes sensitivity to DNA-damaging agents and defects in cell cycle checkpoints. *Embo J* **17**(1), 159-169

Collis, S. J., Swartz, M. J., Nelson, W. G., and DeWeese, T. L. (2003) Enhanced radiation and chemotherapy-mediated cell killing of human cancer cells by small inhibitory RNA silencing of DNA repair factors. *Cancer Res* **63**(7), 1550-1554

Connolly, K. C., Gabra, H., Millwater, C. J., Taylor, K. J., Rabiasz, G. J., Watson, J. E., Smyth, J. F., Wyllie, A. H., and Jodrell, D. I. (1999) Identification of a region of frequent loss of heterozygosity at 11q24 in colorectal cancer. *Cancer Res* **59**(12), 2806-2809

Coppe, J. P., Desprez, P. Y., Krtolica, A., and Campisi, J. (2010) The senescence-associated secretory phenotype: the dark side of tumor suppression. *Annu Rev Pathol* **5**, 99-118

Cortez, D., Wang, Y., Qin, J., and Elledge, S. J. (1999) Requirement of ATM-dependent phosphorylation of brca1 in the DNA damage response to double-strand breaks. *Science* **286**(5442), 1162-1166

Cowell, I. G., Durkacz, B. W., and Tilby, M. J. (2005) Sensitization of breast carcinoma cells to ionizing radiation by small molecule inhibitors of DNA-dependent protein kinase and ataxia telangiectsia mutated. *Biochem Pharmacol* **71**(1-2), 13-20

Craig, A., Scott, M., Burch, L., Smith, G., Ball, K., and Hupp, T. (2003) Allosteric effects mediate CHK2 phosphorylation of the p53 transactivation domain. *EMBO Rep* **4**(8), 787-792

Craig, A. L., and Hupp, T. R. (2004) The regulation of CHK2 in human cancer. *Oncogene* **23**(52), 8411-8418

Cregger, M., Berger, A. J., and Rimm, D. L. (2006) Immunohistochemistry and quantitative analysis of protein expression. *Arch Pathol Lab Med* **130**(7), 1026-1030

Crescenzi, E., Palumbo, G., de Boer, J., and Brady, H. J. (2008) Ataxia telangiectasia mutated and p21CIP1 modulate cell survival of drug-induced senescent tumor cells: implications for chemotherapy. *Clin Cancer Res* **14**(6), 1877-1887

Cuadrado, M., Martinez-Pastor, B., Murga, M., Toledo, L. I., Gutierrez-Martinez, P., Lopez, E., and Fernandez-Capetillo, O. (2006) ATM regulates ATR chromatin loading in response to DNA double-strand breaks. *J Exp Med* **203**(2), 297-303

Culligan, K. M., Robertson, C. E., Foreman, J., Doerner, P., and Britt, A. B. (2006) ATR and ATM play both distinct and additive roles in response to ionizing radiation. *Plant J* **48**(6), 947-961

Cunningham, J. M., Christensen, E. R., Tester, D. J., Kim, C. Y., Roche, P. C., Burgart, L. J., and Thibodeau, S. N. (1998) Hypermethylation of the hMLH1 promoter in colon cancer with microsatellite instability. *Cancer Res* **58**(15), 3455-3460

D'Amours, D., and Jackson, S. P. (2002) The Mre11 complex: at the crossroads of dna repair and checkpoint signalling. *Nat Rev Mol Cell Biol* **3**(5), 317-327

Dasika, G. K., Lin, S. C., Zhao, S., Sung, P., Tomkinson, A., and Lee, E. Y. (1999) DNA damage-induced cell cycle checkpoints and DNA strand break repair in development and tumorigenesis. *Oncogene* **18**(55), 7883-7899

Delavaine, L., and La Thangue, N. B. (1999) Control of E2F activity by p21Waf1/Cip1. *Oncogene* **18**(39), 5381-5392

Deming, P. B., Cistulli, C. A., Zhao, H., Graves, P. R., Piwnica-Worms, H., Paules, R. S., Downes, C. S., and Kaufmann, W. K. (2001) The human decatenation checkpoint. *Proc Natl Acad Sci U S A* **98**(21), 12044-12049

Deng, C., Zhang, P., Harper, J. W., Elledge, S. J., and Leder, P. (1995) Mice lacking p21CIP1/WAF1 undergo normal development, but are defective in G1 checkpoint control. *Cell* **82**(4), 675-684

Diaz, L. A., Jr., Williams, R. T., Wu, J., Kinde, I., Hecht, J. R., Berlin, J., Allen, B., Bozic, I., Reiter, J. G., Nowak, M. A., Kinzler, K. W., Oliner, K. S., and Vogelstein, B. (2012) The molecular evolution of acquired resistance to targeted EGFR blockade in colorectal cancers. *Nature* **486**(7404), 537-540

Diehl, J. A., Zindy, F., and Sherr, C. J. (1997) Inhibition of cyclin D1 phosphorylation on threonine-286 prevents its rapid degradation via the ubiquitin-proteasome pathway. *Genes Dev* **11**(8), 957-972

DiTullio, R. A., Jr., Mochan, T. A., Venere, M., Bartkova, J., Sehested, M., Bartek, J., and Halazonetis, T. D. (2002) 53BP1 functions in an ATM-dependent checkpoint pathway that is constitutively activated in human cancer. *Nat Cell Biol* **4**(12), 998-1002

DiVito, K. A., Charette, L. A., Rimm, D. L., and Camp, R. L. (2004) Long-term preservation of antigenicity on tissue microarrays. *Lab Invest* **84**(8), 1071-1078

Donzelli, M., Busino, L., Chiesa, M., Ganoth, D., Hershko, A., and Draetta, G. F. (2004) Hierarchical order of phosphorylation events commits Cdc25A to betaTrCP-dependent degradation. *Cell Cycle* **3**(4), 469-471

Donzelli, M., Squatrito, M., Ganoth, D., Hershko, A., Pagano, M., and Draetta, G. F. (2002) Dual mode of degradation of Cdc25 A phosphatase. *Embo J* **21**(18), 4875-4884

Dornan, D., and Hupp, T. R. (2001) Inhibition of p53-dependent transcription by BOX-I phospho-peptide mimetics that bind to p300. *EMBO Rep* **2**(2), 139-144

Dulic, V., Kaufmann, W. K., Wilson, S. J., Tlsty, T. D., Lees, E., Harper, J. W., Elledge, S. J., and Reed, S. I. (1994) p53-dependent inhibition of cyclin-dependent kinase activities in human fibroblasts during radiation-induced G1 arrest. *Cell* **76**(6), 1013-1023

Eastman, A. (2004) Cell cycle checkpoints and their impact on anticancer therapeutic strategies. *J Cell Biochem* **91**(2), 223-231

Edge, S. B., and Compton, C. C. (2010) The American Joint Committee on Cancer: the 7th edition of the AJCC cancer staging manual and the future of TNM. *Ann Surg Oncol* **17**(6), 1471-1474

Ejima, Y., Yang, L., and Sasaki, M. S. (2000) Aberrant splicing of the ATM gene associated with shortening of the intronic mononucleotide tract in human colon tumor cell lines: a novel mutation target of microsatellite instability. *Int J Cancer* **86**(2), 262-268

el-Deiry, W. S., Harper, J. W., O'Connor, P. M., Velculescu, V. E., Canman, C. E., Jackman, J., Pietenpol, J. A., Burrell, M., Hill, D. E., Wang, Y., and et al. (1994) WAF1/CIP1 is induced in p53-mediated G1 arrest and apoptosis. *Cancer Res* **54**(5), 1169-1174

el-Deiry, W. S., Tokino, T., Velculescu, V. E., Levy, D. B., Parsons, R., Trent, J. M., Lin, D., Mercer, W. E., Kinzler, K. W., and Vogelstein, B. (1993) WAF1, a potential mediator of p53 tumor suppression. *Cell* **75**(4), 817-825

Enoch, T., and Norbury, C. (1995) Cellular responses to DNA damage: cell-cycle checkpoints, apoptosis and the roles of p53 and ATM. *Trends Biochem Sci* **20**(10), 426-430

Escribano-Diaz, C., Orthwein, A., Fradet-Turcotte, A., Xing, M., Young, J. T., Tkac, J., Cook, M. A., Rosebrock, A. P., Munro, M., Canny, M. D., Xu, D., and Durocher, D. (2013) A cell cycle-dependent regulatory circuit composed of 53BP1-RIF1 and BRCA1-CtIP controls DNA repair pathway choice. *Mol Cell* **49**(5), 872-883

Falck, J., Coates, J., and Jackson, S. P. (2005) Conserved modes of recruitment of ATM, ATR and DNA-PKcs to sites of DNA damage. *Nature* **434**(7033), 605-611

Falck, J., Mailand, N., Syljuasen, R. G., Bartek, J., and Lukas, J. (2001) The ATM-Chk2-Cdc25A checkpoint pathway guards against radioresistant DNA synthesis. *Nature* **410**(6830), 842-847

Falck, J., Petrini, J. H., Williams, B. R., Lukas, J., and Bartek, J. (2002) The DNA damage-dependent intra-S phase checkpoint is regulated by parallel pathways. *Nat Genet* **30**(3), 290-294

Fan, C., Quan, R., Feng, X., Gillis, A., He, L., Matsumoto, E. D., Salama, S., Cutz, J. C., Kapoor, A., and Tang, D. (2006) ATM activation is accompanied with earlier stages of prostate tumorigenesis. *Biochim Biophys Acta* **1763**(10), 1090-1097

Farmer, H., McCabe, N., Lord, C. J., Tutt, A. N., Johnson, D. A., Richardson, T. B., Santarosa, M., Dillon, K. J., Hickson, I., Knights, C., Martin, N. M., Jackson, S. P., Smith, G. C., and Ashworth, A. (2005) Targeting the DNA repair defect in BRCA mutant cells as a therapeutic strategy. *Nature* **434**(7035), 917-921

Fasulo, B., Koyama, C., Yu, K. R., Homola, E. M., Hsieh, T. S., Campbell, S. D., and Sullivan, W. Chk1 and Wee1 kinases coordinate DNA replication, chromosome condensation, and anaphase entry. *Mol Biol Cell* **23**(6), 1047-1057

Fergenbaum, J. H., Garcia-Closas, M., Hewitt, S. M., Lissowska, J., Sakoda, L. C., and Sherman, M. E. (2004) Loss of antigenicity in stored sections of breast cancer tissue microarrays. *Cancer Epidemiol Biomarkers Prev* **13**(4), 667-672

Fishel, R., Lescoe, M. K., Rao, M. R., Copeland, N. G., Jenkins, N. A., Garber, J., Kane, M., and Kolodner, R. (1993) The human mutator gene homolog MSH2 and its association with hereditary nonpolyposis colon cancer. *Cell* **75**(5), 1027-1038

Franken, N. A., Rodermond, H. M., Stap, J., Haveman, J., and van Bree, C. (2006) Clonogenic assay of cells in vitro. *Nat Protoc* **1**(5), 2315-2319

Galaktionov, K., Chen, X., and Beach, D. (1996) Cdc25 cell-cycle phosphatase as a target of c-myc. *Nature* **382**(6591), 511-517

Gamper, A. M., Rofougaran, R., Watkins, S. C., Greenberger, J. S., Beumer, J. H., and Bakkenist, C. J. (2013) ATR kinase activation in G1 phase facilitates the repair of ionizing radiation-induced DNA damage. *Nucleic Acids Res* **41**(22), 10334-10344

Garcia, J. M., Rodriguez, R., Dominguez, G., Silva, J. M., Provencio, M., Silva, J., Colmenarejo, A., Millan, I., Munoz, C., Salas, C., Coca, S., Espana, P., and

Bonilla, F. (2003) Prognostic significance of the allelic loss of the BRCA1 gene in colorectal cancer. *Gut* **52**(12), 1756-1763

Gatei, M., Scott, S. P., Filippovitch, I., Soronika, N., Lavin, M. F., Weber, B., and Khanna, K. K. (2000a) Role for ATM in DNA damage-induced phosphorylation of BRCA1. *Cancer Res* **60**(12), 3299-3304

Gatei, M., Young, D., Cerosaletti, K. M., Desai-Mehta, A., Spring, K., Kozlov, S., Lavin, M. F., Gatti, R. A., Concannon, P., and Khanna, K. (2000b) ATM-dependent phosphorylation of nibrin in response to radiation exposure. *Nat Genet* **25**(1), 115-119

Gatti, R. A., Berkel, I., Boder, E., Braedt, G., Charmley, P., Concannon, P., Ersoy, F., Foroud, T., Jaspers, N. G., Lange, K., and et al. (1988) Localization of an ataxia-telangiectasia gene to chromosome 11q22-23. *Nature* **336**(6199), 577-580

Gayet, J., Zhou, X. P., Duval, A., Rolland, S., Hoang, J. M., Cottu, P., and Hamelin, R. (2001) Extensive characterization of genetic alterations in a series of human colorectal cancer cell lines. *Oncogene* **20**(36), 5025-5032

Gervaz, P., Cerottini, J. P., Bouzourene, H., Hahnloser, D., Doan, C. L., Benhattar, J., Chaubert, P., Secic, M., Gillet, M., and Carethers, J. M. (2002) Comparison of microsatellite instability and chromosomal instability in predicting survival of patients with T3N0 colorectal cancer. *Surgery* **131**(2), 190-197

Giannini, G., Rinaldi, C., Ristori, E., Ambrosini, M. I., Cerignoli, F., Viel, A., Bidoli, E., Berni, S., D'Amati, G., Scambia, G., Frati, L., Screpanti, I., and Gulino, A. (2004) Mutations of an intronic repeat induce impaired MRE11 expression in primary human cancer with microsatellite instability. *Oncogene* **23**(15), 2640-2647

Giannini, G., Ristori, E., Cerignoli, F., Rinaldi, C., Zani, M., Viel, A., Ottini, L., Crescenzi, M., Martinotti, S., Bignami, M., Frati, L., Screpanti, I., and Gulino, A. (2002) Human MRE11 is inactivated in mismatch repair-deficient cancers. *EMBO Rep* **3**(3), 248-254

Goethals, L., Perneel, C., Debucquoy, A., De Schutter, H., Borghys, D., Ectors, N., Geboes, K., McBride, W. H., and Haustermans, K. M. (2006) A new approach to the validation of tissue microarrays. *J Pathol* **208**(5), 607-614

Gorgoulis, V. G., Vassiliou, L. V., Karakaidos, P., Zacharatos, P., Kotsinas, A., Liloglou, T., Venere, M., Ditullio, R. A., Jr., Kastrinakis, N. G., Levy, B., Kletsas, D., Yoneta, A., Herlyn, M., Kittas, C., and Halazonetis, T. D. (2005) Activation of the DNA damage checkpoint and genomic instability in human precancerous lesions. *Nature* **434**(7035), 907-913

Grabsch, H., Dattani, M., Barker, L., Maughan, N., Maude, K., Hansen, O., Gabbert, H. E., Quirke, P., and Mueller, W. (2006) Expression of DNA double-strand break repair proteins ATM and BRCA1 predicts survival in colorectal cancer. *Clin Cancer Res* **12**(5), 1494-1500

Guarente, L. (1993) Synthetic enhancement in gene interaction: a genetic tool come of age. *Trends Genet* **9**(10), 362-366

Guha, C., Guha, U., Tribius, S., Alfieri, A., Casper, D., Chakravarty, P., Mellado, W., Pandita, T. K., and Vikram, B. (2000) Antisense ATM gene therapy: a strategy to increase the radiosensitivity of human tumors. *Gene Ther* **7**(10), 852-858

Guo, C. Y., D'Anna, J. A., Li, R., and Larner, J. M. (1999) The radiation-induced S-phase checkpoint is independent of CDKN1A. *Radiat Res* **151**(2), 125-132

Gupta, S. K., Guo, X., Durkin, S. S., Fryrear, K. F., Ward, M. D., and Semmes, O. J. (2007) Human T-cell leukemia virus type 1 Tax oncoprotein prevents DNA damage-induced chromatin egress of hyperphosphorylated Chk2. *J Biol Chem* **282**(40), 29431-29440

Haber, J. E. (2000) Recombination: a frank view of exchanges and vice versa. *Curr Opin Cell Biol* **12**(3), 286-292

Haince, J. F., Rouleau, M., Hendzel, M. J., Masson, J. Y., and Poirier, G. G. (2005) Targeting poly(ADP-ribosyl)ation: a promising approach in cancer therapy. *Trends Mol Med* **11**(10), 456-463

Ham, M. F., Takakuwa, T., Luo, W. J., Liu, A., Horii, A., and Aozasa, K. (2006) Impairment of double-strand breaks repair and aberrant splicing of ATM and MRE11 in leukemia-lymphoma cell lines with microsatellite instability. *Cancer Sci* **97**(3), 226-234

Harley, C. B., Futcher, A. B., and Greider, C. W. (1990) Telomeres shorten during ageing of human fibroblasts. *Nature* **345**(6274), 458-460

Hartwell, L. H., Szankasi, P., Roberts, C. J., Murray, A. W., and Friend, S. H. (1997) Integrating genetic approaches into the discovery of anticancer drugs. *Science* **278**(5340), 1064-1068

Hatakeyama, M., Brill, J. A., Fink, G. R., and Weinberg, R. A. (1994) Collaboration of G1 cyclins in the functional inactivation of the retinoblastoma protein. *Genes Dev* **8**(15), 1759-1771

Haupt, Y., Maya, R., Kazaz, A., and Oren, M. (1997) Mdm2 promotes the rapid degradation of p53. *Nature* **387**(6630), 296-299

Hayward, R. L., Macpherson, J. S., Cummings, J., Monia, B. P., Smyth, J. F., and Jodrell, D. I. (2003) Antisense Bcl-xl down-regulation switches the response to topoisomerase I inhibition from senescence to apoptosis in colorectal cancer cells, enhancing global cytotoxicity. *Clin Cancer Res* **9**(7), 2856-2865

Hayward, R. L., Schornagel, Q. C., Tente, R., Macpherson, J. S., Aird, R. E., Guichard, S., Habtemariam, A., Sadler, P., and Jodrell, D. I. (2005) Investigation of the role of Bax, p21/Waf1 and p53 as determinants of cellular responses in HCT116 colorectal cancer cells exposed to the novel cytotoxic ruthenium(II) organometallic agent, RM175. *Cancer Chemother Pharmacol* **55**(6), 577-583

Hefferin, M. L., and Tomkinson, A. E. (2005) Mechanism of DNA double-strand break repair by non-homologous end joining. *DNA Repair (Amst)* **4**(6), 639-648

Heffernan, T. P., Simpson, D. A., Frank, A. R., Heinloth, A. N., Paules, R. S., Cordeiro-Stone, M., and Kaufmann, W. K. (2002) An ATR- and Chk1-dependent S checkpoint inhibits replicon initiation following UVC-induced DNA damage. *Mol Cell Biol* **22**(24), 8552-8561

Heikkinen, K., Rapakko, K., Karppinen, S. M., Erkko, H., Nieminen, P., and Winqvist, R. (2005) Association of common ATM polymorphism with bilateral breast cancer. *Int J Cancer* **116**(1), 69-72

Helt, C. E., Cliby, W. A., Keng, P. C., Bambara, R. A., and O'Reilly, M. A. (2005) Ataxia telangiectasia mutated (ATM) and ATM and Rad3-related protein

exhibit selective target specificities in response to different forms of DNA damage. *J Biol Chem* **280**(2), 1186-1192

Hendriks, Y., Franken, P., Dierssen, J. W., De Leeuw, W., Wijnen, J., Dreef, E., Tops, C., Breuning, M., Brocker-Vriends, A., Vasen, H., Fodde, R., and Morreau, H. (2003) Conventional and tissue microarray immunohistochemical expression analysis of mismatch repair in hereditary colorectal tumors. *Am J Pathol* **162**(2), 469-477

Herbig, U., Jobling, W. A., Chen, B. P., Chen, D. J., and Sedivy, J. M. (2004) Telomere shortening triggers senescence of human cells through a pathway involving ATM, p53, and p21(CIP1), but not p16(INK4a). *Mol Cell* **14**(4), 501-513

Hernandez, S., Bessa, X., Bea, S., Hernandez, L., Nadal, A., Mallofre, C., Muntane, J., Castells, A., Fernandez, P. L., Cardesa, A., and Campo, E. (2001) Differential expression of cdc25 cell-cycle-activating phosphatases in human colorectal carcinoma. *Lab Invest* **81**(4), 465-473

Hickson, I., Zhao, Y., Richardson, C. J., Green, S. J., Martin, N. M., Orr, A. I., Reaper, P. M., Jackson, S. P., Curtin, N. J., and Smith, G. C. (2004) Identification and characterization of a novel and specific inhibitor of the ataxia-telangiectasia mutated kinase ATM. *Cancer Res* **64**(24), 9152-9159

Hill, R., Leidal, A. M., Madureira, P. A., Gillis, L. D., Cochrane, H. K., Waisman, D. M., Chiu, A., and Lee, P. W. (2008a) Hypersensitivity to chromium-induced DNA damage correlates with constitutive deregulation of upstream p53 kinases in p21-/- HCT116 colon cancer cells. *DNA Repair (Amst)* **7**(2), 239-252

Hill, R., Leidal, A. M., Madureira, P. A., Gillis, L. D., Waisman, D. M., Chiu, A., and Lee, P. W. (2008b) Chromium-mediated apoptosis: involvement of DNA-dependent protein kinase (DNA-PK) and differential induction of p53 target genes. *DNA Repair (Amst)* **7**(9), 1484-1499

Hirao, A., Kong, Y. Y., Matsuoka, S., Wakeham, A., Ruland, J., Yoshida, H., Liu, D., Elledge, S. J., and Mak, T. W. (2000) DNA damage-induced activation of p53 by the checkpoint kinase Chk2. *Science* **287**(5459), 1824-1827

Hoffmann, I., Draetta, G., and Karsenti, E. (1994) Activation of the phosphatase activity of human cdc25A by a cdk2-cyclin E dependent phosphorylation at the G1/S transition. *Embo J* **13**(18), 4302-4310

Holland, T. A., Elder, J., McCloud, J. M., Hall, C., Deakin, M., Fryer, A. A., Elder, J. B., and Hoban, P. R. (2001) Subcellular localisation of cyclin D1 protein in colorectal tumours is associated with p21(WAF1/CIP1) expression and correlates with patient survival. *Int J Cancer* **95**(5), 302-306

Hollstein, M., Sidransky, D., Vogelstein, B., and Harris, C. C. (1991) p53 mutations in human cancers. *Science* **253**(5015), 49-53

Hoos, A., Urist, M. J., Stojadinovic, A., Mastorides, S., Dudas, M. E., Leung, D. H., Kuo, D., Brennan, M. F., Lewis, J. J., and Cordon-Cardo, C. (2001) Validation of tissue microarrays for immunohistochemical profiling of cancer specimens using the example of human fibroblastic tumors. *Am J Pathol* **158**(4), 1245-1251

Houldsworth, J., and Lavin, M. F. (1980) Effect of ionizing radiation on DNA synthesis in ataxia telangiectasia cells. *Nucleic Acids Res* **8**(16), 3709-3720

Huang, T. T., Wuerzberger-Davis, S. M., Wu, Z. H., and Miyamoto, S. (2003) Sequential modification of NEMO/IKKgamma by SUMO-1 and ubiquitin mediates NF-kappaB activation by genotoxic stress. *Cell* **115**(5), 565-576

Huberman, J. A. (1981) New views of the biochemistry of eucaryotic DNA replication revealed by aphidicolin, an unusual inhibitor of DNA polymerase alpha. *Cell* **23**(3), 647-648

Ionov, Y., Peinado, M. A., Malkhosyan, S., Shibata, D., and Perucho, M. (1993) Ubiquitous somatic mutations in simple repeated sequences reveal a new mechanism for colonic carcinogenesis. *Nature* **363**(6429), 558-561

Iwaya, T., Yokobori, T., Nishida, N., Kogo, R., Sudo, T., Tanaka, F., Shibata, K., Sawada, G., Takahashi, Y., Ishibashi, M., Wakabayashi, G., Mori, M., and Mimori, K. (2012) Downregulation of miR-144 is associated with colorectal cancer progression via activation of mTOR signaling pathway. *Carcinogenesis* **33**(12), 2391-2397

Jaspers, N. G., Gatti, R. A., Baan, C., Linssen, P. C., and Bootsma, D. (1988) Genetic complementation analysis of ataxia telangiectasia and Nijmegen breakage syndrome: a survey of 50 patients. *Cytogenet Cell Genet* **49**(4), 259-263

Jazayeri, A., Falck, J., Lukas, C., Bartek, J., Smith, G. C., Lukas, J., and Jackson, S. P. (2006) ATM- and cell cycle-dependent regulation of ATR in response to DNA double-strand breaks. *Nat Cell Biol* **8**(1), 37-45

Jeggo, P. A., and Lobrich, M. (2005) Artemis links ATM to double strand break rejoining. *Cell Cycle* **4**(3), 359-362

Jiang, H., Reinhardt, H. C., Bartkova, J., Tommiska, J., Blomqvist, C., Nevanlinna, H., Bartek, J., Yaffe, M. B., and Hemann, M. T. (2009) The combined status of ATM and p53 link tumor development with therapeutic response. *Genes Dev* **23**(16), 1895-1909

Jin, J., Ang, X. L., Ye, X., Livingstone, M., and Harper, J. W. (2008) Differential roles for checkpoint kinases in DNA damage-dependent degradation of the Cdc25A protein phosphatase. *J Biol Chem* **283**(28), 19322-19328

Jin, J., Shirogane, T., Xu, L., Nalepa, G., Qin, J., Elledge, S. J., and Harper, J. W. (2003) SCFbeta-TRCP links Chk1 signaling to degradation of the Cdc25A protein phosphatase. *Genes Dev* **17**(24), 3062-3074

Jin, S., Tong, T., Fan, W., Fan, F., Antinore, M. J., Zhu, X., Mazzacurati, L., Li, X., Petrik, K. L., Rajasekaran, B., Wu, M., and Zhan, Q. (2002) GADD45-induced cell cycle G2-M arrest associates with altered subcellular distribution of cyclin B1 and is independent of p38 kinase activity. *Oncogene* **21**(57), 8696-8704

Jinno, S., Suto, K., Nagata, A., Igarashi, M., Kanaoka, Y., Nojima, H., and Okayama, H. (1994) Cdc25A is a novel phosphatase functioning early in the cell cycle. *Embo J* **13**(7), 1549-1556

Jiricny, J., and Nystrom-Lahti, M. (2000) Mismatch repair defects in cancer. *Curr Opin Genet Dev* **10**(2), 157-161

Johnson, R. D., and Jasin, M. (2001) Double-strand-break-induced homologous recombination in mammalian cells. *Biochem Soc Trans* **29**(Pt 2), 196-201

Kakarougkas, A., Ismail, A., Katsuki, Y., Freire, R., Shibata, A., and Jeggo, P. A. (2013) Co-operation of BRCA1 and POH1 relieves the barriers posed by 53BP1 and RAP80 to resection. *Nucleic Acids Res* **41**(22), 10298-10311

Kallioniemi, O. P., Wagner, U., Kononen, J., and Sauter, G. (2001) Tissue microarray technology for high-throughput molecular profiling of cancer. *Hum Mol Genet* **10**(7), 657-662

Kamb, A. (2003) Mutation load, functional overlap, and synthetic lethality in the evolution and treatment of cancer. *J Theor Biol* **223**(2), 205-213

Karin, M., and Ben-Neriah, Y. (2000) Phosphorylation meets ubiquitination: the control of NF-[kappa]B activity. *Annu Rev Immunol* **18**, 621-663

Kastan, M. B., and Bartek, J. (2004) Cell-cycle checkpoints and cancer. *Nature* **432**(7015), 316-323

Kastan, M. B., and Lim, D. S. (2000) The many substrates and functions of ATM. *Nat Rev Mol Cell Biol* **1**(3), 179-186

Kennedy, R. D., Chen, C. C., Stuckert, P., Archila, E. M., De la Vega, M. A., Moreau, L. A., Shimamura, A., and D'Andrea, A. D. (2007) Fanconi anemia pathway-deficient tumor cells are hypersensitive to inhibition of ataxia telangiectasia mutated. *J Clin Invest* **117**(5), 1440-1449

Kerr, J. F., Wyllie, A. H., and Currie, A. R. (1972) Apoptosis: a basic biological phenomenon with wide-ranging implications in tissue kinetics. *Br J Cancer* **26**(4), 239-257

Khanna, K. K., and Jackson, S. P. (2001) DNA double-strand breaks: signaling, repair and the cancer connection. *Nat Genet* **27**(3), 247-254

Kim, C. J., Lee, J. H., Song, J. W., Cho, Y. G., Kim, S. Y., Nam, S. W., Yoo, N. J., Park, W. S., and Lee, J. Y. (2007) Chk1 frameshift mutation in sporadic and hereditary non-polyposis colorectal cancers with microsatellite instability. *Eur J Surg Oncol* **33**(5), 580-585

Kirsch, I. R. (1994) V(D)J recombination and ataxia-telangiectasia: a review. *Int J Radiat Biol* **66**(6 Suppl), S97-108

Kitagawa, R., Bakkenist, C. J., McKinnon, P. J., and Kastan, M. B. (2004) Phosphorylation of SMC1 is a critical downstream event in the ATM-NBS1-BRCA1 pathway. *Genes Dev* **18**(12), 1423-1438

Knappskog, S., Chrisanthar, R., Lokkevik, E., Anker, G., Ostenstad, B., Lundgren, S., Risberg, T., Mjaaland, I., Leirvaag, B., Miletic, H., and Lonning, P. E. (2012) Low expression levels of ATM may substitute for CHEK2 /TP53 mutations predicting resistance towards anthracycline and mitomycin chemotherapy in breast cancer. *Breast Cancer Res* **14**(2), R47

Kolas, N. K., Chapman, J. R., Nakada, S., Ylanko, J., Chahwan, R., Sweeney, F. D., Panier, S., Mendez, M., Wildenhain, J., Thomson, T. M., Pelletier, L., Jackson, S. P., and Durocher, D. (2007) Orchestration of the DNA-damage response by the RNF8 ubiquitin ligase. *Science* **318**(5856), 1637-1640

Kononen, J., Bubendorf, L., Kallioniemi, A., Barlund, M., Schraml, P., Leighton, S., Torhorst, J., Mihatsch, M. J., Sauter, G., and Kallioniemi, O. P. (1998) Tissue microarrays for high-throughput molecular profiling of tumor specimens. *Nat Med* **4**(7), 844-847

Konstantinova, L. N., Fleischman, E. W., Knisch, V. I., Perevozchikov, A. G., and Kopnin, B. P. (1991) Karyotype peculiarities of human colorectal adenocarcinomas. *Hum Genet* **86**(5), 491-496

Kristjansdottir, K., and Rudolph, J. (2004) Cdc25 phosphatases and cancer. *Chem Biol* **11**(8), 1043-1051

Kubbutat, M. H., Jones, S. N., and Vousden, K. H. (1997) Regulation of p53 stability by Mdm2. *Nature* **387**(6630), 299-303

Kuzminov, A. (2001a) DNA replication meets genetic exchange: chromosomal damage and its repair by homologous recombination. *Proc Natl Acad Sci U S A* **98**(15), 8461-8468

Kuzminov, A. (2001b) Single-strand interruptions in replicating chromosomes cause double-strand breaks. *Proc Natl Acad Sci U S A* **98**(15), 8241-8246

LaBaer, J., Garrett, M. D., Stevenson, L. F., Slingerland, J. M., Sandhu, C., Chou, H. S., Fattaey, A., and Harlow, E. (1997) New functional activities for the p21 family of CDK inhibitors. *Genes Dev* **11**(7), 847-862

Lane, D. P., and Crawford, L. V. (1979) T antigen is bound to a host protein in SV40-transformed cells. *Nature* **278**(5701), 261-263

Lavin, M. F. (2004) The Mre11 complex and ATM: a two-way functional interaction in recognising and signaling DNA double strand breaks. *DNA Repair (Amst)* **3**(11), 1515-1520

LeBron, C., Chen, L., Gilkes, D. M., and Chen, J. (2006) Regulation of MDMX nuclear import and degradation by Chk2 and 14-3-3. *Embo J* **25**(6), 1196-1206

Lee, J. H., and Paull, T. T. (2004) Direct activation of the ATM protein kinase by the Mre11/Rad50/Nbs1 complex. *Science* **304**(5667), 93-96

Lee, J. H., and Paull, T. T. (2005) ATM activation by DNA double-strand breaks through the Mre11-Rad50-Nbs1 complex. *Science* **308**(5721), 551-554

Lee, J. H., and Paull, T. T. (2007) Activation and regulation of ATM kinase activity in response to DNA double-strand breaks. *Oncogene* **26**(56), 7741-7748

Lee, S. B., Kim, S. H., Bell, D. W., Wahrer, D. C., Schiripo, T. A., Jorczak, M. M., Sgroi, D. C., Garber, J. E., Li, F. P., Nichols, K. E., Varley, J. M., Godwin, A. K., Shannon, K. M., Harlow, E., and Haber, D. A. (2001) Destabilization of CHK2 by a missense mutation associated with Li-Fraumeni Syndrome. *Cancer Res* **61**(22), 8062-8067

Lempiainen, H., and Halazonetis, T. D. (2009) Emerging common themes in regulation of PIKKs and PI3Ks. *Embo J* **28**(20), 3067-3073

Lengauer, C., Kinzler, K. W., and Vogelstein, B. (1998) Genetic instabilities in human cancers. *Nature* **396**(6712), 643-649

Levack, P. A., Mullen, P., Anderson, T. J., Miller, W. R., and Forrest, A. P. (1987) DNA analysis of breast tumour fine needle aspirates using flow cytometry. *Br J Cancer* **56**(5), 643-646

Lewis, K. A., Bakkum-Gamez, J., Loewen, R., French, A. J., Thibodeau, S. N., and Cliby, W. A. (2007) Mutations in the ataxia telangiectasia and rad3-related-checkpoint kinase 1 DNA damage response axis in colon cancers. *Genes Chromosomes Cancer* **46**(12), 1061-1068

Lewis, K. A., Mullany, S., Thomas, B., Chien, J., Loewen, R., Shridhar, V., and Cliby, W. A. (2005) Heterozygous ATR mutations in mismatch repair-deficient cancer cells have functional significance. *Cancer Res* **65**(16), 7091-7095

Li, H. R., Shagisultanova, E. I., Yamashita, K., Piao, Z., Perucho, M., and Malkhosyan, S. R. (2004) Hypersensitivity of tumor cell lines with microsatellite instability to DNA double strand break producing chemotherapeutic agent bleomycin. *Cancer Res* **64**(14), 4760-4767

Li, J., and Stern, D. F. (2005) DNA damage regulates Chk2 association with chromatin. *J Biol Chem* **280**(45), 37948-37956

Li, L. S., Kim, N. G., Kim, S. H., Park, C., Kim, H., Kang, H. J., Koh, K. H., Kim, S. N., Kim, W. H., Kim, N. K., and Kim, H. (2003) Chromosomal imbalances in the colorectal carcinomas with microsatellite instability. *Am J Pathol* **163**(4), 1429-1436

Li, L. S., Morales, J. C., Veigl, M., Sedwick, D., Greer, S., Meyers, M., Wagner, M., Fishel, R., and Boothman, D. A. (2009) DNA mismatch repair (MMR)-dependent 5-fluorouracil cytotoxicity and the potential for new therapeutic targets. *Br J Pharmacol* **158**(3), 679-692

Li, W., Jian, W., Xiaoping, X., Yingfeng, L., Tao, X., and Xiaoyan, X. (2006) Enhanced radiation-mediated cell killing of human cervical cancer cells by small interference RNA silencing of ataxia telangiectasia-mutated protein. *Int J Gynecol Cancer* **16**(4), 1620-1630

Lim, D. S., Kim, S. T., Xu, B., Maser, R. S., Lin, J., Petrini, J. H., and Kastan, M. B. (2000) ATM phosphorylates p95/nbs1 in an S-phase checkpoint pathway. *Nature* **404**(6778), 613-617

Lindblom, A., Tannergard, P., Werelius, B., and Nordenskjold, M. (1993) Genetic mapping of a second locus predisposing to hereditary non-polyposis colon cancer. *Nat Genet* **5**(3), 279-282

Lisby, M., and Rothstein, R. (2005) Localization of checkpoint and repair proteins in eukaryotes. *Biochimie* **87**(7), 579-589

Liu, Y., and Bodmer, W. F. (2006) Analysis of P53 mutations and their expression in 56 colorectal cancer cell lines. *Proc Natl Acad Sci U S A* **103**(4), 976-981

Loffler, H., Syljuasen, R. G., Bartkova, J., Worm, J., Lukas, J., and Bartek, J. (2003) Distinct modes of deregulation of the proto-oncogenic Cdc25A phosphatase in human breast cancer cell lines. *Oncogene* **22**(50), 8063-8071

Lopez-Girona, A., Furnari, B., Mondesert, O., and Russell, P. (1999) Nuclear localization of Cdc25 is regulated by DNA damage and a 14-3-3 protein. *Nature* **397**(6715), 172-175

Lossaint, G., Besnard, E., Fisher, D., Piette, J., and Dulic, V. (2011) Chk1 is dispensable for G2 arrest in response to sustained DNA damage when the ATM/p53/p21 pathway is functional. *Oncogene* **30**(41), 4261-4274

Lu, Z., and Hunter, T. (2010) Ubiquitylation and proteasomal degradation of the p21(Cip1), p27(Kip1) and p57(Kip2) CDK inhibitors. *Cell Cycle* **9**(12), 2342-2352

Lukas, C., Bartkova, J., Latella, L., Falck, J., Mailand, N., Schroeder, T., Sehested, M., Lukas, J., and Bartek, J. (2001) DNA damage-activated kinase Chk2 is independent of proliferation or differentiation yet correlates with tissue biology. *Cancer Res* **61**(13), 4990-4993

Lukas, C., Melander, F., Stucki, M., Falck, J., Bekker-Jensen, S., Goldberg, M., Lerenthal, Y., Jackson, S. P., Bartek, J., and Lukas, J. (2004a) Mdc1 couples DNA double-strand break recognition by Nbs1 with its H2AX-dependent chromatin retention. *Embo J* **23**(13), 2674-2683

Lukas, J., Lukas, C., and Bartek, J. (2011) More than just a focus: The chromatin response to DNA damage and its role in genome integrity maintenance. *Nat Cell Biol* **13**(10), 1161-1169

Lukas, J., Lukas, C., and Bartek, J. (2004b) Mammalian cell cycle checkpoints: signalling pathways and their organization in space and time. *DNA Repair (Amst)* **3**(8-9), 997-1007

Lundberg, A. S., and Weinberg, R. A. (1998) Functional inactivation of the retinoblastoma protein requires sequential modification by at least two distinct cyclin-cdk complexes. *Mol Cell Biol* **18**(2), 753-761

Luo, G., Yao, M. S., Bender, C. F., Mills, M., Bladl, A. R., Bradley, A., and Petrini, J. H. (1999) Disruption of mRad50 causes embryonic stem cell lethality, abnormal embryonic development, and sensitivity to ionizing radiation. *Proc Natl Acad Sci U S A* **96**(13), 7376-7381

Luo, Y., Lin, F. T., and Lin, W. C. (2004) ATM-mediated stabilization of hMutL DNA mismatch repair proteins augments p53 activation during DNA damage. *Mol Cell Biol* **24**(14), 6430-6444

Lynch, H. T., Smyrk, T. C., Watson, P., Lanspa, S. J., Lynch, J. F., Lynch, P. M., Cavalieri, R. J., and Boland, C. R. (1993) Genetics, natural history, tumor spectrum, and pathology of hereditary nonpolyposis colorectal cancer: an updated review. *Gastroenterology* **104**(5), 1535-1549

Macleod, K. F., Sherry, N., Hannon, G., Beach, D., Tokino, T., Kinzler, K., Vogelstein, B., and Jacks, T. (1995) p53-dependent and independent expression of p21 during cell growth, differentiation, and DNA damage. *Genes Dev* **9**(8), 935-944

Madhusudan, S., and Hickson, I. D. (2005) DNA repair inhibition: a selective tumour targeting strategy. *Trends Mol Med* **11**(11), 503-511

Madhusudan, S., and Middleton, M. R. (2005) The emerging role of DNA repair proteins as predictive, prognostic and therapeutic targets in cancer. *Cancer Treat Rev* **31**(8), 603-617

Mailand, N., Bekker-Jensen, S., Faustrup, H., Melander, F., Bartek, J., Lukas, C., and Lukas, J. (2007) RNF8 ubiquitylates histones at DNA double-strand breaks and promotes assembly of repair proteins. *Cell* **131**(5), 887-900

Mailand, N., Falck, J., Lukas, C., Syljuasen, R. G., Welcker, M., Bartek, J., and Lukas, J. (2000) Rapid destruction of human Cdc25A in response to DNA damage. *Science* **288**(5470), 1425-1429

Mailand, N., Podtelejnikov, A. V., Groth, A., Mann, M., Bartek, J., and Lukas, J. (2002) Regulation of G(2)/M events by Cdc25A through phosphorylation-dependent modulation of its stability. *Embo J* **21**(21), 5911-5920

Malumbres, M., and Barbacid, M. (2005) Mammalian cyclin-dependent kinases. *Trends Biochem Sci* **30**(11), 630-641

Mandell, J. W. (2003) Phosphorylation state-specific antibodies: applications in investigative and diagnostic pathology. *Am J Pathol* **163**(5), 1687-1698

Markowitz, S. (2000) DNA repair defects inactivate tumor suppressor genes and induce hereditary and sporadic colon cancers. *J Clin Oncol* **18**(21 Suppl), 75S-80S

Martin, N. M. (2001) DNA repair inhibition and cancer therapy. *J Photochem Photobiol B* **63**(1-3), 162-170

Matsuoka, S., Ballif, B. A., Smogorzewska, A., McDonald, E. R., 3rd, Hurov, K. E., Luo, J., Bakalarski, C. E., Zhao, Z., Solimini, N., Lerenthal, Y., Shiloh, Y., Gygi, S. P., and Elledge, S. J. (2007) ATM and ATR substrate analysis

reveals extensive protein networks responsive to DNA damage. *Science* **316**(5828), 1160-1166

Matsuoka, S., Huang, M., and Elledge, S. J. (1998) Linkage of ATM to cell cycle regulation by the Chk2 protein kinase. *Science* **282**(5395), 1893-1897

McCabe, N., Turner, N. C., Lord, C. J., Kluzek, K., Bialkowska, A., Swift, S., Giavara, S., O'Connor M, J., Tutt, A. N., Zdzienicka, M. Z., Smith, G. C., and Ashworth, A. (2006) Deficiency in the Repair of DNA Damage by Homologous Recombination and Sensitivity to Poly(ADP-Ribose) Polymerase Inhibition. *Cancer Res* **66**(16), 8109-8115

McCarty, K. S., Jr., Szabo, E., Flowers, J. L., Cox, E. B., Leight, G. S., Miller, L., Konrath, J., Soper, J. T., Budwit, D. A., Creasman, W. T., and et al. (1986) Use of a monoclonal anti-estrogen receptor antibody in the immunohistochemical evaluation of human tumors. *Cancer Res* **46**(8 Suppl), 4244s-4248s

Meyn, M. S. (1995) Ataxia-telangiectasia and cellular responses to DNA damage. *Cancer Res* **55**(24), 5991-6001

Midgley, C. A., and Lane, D. P. (1997) p53 protein stability in tumour cells is not determined by mutation but is dependent on Mdm2 binding. *Oncogene* **15**(10), 1179-1189

Miquel, C., Jacob, S., Grandjouan, S., Aime, A., Viguier, J., Sabourin, J. C., Sarasin, A., Duval, A., and Praz, F. (2007) Frequent alteration of DNA damage signalling and repair pathways in human colorectal cancers with microsatellite instability. *Oncogene* **26**(40), 5919-5926

Misale, S., Yaeger, R., Hobor, S., Scala, E., Janakiraman, M., Liska, D., Valtorta, E., Schiavo, R., Buscarino, M., Siravegna, G., Bencardino, K., Cercek, A., Chen, C. T., Veronese, S., Zanon, C., Sartore-Bianchi, A., Gambacorta, M., Gallicchio, M., Vakiani, E., Boscaro, V., Medico, E., Weiser, M., Siena, S., Di Nicolantonio, F., Solit, D., and Bardelli, A. (2012) Emergence of KRAS mutations and acquired resistance to anti-EGFR therapy in colorectal cancer. *Nature* **486**(7404), 532-536

Mittnacht, S., Lees, J. A., Desai, D., Harlow, E., Morgan, D. O., and Weinberg, R. A. (1994) Distinct sub-populations of the retinoblastoma protein show a distinct pattern of phosphorylation. *Embo J* **13**(1), 118-127

Miyaki, M., Konishi, M., Tanaka, K., Kikuchi-Yanoshita, R., Muraoka, M., Yasuno, M., Igari, T., Koike, M., Chiba, M., and Mori, T. (1997) Germline mutation of MSH6 as the cause of hereditary nonpolyposis colorectal cancer. *Nat Genet* **17**(3), 271-272

Molitor, J. A., Walker, W. H., Doerre, S., Ballard, D. W., and Greene, W. C. (1990) NF-kappa B: a family of inducible and differentially expressed enhancer-binding proteins in human T cells. *Proc Natl Acad Sci U S A* **87**(24), 10028-10032

Momand, J., Wu, H. H., and Dasgupta, G. (2000) MDM2--master regulator of the p53 tumor suppressor protein. *Gene* **242**(1-2), 15-29

Mouradov, D., Domingo, E., Gibbs, P., Jorissen, R. N., Li, S., Soo, P. Y., Lipton, L., Desai, J., Danielsen, H. E., Oukrif, D., Novelli, M., Yau, C., Holmes, C. C., Jones, I. T., McLaughlin, S., Molloy, P., Hawkins, N. J., Ward, R., Midgely, R., Kerr, D., Tomlinson, I. P., and Sieber, O. M. (2010) Survival in stage II/III colorectal cancer is independently predicted by chromosomal and

microsatellite instability, but not by specific driver mutations. *Am J Gastroenterol* **108**(11), 1785-1793

Mukhopadhyay, U. K., Senderowicz, A. M., and Ferbeyre, G. (2005) RNA silencing of checkpoint regulators sensitizes p53-defective prostate cancer cells to chemotherapy while sparing normal cells. *Cancer Res* **65**(7), 2872-2881

Myers, J. S., and Cortez, D. (2006) Rapid activation of ATR by ionizing radiation requires ATM and Mre11. *J Biol Chem* **281**(14), 9346-9350

Nagasaki, T., Hara, M., Nakanishi, H., Takahashi, H., Sato, M., and Takeyama, H. (2014) Interleukin-6 released by colon cancer-associated fibroblasts is critical for tumour angiogenesis: anti-interleukin-6 receptor antibody suppressed angiogenesis and inhibited tumour-stroma interaction. *Br J Cancer* **110**(2), 469-478

Nghiem, P., Park, P. K., Kim, Y., Vaziri, C., and Schreiber, S. L. (2001) ATR inhibition selectively sensitizes G1 checkpoint-deficient cells to lethal premature chromatin condensation. *Proc Natl Acad Sci U S A* **98**(16), 9092-9097

NICECG131. (2011) Clinical Guideline: Colorectal cancer: the diagnosis and management of colorectal cancer. *NICE* **CG131**, 1-186

NICETA242. (2012) Cetuximab, bevacizumab and panitumumab for the treatment of metastatic colorectal cancer after first-line chemotherapy

Nicolaides, N. C., Papadopoulos, N., Liu, B., Wei, Y. F., Carter, K. C., Ruben, S. M., Rosen, C. A., Haseltine, W. A., Fleischmann, R. D., Fraser, C. M., and et al. (1994) Mutations of two PMS homologues in hereditary nonpolyposis colon cancer. *Nature* **371**(6492), 75-80

Niida, H., and Nakanishi, M. (2006) DNA damage checkpoints in mammals. *Mutagenesis* **21**(1), 3-9

Nishida, N., Nagahara, M., Sato, T., Mimori, K., Sudo, T., Tanaka, F., Shibata, K., Ishii, H., Sugihara, K., Doki, Y., and Mori, M. (2012) Microarray analysis of colorectal cancer stromal tissue reveals upregulation of two oncogenic miRNA clusters. *Clin Cancer Res* **18**(11), 3054-3070

Norbury, C. J., and Hickson, I. D. (2001) Cellular responses to DNA damage. *Annu Rev Pharmacol Toxicol* **41**, 367-401

Noske, A., Lipka, S., Budczies, J., Muller, K., Loddenkemper, C., Buhr, H. J., and Kruschewski, M. (2009) Combination of p53 expression and p21 loss has an independent prognostic impact on sporadic colorectal cancer. *Oncol Rep* **22**(1), 3-9

Nuciforo, P. G., Luise, C., Capra, M., Pelosi, G., and d'Adda di Fagagna, F. (2007) Complex engagement of DNA damage response pathways in human cancer and in lung tumor progression. *Carcinogenesis* **28**(10), 2082-2088

Nyiraneza, C., Jouret-Mourin, A., Kartheuser, A., Camby, P., Plomteux, O., Detry, R., Dahan, K., and Sempoux, C. (2011) Distinctive patterns of p53 protein expression and microsatellite instability in human colorectal cancer. *Hum Pathol* **42**(12), 1897-1910

O'Connor, P. M., Jackman, J., Bae, I., Myers, T. G., Fan, S., Mutoh, M., Scudiero, D. A., Monks, A., Sausville, E. A., Weinstein, J. N., Friend, S., Fornace, A. J., Jr., and Kohn, K. W. (1997) Characterization of the p53 tumor suppressor pathway in cell lines of the National Cancer Institute anticancer drug screen

and correlations with the growth-inhibitory potency of 123 anticancer agents. *Cancer Res* **57**(19), 4285-4300

Ogino, S., Nosho, K., Shima, K., Baba, Y., Irahara, N., Kirkner, G. J., Hazra, A., De Vivo, I., Giovannucci, E. L., Meyerhardt, J. A., and Fuchs, C. S. (2009) p21 expression in colon cancer and modifying effects of patient age and body mass index on prognosis. *Cancer Epidemiol Biomarkers Prev* **18**(9), 2513-2521

Ohtsubo, M., Theodoras, A. M., Schumacher, J., Roberts, J. M., and Pagano, M. (1995) Human cyclin E, a nuclear protein essential for the G1-to-S phase transition. *Mol Cell Biol* **15**(5), 2612-2624

Oka, K., Tanaka, T., Enoki, T., Yoshimura, K., Ohshima, M., Kubo, M., Murakami, T., Gondou, T., Minami, Y., Takemoto, Y., Harada, E., Tsushimi, T., Li, T. S., Traganos, F., Darzynkiewicz, Z., and Hamano, K. (2010) DNA damage signaling is activated during cancer progression in human colorectal carcinoma. *Cancer Biol Ther* **9**(3), 246-252

Osborn, A. J., Elledge, S. J., and Zou, L. (2002) Checking on the fork: the DNA-replication stress-response pathway. *Trends Cell Biol* **12**(11), 509-516

Ottini, L., Falchetti, M., Saieva, C., De Marco, M., Masala, G., Zanna, I., Paglierani, M., Giannini, G., Gulino, A., Nesi, G., Mariani Costantini, R., and Palli, D. (2004) MRE11 expression is impaired in gastric cancer with microsatellite instability. *Carcinogenesis* **25**(12), 2337-2343

Painter, R. B., and Young, B. R. (1980) Radiosensitivity in ataxia-telangiectasia: a new explanation. *Proc Natl Acad Sci U S A* **77**(12), 7315-7317

Pang, L. Y., Scott, M., Hayward, R. L., Mohammed, H., Whitelaw, C. B., Smith, G. C., and Hupp, T. R. (2011) p21(WAF1) is component of a positive feedback loop that maintains the p53 transcriptional program. *Cell Cycle* **10**(6), 932-950

Parsels, L. A., Parsels, J. D., Tai, D. C., Coughlin, D. J., and Maybaum, J. (2004) 5-fluoro-2'-deoxyuridine-induced cdc25A accumulation correlates with premature mitotic entry and clonogenic death in human colon cancer cells. *Cancer Res* **64**(18), 6588-6594

Passos, J. F., Nelson, G., Wang, C., Richter, T., Simillion, C., Proctor, C. J., Miwa, S., Olijslagers, S., Hallinan, J., Wipat, A., Saretzki, G., Rudolph, K. L., Kirkwood, T. B., and von Zglinicki, T. (2010) Feedback between p21 and reactive oxygen production is necessary for cell senescence. *Mol Syst Biol* **6**, 347

Petrini, J. H. (2000) The Mre11 complex and ATM: collaborating to navigate S phase. *Curr Opin Cell Biol* **12**(3), 293-296

Pietenpol, J. A., Tokino, T., Thiagalingam, S., el-Deiry, W. S., Kinzler, K. W., and Vogelstein, B. (1994) Sequence-specific transcriptional activation is essential for growth suppression by p53. *Proc Natl Acad Sci U S A* **91**(6), 1998-2002

Piret, B., Schoonbroodt, S., and Piette, J. (1999) The ATM protein is required for sustained activation of NF-kappaB following DNA damage. *Oncogene* **18**(13), 2261-2271

Pommier, Y., Leo, E., Zhang, H., and Marchand, C. DNA topoisomerases and their poisoning by anticancer and antibacterial drugs. *Chem Biol* **17**(5), 421-433

Ponz de Leon, M., Benatti, P., Percesepe, A., Rossi, G., Viel, A., Santarosa, M., Pedroni, M., and Roncucci, L. (1999) Clinical and molecular diagnosis of

hereditary non-polyposis colorectal cancer: problems and pitfalls in an extended pedigree. *Ital J Gastroenterol Hepatol* **31**(6), 476-480

Rasio, D., Negrini, M., Manenti, G., Dragani, T. A., and Croce, C. M. (1995) Loss of heterozygosity at chromosome 11q in lung adenocarcinoma: identification of three independent regions. *Cancer Res* **55**(18), 3988-3991

Raynaud, C. M., Jang, S. J., Nuciforo, P., Lantuejoul, S., Brambilla, E., Mounier, N., Olaussen, K. A., Andre, F., Morat, L., Sabatier, L., and Soria, J. C. (2008a) Telomere shortening is correlated with the DNA damage response and telomeric protein down-regulation in colorectal preneoplastic lesions. *Ann Oncol* **19**(11), 1875-1881

Raynaud, C. M., Sabatier, L., Philipot, O., Olaussen, K. A., and Soria, J. C. (2008b) Telomere length, telomeric proteins and genomic instability during the multistep carcinogenic process. *Crit Rev Oncol Hematol* **66**(2), 99-117

Reaper, P. M., Griffiths, M. R., Long, J. M., Charrier, J. D., Maccormick, S., Charlton, P. A., Golec, J. M., and Pollard, J. R. (2011) Selective killing of ATM- or p53-deficient cancer cells through inhibition of ATR. *Nat Chem Biol* **7**(7), 428-430

Renwick, A., Thompson, D., Seal, S., Kelly, P., Chagtai, T., Ahmed, M., North, B., Jayatilake, H., Barfoot, R., Spanova, K., McGuffog, L., Evans, D. G., Eccles, D., Easton, D. F., Stratton, M. R., and Rahman, N. (2006) ATM mutations that cause ataxia-telangiectasia are breast cancer susceptibility alleles. *Nat Genet* **38**(8), 873-875

Ribic, C. M., Sargent, D. J., Moore, M. J., Thibodeau, S. N., French, A. J., Goldberg, R. M., Hamilton, S. R., Laurent-Puig, P., Gryfe, R., Shepherd, L. E., Tu, D., Redston, M., and Gallinger, S. (2003) Tumor microsatellite-instability status as a predictor of benefit from fluorouracil-based adjuvant chemotherapy for colon cancer. *N Engl J Med* **349**(3), 247-257

Ricciardiello, L., Ceccarelli, C., Angiolini, G., Pariali, M., Chieco, P., Paterini, P., Biasco, G., Martinelli, G. N., Roda, E., and Bazzoli, F. (2005) High thymidylate synthase expression in colorectal cancer with microsatellite instability: implications for chemotherapeutic strategies. *Clin Cancer Res* **11**(11), 4234-4240

Rich, T., Allen, R. L., and Wyllie, A. H. (2000) Defying death after DNA damage. *Nature* **407**(6805), 777-783

Richardson, C., and Jasin, M. (2000) Frequent chromosomal translocations induced by DNA double-strand breaks. *Nature* **405**(6787), 697-700

Rimm, D. L., Camp, R. L., Charette, L. A., Costa, J., Olsen, D. A., and Reiss, M. (2001a) Tissue microarray: a new technology for amplification of tissue resources. *Cancer J* **7**(1), 24-31

Rimm, D. L., Camp, R. L., Charette, L. A., Olsen, D. A., and Provost, E. (2001b) Amplification of tissue by construction of tissue microarrays. *Exp Mol Pathol* **70**(3), 255-264

Rochette, P. J., Bastien, N., Lavoie, J., Guerin, S. L., and Drouin, R. (2005) SW480, a p53 double-mutant cell line retains proficiency for some p53 functions. *J Mol Biol* **352**(1), 44-57

Roos, W. P., and Kaina, B. (2006) DNA damage-induced cell death by apoptosis. *Trends Mol Med* **12**(9), 440-450

Roos, W. P., and Kaina, B. (2013) DNA damage-induced cell death: from specific DNA lesions to the DNA damage response and apoptosis. *Cancer Lett* **332**(2), 237-248

Rosner, M., Schipany, K., and Hengstschlager, M. (2013) Merging high-quality biochemical fractionation with a refined flow cytometry approach to monitor nucleocytoplasmic protein expression throughout the unperturbed mammalian cell cycle. *Nat Protoc* **8**(3), 602-626

Russell, P. (1998) Checkpoints on the road to mitosis. *Trends Biochem Sci* **23**(10), 399-402

Russell, P., and Nurse, P. (1986) cdc25+ functions as an inducer in the mitotic control of fission yeast. *Cell* **45**(1), 145-153

Sancar, A., Lindsey-Boltz, L. A., Unsal-Kacmaz, K., and Linn, S. (2004) Molecular mechanisms of mammalian DNA repair and the DNA damage checkpoints. *Annu Rev Biochem* **73**, 39-85

Sanchez, Y., Wong, C., Thoma, R. S., Richman, R., Wu, Z., Piwnica-Worms, H., and Elledge, S. J. (1997) Conservation of the Chk1 checkpoint pathway in mammals: linkage of DNA damage to Cdk regulation through Cdc25. *Science* **277**(5331), 1497-1501

Saretzki, G. (2010) Cellular senescence in the development and treatment of cancer. *Curr Pharm Des* **16**(1), 79-100

Sarkaria, J. N., Busby, E. C., Tibbetts, R. S., Roos, P., Taya, Y., Karnitz, L. M., and Abraham, R. T. (1999) Inhibition of ATM and ATR kinase activities by the radiosensitizing agent, caffeine. *Cancer Res* **59**(17), 4375-4382

Sarkaria, J. N., Tibbetts, R. S., Busby, E. C., Kennedy, A. P., Hill, D. E., and Abraham, R. T. (1998) Inhibition of phosphoinositide 3-kinase related kinases by the radiosensitizing agent wortmannin. *Cancer Res* **58**(19), 4375-4382

Savitsky, K., Bar-Shira, A., Gilad, S., Rotman, G., Ziv, Y., Vanagaite, L., Tagle, D. A., Smith, S., Uziel, T., Sfez, S., Ashkenazi, M., Pecker, I., Frydman, M., Harnik, R., Patanjali, S. R., Simmons, A., Clines, G. A., Sartiel, A., Gatti, R. A., Chessa, L., Sanal, O., Lavin, M. F., Jaspers, N. G., Taylor, A. M., Arlett, C. F., Miki, T., Weissman, S. M., Lovett, M., Collins, F. S., and Shiloh, Y. (1995) A single ataxia telangiectasia gene with a product similar to PI-3 kinase. *Science* **268**(5218), 1749-1753

Schmitt, E., Paquet, C., Beauchemin, M., and Bertrand, R. (2007) DNA-damage response network at the crossroads of cell-cycle checkpoints, cellular senescence and apoptosis. *J Zhejiang Univ Sci B* **8**(6), 377-397

Schultz, L. B., Chehab, N. H., Malikzay, A., and Halazonetis, T. D. (2000) p53 binding protein 1 (53BP1) is an early participant in the cellular response to DNA double-strand breaks. *J Cell Biol* **151**(7), 1381-1390

Sherr, C. J., and Roberts, J. M. (1995) Inhibitors of mammalian G1 cyclin-dependent kinases. *Genes Dev* **9**(10), 1149-1163

Shieh, S. Y., Ahn, J., Tamai, K., Taya, Y., and Prives, C. (2000) The human homologs of checkpoint kinases Chk1 and Cds1 (Chk2) phosphorylate p53 at multiple DNA damage-inducible sites. *Genes Dev* **14**(3), 289-300

Shieh, S. Y., Ikeda, M., Taya, Y., and Prives, C. (1997) DNA damage-induced phosphorylation of p53 alleviates inhibition by MDM2. *Cell* **91**(3), 325-334

Shiloh, Y. (2001) ATM and ATR: networking cellular responses to DNA damage. *Curr Opin Genet Dev* **11**(1), 71-77

Shiloh, Y. (2006) The ATM-mediated DNA-damage response: taking shape. *Trends Biochem Sci* **31**(7), 402-410

Shiloh, Y. (2003) ATM and related protein kinases: safeguarding genome integrity. *Nat Rev Cancer* **3**(3), 155-168

Skehan, P., Storeng, R., Scudiero, D., Monks, A., McMahon, J., Vistica, D., Warren, J. T., Bokesch, H., Kenney, S., and Boyd, M. R. (1990) New colorimetric cytotoxicity assay for anticancer-drug screening. *J Natl Cancer Inst* **82**(13), 1107-1112

Sorensen, C. S., Syljuasen, R. G., Falck, J., Schroeder, T., Ronnstrand, L., Khanna, K. K., Zhou, B. B., Bartek, J., and Lukas, J. (2003) Chk1 regulates the S phase checkpoint by coupling the physiological turnover and ionizing radiation-induced accelerated proteolysis of Cdc25A. *Cancer Cell* **3**(3), 247-258

Stewart, G. S., Maser, R. S., Stankovic, T., Bressan, D. A., Kaplan, M. I., Jaspers, N. G., Raams, A., Byrd, P. J., Petrini, J. H., and Taylor, A. M. (1999) The DNA double-strand break repair gene hMRE11 is mutated in individuals with an ataxia-telangiectasia-like disorder. *Cell* **99**(6), 577-587

Stolfi, C., Fina, D., Caruso, R., Caprioli, F., Fantini, M. C., Rizzo, A., Sarra, M., Pallone, F., and Monteleone, G. (2008) Mesalazine negatively regulates CDC25A protein expression and promotes accumulation of colon cancer cells in S phase. *Carcinogenesis* **29**(6), 1258-1266

Stucki, M., and Jackson, S. P. (2006) gammaH2AX and MDC1: anchoring the DNA-damage-response machinery to broken chromosomes. *DNA Repair (Amst)* **5**(5), 534-543

Sugai, T., Habano, W., Uesugi, N., Jiao, Y. F., Nakamura, S. I., Yoshida, T., and Higuchi, T. (2001) Frequent allelic imbalance at the ATM locus in DNA multiploid colorectal carcinomas. *Oncogene* **20**(42), 6095-6101

Swift, M., Morrell, D., Massey, R. B., and Chase, C. L. (1991) Incidence of cancer in 161 families affected by ataxia-telangiectasia. *N Engl J Med* **325**(26), 1831-1836

Takata, M., Sasaki, M. S., Sonoda, E., Morrison, C., Hashimoto, M., Utsumi, H., Yamaguchi-Iwai, Y., Shinohara, A., and Takeda, S. (1998) Homologous recombination and non-homologous end-joining pathways of DNA double-strand break repair have overlapping roles in the maintenance of chromosomal integrity in vertebrate cells. *Embo J* **17**(18), 5497-5508

Takemasa, I., Yamamoto, H., Sekimoto, M., Ohue, M., Noura, S., Miyake, Y., Matsumoto, T., Aihara, T., Tomita, N., Tamaki, Y., Sakita, I., Kikkawa, N., Matsuura, N., Shiozaki, H., and Monden, M. (2000) Overexpression of CDC25B phosphatase as a novel marker of poor prognosis of human colorectal carcinoma. *Cancer Res* **60**(11), 3043-3050

Takemura, H., Rao, V. A., Sordet, O., Furuta, T., Miao, Z. H., Meng, L., Zhang, H., and Pommier, Y. (2006) Defective Mre11-dependent activation of Chk2 by ataxia telangiectasia mutated in colorectal carcinoma cells in response to replication-dependent DNA double strand breaks. *J Biol Chem* **281**(41), 30814-30823

Tauchi, H., Matsuura, S., Kobayashi, J., Sakamoto, S., and Komatsu, K. (2002) Nijmegen breakage syndrome gene, NBS1, and molecular links to factors for genome stability. *Oncogene* **21**(58), 8967-8980

Thibodeau, S. N., Bren, G., and Schaid, D. (1993) Microsatellite instability in cancer of the proximal colon. *Science* **260**(5109), 816-819

Thibodeau, S. N., French, A. J., Cunningham, J. M., Tester, D., Burgart, L. J., Roche, P. C., McDonnell, S. K., Schaid, D. J., Vockley, C. W., Michels, V. V., Farr, G. H., Jr., and O'Connell, M. J. (1998) Microsatellite instability in colorectal cancer: different mutator phenotypes and the principal involvement of hMLH1. *Cancer Res* **58**(8), 1713-1718

Thibodeau, S. N., French, A. J., Roche, P. C., Cunningham, J. M., Tester, D. J., Lindor, N. M., Moslein, G., Baker, S. M., Liskay, R. M., Burgart, L. J., Honchel, R., and Halling, K. C. (1996) Altered expression of hMSH2 and hMLH1 in tumors with microsatellite instability and genetic alterations in mismatch repair genes. *Cancer Res* **56**(21), 4836-4840

Tort, F., Bartkova, J., Sehested, M., Orntoft, T., Lukas, J., and Bartek, J. (2006) Retinoblastoma pathway defects show differential ability to activate the constitutive DNA damage response in human tumorigenesis. *Cancer Res* **66**(21), 10258-10263

Uhrhammer, N., Bay, J., Pernin, D., Rio, P., Grancho, M., Kwiatkowski, F., Gosse-Brun, S., Daver, A., and Bignon, Y. (1999) Loss of heterozygosity at the ATM locus in colorectal carcinoma. *Oncol Rep* **6**(3), 655-658

Uziel, T., Lerenthal, Y., Moyal, L., Andegeko, Y., Mittelman, L., and Shiloh, Y. (2003) Requirement of the MRN complex for ATM activation by DNA damage. *Embo J* **22**(20), 5612-5621

Vahteristo, P., Tamminen, A., Karvinen, P., Eerola, H., Eklund, C., Aaltonen, L. A., Blomqvist, C., Aittomaki, K., and Nevanlinna, H. (2001) p53, CHK2, and CHK1 genes in Finnish families with Li-Fraumeni syndrome: further evidence of CHK2 in inherited cancer predisposition. *Cancer Res* **61**(15), 5718-5722

Valerie, K., and Povirk, L. F. (2003) Regulation and mechanisms of mammalian double-strand break repair. *Oncogene* **22**(37), 5792-5812

van den Bosch, M., Bree, R. T., and Lowndes, N. F. (2003) The MRN complex: coordinating and mediating the response to broken chromosomes. *EMBO Rep* **4**(9), 844-849

Varon, R., Vissinga, C., Platzer, M., Cerosaletti, K. M., Chrzanowska, K. H., Saar, K., Beckmann, G., Seemanova, E., Cooper, P. R., Nowak, N. J., Stumm, M., Weemaes, C. M., Gatti, R. A., Wilson, R. K., Digweed, M., Rosenthal, A., Sperling, K., Concannon, P., and Reis, A. (1998) Nibrin, a novel DNA double-strand break repair protein, is mutated in Nijmegen breakage syndrome. *Cell* **93**(3), 467-476

Vermeulen, K., Van Bockstaele, D. R., and Berneman, Z. N. (2003) The cell cycle: a review of regulation, deregulation and therapeutic targets in cancer. *Cell Prolif* **36**(3), 131-149

Vermeulen, S. J., Chen, T. R., Speleman, F., Nollet, F., Van Roy, F. M., and Mareel, M. M. (1998) Did the four human cancer cell lines DLD-1, HCT-15, HCT-8, and HRT-18 originate from one and the same patient? *Cancer Genet Cytogenet* **107**(1), 76-79

Veuger, S. J., Curtin, N. J., Smith, G. C., and Durkacz, B. W. (2004) Effects of novel inhibitors of poly(ADP-ribose) polymerase-1 and the DNA-dependent protein kinase on enzyme activities and DNA repair. *Oncogene* **23**(44), 7322-7329

Vigneron, A., Cherier, J., Barre, B., Gamelin, E., and Coqueret, O. (2006) The cell cycle inhibitor p21waf1 binds to the myc and cdc25A promoters upon DNA damage and induces transcriptional repression. *J Biol Chem* **281**(46), 34742-34750

Vigo, E., Muller, H., Prosperini, E., Hateboer, G., Cartwright, P., Moroni, M. C., and Helin, K. (1999) CDC25A phosphatase is a target of E2F and is required for efficient E2F-induced S phase. *Mol Cell Biol* **19**(9), 6379-6395

Vindelov, L. L., Christensen, I. J., and Nissen, N. I. (1983) A detergent-trypsin method for the preparation of nuclei for flow cytometric DNA analysis. *Cytometry* **3**(5), 323-327

Waldman, T., Kinzler, K. W., and Vogelstein, B. (1995) p21 is necessary for the p53-mediated G1 arrest in human cancer cells. *Cancer Res* **55**(22), 5187-5190

Waldman, T., Lengauer, C., Kinzler, K. W., and Vogelstein, B. (1996) Uncoupling of S phase and mitosis induced by anticancer agents in cells lacking p21. *Nature* **381**(6584), 713-716

Wang, T. L., Diaz, L. A., Jr., Romans, K., Bardelli, A., Saha, S., Galizia, G., Choti, M., Donehower, R., Parmigiani, G., Shih Ie, M., Iacobuzio-Donahue, C., Kinzler, K. W., Vogelstein, B., Lengauer, C., and Velculescu, V. E. (2004a) Digital karyotyping identifies thymidylate synthase amplification as a mechanism of resistance to 5-fluorouracil in metastatic colorectal cancer patients. *Proc Natl Acad Sci U S A* **101**(9), 3089-3094

Wang, Y., Cortez, D., Yazdi, P., Neff, N., Elledge, S. J., and Qin, J. (2000) BASC, a super complex of BRCA1-associated proteins involved in the recognition and repair of aberrant DNA structures. *Genes Dev* **14**(8), 927-939

Wang, Y. A., Elson, A., and Leder, P. (1997) Loss of p21 increases sensitivity to ionizing radiation and delays the onset of lymphoma in atm-deficient mice. *Proc Natl Acad Sci U S A* **94**(26), 14590-14595

Wang, Z., Cummins, J. M., Shen, D., Cahill, D. P., Jallepalli, P. V., Wang, T. L., Parsons, D. W., Traverso, G., Awad, M., Silliman, N., Ptak, J., Szabo, S., Willson, J. K., Markowitz, S. D., Goldberg, M. L., Karess, R., Kinzler, K. W., Vogelstein, B., Velculescu, V. E., and Lengauer, C. (2004b) Three classes of genes mutated in colorectal cancers with chromosomal instability. *Cancer Res* **64**(9), 2998-3001

Watanabe, N., Broome, M., and Hunter, T. (1995) Regulation of the human WEE1Hu CDK tyrosine 15-kinase during the cell cycle. *Embo J* **14**(9), 1878-1891

Weinberg, R. A. (1995) The retinoblastoma protein and cell cycle control. *Cell* **81**(3), 323-330

Wheeler, J. M., Beck, N. E., Kim, H. C., Tomlinson, I. P., Mortensen, N. J., and Bodmer, W. F. (1999) Mechanisms of inactivation of mismatch repair genes in human colorectal cancer cell lines: the predominant role of hMLH1. *Proc Natl Acad Sci U S A* **96**(18), 10296-10301

Wheeler, J. M., Bodmer, W. F., and Mortensen, N. J. (2000) DNA mismatch repair genes and colorectal cancer. *Gut* **47**(1), 148-153

Williams, L. H., Choong, D., Johnson, S. A., and Campbell, I. G. (2006) Genetic and epigenetic analysis of CHEK2 in sporadic breast, colon, and ovarian cancers. *Clin Cancer Res* **12**(23), 6967-6972

Wright, J. A., Keegan, K. S., Herendeen, D. R., Bentley, N. J., Carr, A. M., Hoekstra, M. F., and Concannon, P. (1998) Protein kinase mutants of human ATR increase sensitivity to UV and ionizing radiation and abrogate cell cycle checkpoint control. *Proc Natl Acad Sci U S A* **95**(13), 7445-7450

Wu, X., Webster, S. R., and Chen, J. (2001) Characterization of tumor-associated Chk2 mutations. *J Biol Chem* **276**(4), 2971-2974

Xiao, Y., and Weaver, D. T. (1997) Conditional gene targeted deletion by Cre recombinase demonstrates the requirement for the double-strand break repair Mre11 protein in murine embryonic stem cells. *Nucleic Acids Res* **25**(15), 2985-2991

Xiao, Z., Chen, Z., Gunasekera, A. H., Sowin, T. J., Rosenberg, S. H., Fesik, S., and Zhang, H. (2003) Chk1 mediates S and G2 arrests through Cdc25A degradation in response to DNA-damaging agents. *J Biol Chem* **278**(24), 21767-21773

Xie, A., Hartlerode, A., Stucki, M., Odate, S., Puget, N., Kwok, A., Nagaraju, G., Yan, C., Alt, F. W., Chen, J., Jackson, S. P., and Scully, R. (2007) Distinct roles of chromatin-associated proteins MDC1 and 53BP1 in mammalian double-strand break repair. *Mol Cell* **28**(6), 1045-1057

Xu, B., O'Donnell, A. H., Kim, S. T., and Kastan, M. B. (2002) Phosphorylation of serine 1387 in Brca1 is specifically required for the Atm-mediated S-phase checkpoint after ionizing irradiation. *Cancer Res* **62**(16), 4588-4591

Yamamoto, H., Min, Y., Itoh, F., Imsumran, A., Horiuchi, S., Yoshida, M., Iku, S., Fukushima, H., and Imai, K. (2002) Differential involvement of the hypermethylator phenotype in hereditary and sporadic colorectal cancers with high-frequency microsatellite instability. *Genes Chromosomes Cancer* **33**(3), 322-325

Yamashita, S., Yamamoto, H., Mimori, K., Nishida, N., Takahashi, H., Haraguchi, N., Tanaka, F., Shibata, K., Sekimoto, M., Ishii, H., Doki, Y., and Mori, M. (2012) MicroRNA-372 is associated with poor prognosis in colorectal cancer. *Oncology* **82**(4), 205-212

Yang, J., Xu, Z. P., Huang, Y., Hamrick, H. E., Duerksen-Hughes, P. J., and Yu, Y. N. (2004) ATM and ATR: sensing DNA damage. *World J Gastroenterol* **10**(2), 155-160

Yarden, R. I., Pardo-Reoyo, S., Sgagias, M., Cowan, K. H., and Brody, L. C. (2002) BRCA1 regulates the G2/M checkpoint by activating Chk1 kinase upon DNA damage. *Nat Genet* **30**(3), 285-289

Young, B. R., and Painter, R. B. (1989) Radioresistant DNA synthesis and human genetic diseases. *Hum Genet* **82**(2), 113-117

Zhan, Q., Antinore, M. J., Wang, X. W., Carrier, F., Smith, M. L., Harris, C. C., and Fornace, A. J., Jr. (1999) Association with Cdc2 and inhibition of Cdc2/Cyclin B1 kinase activity by the p53-regulated protein Gadd45. *Oncogene* **18**(18), 2892-2900

Zhang, J., Willers, H., Feng, Z., Ghosh, J. C., Kim, S., Weaver, D. T., Chung, J. H., Powell, S. N., and Xia, F. (2004) Chk2 phosphorylation of BRCA1 regulates DNA double-strand break repair. *Mol Cell Biol* **24**(2), 708-718

Zhao, H., Watkins, J. L., and Piwnica-Worms, H. (2002) Disruption of the checkpoint kinase 1/cell division cycle 25A pathway abrogates ionizing radiation-induced S and G2 checkpoints. *Proc Natl Acad Sci U S A* **99**(23), 14795-14800

Zhao, S., Weng, Y. C., Yuan, S. S., Lin, Y. T., Hsu, H. C., Lin, S. C., Gerbino, E., Song, M. H., Zdzienicka, M. Z., Gatti, R. A., Shay, J. W., Ziv, Y., Shiloh, Y., and Lee, E. Y. (2000) Functional link between ataxia-telangiectasia and Nijmegen breakage syndrome gene products. *Nature* **405**(6785), 473-477

Zhou, B. B., and Elledge, S. J. (2000) The DNA damage response: putting checkpoints in perspective. *Nature* **408**(6811), 433-439

Zhu, J., Petersen, S., Tessarollo, L., and Nussenzweig, A. (2001) Targeted disruption of the Nijmegen breakage syndrome gene NBS1 leads to early embryonic lethality in mice. *Curr Biol* **11**(2), 105-109

Zoppoli, G., Solier, S., Reinhold, W. C., Liu, H., Connelly, J. W., Jr., Monks, A., Shoemaker, R. H., Abaan, O. D., Davis, S. R., Meltzer, P. S., Doroshow, J. H., and Pommier, Y. (2012) CHEK2 genomic and proteomic analyses reveal genetic inactivation or endogenous activation across the 60 cell lines of the US National Cancer Institute. *Oncogene* **31**(4), 403-418

Zou, L., and Elledge, S. J. (2003) Sensing DNA damage through ATRIP recognition of RPA-ssDNA complexes. *Science* **300**(5625), 1542-1548

Appendix A EC50 ATM Assay Cell Lines

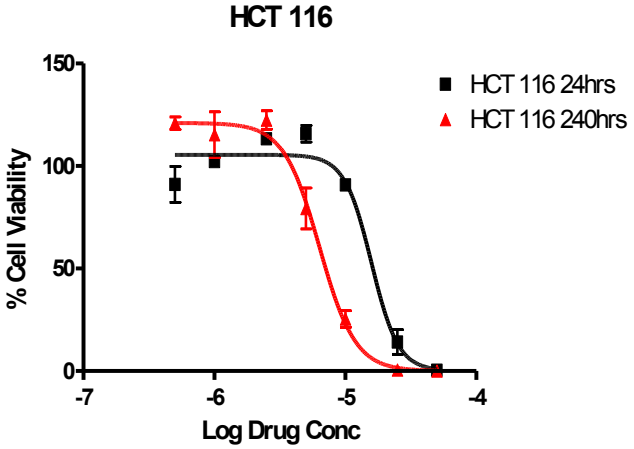

	HCT 116 24 hours	HCT 116 240 hours
EC50	1.5832e-005	6.3466e-006
95% CI	1.1498e-005 to 2.1799e-005	5.4183e-006 to 7.4340e-006
R^2	0.9606	0.9674

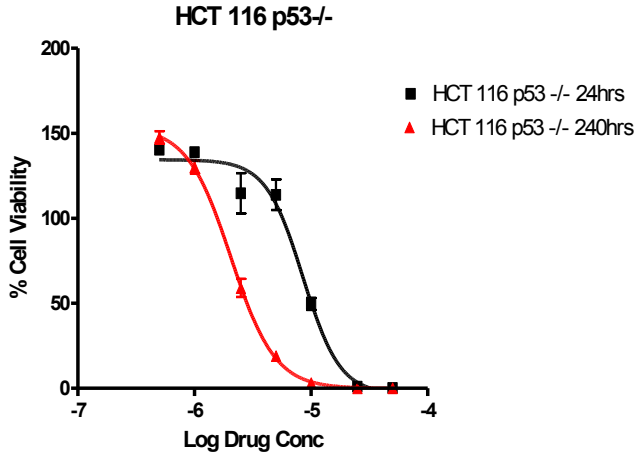

	HCT 116 p53 24 hours	HCT 116 p53 240 hours
EC50	8.5219e-006	2.0607e-006
95% CI	7.1447e-006 to 1.0165e-005	1.8663e-006 to 2.2754e-006
R^2	0.9653	0.9971

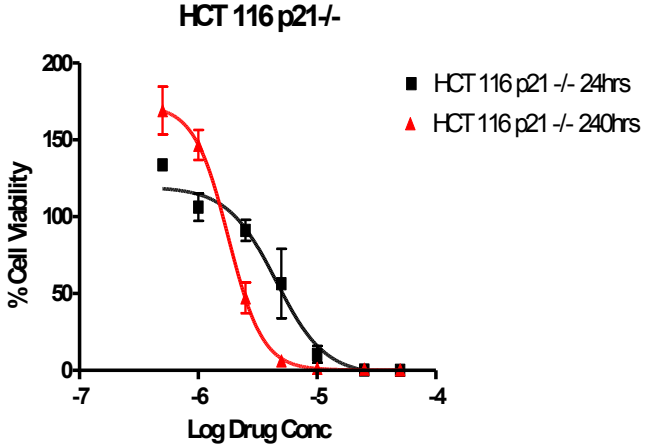

	HCT 116 p21 24 hours	HCT 116 p21 240 hours
EC50	4.5261e-006	1.7945e-006
95% CI	3.0306e-006 to 6.7596e-006	1.4726e-006 to 2.1868e-006
R^2	0.9411	0.9735

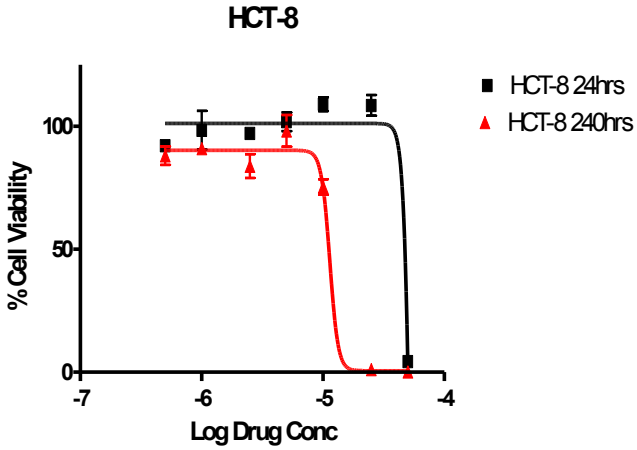

	HCT-8 24 hours	HCT-8 240 hours
EC50	5.4380e-005	1.1358e-005
95% CI		1.2641e-016 to 1.0206e+006
R^2	0.9471	0.9822

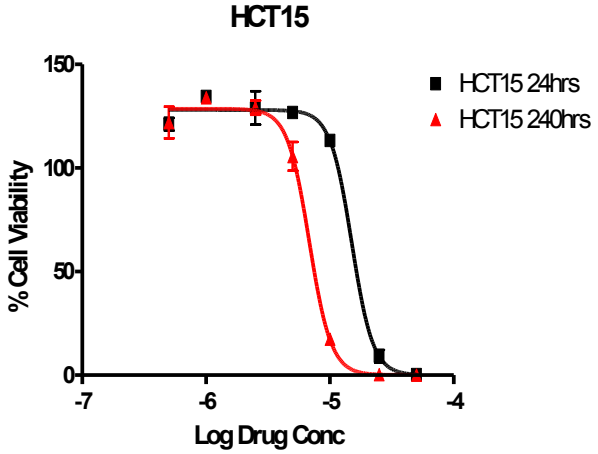

	SW-480 24 hours	SW-480 240 hours
EC50	1.2812e-005	8.9987e-006
95% CI	8.5638e-006 to 1.9166e-005	8.1632e-010 to 0.09920
R^2	0.9460	0.8998

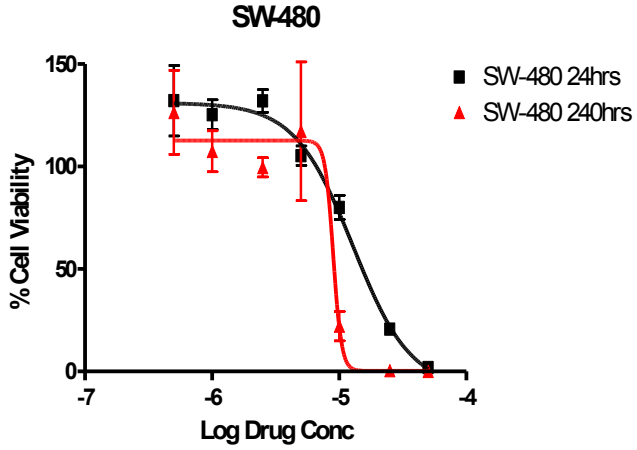

	SW-480 24 hours	SW-480 240 hours
EC50	1.2812e-005	8.9987e-006
95% CI	8.5638e-006 to 1.9166e-005	8.1632e-010 to 0.09920
R^2	0.9460	0.8998

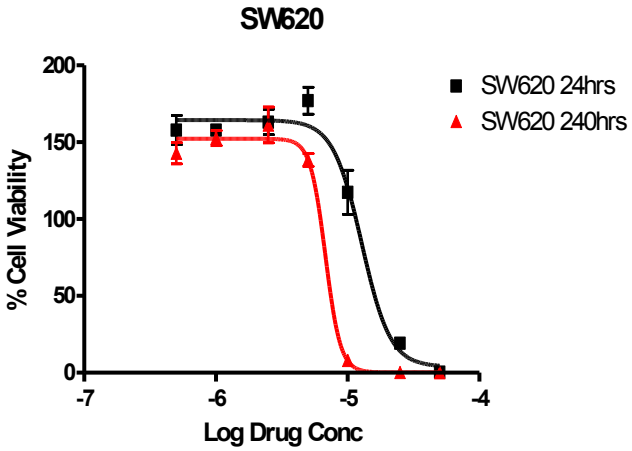

	SW620 24 hours	SW620 240 hours
EC50	1.2800e-005	6.7902e-006
95% CI	9.8065e-006 to 1.6706e-005	5.8280e-006 to 7.9114e-006
R^2	0.9740	0.9833

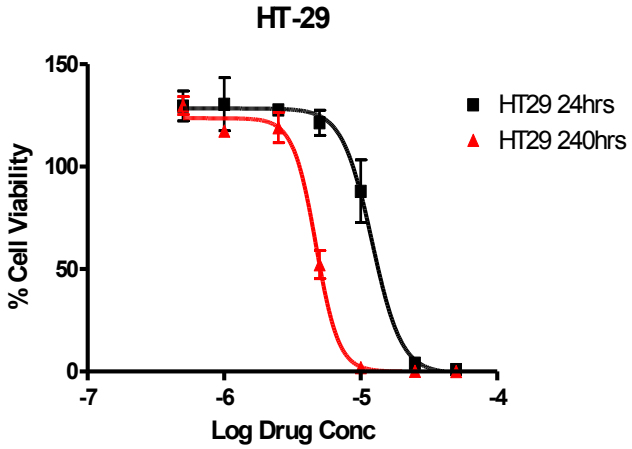

	HT-29 24 hours	HCT-29 240 hours
EC50	1.2087e-005	4.7069e-006
95% CI	9.4613e-006 to 1.5442e-005	4.3441e-006 to 5.1000e-006
R^2	0.9535	0.9911